

Abstract

JOHNSON, MATTHEW ROBERT. Intercellular Communication in Hyperthermophilic Microorganisms. (Under the direction of Dr. Robert M. Kelly).

In the microbial world it is becoming apparent that many syntrophic, symbiotic and competitive interactions that occur within and between species are driven largely by a form of cell-to-cell communication known as quorum sensing, in which communication within and between species occurs through the use of highly specific signal molecules. In this work, evidence is presented through functional-genomics approaches that cell-to-cell signaling is a phenomenon not limited to mesophilic bacteria. In *Thermotoga maritima*, a hyperthermophilic bacterium, a previously uncharacterized small peptide (TM0504) that is very highly expressed under syntrophic growth conditions was found to have quorum sensing properties, inducing the cell-density dependent expression of glycosyltransferases to form exopolysaccharides. Exopolysaccharide production enabled the close association of *T. maritima* to the hyperthermophilic methanogen *Methanococcus jannaschii*, underlying the syntrophic transfer of hydrogen between species. Upon further examination, it was found that distinct life cycles exist within this syntrophic relationship, with rapid growth and aggregation in the co-culture followed by detachment of the two species in stationary phase. This process is postulated to be driven by an unknown quorum sensing system, allowing the detachment and spread of these organisms into new growth environments.

In addition, evidence was provided that showed that *Pyrococcus furiosus*, a hyperthermophilic archaeon growing optimally near 100°C, both produces and responds to a recognizable form of AI-2, a furanosyl borate diester and known universal

autoinducer of quorum sensing in mesophilic bacteria. As *P. furiosus* and all other members of the Archaea lack the LuxS enzyme involved in AI-2 biosynthesis in mesophilic bacteria, an alternative pathway must be involved. Purification of native AI-2 biosynthetic enzymes from *P. furiosus* crude cell extracts using a biological reporter assay allowed for the isolation of fractionated cell-free extracts that could convert adenosine to a species that triggered quorum sensing in a reporter strain of *Vibrio harveyi*. Through the use of the available genome sequence, it was proposed the production pathway for AI-2 involves the phosphorylation of ribose from adenosine through the activity of a eukaryotic-like MTA-phosphorylase (PF0016). In fact, the recombinantly produced MTA phosphorylase could complement fractionated *P. furiosus* biomass to produce enhanced levels of AI-2 activity from adenosine at 90°C. Other components of the pathway are under investigation, but likely includes a ribose phosphoisomerase (PF1258) to produce phosphorylated ribulose, which can be non-enzymatically converted to (4S)-4,5-dihydroxy-2,3-pentanedione (DPD). A potentially unique contribution of thermal energy in the conversion is proposed as this step is significantly accelerated at hyperthermophilic temperatures over rates observed at mesophilic temperatures, suggesting temperature may have had a role in directing the evolution of cell-to-cell signaling systems. Overall, these results suggest quorum sensing phenomena occurs in hyperthermophilic microorganisms, where it likely plays an important role in regulating intra- and inter-species interactions and defining microbial phenotypes.

Intercellular Communication in Hyperthermophilic Microorganisms

By

Matthew Robert Johnson

Submitted to the Graduate Faculty of North Carolina State University in partial fulfillment of the requirements for the Degree of Doctor of Philosophy.

Chemical Engineering

Raleigh, NC
August 2005

APPROVED BY

Dr. David F. Ollis

Dr. James W. Brown

Dr. Jason M. Haugh

Dr. Robert M. Kelly
Chair of Advisory Committee

Dedication

I would like to dedicate this thesis work to my parents and grandparents, whom taught me throughout my life the importance of education, and who made sure that I all the opportunities the world can offer.

Biography

Matthew Robert Johnson was born in Jackson, MI on January 24th 1979. After the third grade he moved with his family to Poughkeepsie, NY where they lived for three years. After relocating to the small town of Hilton, NY outside of Rochester, he completed grades 6-12 grade and earned his Regents Diploma while being a three-time letter winner with the varsity football program. After high school he attended Cornell University in Ithaca, NY where he earned his Bachelors of Science in Agricultural and Biological Engineering cum laude, while playing football with the Division IAA varsity football team. After Cornell, he attended North Carolina State University to pursue his Ph.D in Chemical Engineering. On July 13th, 2002 he was happily married to his wife Angelica Marie Toulis, whom he had met at Cornell, and together they enjoyed a wonderful honeymoon in Greece. In December 2002 he earned his Masters of Science in Chemical Engineering, followed by his Masters of Business Administration degree in May of 2005.

Acknowledgments

The French have a saying that to make great wine the grapes must suffer, and to make it through the Ph.D process sacrifices have to be made on both the part of the candidate, and most importantly, their family. The fruits of this work could not have been accomplished without the incredible love and support of my wife Angelica, who has been by my side through four college degrees, relocations, and many nights and weekends busy at work. She knows more than anyone else what it has taken to get through graduate school, and without her it would not have been possible.

I also must thank my parents, grandparents, sisters and friends who have served supported me through the past five years and all the proceeding years of my education. They have always been there and have been the drive that has kept me going, always taking interest in the work I have completed.

Finally I have to thank the team of incredible researchers that I have spent the past five years with. Dr. Robert Kelly has been a wonderful mentor and I have enjoyed and appreciated the time he has invested in me, and the classes we have taught together. The work we complete in the Kelly Group could not be possible if it were not for the dedication and passion he has for great research, and for being a great mentor. In addition I would like to thank the faculty of the NCSU Biotechnology program including Dr. John Chisnell and Dr. Sue Carson, who have supported me through my research and have been great to work with.

The fellow grad students in the Kelly group have been fun to work with and I have enjoyed being part of such a wonderful team. There is no way that my thesis could have come together without the help of Clemente Montero, Keith Shockley, Shannon

Conners, Don Comfort, Josh Michel, Sabrina Tachdjian, Hank Chou, Jason Nichols, Don Ward, Amy Van Fossen, Kate Auernik, Derrick Lewis, Morgan Harris and Steven Gray.

Finally, last but certainly not least, the undergraduate students who have worked with me on my projects have taught me so much, and have been a pleasure to work with. Tom Van Blarcom, Brian Pridgen, Kristen Jones, Jonathon Bendas, Jim Furgurson and Stephanie Bridger have all contributed to the research I have presented and published, and I appreciate their hard work and dedication very much.

Table of Contents

	<u>Page</u>
List of Tables	ix
List of Figures	x
Chapter 1: Intercellular Communication in Hyperthermophilic Microorganisms	1
Communication-driven ecological interactions	2
Characterized quorum sensing systems in bacteria	5
Interspecies quorum sensing	7
Intraspecies communication	10
The search for quorum sensing in hyperthermophiles	13
References cited	16
Chapter 2: Functional Genomics-based Studies of the Microbial Ecology of Hyperthermophilic Microorganisms	20
Abstract	21
Introduction	22
Mixed species studies: an essential part of microbial ecology	23
Biofilms	25
Genetic transfer	27
Challenges and future work	29
Conclusions	30
Acknowledgements	31
References cited	31
Chapter 3: Population Density-Dependent Regulation of Exopolysaccharide Formation in the Hyperthermophilic Bacterium <i>Thermotoga maritima</i>	34
Abstract	35
Introduction	36
Results and discussion	39
High cell-density <i>T. maritima</i> and the formation of polysaccharide cellular aggregates	39
Whole genome transcriptional response of <i>T. maritima</i> in co-culture	40
Proposed pathway for EPS production and regulation in <i>T. maritima</i>	41
Evidence for cell-to-cell communication	45
Summary	47
Experimental procedures	48
Bacterial strains, growth, and handling	48
Fluorescence microscopy	49

Microarray protocols	50
Exopolysaccharide Analysis	51
Acknowledgements	52
References cited	53
Chapter 4: <i>Thermotoga maritima</i> phenotype is impacted by syntrophic with <i>Methanococcus jannaschii</i> in hyperthermophilic co-culture	66
Abstract	67
Introduction	68
Materials and methods	71
Growth of microorganisms	71
Fluorescence microscopy	73
Microarray protocols	73
Independent confirmation with Real-Time PCR	74
Results and discussion	75
Transition from log to stationary phase in <i>T. maritima</i> pure and co-culture	75
Comparisons between phase-dependent phenotypes in pure culture and co-culture	79
Differential expression of regulatory proteins	80
Secondary messengers	83
Summary	84
Acknowledgements	85
References cited	86
Supplemental Data	96
Chapter 5: Evidence for AI-2 Based Cell-to-Cell Signaling in Hyperthermophilic Archaea and Bacteria: Proposed Pathway for AI-2 Biosynthesis in <i>Pyrococcus furiosus</i>	127
Abstract	128
Introduction	130
Materials and methods	132
Growth of microorganisms	132
Screening of hyperthermophiles for autoinducer production	133
Fractionation of native <i>P. furiosus</i> cell-free extract	134
Large scale in-vitro production of AI-2	135
Microarray protocols	137
Recombinant production of <i>P. furiosus</i> methylthioladenosine phosphorylase (PF0016)	137
Results	138
Autoinducer activity in hyperthermophilic supernatants	138
Crude extract autoinducer synthesis activity in <i>P. furiosus</i>	140

The production of AI-2 is an enzymatic reaction with adenosine as the substrate	140
Proposed pathway for AI-2 production in <i>P. furiosus</i>	142
Transcriptional response to <i>in-vitro</i> produced AI-2	145
Discussion	148
Acknowledgements	150
References cited	151
Chapter 6: Appendixes	154
Appendix 1: Microarray and Real-Time PCR protocols and manual	154
Appendix 2: Growth of <i>Vibrio harveyi</i> for the detection of homoserine lactones and the autoinducer AI-2	179

List of Tables

	<u>Page</u>
1.1 Peptide-based quorum sensing systems in Bacteria	11
1.2 Distribution of predicted open reading frames in microbial genomes	15
2.1 Predicted lateral gene transfer in hyperthermophiles	28
3.1 Differential expression of genes in the co-culture	56
4.1 Differentially expressed genes in <i>T. maritima</i> during the transition from mid-log to early stationary phase in pure culture	90
4.2 Differentially expressed carbohydrate active enzymes and transporters	91
4.3 Confirmation of microarray results with Real-Time PCR	92
4.S1 Supplemental: Genes differentially expressed in sparged or co-culture	96
4.S2 Supplemental: Genes differentially expressed in mid-log to stationary phase transition in the co-culture	113
4.S3 Supplemental: Differential gene expression between pure and co-culture in similar growth phases	117
5.1 The induction of luminescence in <i>V. harveyi</i> strain MM32 by crude Extracts from <i>P. furiosus</i>	140
5.2 Differential gene expression in between an AI-2 and control dosed culture of <i>P. furiosus</i>	146
5.3 The induction of luminescence in MM32 by the supernatants of <i>P. furiosus</i> at different phases of growth	147

List of Figures

	<u>Page</u>
1.1 The three main systems of quorum sensing in bacteria	8
1.2 The activated methyl cycle	9
2.1 Epifluorescence images of <i>T. maritima</i> pure and co-cultures	24
3.1 Mono and co-culture samples stained with Acridine orange and Calcofluor	58
3.2A The log ₂ fold change in gene expression between the pure culture and the co-culture	59
3.2B Gene expression changes broken down into functional categories as defined by the COG database	60
3.3 Putative pathway for exopolysaccharide production under high cell density conditions in <i>T. maritima</i>	61
3.4 Putative diguanylate cyclase and cyclic di-GMP phosphodiesterase GGDEF domain proteins from <i>T. maritima</i>	62
3.5 Putative signaling peptide from <i>T. maritima</i>	63
3.6 Acridine orange and Calcofluor stained cultures of <i>T. maritima</i> 30 minutes after dosing with either buffer (PBS) (left), or synthetic peptide	64
3.7 Putative glycosyl transferase operon related to EPS production	65
4.1 Growth of <i>T. maritima</i> in pure culture and in co-culture with <i>M. jannaschii</i>	94
4.2 Relative expression of putative sigma factors	95
5.1 The induction of luminescence in <i>V. harveyi</i> strain MM32 by hyperthermophilic supernatants	139
5.2 The production pathway for AI-2 in mesophilic organisms and the proposed pathway in <i>P. furiosus</i>	142
5.3 The effect of adenosine concentration on activity of <i>P. furiosus</i> crude extract	143
5.4 Background subtracted mass spectra analysis of <i>in-vitro</i> produced AI-2	144
5.5 Alignment of the mouse class I PNP with PF0016	149

Chapter 1: Intercellular Communication in Hyperthermophilic Microorganisms

M. R. Johnson and R.M. Kelly

**Department of Chemical and Biomolecular Engineering
North Carolina State University
Raleigh, NC 27695-7905**

Communication-Driven Ecological Interactions

Fundamental to microbial ecology is the interaction of microorganisms with other organisms both within, and outside of, their own species or genus. Such interactions among a diverse community of cells offers advantages of coordinated growth, movement, and biochemical activity (52, 63), while at the same time improving competitiveness within a heterogeneous environment. A recent discovery that has proven key to understanding microbial interactions is the phenomena known as *quorum sensing* in which microbial cells can signal within and between species (17).

Quorum sensing has been found in environments ranging from the gastrointestinal tract of mammals to marine environments. Given the widespread (48) and highly conserved (21) occurrence of quorum sensing throughout the Bacteria, it is plausible that quorum sensing exists in hydrothermal environments as well. Several quorum sensing signal molecules have been shown to be stable at temperatures characteristic of high temperature microbial habitats (19, 58). Evidence for species interactions is strong in cases such as the co-culture of hyperthermophilic heterotrophs and methanogens (those with optimal growth temperatures of 80°C and higher) (38), but it remains to be seen if this high level of syntrophy is dependent upon quorum sensing. If quorum sensing is shown to occur among hyperthermophiles, questions arise about whether this phenomenon evolved from within hyperthermophilic niches, or if it was acquired via genetic transfer.

Benefits that could be derived from intercellular communication in high temperature environments are important to investigate, as signaling is a metabolically expensive process and, therefore, would only occur if the resulting quorum sensing regulated phenotype enhances the survivability of the organism. Cell-to-cell communication could be important

in high temperature syntrophic interactions in which delicate interactions are required between species in order for the individual cells to survive. In order for organisms to inhabit extreme environments, it must be thermodynamically favorable for them to do so. While it has been estimated that the minimal quantum free energy level in growth substrates of -20 KJ/mol required for the biological conversion of free energy in single species (40), recent work has shown that in syntrophic co-cultures containing methanogens can utilize substrates with quantum free energy levels as low as -4.5 KJ/mol. Such low energy conditions are found in such biologically inhospitable areas as the deep sea and the subsurface of Earth (40), and could be representative of the first ecosystems that evolved on Earth or other planets where the potential for life could exist (55).

In both artificial and native hyperthermophilic environments, syntrophic methanogen to heterotroph ratios are approximately 1:100 (5, 38). The species are very inter-dependent when grown in co-culture, and must exist in close proximity to one another in order for efficient hydrogen transfer to occur (38). Such organisms are believed to be closely related to the earliest forms of life based on 16S rRNA typing (26), and exist in environments quite similar to the environmental conditions found on early Earth (46). Therefore, understanding how interactions between species occur in these environments should aid in elucidating the origins of microbial interactions and multicellularity. In addition, recent studies have suggested that eukaryotic may have first arose from a mixed culture environment consisting of archaeal methanogen and a heterotrophic bacterium (32, 35), instead of the widely accepted theory that depicts eukaryotes evolving from the endosymbiosis of plastids which formed primitive mitochondria (34).

Based off the known interactions between heterotrophs and methanogens, several species of interest have been chosen as targets for quorum sensing investigation. *Methanococcus jannaschii*, which was originally isolated from white smoker submarine hydrothermal vents located along the East Pacific Rise, is a hyperthermophilic member of the domain Archaea, and a methanogenic autotroph utilizing hydrogen and carbon dioxide for metabolic energy production (22). Since the genome has been sequenced (6), *M. jannaschii* makes is an attractive target for functional genomic and bioinformatic-based studies. In addition, *M. jannaschii* cannot utilize extracellular sugars for growth (29) and, therefore, when cultured in environments without abundant hydrogen and carbon dioxide it is dependant upon syntrophic interactions for growth.

Two other organisms of interest here include *Thermotoga maritima* and *Pyrococcus furiosus*, both of which are hyperthermophilic heterotrophs isolated from geothermally-heated sediment off the coast of Volcano Island, Italy (18, 27). *T. maritima*, a bacterium, has been isolated in diverse thermophilic environments ranging from terrestrial hot springs to deep sea hydrothermal vents (33), has a fully sequenced genome (39). *T. maritima* can metabolize many simple and complex carbohydrates producing fermentative byproducts, such as hydrogen and carbon dioxide (14). Studies have shown that *T. maritima*, a hydrogen-producing heterotroph, benefits from being grown in co-cultivation with *M. jannaschii*, as accumulating hydrogen is inhibitory to the growth of *T. maritima* (38). Functional genomic studies have been conducted with *T. maritima* examining the effects of heat stress (44), biofilm phenotype (45), and sugar utilization pathways (9), but to date no studies have been completed focusing on the effects of growth phase or species interactions.

P. furiosus is very similar in growth habits to *T. maritima* with the key differences that it is a member of the Archaea, and capable of growth at higher temperatures (18). Its metabolism is dependent on a modified Embden-Meyerhof (EM) pathway utilizing a wide variety of carbohydrates and peptides for energy metabolism with hydrogen, carbon dioxide, and acetate as the main metabolic byproducts (37). As a member of the Archaea, *P. furiosus* is significantly different from bacterial hyperthermophiles; instead of relying on sigma factors for regulation of transcription, it uses transcription factors and TATA-box promoters for regulation of transcription (41). This is a significant difference as stress responses and most of the microbial phenotypes found in bacteria are controlled through sigma factors, and so how these processes are regulated in the archaea remains largely unknown. The genome sequence of *P. furiosus* was completed in 2001 (47), followed soon thereafter by functional genomics studies for a variety of growth conditions including heat shock response (53), sulfur metabolism (51), and growth substrate preferences (50), but as with *T. maritima*, no studies have been completed analyzing growth phase phenotypes or cell-to-cell interactions.

Characterized Quorum Sensing Systems in Bacteria

Quorum sensing is a term assigned to a particular form of bacterial cell-to-cell communication in which genes are expressed in a cell-density-dependent manner after reaching a critical concentration of signal molecules (20). Cells participating in quorum sensing continuously secrete a signal molecule into the surrounding environment, and then utilize specific receptors to determine the concentration of the signal molecule outside of the cell, triggering a cell density dependent response (62). Autoinducers, the common name for these signal molecules, comes from the fact that, in many characterized species, one primary

response to accumulating signal molecules is an increase in the expression of the genes responsible for signal molecule production (2).

A decade ago, only a handful of bacteria were known to be capable of such communication (62). But, with the advent of modern molecular biology techniques, it now appears that quorum sensing is highly conserved and that many characterized bacteria possess at least one quorum sensing system (1, 49).

Currently, two functional classes of quorum sensing have been identified: one which is highly specific and used for intraspecies communication, and one that is widely shared by bacteria and believed to be used for interspecies communication (48). In addition to the cell-to-cell microbial signaling, it is known that eukaryotes, while not utilizing their own quorum sensing system, can interfere with the quorum sensing systems of bacteria either to thwart virulent attacks, or increase the efficiency of symbiosis (15, 48). The importance of quorum sensing in coordinating bacterial communities can be seen in examples spanning from virulence to the formation of biofilms (48). Microbial cells produce biofilms to provide protection against such stresses as desiccation, toxins, antibiotics, and to bind and hold nutrients and enhance physiological stability in comparison to single cells (4, 10). It has been shown that without intercellular communication, biofilm health and stability are substantially compromised due to the loss of coordinated activities such as exopolysaccharide production (12).

To date no known quorum sensing system has been identified in the Archaea. Quorum sensing systems have been mainly identified in pathogenic bacteria, but this finding may be due in part to the bias of genome sequencing projects toward medically relevant species (60). Archaea, however, offer an interesting case to search for cell-to-cell signaling

as they share characteristics of both the Bacteria and Eukaryotes (32), and represent a large portion of the biomass on Earth, comprising approximately one-fourth of the prokaryote biomass of the oceans, and a significant portion of the digestive-system flora of higher eukaryotes (7). Determining whether or not members of the Archaea participate in quorum sensing is important for understanding how cell-to-cell signaling may have originated and evolved, and also to better understand the impact archaea have on microbial ecology and human health.

Interspecies Quorum Sensing

Interspecies communication requires a common molecule that is universally identified by all species involved in group communication (48). Recently, an autoinducer named AI-2 has been identified that has been proven to be utilized by a broad spectrum of bacteria (8, 49). The structure of AI-2 has been determined to be a furanosyl borate diester with a molecular weight of approximately 193 Da (8). AI-2 is produced in a three step process (Figure 5) (8, 49). S-adenosylmethionine (SAM), an essential metabolite utilized for methylating DNA, RNA, and proteins, is first converted by non-specific methyl transferases to S-adenosylhomocysteine (SAH). Another enzyme, Pfs nucleosidase, removes the adenine from SAH and forms S-ribosylhomocysteine (SRH), which is rapidly utilized by a third enzyme, *LuxS*, to form AI-2 (Figure 2). Of importance is the action of Pfs nucleosidase. Its substrate, SAH, is an extremely toxic methyl transferase inhibitor, and must be rapidly degraded to avoid cell death (48). Most bacteria genomes sequenced so far contain either a SAH hydrolase, or the AI-2 signaling system for SAH detoxification (56).

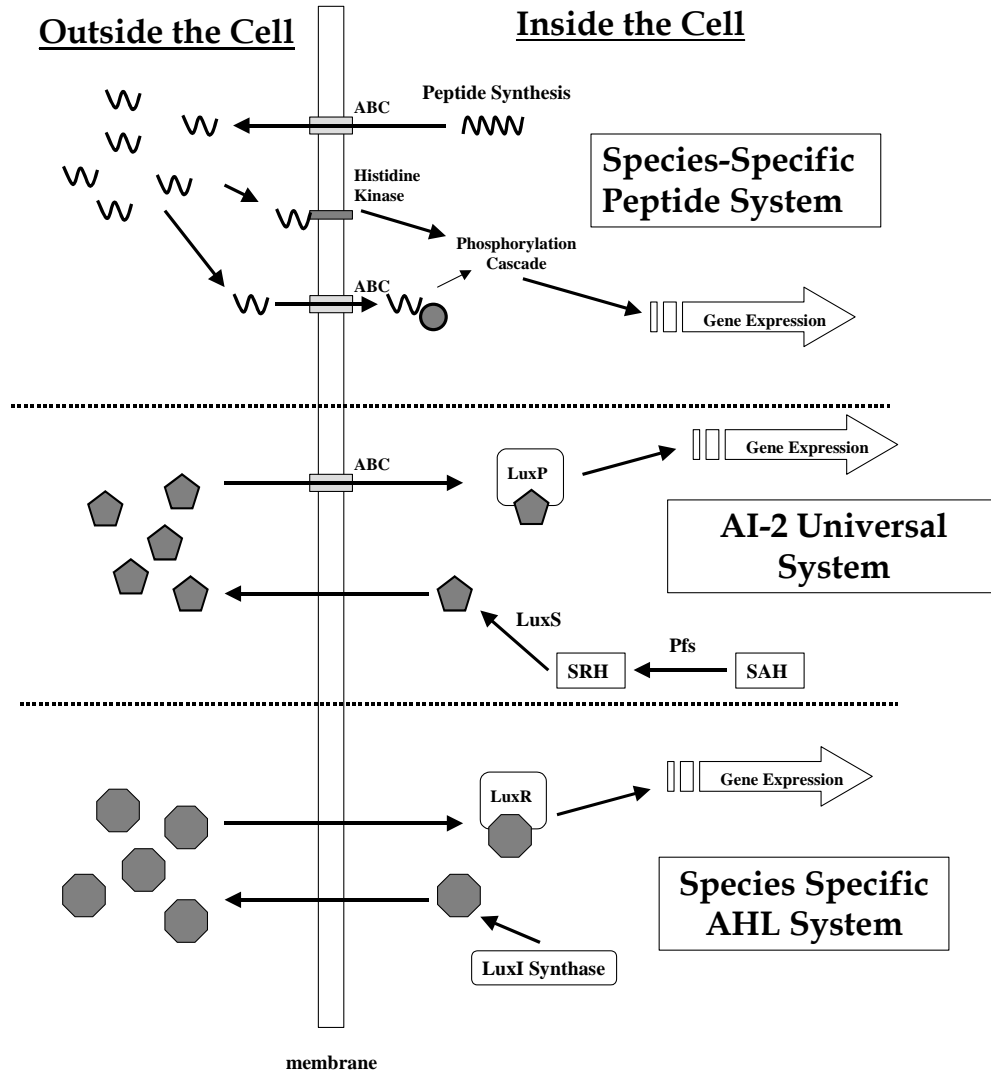


Figure 1. The three main systems of quorum sensing in bacteria. **Top:** The peptide based system found mainly in gram-positive Bacteria. **Middle:** The autoinducer-2 (AI-2) system that has been characterized as being both produced and detected in many modern pathogenic organisms, including those in the gram-positive and gram-negative classifications. **Bottom:** The homoserine lactone-(HSL)-based quorum sensing system found primarily in the gram-negative bacteria.

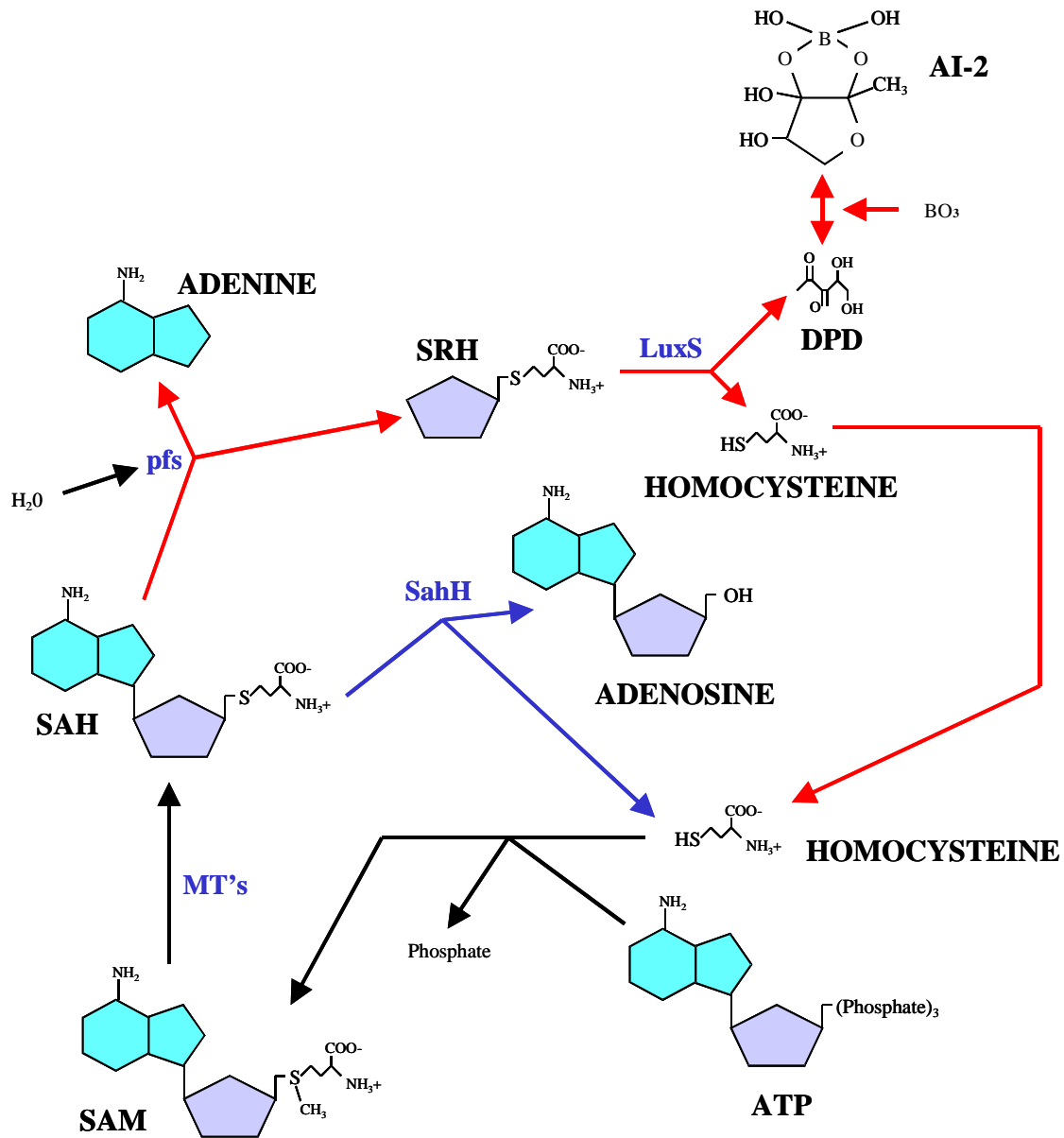


Figure 2. The activated methyl cycle (60). The black pathways are those utilized by both AI-2 producing and non-AI-2 producing organisms. The blue pathways are those utilized by organisms that do not contain LuxS, while the red pathways are used for the production of AI-2. Abbreviations: SAM (S-adenosyl methionine), SAH (S-adenosyl homocysteine), SRH (S-ribosyl homocysteine), DPD (4,5-dihydroxy-2,3-pentanedione), AI-2 (3-methyl-5,6-dihydro-furo(2,3-D)(1,3,2)dioxaborole-2,2,6,6A-tetraol).

The sensory systems for AI-2 have been determined for a few species, including the LuxP system in *V. harveyi* (24), and the Lsr system in *Salmonella typhimurium* (58). LuxP in *V. harveyi* is a AI-2 binding protein that interacts with a protein histidine kinase (LuxQ) which regulates a phosphorylation cascade leading to transcriptional regulation (24). In the Lsr system in *Salmonella typhimurium* and *Escherichia coli*, an ATP-binding cassette (ABC) transporter, Lsr, with homologies to ribose, histidine, and galactose transporters, actively transports AI-2 into the cell (58). Since transporting molecules across the membrane is an energetically expensive process, a repressor molecule, known as *LsrR*, actively suppresses the synthesis of the transporter. When AI-2 encounters the outer membrane, it binds to membrane-bound receptors that in turn antagonistically bind a repressor agent to *LsrR*. The ABC transporter can then be expressed and AI-2 is transported into the cell to effect gene expression regulated under interspecies quorum sensing. The action of AI-2 once inside of the cell is thought to involve the phosphorylation of AI-2, which is then able to interact with regulator proteins and modulate gene expression (57).

Intraspecies Communication

The known pathways of intraspecies quorum sensing in bacteria consist of peptide-based signaling in gram-positive and in some gram-negative Bacteria, and homoserine lactone (HSL)-based signaling in gram-negative bacteria (48). In addition, cAMP has been found to be utilized in several species for the purpose of swarming under stress (16), and is essential for some HSL-based intraspecies signaling systems (54).

Peptide-based Quorum Sensing

In gram-positive bacterial signaling systems, oligopeptide signaling molecules are synthesized in the cell and exported by ABC transporters (31). Membrane-bound receptors related to the two component protein kinase regulatory system can detect oligopeptides that are present in the extracellular environment (52). Additionally, it has been shown that cells can either transport the oligopeptides into the cell via ABC transporters to bind with phosphatase receptors, or the ABC transporter itself acts as a receptor (31). Upon recognition by a receptor, genetic response ensues by a cascade of phosphorylation that concludes in activating transcription regulators (31). In Table 1 several of the characterized peptide-signaling systems and classes are listed in detail.

Table 1. Peptide-based quorum sensing systems in Bacteria (31).

Class I Signaling Peptides – Characterized by signaling peptides that often function as an anti-microbial peptide, and which are detected through a histidine kinase / response regulator two-component system. These peptides may be post-translationally modified.	
<i>Streptomyces pyogenes</i>	A heavily modified signaling peptide is utilized ScnA. ScnM, modifies the peptide, and ScnT transports the mature peptide outside of the cell. ScnFEG are immunity genes against SnnA.
<i>Lactococcus lactis</i>	The signaling peptides cleaved at GG motif, NisBC post-translationally modifies peptides after export. Signaling peptides include NisA and NisZ (31).
Class II Signaling Peptides – Characterized by signaling peptides that are sometimes anti-microbial. These peptides are unmodified, cleaved at a glycine-glycine motif (The C-terminus portion is functional), and detected by histidine kinase / response regulator pair. The peptides are a C39 peptidase transporter.	
<i>Lactobacillus plantarum</i>	PlnA is cleaved at a GG motif. The signal peptide structure is helical. Additional peptides are produced that aid in forming immunity against the mature signal peptide, which is an anti-microbial agent.
<i>Lactobacillus sakei</i>	This system is very similar to <i>L. plantarum</i> , with a 19-23 AA peptide.
<i>Carnobacterium pisciocola</i>	The signaling peptide is an anti-microbial agent, cleaved at a GG motif, and is unmodified. One gene that has been identified as a signaling peptide is CbnX.
<i>Streptococcus pneumoniae</i>	GG-cleaved peptides have been identified, e.g. BlpC and CSP. They are transported by an ABC transporter with peptidase activity, for control of competence and anti-microbial production. They are detected by a histidine kinase / response regulator two-component system. (11, 13, 43).

Table 1, Continued	
Unclassified Signaling Peptides	
<i>Streptomyces coelicolor</i>	Uses the OPP peptide transport system to export signaling peptides. Modifications occur to the signaling peptides. The function of the signal is to initiate mycelium production and spore formation. (31).
<i>Bacillus subtilis</i>	<i>B. subtilis</i> utilizes both unmodified and modified signaling peptides for competence and sporulation. All signaling peptides identified are flagged for transport by conserved signal peptide sequences. This is the only bacterium to date that exports signaling peptides this way (with the Sec apparatus). They are detected both through histidine kinases and through an OPP transport system where they inhibit phosphatases. (31)
<i>Staphylococcus epidermis</i>	AgrB is the precursor to a signaling peptide, AgrB modifies and transports the peptide, and AgrCA detects the signal. AgrB is cleaved and modified with a thiolester bond to form a mature signal molecule. No ABC transporters are used for transporting the peptide in or outside of the cell.
<i>Staphylococcus aureus</i>	Very similar to <i>S. epidermis</i> . The signaling peptide used is called AIP-1 (64).

Homoserine Lactone-Based Quorum Sensing

HSL-based signaling systems in gram-negative Bacteria do not require transporters to cross the cell membrane, as they diffuse freely into and out of the cell (31, 48). The specific HSL used varies between species, but the mechanisms of their use is highly conserved (48). First the HSL molecule is synthesized via a protein known as LuxI. The HSL diffuses across the membrane and into the environment surrounding the cell. The HSL enters back into the cell via diffusion and is recognized by a protein called LuxR. LuxR in turn activates transcription factors and initiates a genetic response (48). The production of HSL is under the control of feedback mechanisms and helps control activities, such as biofilm formation, clustering of cells, and cell density (52). To date many HSL-based signaling systems have been identified due to the conserved sequence of HSL synthesis enzymes such as LuxI.

The Search for Quorum-Sensing in Hyperthermophiles

Bioinformatic analysis has suggested that HSL-based signaling may not exist in the hyperthermophilic organisms sequenced to date. In addition, all of the archaeal genomes that have been sequenced to date contain a SAH hydrolase and not LuxS, and only one genome, that of *Methanosarcina acetivorans* C2A, contains a putative Pfs nucleosidase (56). In most genome-sequenced hyperthermophilic bacteria, only a putative SAH hydrolase is encoded, with the exception being in *T. maritima*, which appears to contain both a Pfs enzyme from the AI-2 pathway, and the SAH hydrolase, while a LuxS homologue has yet to be identified (56). The difficulty in examining hyperthermophilic genomes for the presence of putative small peptide signaling molecules lies in the fact that signaling peptides are often produced from genes predicted to code for proteins less than 100 amino acids in size. Such genes constitute a large portion of every sequenced genome. As shown in Table 2, even for relatively well-characterized organisms such as *E. coli*, the number of predicted sub-100 amino acid proteins is around 389 with greater than 76% of them of unknown function.

While genomic information does not provide evidence for quorum sensing in hyperthermophiles, the ecological interactions that occur in these environments suggest that it is highly unlikely that actively growing cells grow independently from the other microorganisms. Phenomena such as multi-species biofilm formation (38), parasitic symbiosis (61), apparent lateral gene transfer (39), and even possible virulence functions (25) all point toward interactions occurring within and between species in hyperthermophilic environments, with each of these phenomena demonstrated to be quorum sensing regulated in mesophilic organisms (23, 28, 36, 64). Given the presence of these interactions, and the fact that significant evolutionary differences exist between the hyperthermophiles and

mesophiles, approaches other than genomic comparisons need to be utilized in order to screen for the presence of cell-to-cell signaling.

Because the genes that could be responsible for cell-to-cell signaling in the hyperthermophiles are unknown, techniques such as transcriptional profiling over a variety of phenotypes can be very useful for identifying quorum-sensing gene candidates. In the examination of small unknown peptides in particular, a transcriptional approach such as cDNA microarrays is very useful for screening large numbers of unknown open reading frames (ORFs), as expressing all possible unknown candidates would not be feasible (Table 2). A very rapid screening of these small peptide-encoding genes can be completed through microarray expression of the entire genome of the target organism under growth conditions relevant to quorum sensing, such as biofilm formation and growth phase transitions. In addition to screening transcriptional response, additional techniques may be utilized to explore for the production of quorum sensing molecules, such as bioassays to detect the presence of signal molecules in culture supernatants (3, 42), and analysis of expressed small peptides found in culture supernatants (30).

TABLE 2. Distribution of predicted open reading frames (ORFs) in microbial genomes as a function of the size of the ORFs in terms of amino acid length of predicted encoded proteins. All data is from the COG database (59).

ORG*	Number of Amino Acids Encoded in Predicted ORF (#) / Number of Hypotheticals (?)																			
	1-100		101-200		201-300		301-400		401-500		501-600		601-700		701-800		801-900		>900	
	#	?	#	?	#	?	#	?	#	?	#	?	#	?	#	?	#	?	#	?
Tma	160	109	385	211	465	195	384	113	240	71	89	26	69	14	30	7	24	4	28	10
Pfu	238	176	537	352	496	239	396	147	225	69	64	18	45	10	20	6	15	4	28	6
Ban	1007	848	1366	655	1208	327	890	154	531	50	237	19	115	15	52	5	42	8	59	8
Mka	294	203	560	275	481	196	317	105	177	50	64	15	43	7	16	5	10	3	25	6
Hpy	182	138	358	202	355	151	266	81	191	58	84	20	59	14	30	4	27	4	35	4
Eco	389	262	983	507	982	288	804	155	543	73	241	40	120	18	86	16	63	6	74	7
TOT	2270	1736	4189	2202	3987	1396	3057	755	1907	371	779	138	451	78	234	43	181	29	249	41
%?	76.5%		52.6%		35.0%		24.7%		19.5%		17.7%		17.3%		18.4%		16.0%		16.5%	

*Tma = *Thermotoga maritima*; Pfu = *Pyrococcus furiosus*; Ban = *Bacillus anthracis*; Mka = *Methanopyrus kandleri*; Hpy = *Helicobacter pylori*; Eco = *Escherichia coli*

References Cited

1. **Bartlett, D. H.** 2000. Editor in Chief, Molecular Marine Microbiology. Horizon Press.
2. **Bassler, B. L.** 2002. Small talk: Cell-to-cell communication in bacteria. *Cell* **109**:421-424.
3. **Bassler, B. L., E. P. Greenberg, and A. M. Stevens.** 1997. Cross-species induction of luminescence in the quorum-sensing bacterium *Vibrio harveyi*. *J. Bacteriol.* **179**:4043-4045.
4. **Beveridge, T., S. Makin, and Z. Kadurugamuwa.** 1997. Interactions between biofilms and the environment. *FEMS Microbiol. Rev.*:291-303.
5. **Bonchosmolovskaya, E. A., and K. O. Stetter.** 1991. Interspecies hydrogen transfer in cocultures of thermophilic Archaea. *Syst. Appl. Microbiol.* **14**:205-208.
6. **Bult, C. J., O. White, G. J. Olsen, L. Zhou, R. D. Fleischmann, G. G. Sutton, J. A. Blake, L. M. FitzGerald, R. A. Clayton, J. D. Gocayne, A. R. Kerlavage, B. A. Dougherty, J. F. Tomb, M. D. Adams, C. I. Reich, R. Overbeek, E. F. Kirkness, K. G. Weinstock, J. M. Merrick, A. Glodek, J. L. Scott, N. S. Geoghagen, and J. C. Venter.** 1996. Complete genome sequence of the methanogenic Archaeon, *Methanococcus jannaschii*. *Science*:1058-1073.
7. **Cavicchioli, R., P. M. G. Curmi, N. Saunders, and T. Thomas.** 2003. Pathogenic archaea: do they exist? *Bioessays* **25**:1119-1128.
8. **Chen, X., S. Schauder, N. Potier, A. Van Dorselaer, I. Pelczer, B. L. Bassler, and F. M. Hughson.** 2002. Structural identification of a bacterial quorum-sensing signal containing boron. *Nature* **415**:545-549.
9. **Chhabra, S., K. R. Shockley, S. Connors, K. Scott, R. Wolfinger, and R. Kelly.** 2003. Carbohydrate induced differential gene expression patterns in the hyperthermophilic bacterium *Thermotoga maritima*. *J. Biol. Chem.* **278**:7540-7552.
10. **Crespi, B. J.** 2001. The evolution of social behavior in microorganisms. *Trends Ecol. Evol.* **16**:178-183.
11. **Cvitkovitch, D. G., Y.-h. Li, and R. P. Ellen.** 2003. Quorum sensing and biofilm formation in *streptococcal* infections. *J. Clin. Invest.* **112**:1626-1632.
12. **Davies, D. G., M. R. Parsek, J. P. Pearson, B. H. Iglewski, J. W. Costerton, and E. P. Greenberg.** 1998. The involvement of cell-to-cell signals in the development of a bacterial biofilm. *Science* **280**:295-298.
13. **de Saizieu, A., C. Gardes, N. Flint, C. Wagner, M. Kamber, T. Mitchell, W. Keck, K. Amrein, and R. Lange.** 2000. Microarray-based identification of a novel *Streptococcus pneumoniae* regulon controlled by an autoinduced peptide. *J. Bacteriol.* **182**:4696-4703.
14. **de Vos, W. M., S. W. M. Kengen, W. G. B. Voorhorst, and J. van der Oost.** 1998. Sugar utilization and its control in hyperthermophiles. *Extremophiles* **2**:201-205.
15. **Dong, Y. H., A. R. Gusti, Q. Zhang, J. L. Xu, and L. H. Zhang.** 2002. Identification of quorum-quenching N-acyl homoserine lactonases from *Bacillus* species. *Appl. Environ. Microbiol.* **68**:1754-1759.
16. **Fedoroff, N., and W. Fontana.** 2002. Genetic networks: Small numbers of big molecules. *Science* **297**:1129-1131.
17. **Fenchel, T.** 2002. Microbial behavior in a heterogeneous world. *Science* **296**:1068-1071.
18. **Fiala, G., and K. O. Stetter.** 1986. *Pyrococcus furiosus* sp. nov. represents a novel genus of marine heterotrophic archaeobacteria growing optimally at 100°C. *Arch. Microbiol.* **145**:56-61.
19. **Freestone, P. P. E., R. D. Haigh, P. H. Williams, and M. Lyte.** 1999. Stimulation of bacterial growth by heat-stable, norepinephrine- induced autoinducers. *FEMS Microbiol. Lett.* **172**:53-60.

20. **Fuqua, W., S. Winans, and E. Greenberg.** 1994. Quorum sensing in bacteria: the LuxR-LuxI family of cell density response transcription regulators. *J. Bacteriol.*:269-275.
21. **Gray, K. M., and J. R. Garey.** 2001. The evolution of bacterial LuxI and LuxR quorum sensing regulators. *Microbiology-Sgm* **147**:2379-2387.
22. **Haney, P. J., J. H. Badger, G. L. Buldak, C. I. Reich, C. R. Woese, and G. J. Olsen.** 1999. Thermal adaptation analyzed by comparison of protein sequences from mesophilic and extremely thermophilic *Methanococcus* species. *P. Natl. Acad. Sci. USA* **96**:3578-3583.
23. **Havarstein, L., G. Coomaraswamy, and D. Morrison.** 1995. An unmodified heptadecapeptide pheromone induces competence for genetic transformation in *Streptococcus pneumoniae*. *P. Natl. Acad. Sci. USA* **92**:11140-11144.
24. **Henke, J. M., and B. L. Bassler.** 2004. Three parallel quorum-sensing systems regulate gene expression in *Vibrio harveyi*. *J. Bacteriol.* **186**:6902-6914.
25. **Hicks, P., K. Rinker, J. Baker, and R. Kelly.** 1998. Homomultimeric protease in the hyperthermophilic bacterium *Thermotoga maritima* has structural and amino acid sequence homology to bacteriocins in mesophilic bacteria. *FEBS Lett.* **440**:393-398.
26. **Huber, R., H. Huber, and K. O. Stetter.** 2000. Towards the ecology of hyperthermophiles: biotopes, new isolation strategies and novel metabolic properties. *FEMS Microbiol. Rev.* **24**:615-623.
27. **Huber, R., T. A. Langworthy, H. Konig, M. Thomm, C. R. Woese, U. B. Sleytr, and K. O. Stetter.** 1986. *Thermotoga maritima* sp-nov represents a new genus of unique extremely thermophilic eubacteria growing up to 90 degrees C. *Arch. Microbiol.* **144**:324-333.
28. **Joint, I., K. Tait, M. E. Callow, J. A. Callow, D. Milton, P. Williams, and M. Camara.** 2002. Cell-to-cell communication across the prokaryote-eukaryote boundary. *Science* **298**:1207.
29. **Jones, W. J., D. P. Nagle, and W. B. Whitman.** 1987. Methanogens and the diversity of archaeobacteria. *Microbiol. Rev.* **51**:135-177.
30. **Kalkum, M., G. J. Lyon, and B. T. Chait.** 2003. Detection of secreted peptides by using hypothesis-driven multistage mass spectrometry. *P. Natl. Acad. Sci. USA* **100**:2795-2800.
31. **Lazazzera, B. A., and A. D. Grossman.** 1998. The Ins and Outs of Peptide Signalling. *Trends Microbiol.* **6**:288-294.
32. **Lopez-Garcia, P., and D. Moreira.** 1999. Metabolic symbiosis at the origin of eukaryotes. *Trends Biochem. Sci.* **24**:88-93.
33. **Madigan, M., J. Martinko, and J. Parker.** 2000. *Brock Biology of Microorganisms*, 9th ed. Prentice Hall, Upper Saddle River, NJ.
34. **Margulis, L.** 1970. *Origin of Eukaryotic Cells*. Yale University Press.
35. **Martin, W., and M. Muller.** 1998. The hydrogen hypothesis for the first eukaryote. *Nature* **392**:37-41.
36. **Miller, M. B., K. Skorupski, D. H. Lenz, R. K. Taylor, and B. L. Bassler.** 2002. Parallel quorum sensing systems converge to regulate virulence in *Vibrio cholerae*. *Cell* **110**:303-314.
37. **Mukund, S., and M. W. Adams.** 1995. Glyceraldehyde-3-phosphate ferredoxin oxidoreductase, a novel tungsten-containing enzyme with a potential glycolytic role in the hyperthermophilic archaeon *Pyrococcus furiosus*. *J. Biol. Chem.* **270**:8389-8392.
38. **Muralidharan, V., K. D. Rinker, I. S. Hirsh, E. J. Bouwer, and R. M. Kelly.** 1997. Hydrogen transfer between methanogens and fermentative heterotrophs in hyperthermophilic cocultures. *Biotechnol. Bioeng.* **56**:268-278.
39. **Nelson, K. E., R. A. Clayton, S. R. Gill, M. L. Gwinn, R. J. Dodson, D. H. Haft, E. K. Hickey, L. D. Peterson, W. C. Nelson, K. A. Ketchum, L. McDonald, T. R. Utterback, J. A. Malek, K. D. Linher, M. M. Garrett, A. M. Stewart, M. D. Cotton, M. S. Pratt, C. A. Phillips, D. Richardson, J. Heidelberg, G. G. Sutton, R. D. Fleischmann, J. A. Eisen, O.**

- White, S. L., Salzberg, H. O., Smith, J. C., Venter, and C. M. Fraser.** 1999. Evidence for lateral gene transfer between Archaea and Bacteria from genome sequence of *Thermotoga maritima*. *Nature* **399**:323-329.
40. **Newman, D. K., and J. F. Banfield.** 2002. Geomicrobiology: How molecular-scale interactions underpin biogeochemical systems. *Science* **296**:1071-1077.
41. **Ouhammouch, M.** 2004. Transcriptional regulation in Archaea. *Curr. Opin. Genet. Dev.* **14**:133-138.
42. **Paggi, R. A., C. B. Martone, C. Fuqua, and R. E. De Castro.** 2003. Detection of quorum sensing signals in the haloalkaliphilic archaeon *Natronococcus occultus*. *FEMS Microbiol. Lett.* **221**:49-52.
43. **Peterson, S. N., C. K. Sung, R. Cline, and e. al.** 2004. Identification of competence pheromone responsive genes in *Streptococcus pneumoniae* by use of DNA microarrays. *Mol. Microbiol.* **in press**.
44. **Pysz, M., D. Ward, K. Shockley, C. Montero, S. Conners, M. Johnson, and R. Kelly.** 2004. Transcriptional analysis of dynamic heat-shock response by the hyperthermophilic bacterium *Thermotoga maritima*. *Extremophiles* **8**:209-217.
45. **Pysz, M. A., S. C. Conners, C. I. Montero, K. R. Shockley, M. R. Johnson, D. E. Ward, and R. M. Kelly.** 2004. Transcriptional analysis of biofilm formation in the anaerobic hyperthermophilic bacterium *Thermotoga maritima*. *Appl. Environ. Microbiol.* **70**:6098-6112.
46. **Reysenbach, A. L., and S. L. Cady.** 2001. Microbiology of ancient and modern hydrothermal systems. *Trends Microbiol.* **9**:79-86.
47. **Robb, F. T., D. L. Maeder, J. R. Brown, J. DiRuggiero, M. D. Stump, R. K. Yeh, R. B. Weiss, and D. M. Dunn.** 2001. Genomic sequence of hyperthermophile, *Pyrococcus furiosus*: implications for physiology and enzymology. *Methods Enzymol.* **330**:134-157.
48. **Schauder, S., and B. L. Bassler.** 2001. The Languages of Bacteria. *Genes Dev.* **15**:1468-1480.
49. **Schauder, S., K. Shokat, M. G. Surette, and B. L. Bassler.** 2001. The LuxS family of bacterial autoinducers: biosynthesis of a novel quorum-sensing signal molecule. *Mol. Microbiol.* **41**:463-476.
50. **Schut, G. J., S. D. Brehm, S. Datta, and M. W. Adams.** 2003. Whole-genome DNA microarray analysis of a hyperthermophile and an archaeon: *Pyrococcus furiosus* grown on carbohydrates or peptides. *J. Bacteriol.* **185**:3935-3947.
51. **Schut, G. J., J. Zhou, and M. W. Adams.** 2001. DNA microarray analysis of the hyperthermophilic archaeon *Pyrococcus furiosus*: evidence for a new type of sulfur-reducing enzyme complex. *J. Bacteriol.* **183**:7027-7036.
52. **Shapiro, J.** 1998. Thinking About Bacterial Populations as Multicellular Organisms. *Annu. Rev. Microbiol.*:81-104.
53. **Shockley, K. R., D. E. Ward, S. Chhabra, S. Conners, C. Montero, and R. Kelly.** 2003. Heat shock response by the hyperthermophilic archaeon *Pyrococcus furiosus*. *Appl. Environ. Microbiol.* **69**:2365-2371.
54. **Stevens, A., and E. Greenberg.** 1999. Transcription activation by LuxR. *In* G. W. Dunny, S.; (ed.), *Cell-Cell Signaling in Bacteria*. ASM Press, Washington, DC.
55. **Summit, M., and J. A. Baross.** 2001. A novel microbial habitat in the mid-ocean ridge seafloor. *P. Natl. Acad. Sci. USA* **98**:2158-2163.
56. **Sun, J., R. Daniel, I. Wagner-Dobler, and A. P. Zeng.** 2004. Is autoinducer-2 a universal signal for interspecies communication: a comparative genomic and phylogenetic analysis of the synthesis and signal transduction pathways. *BMC Evol. Biol.* **4**:36.

57. **Taga, M., S. T. Miller, and B. L. Bassler.** 2003. Lsr-mediated transport and processing of AI-2 in *Salmonella typhimurium*. *Mol. Microbiol.* **50**:1411-1427.
58. **Taga, M., J. Semmelhack, and B. Bassler.** 2001. The LuxS dependant autoinducer AI-2 controls the expression of an ABC transporter that functions in AI-2 uptake in *Salmonella typhimurium*. *Mol. Microbiol.* **42**:777-793.
59. **Tatusov, R., D. Natale, I. Garkavtsev, T. Tatusova, U. Shankavaram, B. Rao, B. Kiryutin, M. Galperin, N. Fedorova, and E. Koonin.** 1997. The COG database: new developments in phylogenetic classification of proteins from complete genomes. *Nucleic Acids Res.* **29**:22-28.
60. **Vendeville, A., K. Winzer, K. Heurlier, C. M. Tang, and K. R. Hardie.** 2005. Making 'sense' of metabolism: autoinducer-2, LuxS and pathogenic bacteria. *Nat. Rev. Microbiol.* **3**:383-396.
61. **Waters, E., M. J. Hohn, I. Ahel, D. E. Graham, M. D. Adams, M. Barnstead, K. Y. Beeson, L. Bibbs, R. Bolanos, M. Keller, K. Kretz, X. Lin, E. Mathur, J. Ni, M. Podar, T. Richardson, G. G. Sutton, M. Simon, D. Soll, K. O. Stetter, J. M. Short, and M. Noordewier.** 2003. The genome of *Nanoarchaeum equitans*: insights into early archaeal evolution and derived parasitism. *Proc. Natl. Acad. Sci. USA* **100**:12984-12988.
62. **Winzer, K., K. R. Hardie, and P. Williams.** 2002. Bacterial cell-to-cell communication: Sorry, can't talk now - gone to lunch! *Curr. Opin. Microbiol.* **5**:216-222.
63. **Woese, C. R.** 1998. The universal ancestor. *P. Natl. Acad. Sci. USA*:6854-6859.
64. **Yarwood, J. M., D. J. Bartels, E. M. Volper, and E. P. Greenberg.** 2004. Quorum sensing in *Staphylococcus aureus* biofilms. *J. Bacteriol.* **186**:1838-1850.

**Chapter 2: Functional Genomics-based Studies of the Microbial Ecology
of Hyperthermophilic Microorganisms**

M.R. Johnson, C.I. Montero, S.B. Connors, K.R. Shockley, M.A. Pysz, and R.M. Kelly
Department of Chemical Engineering, North Carolina State University, Raleigh, NC 27695

Published in: *Biochemical Society Transactions* (April, 2004)
32: 188-192

ABSTRACT

Although much attention has been paid to the genetic, biochemical and physiological aspects of individual hyperthermophiles, how these unique microorganisms relate to each other and to their natural habitats must be addressed in order to develop a comprehensive understanding of life at high temperatures. Phylogenetic 16S rRNA-based profiling of samples from various geothermal sites has provided insights into community structure, but this must be complemented with efforts to relate metabolic strategies to biotic and abiotic characteristics in high temperature habitats. Described here are functional genomics-based approaches, using cDNA microarrays, to gain insight into how ecological features such as biofilm formation, species interaction, and possibly even gene transfer may occur in native environments, as well as to determine what genes or sets of genes may be tied to environmental functionality.

INTRODUCTION

Microbial life as we know it depends on complex chemical, physical and biological interactions, factors that are often ignored in determining the salient metabolic and physiological features of individual microorganisms. It can be challenging enough to understand how various metabolic pathways in an individual organism affect one another, but even more so when considering the possibility that intra- and interspecies interactions and other biological/abiological factors play a significant role. However, as the post-genomic era unfurls, and a myriad of powerful functional genomic tools have become available, holistic frameworks for complex biological phenomena can be envisioned. Among the opportunities presenting themselves is the prospect of examining comprehensive transcriptional and translational response patterns in a single organism or in a microbial community to various environment-based biological and abiological stimuli. While analyses based on 16S rRNA sequences have enabled the detection of species in a particular environment [1,2,3], functional assessments must be used to understand how species interact and what role specific microorganisms play in their particular niche. Genetic systems for hyperthermophiles have yet to be developed, but genomic-based tools such as DNA microarrays offer an alternative approach for deciphering novel physiological and ecological phenomena underlying life at high temperatures [4].

MIXED SPECIES STUDIES: AN ESSENTIAL PART OF MICROBIAL ECOLOGY

It has been hypothesized that life in any niche evolves as a diverse collection of species [5] in which the sharing of genes and synergistic interactions are intrinsic features. In order to understand how species interact in a natural environment, it is important to look past the limitations of pure culture studies and instead examine how mixed populations respond to stimuli. Among the issues that need to be examined in high temperature microbial ecology are how hyperthermophiles sense their biological environment, how they interact with each other, and how they fulfill specific roles in their environment. The ways in which specific phenotypes are regulated in hyperthermophiles are not known, and this prompts a number of interesting questions concerning intra- and interspecies interactions in geothermal environments. What triggers biofilm formation [6] in hyperthermophiles and how does this relate to species interactions within the sessile consortia? What mechanisms enable interspecies transfer of metabolites and what synergistic interactions are formed to enhance such exchanges? It has been suggested through analysis of sequencing data that massive lateral gene transfer has occurred between certain hyperthermophilic species [4]. If so, to what extent is genetic material exchanged among currently extant hyperthermophiles and how does such a process proceed? If in fact evolution occurs as a diverse biological unit [5], the nature of interactions within that unit must be examined at the cellular and, ultimately, the community level. If quorum sensing [7] is used by hyperthermophiles, by what mechanisms does communication take place?

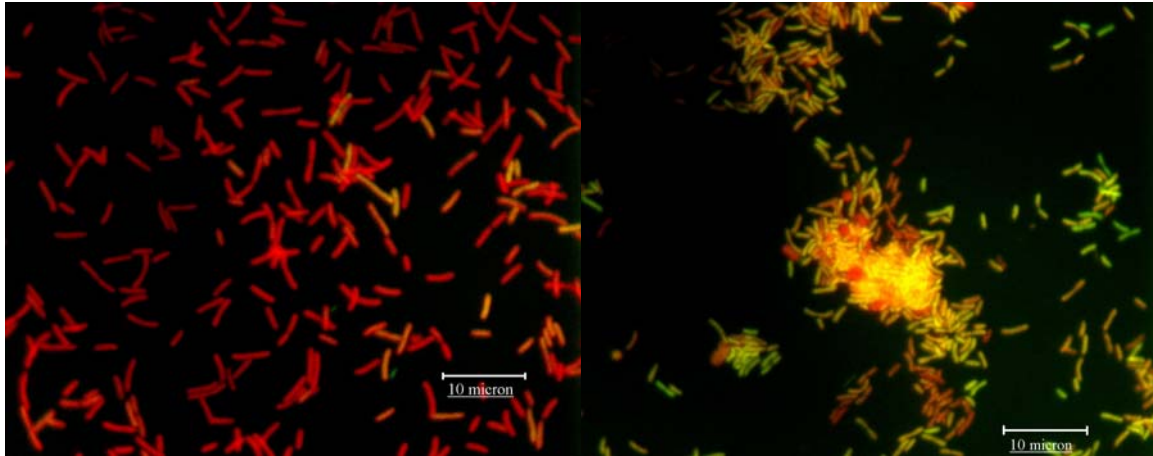


Figure 1. Epifluorescence images of *T. maritima* pure culture (left), and *T. maritima* and *M. jannaschii* coculture (right). *T. maritima* displays a rod morphology while *M. jannaschii* is the cocci bound up in the middle of the clumps.

A challenge in conducting mixed culture studies is that not all species are culturable, and relatively few species have been isolated and grown successfully under laboratory conditions. One approach is to select representative model organisms to cultivate together to begin to understand the interactions taking place. One classical example of hyperthermophilic symbiosis is the pairing of a heterotroph with a methanogen. Many hyperthermophilic heterotrophs produce hydrogen, and hyperthermophilic methanogens utilize this hydrogen as an energy source for growth [8]. Hydrogen is a potent growth inhibitor for certain hyperthermophilic heterotrophs [9], so when the two physiological types are paired together the heterotroph benefits from the abatement of growth inhibition, while the methanogen secures a supply of its limiting growth reagent [8]. This defined coculture is an initial step toward gaining an understanding of how species interact. While not a true representation of ecology in a natural setting, it enables the observation of species

interactions in a controlled environment, a necessity when utilizing molecular tools such as microarrays where cross contamination between species can be problematic. The result of such a simple pairing can be dramatic, yielding such results as a ten-fold gain in maximum cell density for the mixed species when compared to the pure culture [8], and highlighting drastic differences in global gene expression patterns (Johnson and Kelly, unpublished data). In addition, microbial interactions in hyperthermophiles are not limited to synergistic relationships. Recently, an example of the first parasitic relationship between a hyperthermophile with a genome size of only 0.5 Mb and an archaeal host has been described [10], opening up new questions as to how the species perceives the presence of the host and subsequently attaches to it.

BIOFILMS

Biofilms found in hydrothermal systems contain microorganisms that can form a matrix and adhere to a surface as a community [3]. In general, biofilms often allow cooperation among individuals and enhanced defense mechanisms [11]. However, the specific functions of biofilms in hyperthermophilic niches have yet to be understood. In the better characterized mesophiles, biofilm cells have been shown to be involved in cell-to-cell signaling, pathogenesis, communal feeding, and the formation of a complex biofilm secondary structure [12]. Many questions remain about the roles, composition and structures of hyperthermophilic biofilms as well as possible signaling processes that may contribute to their formation. While biochemical analysis can yield information about biofilm composition, it offers little insight into the pathways used to form the biofilm, or

how the biofilm is degraded or maintained. Actively growing mesophilic biofilms first develop a matrix of growing cells, then expand the colony size, and finally detach portions of the colony from the biofilm in order to form new biofilms [13, 14]. If a similar feature pattern of growth occurs in hyperthermophilic biofilms, by what methods do they detach? If the biofilm is formed with a scaffold of polysaccharides, then the gene expression pattern of the cell's hydrolase inventory could prove very interesting. This information would not only offer insight into the genes needed for biofilm sloughing, but also information on the types of chemical linkages present in the biofilm material.

Hyperthermophile-based biofilms have been observed for *P. furiosus* and *T. maritima* [15] and in co-cultures of *T. maritima* and *M. jannaschii* [16]. The use of continuous culture (chemostat) is the method of choice for the efficient and consistent growth of hyperthermophilic biofilms [17]. This method allows for the production of sufficient biofilm material for RNA extractions and has been used in microarray studies comparing planktonic versus biofilm cells in *T. maritima* cultures (Pysz and Kelly, unpublished data). Polycarbonate filters have provided a useful surface in hyperthermophilic continuous cultures for imaging biofilm growth by fluorescent microscopy, confocal laser scanning microscopy, scanning electron microscopy, and environmental scanning electron microscopy [15]. Pairing such biochemical and image-based analysis of biofilm matrix with transcriptional information offers great potential for characterizing the structures formed by a hyperthermophilic biofilm community.

GENETIC TRANSFER

With the complete genome sequences now available for a number of hyperthermophilic microorganisms, it has become clear that gene transfer has played an important part in their evolution [18]. As seen in the table below, 4-24% of genes within genomes of sequenced hyperthermophilic species are predicted to be the direct result of lateral gene transfer. The mechanism underlying these gene transfer events is unknown. Could the transfer be via pili formed by the cells to transfer DNA (conjugation), bacteriophage-mediated transduction, or transformation through direct DNA uptake? In the example of *T. maritima*, which has an astonishingly large number of predicted laterally transferred genes, no bacteriophage or conjugation-related genes have been identified from genome sequence analysis [4,19]. There is a possibility that transformation could occur via competence due to the presence of putative competence genes (*drpA*, *comM*, *comE*, *comEA*, *comFC*) similar to a type II secretion pathway and a type IV pilin-related protein, both of which are systems used in mesophiles for competence [4]. However, such a system has yet to be confirmed in a functional setting.

TABLE 1. PREDICTED LATERAL GENE TRANSFER IN HYPERTHERMOPHILES		
Species	Percent of genome predicted from LGT	Reference
<i>Aeropyrum pernix</i>	14.6	18
<i>Aquifex aeolicus</i>	4.6	18
<i>Archaeoglobus fulgidus</i>	6.6	18
<i>Methanococcus jannaschii</i>	4.2	18
<i>Methanopyrus kandleri</i>	10.6	18
<i>Pyrobaculum aerophilum</i>	11.8	18
<i>Pyrococcus abyssii</i>	6.8	18
<i>Pyrococcus furiosus</i>	6.4	18
<i>Pyrococcus horikoshii</i>	6.8	18
<i>Sulfolobus solfataricus</i>	4.9	18
<i>Sulfolobus tokodaii</i>	4.7	18
<i>Thermoanaerobacterium tengcongensis</i>	13.2	18
<i>Thermotoga maritima</i>	24	4

One way to begin to probe for the mechanisms of gene transfer in hyperthermophiles is to stress cultures and look for the induction of putative competence-related genes. Common competence inducing events such as osmotic shock, heat shock, and entrance into stationary growth phase can be examined for the ability to induce the expression of these putative competence genes. Ideally, the experiments should be conducted utilizing a large-scale cultivation approach. This methodology offers optimal control over growth conditions, and allows for the sampling of multiple time points over the course of a stimulation experiment from the same population, in essence building the statistical power of the study. In the mesophile *Streptococcus pneumoniae*, sampling many time points has proven to be important as competence-related genes are expressed within 5 minutes of stimulation, and quickly fall off to basal transcriptional levels within 15 minutes of stimulation [20].

CHALLENGES AND FUTURE WORK

When using microarrays with mixed species studies, it is necessary to minimize or prevent cross contamination of RNA from multiple species hybridizing onto the microarray designed for a single species. In the simple example of a coculture with two species, two factors exist that can help determine the significance of this problem. First is the similarity at the sequence level of one species to another. It has been suggested that at least 80% identity at the nucleotide level is needed for a DNA target to hybridize to a microarray probe [21], and it can be hypothesized that a similar stringency would exist for a cDNA:DNA hybridization, with the cDNA target representing the sequence of mRNA present in the culture. In cocultures of Archaea and Bacteria, such a high degree of identity is usually not a problem between the species due to the divergence between the kingdoms, but is a point to note when selecting species to grow in a mixed culture. A simple method of checking for cross hybridization is to pool RNA from the contaminating species grown under several conditions, produce the corresponding labeled cDNA, and test for the ability to hybridize to the array of interest. No hybridization was detected, for instance, when hybridizing *M. jannaschii* RNA against a *T. maritima* full genome cDNA microarray (Johnson and Kelly, unpublished data). The second factor to take into account is the population dynamic of the culture. In the case of *T. maritima* cocultured with *M. jannaschii*, *M. jannaschii* comprises less than 2% of the cells in the culture [8]. As such, the contamination of *M. jannaschii* RNA will have minimal effects on *T. maritima* expression data. Many times microarray results can be validated, and gene function deciphered, by eliminating a gene from an organism's genome and monitoring the resulting effect of the knockout. While genetic

systems are currently unavailable for hyperthermophiles, further efforts to establish stimuli that induce competence may lead to the development of these tools in the future.

Certainly, one area of future work is to link transcriptional data to information about actual translated and functional proteins. As tools like high throughput mass spectrometry are developed that allow for the rapid detection of all the proteins in a given sample [22], the response rate to environmental stimuli could be followed on a genome scale. It has been shown that in hyperthermophiles transcriptional response time to stimuli is very fast, and gene expression changes in response to heat shock have been shown to occur within minutes of stimulation [Pysz et al., in press]. However, little is known about how rapidly the encoded proteins can be produced, and even less about how the groups of proteins that act together (e.g. chaperones) are expressed. The ability to detect or even quantitate protein production would offer huge advantages in understanding response to stimuli, protein functionality, and feedback mechanisms in hyperthermophiles.

CONCLUSIONS

It is impossible to understand the ecology of hyperthermophilic environments without understanding how species interact and respond to environmental changes. Environmental sampling techniques (e.g., 16s rRNA sequencing) enable species identification in native environments, while pure culture studies have enabled the further characterization of individual species. However, it is important to investigate how organisms grow under conditions encountered in their natural environment to examine issues such as species interaction, stress response, and biofilm formation. DNA microarrays have enabled the

study of gene expression under a variety of conditions, and if paired with developing technologies, such as high throughput protein identification and quantification, they offer the prospect of determining the underlying functions of genes and how species thrive in extreme niches.

ACKNOWLEDGMENTS

This work was supported in part by grants from NASA, NSF and DOE. M.R. Johnson acknowledges the support of a DoEd GAANN Fellowship. S.B. Connors acknowledges the support of a NIEHS Bioinformatics Traineeship.

REFERENCES CITED

- 1 Barns, S.M., Delwiche, C. F., Palmer, J. D., Dwason, S.C., Hershberger, H. L., and Pace, N.R. (1996) *Ciba*. **202**, 24-32
- 2 Bonch-Osmolovskaya, E. A., and Stetter, K.O. (1991) *Syst. Appl. Microbiol.* **14**, 205-208
- 3 Reysenbach, A.L., and Shock, E. (2002) *Science*. **296**, 1077-1082
- 4 Nelson, K.E., Paulsen, I.T., Heidelberg, J. F., and Fraser, C. M. (2000) *Nat. Biotechnol.* **18**, 1049-1054

- 5 Woese, C. (1998) P. Natl. Acad. Sci. U.S.A. **95**, 6854-6859
- 6 O'Toole, G., Kaplan, H., and Kolter, R.. (2000) Annu. Rev. Microbiol. **54**, 49-49
- 7 Fuqua, W.S., Winans, S., and Greenberg, E., (1994). J. Bacteriol. **176**, 269-275
- 8 Muralidhuran, V., Rinker, K.D., Hirsh, I. S., Bouwer, E. J., and Kelly, R.M.. (1997)
Biotechnol. Bioeng. **56** 268-278
- 9 Huber, R., and Stetter, K.O. Method. Enzymol. (2001) **330**, 11-24
- 10 Beveridge, T. J., Makin, S.A., Kadurugamuwa, J.L. and Li, Z. (1997) FEMS Microbiol.
Rev. **20** 291-303
- 11 Costerton, J.W., Lewandowski, Z., Caldwell, D.E., Korber, D.R., and Lappin-Scott H.M.
(1995) Annu. Rev. Microbiol. **49**, 711-745
- 12 Kolter, R., and Losick R.. (1998) Science. **280**, 226-227.
- 13 Kaplan, J.B., Ragunath, C., Ramasubbu, N., and Fine, D.H. (2003) J. Bacteriol. **185**,
4693-4698

- 14 Allison, D. G., Ruiz, B., SanJose, C., Jaspe, A., and Gilbert, P. (1998). *FEMS Microbiol. Lett.* **167**, 179-184
- 15 Rinker, K.D. (1998) PhD Thesis North Carolina State University, Raleigh, NC.
- 16 Thomas, N.A., and Jarrell, K.F. (2001) *J. Bacteriol.* **183**, 7154-7164
- 17 Pysz, M.A., Rinker, K.D., Shockley, K.R., and Kelly, R.M. (2001) *Method. Enzymol.* **330**, 31-40
- 18 Campbell, A.M. (2000) *Theor. Popul. Biol.* **57**, 71-77
- 19 Nesbo, C.L., Nelson, K.E., and Doolittle, W. (2002) *J. Bacteriol.* **184**, 4475-4488
- 20 Peterson, S., Cline, R.T., Tettelin, H., Sharov, V., and Morrison, D.A. (2000) *J. Bacteriol.* **182**, 6192-6202
- 21 Wu, L.Y., Thompson, D.K., Li, G.S., Hurt, R.A., Tiedje, J.M., and Zhou, J.Z. (2001) *Appl. Environ. Microbiol.* **67**, 5780-5790
- 22 Cargile, B.J., Bundy, J.L., Grunden, A.M., and Stephenson, J.L. (2003) *Anal. Chem.* **76**, 86-97

**Chapter 3: Population density-dependent regulation of
exopolysaccharide formation in the hyperthermophilic bacterium**

Thermotoga maritima

*M.R. Johnson, C.I. Montero, S.B. Connors, K.R. Shockley, S.L. Bridger and R.M. Kelly**

Department of Chemical Engineering
North Carolina State University
Raleigh, NC 27695-7905

Published in: *Molecular Microbiology* (February, 2005)
55: 664-674

Running title: Exopolysaccharide formation in *Thermotoga maritima*

***Address correspondence to:**

Robert M. Kelly
Department of Chemical Engineering
North Carolina State University
Raleigh, NC 27695-7905

Phone: (919) 515-6396

Fax: (919) 515-3465

Email: rmkelly@eos.ncsu.edu

Abstract

Co-cultivation of the hyperthermophiles *Thermotoga maritima* and *Methanococcus jannaschii* resulted in five-fold higher *T. maritima* cell densities when compared to monoculture as well as concomitant formation of exopolysaccharide and flocculation of heterotroph-methanogen cellular aggregates. Transcriptional analysis of *T. maritima* cells from these aggregates using a whole genome cDNA microarray revealed the induction of a putative exopolysaccharide synthesis pathway, regulated by intracellular levels of cyclic di-guanosine 3',5'-(cyclic)phosphate (cyclic di-GMP) and mediated by the action of several GGDEF proteins, including a putative diguanylate cyclase (TM1163) and a putative phosphodiesterase (TM1184). Transcriptional analysis also showed that TM0504, which encodes a polypeptide containing a motif common to known peptide-signaling molecules in mesophilic bacteria, was strongly up-regulated in the co-culture. Indeed, when a synthetically produced peptide based on TM0504 was dosed into the culture at ecologically relevant levels, the production of exopolysaccharide was induced at significantly lower cell densities than was observed in cultures lacking added peptide. In addition to identifying a pathway for polysaccharide formation in *T. maritima*, these results point to the existence of peptide-based quorum sensing in hyperthermophilic bacteria and indicate that cellular communication should be considered as a component of the microbial ecology within hydrothermal habitats.

Introduction

Hyperthermophiles, or microorganisms having an optimum temperature for growth at or above 80°C, include members of both the Archaea and Bacteria (Stetter *et al.*, 1990), and are believed to be closely related to the earliest forms of life on earth (Huber *et al.*, 2000). While numerous efforts have been directed at the biochemical attributes of biomolecules produced by these organisms, relatively little is known about how hyperthermophiles function in their native environments, especially with respect to intraspecies and interspecies interactions. Given the challenges involved in assessing high temperature biotopes, especially deep seas hydrothermal vents, it is not surprising that the microbial ecology of these environments has not been investigated to any great extent (Reysenbach and Shock, 2002). However, this perspective is important to appreciate the biological basis for microbial life in extremely hot niches.

Characteristic of anaerobic high temperature environments is the biological production and consumption of molecular hydrogen (Adams, 1990). Laboratory cultures of Thermococcales and Thermotogales, the most studied hyperthermophilic fermentative heterotrophs, produce significant amounts of molecular hydrogen that can ultimately inhibit growth under accumulating conditions (Huber *et al.*, 1986). Biological methanogenesis can serve as a H₂ sink (Muralidharan *et al.*, 1997), and it is common to find heterotrophs co-localized with methanogens in natural environments. Indeed, laboratory co-culture of hyperthermophilic methanogens and hyperthermophilic fermentative anaerobes has been shown to enhance biomass yields compared to pure cultures (Bonchosmolovskaya and Stetter, 1991; Muralidharan *et al.*, 1997). This mutually beneficial relationship likely extends to natural hydrothermal environments,

given that microorganisms seldom behave in an isolated manner (Kolter and Losick, 1998). In fact, it has been suggested that multicellularity may have first arisen on Earth in the form of a symbiotic relationship between a methanogen and a heterotroph (Lopez-Garcia and Moreira, 1999; Martin and Muller, 1998). Although multicellularity has yet to be investigated in any detail in hydrothermal environments, it would seem that some form of cellular communication, now known to be widespread among mesophilic microbial taxa (Bassler, 2002), should exist. If so, questions arise about the nature of such communication and interspecies and intraspecies consequences among hyperthermophiles.

Microbial interactions in many environments are enhanced by the formation of biofilms held together or engulfed by exopolysaccharides (EPS) (Costerton, 1995). It has been observed that EPS formation is regulated several species such as *Salmonella typhimurium* and *Gluconacetobacter xylinium* by the cellular levels of cyclic di-GMP (Jenal, 2004; Tal *et al.*, 1998). In these organisms, free cyclic di-GMP binds to a cellulose synthesis complex, consisting of binding proteins and glycosyl transferases, thereby creating an activated complex capable of synthesizing EPS (Jenal, 2004). Regulation of cyclic di-GMP levels involves the opposing activity of several GGDEF-domain containing proteins (COG2199), including a diguanylate cyclase, which produces cyclic di-GMP from GTP, and a phosphodiesterase that cleaves cyclic di-GMP back to two GTP molecules (Tal *et al.*, 1998). In GGDEF domain proteins from *S. typhimurium* (Zogaj *et al.*, 2001) and *G. xylinium* (Tal *et al.*, 1998), PAS and PAC domains (SMART SM00086 and SM00091) act as sensors for light, oxygen, redox, and, perhaps, many other stimuli yet to be determined, and effect regulation through interactions with other domains

similar to that in two component systems (Zhulin and Taylor, 1997). These domains are thought to be involved in the regulation of catabolic and anabolic cyclic di-GMP levels after translation, in response to environmental stimuli (Jenal, 2004);(Chang *et al.*, 2001). The GGDEF domain, also referred to as the DUF1 domain, is believed to contain the catalytic site for cyclic di-GMP modification (Paul *et al.*, 2004). The GAF domain, found in bacterial cyclic di-GMP phosphodiesterases, is similar to a cyclic GMP binding domain in eukaryotes and may function to bind the molecule for cleavage (Sopory *et al.*, 2003).

Global regulators that induce cells to form biofilms have been studied for several mesophilic bacteria, and it has been shown that quorum sensing is often utilized to control population density-dependent biofilm development (Cvitkovitch *et al.*, 2003; Stanley and Lazazzera, 2004). However, regulation of biofilm formation processes can be highly specific to a particular microorganism's ecological niche. For example, *Pseudomonas aeruginosa* uses quorum sensing-driven biofilm formation as a defense mechanism for extended survival within a host. In fact, deletion of the homoserine lactone-based signaling system in *P. aeruginosa* yields a strain unable to produce properly structured biofilms, such that it is similar to undifferentiated planktonic cells (Davies and al., 1998). In contrast, biofilm formation in *Vibrio cholerae* is enhanced by the deletion of a functional quorum sensing system, such that signaling for this species actually helps repress biofilm formation (Hammer and Bassler, 2003). This strategy is consistent with the relatively short lifecycle of *V. cholerae* within a host's digestive tract, which promotes rapid dispersal back into the environment to re-infect another host (Hammer and Bassler, 2003).

Although it has been shown that hyperthermophiles form biofilms (LaPaglia and Hartzell, 1997; Rinker and Kelly, 2000), the pathways by which this occurs and the role that quorum sensing might play in this process have not been determined. Here, a functional genomics approach was used to determine the basis for exopolysaccharide formation and regulation by the hyperthermophilic bacterium *Thermotoga maritima* as well as to determine if quorum sensing plays a role in the population density-dependent formation of EPS.

Results and Discussion

High cell-density T. maritima and the formation of polysaccharide cellular aggregates

For hyperthermophilic fermentative anaerobes in laboratory pure cultures, such as *T. maritima*, biologically-produced H₂ is inhibitory and, ultimately, population-limiting. While this inhibition can be overcome partially by mechanically sparging the culture with inert gas, the use of a biological H₂ sink can be more effective. It was previously shown that in co-cultures of *T. maritima* and *Methanococcus jannaschii* significant enhancement of *T. maritima* maximum cell density compared to pure culture could be achieved, with a final heterotroph to methanogen ratio of 50:1 (Muralidharan *et al.*, 1997). Here, *M. jannaschii* was utilized as a means to increase the maximum cell density of *T. maritima* five-fold in order to explore the response to an increase in population density. Under such co-culture conditions, cellular aggregates containing both *T. maritima* and *M. jannaschii* formed, and a maximum cell density of over 10⁹ cells/ml was obtained.

Composition analysis of the high cell-density coculture aggregates determined that 5% of the dry mass in the aggregates was polysaccharide consisting of 91.2%

glucose, 5.2% ribose, and 2.7% mannose; the presence of alginate was not detected. Figure 1 shows the results of fluorescence microscopy on the cell aggregates stained with acridine orange (for visualization of cells) and/or Calcofluor (to detect the presence of β -linked glycan polysaccharides). Figure 1a reveals the formation of cell aggregates in the acridine orange stained co-culture. When Calcofluor was added to glutaraldehyde-fixed culture samples, both the pure and co-culture exhibited a blue fluorescence, which was more pronounced in the co-culture (Figure 1b). When both dyes were utilized simultaneously to visualize both the cells and the polysaccharide, it became apparent that the aggregates were engulfed and possibly even held together by EPS (Figure 1c). Both *T. maritima* and *M. jannaschii* were evident in the aggregates, distinguished by their rod-like and coccoid-like morphologies, respectively.

Whole genome transcriptional response of T. maritima in co-culture

Transcriptional analysis of cells isolated from the high cell density co-culture, using a whole *T. maritima* genome cDNA microarray, revealed that 420 genes (22% of the *T. maritima* genome) were differentially expressed 2-fold or more with a high level of statistical significance (experiment-wide p-value of $\alpha = 0.05$) when compared to the lower density pure culture (see Figure 2a). Figure 2b shows the contributions from various functional categories (COG) (Tatusov *et al.*, 1997) to the overall transcriptional response. Genes related to transcription and translation were substantially down-regulated in the high cell density co-culture, as were genes encoding chaperones and protein/DNA repair proteins. On the contrary, genes involved in energy production/conversion and ion and carbohydrate transport/metabolism were up-regulated at high cell density. Patterns of

gene expression reflected a more actively growing culture in the presence of the methanogen, which was borne out by the higher cell yields (see Figure 1).

In addition, several genes belonging to COG category V, “defense mechanisms,” were up-regulated in the co-culture. These include TM0765, TM0043, and TM0815, all possible multi-drug transporter subunits that could function to either remove harmful antibiotics or to export antibiotics synthesized by *T. maritima*. TM0043 was particularly interesting as it contained an N-terminal double-glycine peptidase domain (COG2274) similar to that found in *Streptococcus pneumoniae* and lactic acid bacteria. In these species, the N-terminal domain cleaves small bacteriocins and small auto-inducing peptides (quorum sensing signals) forming a mature signaling peptide or bacteriocin as the peptide is exported from the cell (Havarstein *et al.*, 1995a; Havarstein *et al.*, 1995b). No other subunits of an ABC transporter are proximate to TM0043 in the genome, and this subunit, therefore, may interact with other transporter components in distant operons to export small peptides for signaling or defense.

Proposed pathway for EPS production and regulation in T. maritima

The positive calcofluor staining of cellular aggregates and the detection of polysaccharides in the high cell density aggregates indicates the production of β -linked glucan exopolysaccharide (EPS). Previously, EPS production has been observed in *T. maritima* (Pysz *et al.*, 2004b; Rinker and Kelly, 2000), although the pathway for its production has not been determined. Transcriptional response data obtained here, in conjunction with previous studies of EPS production in mesophilic bacteria, provides the basis for a putative EPS production pathway in *T. maritima* (Figure 3). Numerous

complete or partial ABC sugar transporter cassettes were up-regulated in the high cell density culture, including TM0102-05, TM0277-79, TM0419-24, TM0594-98, and TM0810-12, presumably to import mono- or oligosaccharides. In studies with *S. typhimurium* and *G. xylinus*, it has been noted that an endoglucanase was co-expressed with the cellulose synthesis operon in EPS-producing cells (Tal *et al.*, 1998; Zogaj *et al.*, 2001). Here, both a putative *T. maritima* endoglucanase (TM1752, +2.2 fold), previously demonstrated to be induced during growth on glucomannans (Chhabra *et al.*, 2002), and a glucosidase (TM1834, +4.0 fold), with activity against both maltose and small oligosaccharides (Bibel *et al.*, 1998), were up-regulated. These glycosyl hydrolases may be involved in processing simple sugars for use in EPS production.

In the high cell density culture, seven of ten enzymes involved in glycolysis were down-regulated compared to the pure culture (Table 1), suggesting that transported sugars were not being used solely for energy metabolism. Furthermore, genes involved in producing GDP-mannose, a putative phosphomannomutase (TM0769, -1414.0 fold) and a putative mannose guanyltransferase (TM1033, -4.5 fold), were down-regulated at high cell densities along with genes possibly involved in making mannose based compatible solutes (mannosyl phosphoglycerate synthase [TM0756, -3.0 fold], mannosyl phosphoglycerate phosphatase [TM0171, -1.4 fold]). The first enzyme in the GDP mannose pathway, mannose 6-P isomerase (TM0736, +1.7 fold), was up-regulated slightly during growth at high cell densities. However, this enzyme catalyses the only reversible reaction in the pathway and may allow for the conversion of the first intermediate back to phosphorylated fructose, where it can be utilized for a variety of purposes including glycolysis or exopolysaccharide formation. In addition the first

enzyme in the pathway for the compatible solute di-myo-inositol-1,1-phosphate (DIP), myo-inositol-1-phosphate synthase (TM1419, -3.0 fold), was also down-regulated in the high cell density culture, while a putative myo-inositol degradation pathway encoded by the ORFs TM0414, TM0416, TM0419, and TM0420 was induced in the high cell density co-culture.

In light of apparent intracellular accumulation of carbohydrates, along with the corresponding decrease in glycolysis and compatible solute formation, it is plausible that free sugars are utilized for EPS production. Of the *T. maritima* glycosyl transferase inventory, as defined by the CAZY carbohydrate active enzyme database (Coutinho and Henrissat, 1999), five glycosyl transferases were found to be up-regulated in the high cell density culture. The first three proteins, TM0624 (+2.6 fold), TM0627 (+3.4 fold), and TM0628 (+1.6 fold) are family four glycosyl transferases with putative activity for utilizing a variety of sugars to form saccharide-based polymers. The fourth protein is TM0767 (+9.0 fold), a characterized glycosyl transferase, which contains both active sites for degrading starches and for forming glucan polymers from oligosaccharides created by the hydrolytic activity (Meissner and Liebl, 1998). In addition, TM0818 (+2.0 fold), has putative activity for forming β -1,4-linked mannan from GDP mannose. Since the synthesis pathway for GDP mannose and mannosyl glycerate are both down-regulated, this may allow *T. maritima* to scavenge any remaining GDP mannose for use in EPS production.

In known EPS producers, such as *G. xylinum* and *S. typhimurium*, the production of EPS not only relies upon the expression of glycosyl transferases, but also on the presence of cyclic di-GMP (Tal *et al.*, 1998; Zogaj *et al.*, 2001). As explained above, the

concentration of cyclic di-GMP depends upon the opposing activities of a cyclase and phosphodiesterase that both contain a GGDEF domain. To investigate possible GGDEF-domain proteins in *T. maritima*, amino acid sequences for the characterized *G. xylinum* cyclic di-GMP cyclase (accession number O87374) and phosphodiesterase (O87373) were dissected into individual domains using the SMART database (Letunic *et al.*, 2004) (Figure 4). Both proteins contain PAS and PAC sensor domains, and DUF1 and DUF2 domains, while the phosphodiesterase also contains a GAF domain. When comparing the ten GGDEF containing proteins in *T. maritima* to GGDEF proteins in *G. xylinum* using the SMART database, it was found that three of the *T. maritima* proteins contained multiple domains similar to ones found in the adenylate cyclase and phosphodiesterase of *G. xylinum*. Aligning separate sections of the *T. maritima* GGDEF proteins against the characterized *G. xylinum* diguanylate cyclase and cyclic di-GMP phosphodiesterase using the alignment tool T-Coffee (<http://www.ch.embnet.org/software/TCoffee.html>) yielded two matches. The first, TM1163, contained a mixed ordering of domains when compared to the diguanylate cyclase in *G. xylinum* (O87374), with the DUF1 and DUF2 domains switched in orientation compared to O87374, a phenomena often seen in GGDEF domain proteins (Jenal, 2004). A putative PAS-PAC domain was found in residues 1-106, followed by the putative DUF2 (residues 134-325) and DUF1 (residues 326-490) domains. The second protein, TM1184, displayed the same ordering of domains when compared to the cyclic di-GMP phosphodiesterase in *G. xylinum* (O87373): the PAS-PAC domain followed by the GAF and DUF1 domains, with the DUF2 domain of unknown function not being identified. Expression data for these two genes indicated a slight up-regulation for the putative diguanylate cyclase TM1163 (+1.7 fold) and a down-

regulation for the putative cyclic di-GMP phosphodiesterase TM1184 (-2.6 fold) in the high cell density culture.

The third GGDEF protein, TM1788, has a high degree of similarity (61% similarity over 50% of the sequence) to the cyclic di-GMP binding regulatory protein AdrA in *S. typhimurium* (Zogaj *et al.*, 2001), and was up-regulated 4.2 fold in the high cell density co-culture. AdrA has been found to co-purify with glycosyl transferases in *S. typhimurium*, be capable of producing cyclic di-GMP (Simm *et al.*, 2004), and *adrA* mutants have been both shown to be deficient in extracellular matrix production (Romling *et al.*, 2000). Finally, TM1788 contains a putative signal peptide as identified in SMART, suggesting a membrane or extracellular localization.

While there are two species present in this high density co-culture, it is likely that *T. maritima* plays the primary role in the formation of EPS. Not only does *T. maritima* greatly outnumber *M. jannaschii* in the co-culture (95% of the cells are *T. maritima*), but it also has a far greater number of carbohydrate active enzymes (Chhabra *et al.*, 2003). The identifiable carbohydrate active enzymes in the *M. jannaschii* genome are related to glycogen production and degradation for energy storage (Coutinho and Henrissat, 1999).

Evidence for cell-to-cell communication

In light of the fact EPS formation was observed at high cell densities, the possibility of quorum sensing playing a role in this process was considered. To date, three types of signaling mechanisms have been identified in bacteria (Bassler, 2002). Although acyl homoserine lactone (AHL)-based signaling is prevalent in gram-negative bacteria, within which *T. maritima* appears to group (Huber *et al.*, 1986), AHL signals are not

thermostable (Surette and Bassler, 1998) and are, therefore, unlikely to be important in high temperature biotopes. While the cross-species quorum sensing molecule, AI-2, is known to act as a signal both within and between gram-positive and gram-negative bacteria (Schauder *et al.*, 2001), the *luxS* gene that is necessary for production of AI-2 is not evident in either the *T. maritima* or *M. jannaschii* genomes.

Peptide-based signaling has been, to this point, restricted to gram-positive bacteria. Peptide signaling involves species-specific small peptides, usually under 40 amino acids (Lazazzera and Grossman, 1998), the production of which can be cell-density dependent (Bassler, 2002). The inherent thermostability of small peptides makes them more likely candidates for signaling processes in hydrothermal environments. In the high cell density co-culture, a gene encoding a polypeptide of 43 amino acids (TM0504) was up-regulated +13-fold compared to the lower density pure culture. Located immediately upstream of this gene in the *T. maritima* genome are the permeases (TM0503, TM0502) and ATP-binding subunits (TM0501, TM0500) comprising an oligopeptide ATP-binding cassette (ABC) transporter (see Figure 5B); anti-microbial peptide transporter domains exist in both TM0500 and TM0501 (COG4167 and 4170). Since a periplasmic-binding protein is missing from this operon, this cluster of genes may function to export a small peptide derived from the protein product of TM0504. In addition, TM0504 contains a GG motif (Figure 5A), similar to the cleavage point for the active form of auto-inducing peptides found in *S. pneumoniae* and lactic acid bacteria (Havarstein *et al.*, 1995a).

Because a genetic system for *T. maritima* is not available to construct knockout mutants lacking TM0504, the function of the corresponding polypeptide was examined

directly by adding a truncated version (consisting of 28 amino acids following the second GG motif) to a pure culture of *T. maritima*. When the predicted mature peptide from TM0504 was dosed into the pure culture during early log phase, EPS production was noted within 30 minutes while no EPS formation was noted at this point without peptide addition (Figure 6). Transcriptional analysis revealed that genes in an operon containing putative family 4 glycosyl transferases were up-regulated in the pure culture 30 minutes after peptide dosing, some of which were found to respond in a similar way in the high density co-culture (see Figure 7). Variations in gene expression observed between the pure and co-culture likely reflect the complexity of the signaling process and other factors related to growth conditions (e.g., 5- to 10-fold different cell densities, presence of methanogen). It was interesting that no significant transcriptional changes were noted 10 minutes after peptide dosing into the pure culture (unpublished data), suggesting that a period of time is required for peptide uptake and response.

Summary

Co-cultivation of *T. maritima* with a hyperthermophilic methanogen generated high cell densities of the heterotroph, concomitant with EPS production, apparently regulated by several GGDEF domain proteins in conjunction with a quorum sensing peptide TM0504. Pathways for carbohydrate acquisition and processing to EPS were identified in *T. maritima* from differential gene expression data, using information available for such systems in mesophilic bacteria. In the co-culture condition, the proposed mechanism for EPS synthesis is proposed to begin with simple sugars that are made available through

the concerted action of hydrolases and ABC transporters. Glycolysis and compatible solute pathways were down-regulated, presumably enabling sugars to be shuttled toward the production of EPS. Though it is not clear what regulates GGDEF protein expression in *T. maritima*, or for that matter in other bacteria, stimulation of EPS production in the presence of the signaling peptide indicates that a quorum sensing mechanism is in place and operational in *T. maritima*. This is the first such indication that these processes occur in hydrothermal environments and raises the prospect that other hyperthermophiles rely on quorum sensing as a component of their ecological strategy.

Experimental procedures

Bacterial strains, growth, and handling

T. maritima strain MSB8 and *M. jannaschii* strain DSM2661 were grown at 80°C in BSMII media in a 100% N₂ atmosphere (pure culture) or in 80% H₂/20% CO₂ pressurized to 2 bar, respectively. BSMII media contained 40 g/l sea salts, 5 g/l tryptone, 3 g/l yeast extract, 3 g/l maltose, 3 g/l Piperazine-1,4-bis(2-ethanesulfonic acid) (PIPES), 0.5 mg/l NaSeO₃•5H₂O, 0.5 mg/l NiCl₂•6H₂O, 0.25 g/l NH₄Cl, 10 mg/l Fe(NH₄)₂(SO₄)₂•6H₂O, 1.25 g/l sodium acetate anhydrate, 1 ml/l 1% Resazurin, and 10 ml/l Wolfe's trace elements and 10 ml/l Wolfe's trace vitamins solution (all Sigma Aldrich, Wolfe's solutions ATCC). The medium was adjusted to pH 7.0, autoclaved for sterility, and stored at 4 °C until use. For microarray comparisons of pure and co-culture growth, 400 ml of media were dispensed into a glass jar (Corning, Corning, NY) and heated to 80°C with the jar sealed with a rubber septum. The medium was then sparged

with the appropriate gas as described above for 60 sec and reduced with 4 ml of a 10% sodium sulfide / 10% L-cysteine/HCl solution (Sigma-Aldrich) at pH 8.0. All cultures were inoculated (1%) after addition of reducing agent with log phase cells. Cultures were agitated at 100 rpm in an oil bath at 80°C. For the co-culture, *T. maritima* and *M. jannaschii* were inoculated together under an initial atmosphere of 80% H₂ / 20% CO₂ pressurized at 2 bar. For the comparison of pure and co-culture, the cells were grown in duplicate and harvested at mid-log phase.

To test the effect of the putative signaling peptide, the predicted mature region of TM0504 (PWASPSAARV FALGRDLPRAGCPLPQPS) was synthesized (University of Georgia Synthesis and Sequencing Facility). A pure culture of *T. maritima* was grown in a 2-liter working volume fermenter (Applikon) that was stirred using an impellor at 350 RPM, sparged with nitrogen at 150 ml/min, and controlled at a temperature set point of 80 °C. After inoculating with a 1% inoculum, the culture was grown to early log phase, and dosed with the synthetic peptide to a final concentration of 5 mg/L. Samples for microarray analysis were taken before dosing, and at 10 minutes and 30 minutes after dosing. Calcofluor staining confirmed the presence of polysaccharide after 30 minutes as shown in figure six.

Fluorescence microscopy

Cells were enumerated by fixing culture samples with glutaraldehyde (Sigma Chemical, 0.25% final concentration), vortexing to break up cell aggregates, then adding fixed culture samples to 5 ml of 0.05% acridine orange (Sigma), filtering onto 0.2 micron polycarbonate filter membranes (Osmonics), and counted using an eyepiece grid (Nikon).

For detection of polysaccharide, 3 ml of 0.05% Calcofluor (fluorescent whitener 28, Sigma) was added to 0.2 ml of glutaraldehyde fixed cells and filtered onto a polycarbonate filter, as explained above. For visualizing cells and polysaccharides, 100 μ L of 1% acridine orange were added to Calcofluor-stained fixed cells and filtered. For visualization, an epifluorescence microscope was utilized (Nikon) with the appropriate filter sets (Southern Micro Instruments, Marietta GA). Images were captured using the Spot system (Diagnostic Instruments Inc.).

Microarray protocols

A *T. maritima* cDNA microarray was constructed and utilized using methodologies discussed previously (Chhabra *et al.*, 2003). Briefly, PCR products representing over 99% of the open reading frames in the sequenced genome (1928 ORFs) were generated and printed onto UltraGAPS microarray slides (Corning) with six replicates of each gene per slide using a Qarray mini printer (Genetix), with PCR products suspended in 50% Dimethyl sulfoxide. For RNA extraction, 400 ml of culture were harvested and cooled rapidly to 0°C by immersing the jars in ice water and then immediately centrifuging the cells at 13,000 x g for 20 min at 4°C. cDNA was generated from the extracted RNA and labeled using the amino-allyl method discussed previously (Chhabra *et al.*, 2003). Hybridizations were carried out for 18 hours and hybridized slides were scanned on a PerkinElmer ExpressLite Scanner (Perkin Elmer) and quantitated using ScanArray (Perkin Elmer). The data analysis was completed as discussed previously (Pysz *et al.*, 2004a), utilizing the Bonferroni correction ($\alpha = 0.05$) to account for multiple testing (Wolfinger *et al.*, 2001). Unless otherwise noted, gene annotation is from the COG

database at NCBI (Tatusov *et al.*, 1997), and was identified using the Conserved Domain Database at NCBI (Marchler-Bauer *et al.*, 2003).

As a precaution, RNA from *M. jannaschii* was tested for cross hybridization by utilizing the protocols explained above and hybridizing labeled *M. jannaschii* cDNA samples to the *T. maritima* microarray. No hybridization was detected on the scanned slides. In addition, a genome sequence comparison was made between *M. jannaschii* and *T. maritima* searching for sequence homology. It has been suggested that an 80% identity at the nucleotide level will lead to cross hybridization of a contaminating gene against a designated probe (Wu *et al.*, 2001). Utilizing the Comprehensive Microbial Resource developed by the Institute for Genomic Research (TIGR), it was determined that at the 80% identity level no cross hybridization should occur between *M. jannaschii* and *T. maritima* (Peterson *et al.*, 2001).

Exopolysaccharide Analysis

Exopolysaccharide analysis was performed by growing two 400 ml cultures containing co-cultures to late log phase as described above. The cultures were centrifuged and the resulting pellet was resuspended in 1 liter of 40 g/l sea salts (Sigma-Aldrich) and centrifuged. The sea salts wash was repeated once more and the resulting pellet was resuspended in 10 ml of water and loaded into a 10 kDa dialysis cartridge (Pierce) and dialyzed against 4 liters of deionized water overnight at 4 °C. After 24 hours the water was exchanged with fresh water and the sample was dialyzed again overnight. The resulting desalted sample was frozen and analyzed for monosaccharide content by the Complex Carbohydrate Research Center at the University of Georgia.

Acknowledgments

This work was supported in part by grants from the NASA Exobiology, DOE Energy Biosciences, and NSF Biotechnology Programs. MRJ acknowledges support from a Department of Education GAANN Fellowship and SBC acknowledges support from an NIEHS Bioinformatics Traineeship. Assistance from J.R. Brown and C. Jellis, Department of Microbiology, NCSU, with cultivation of *M. jannaschii* is also appreciated.

References Cited

- Adams, M.W.W. (1990) The metabolism of hydrogen by extremely thermophilic, sulfur-dependent archaeobacteria. *FEMS Microbiol. Rev.* **75**: 219-238.
- Bassler, B.L. (2002) Small talk: Cell-to-cell communication in bacteria. *Cell* **109**: 421-424.
- Bibel, M., Brettl, C., Gossler, U., Kriegshauser, G., and Liebl, W. (1998) Isolation and analysis of genes for amylolytic enzymes of the hyperthermophilic bacterium *Thermotoga maritima*. *FEMS Microbiol. Lett.* **158**: 9-15.
- Bonchosmolovskaya, E.A., and Stetter, K.O. (1991) Interspecies hydrogen transfer in cocultures of thermophilic Archaea. *Syst. Appl. Microbiol.* **14**: 205-208.
- Chang, A., Tuckerman, J., Gonzalez, G., Mayer, R., Weinhouse, H., Volman, G., Amikam, D., Benziman, M., and Gilles-Gonzalez, M. (2001) Phosphodiesterase A1, a regulator of cellulose synthesis in *Acetobacter xylinum*, is a heme-based sensor. *Biochemistry* **40**: 3420-3426.
- Chhabra, S., Shockley, K., Ward, D., and Kelly, R. (2002) Regulation of endo-acting glycosyl hydrolases in the hyperthermophilic bacterium *Thermotoga maritima* grown on glucan- and mannan-based polysaccharides. *Appl. Environ. Microbiol.* **68**: 545-554.
- Chhabra, S., Shockley, K.R., Conners, S., Scott, K., Wolfinger, R., and Kelly, R. (2003) Carbohydrate induced differential gene expression patterns in the hyperthermophilic bacterium *Thermotoga maritima*. *J. Biol. Chem.* **278**: 7540-7552.
- Costerton, J.W. (1995) Overview of Microbial Biofilms. *J. Indust. Microbiol.* **15**: 137-140.
- Coutinho, P.M., and Henrissat, B. (1999) Carbohydrate-active enzymes: an integrated database approach. *Recent Advances in Carbohydrate Bioengineering* The Royal Society of Chemistry, Cambridge: 3-12.
- Cvitkovitch, D.G., Li, Y.-h., and Ellen, R.P. (2003) Quorum sensing and biofilm formation in *streptococcal* infections. *J. Clin. Invest.* **112**: 1626-1632.
- Davies, D.G., and al., e. (1998) The involvement of cell-to-cell signals in the development of a bacterial biofilm. *Science*: 295-298.
- Dewey, T., and Hammes, G. (1980) Calculation on fluorescence resonance energy transfer on surfaces. *Biophys. J.* **32**: 1023-1035.
- Hammer, B.K., and Bassler, B. (2003) Quorum sensing controls biofilm formation in *Vibrio cholerae*. *Mol. Microbiol.* **50**: 101-114.
- Havarstein, L., Coomaraswamy, G., and Morrison, D. (1995a) An unmodified heptadecapeptide pheromone induces competence for genetic transformation in *Streptococcus pneumoniae*. *P. Natl. Acad. Sci. USA* **92**: 11140-11144.
- Havarstein, L., Diep, D., and Nes, I. (1995b) A family of bacteriocin ABC transporters carry out proteolytic processing of their substrates concomitant with export. *Mol. Microbiol.* **16**: 229-240.
- Huber, R., Langworthy, T.A., Konig, H., Thomm, M., Woese, C.R., Sleytr, U.B., and Stetter, K.O. (1986) *Thermotoga maritima* sp-nov represents a new genus of

- unique extremely thermophilic eubacteria growing up to 90 degrees C. *Arch. Microbiol.* **144**: 324-333.
- Huber, R., Huber, H., and Stetter, K.O. (2000) Towards the ecology of hyperthermophiles: biotopes, new isolation strategies and novel metabolic properties. *FEMS Microbiol. Rev.* **24**: 615-623.
- Jenal, U. (2004) Cyclic di-guanosine-monophosphate comes of age: a novel secondary messenger involved in modulating cell surface structures in bacteria. *Curr. Opin. Microbiol.* in press.
- Kolter, R., and Losick, R. (1998) One for All and All for One. *Science*: 226-227.
- LaPaglia, C., and Hartzell, P.L. (1997) Stress-induced production of biofilm in the hyperthermophile *Archaeoglobus fulgidus*. *Appl. Environ. Microbiol.* **63**: 3158-3163.
- Lazazzera, B.A., and Grossman, A.D. (1998) The Ins and Outs of Peptide Signalling. *Trends Microbiol.* **6**: 288-294.
- Letunic, I., Copley, R., Schmidt, S., Ciccarelli, F., Doerks, T., Schultz, J., Ponting, C., and Bork, P. (2004) SMART 4.0: towards genomic data integration. *Nucleic Acids Res.* **32**: D142-D144.
- Lopez-Garcia, P., and Moreira, D. (1999) Metabolic symbiosis at the origin of eukaryotes. *Trends Biochem. Sci.* **24**: 88-93.
- Marchler-Bauer, A., Anderson, J., DeWeese-Scott, C., Fedorova, N., Geer, L., He, S., Hurwitz, D., Jackson, J., Jacobs, A., Lanczycki, C., Liebert, C., Liu, C., Madej, T., Marchler, G., Mazumder, R., Nikolskaya, A., Panchenko, A., Rao, B., Shoemaker, B., Simonyan, V., Song, J., Thiessen, P., Vasudevan, S., Wang, Y., Yamashita, R., Yin, J., and Bryant, S. (2003) CDD: a curated Entrez database of conserved domain alignments. *Nucleic Acids Res.* **31**: 383-387.
- Martin, W., and Muller, M. (1998) The hydrogen hypothesis for the first eukaryote. *Nature*: 37-41.
- Meissner, H., and Liebl, W. (1998) *Thermotoga maritima* maltosyltransferase, a novel type of matlodextrin glycosyltransferase acting on starch and malto-oligosaccharides. *Eur. J. Biochem.* **250**: 1050-1058.
- Muralidharan, V., Rinker, K.D., Hirsh, I.S., Bouwer, E.J., and Kelly, R.M. (1997) Hydrogen transfer between methanogens and fermentative heterotrophs in hyperthermophilic cocultures. *Biotechnol. Bioeng.* **56**: 268-278.
- Paul, R., Weiser, S., Amiot, N., Chan, C., Schirmer, T., Giese, B., and Jenal, U. (2004) Cell cycle-dependent dynamic localization of a bacterial response regulator with a novel di-guanylate cyclase output domain. *Genes Dev.* **18**: 715-727.
- Peterson, J., Umayam, L., Dickinson, T., Hickey, E.K., and White, O. (2001) The comprehensive microbial resource. *Nucleic Acids Res.* **29**: 123-125.
- Pysz, M., Ward, D., Shockley, K., Montero, C., Conners, S., Johnson, M., and Kelly, R. (2004a) Transcriptional analysis of dynamic heat-shock response by the hyperthermophilic bacterium *Thermotoga maritima*. *Extremophiles* **8**: 209-217.
- Pysz, M.A., Conners, S.C., Montero, C.I., Shockley, K.R., Johnson, M.R., Ward, D.E., and Kelly, R.M. (2004b) Transcriptional analysis of biofilm formation in the anaerobic hyperthermophilic bacterium *Thermotoga maritima*. *Appl. Environ. Microbiol.* **70**: in press.

- Reysenbach, A.L., and Shock, E. (2002) Merging genomes with geochemistry in hydrothermal ecosystems. *Science* **296**: 1077-1082.
- Rinker, K.D., and Kelly, R.M. (2000) Effect of carbon and nitrogen sources on growth dynamics and exopolysaccharide production for the hyperthermophilic archaeon *Thermococcus litoralis* and bacterium *Thermotoga maritima*. *Biotechnol. Bioeng.* **69**: 537-547.
- Romling, U., Rohde, M., Olsen, A., Normark, S., and Reinkoster, J. (2000) AgfD, the checkpoint of multicellular and aggressive behavior in *Salmonella typhimurium* regulates at least two independent pathways. *Mol. Microbiol.* **36**: 10-23.
- Schauder, S., Shokat, K., Surette, M.G., and Bassler, B.L. (2001) The LuxS family of bacterial autoinducers: biosynthesis of a novel quorum-sensing signal molecule. *Mol. Microbiol.* **41**: 463-476.
- Simm, R., Morr, M., Kader, A., Nimtz, M., and Römling, U. (2004) GGDEF and EAL domains inversely regulate cyclic di-GMP levels and transition from sessility to motility. *Mol. Microbiol.* **53**: 1123-1134.
- Sopory, S., Balaji, S., Srinivasan, N., and Visweswariah, S. (2003) Modeling and mutational analysis of the GAF domain of the cGMP-binding, cGMP-specific phosphodiesterase, PDE5. *FEBS Lett.* **539**: 161-166.
- Stanley, N., and Lazazzera, B.A. (2004) Environmental signals and regulatory pathways that influence biofilm formation. *Mol. Microbiol.* **52**: 917-924.
- Stetter, K.O., Fiala, G., Huber, G., and Seegerer, A. (1990) Hyperthermophilic microorganisms. *FEMS Microbiol. Rev.*: 117-124.
- Surette, M.G., and Bassler, B. (1998) Quorum sensing in *Escherichia coli* and *Salmonella typhimurium*. *P. Natl. Acad. Sci. USA* **95**: 7046-7050.
- Tal, R., Wong, H.C., Calhoon, R., Gelfand, D., Fear, A.L., Volman, G., Mayer, R., Ross, P., Amikam, D., Weinhouse, H., Cohen, A., Sapir, S., Ohana, P., and Benziman, M. (1998) Three *cdg* operons control cellular turnover of cyclic di-GMP in *Acetobacter xylinum*: Genetic organization and occurrence of conserved domains in isoenzymes. *J. Bacteriol.* **180**: 4416-4425.
- Tatusov, R., Natale, D., Garkavtsev, I., Tatusova, T., Shankavaram, U., Rao, B., Kiryutin, B., Galperin, M., Fedorova, N., and Koonin, E. (1997) The COG database: new developments in phylogenetic classification of proteins from complete genomes. *Nucleic Acids Res.* **29**: 22-28.
- Wolfinger, R., Gibson, G., Wolfinger, E., Bennet, L., Hamadeh, H., Bushel, P., Afshari, C., and Paules, R. (2001) Assessing gene significance from cDNA microarray expression data via mixed models. *J. Comp. Biol.* **8**: 625-637.
- Wu, L.Y., Thompson, D.K., Li, G.S., Hurt, R.A., Tiedje, J.M., and Zhou, J.Z. (2001) Development and evaluation of functional gene arrays for detection of selected genes in the environment. *Appl. Environ. Microbiol.* **67**: 5780-5790.
- Zhulin, I., and Taylor, B. (1997) PAS domain S-boxes in archaea, bacteria and sensors for oxygen and redox. *Protein Sequence Motif* **22**: 331-333.
- Zogaj, X., Nimtz, M., Rohde, M., Bokranz, W., and Romling, U. (2001) The multicellular morphotypes of *Salmonella typhimurium* and *Escherichia coli* produce cellulose as the second component of the extracellular matrix. *Mol. Microbiol.* **39**: 1452-1463.

TABLE 1. Differential expression of genes in the co-culture, shown in Figure 2. Annotations are based on information from the CAZY database for the carbohydrate active enzymes, or from the COG database.

Role	Gene ID	Name	Fold Change Co- vs. Mono-culture
Maltose Transport	TM1838	ABC Permease	2.6
	TM1839	ABC ATP Binding Protein	5.5
Sugar Transport	TM0102	ABC Periplasmic Binding Protein	2.6
	TM0103	ABC ATP Binding Protein	1.4
	TM0104	ABC Permease	2.0
	TM0105	ABC Permease	3.0
	TM0277	ABC Periplasmic Binding Protein	3.3
	TM0278	ABC Permease	3.3
	TM0279	ABC Permease	3.1
	TM0419	ABC Permease	2.3
	TM0420	ABC Permease	2.8
	TM0421	ABC ATP Binding Protein	1.0
	TM0424	ABC Permease	1.5
	TM0594	ABC Permease	2.7
	TM0595	ABC Binding Protein	3.2
	TM0596	ABC Permease	2.6
	TM0597	ABC Permease	2.7
	TM0598	ABC Permease	2.7
	TM0810	ABC Binding Protein	2.1
TM0811	ABC Permease	2.8	
TM0812	ABC Permease	2.6	
Sugar Catabolism	TM1752	Endoglucanase	2.2
	TM1834	alpha Glucosidase	4.0
Glycolysis	TM0208	Pyruvate Kinase	-17.8
	TM0209	Phosphofructokinase	-4.7
	TM0273	Fructose Bisphosphate Aldolase	-4.4
	TM0688	Glyceraldehyde 3-P Dehydrogenase	-5.0
	TM0689	3-Phosphoglycerate Kinase	-7.0
	TM0877	Enolase	-2.9
	TM1469	Glucokinase	-2.2
Myo Inositol Metabolism	TM0414	Myo Inositol Dehydrogenase	2.7
	TM0416	Sugar Phosphate Isomerase	2.3

	TM0417	ABC Permease	1.5
	TM0419	ABC Permease	2.3
	TM0420	ABC Permease	2.8
	TM1419	Myo Inositol Synthase	-3.0
Mannosyl Glycerate Synthesis	TM0171	mannosyl phosphoglycerate phosphatase	-1.4
	TM0736	Phosphomannose isomerase	1.7
	TM0756	mannosyl phosphoglycerate synthase	-3.0
	TM0769	Phosphomannomutase	-1400
	TM1033	Mannose 1-P guanylyltransferase	-4.5
Exopolysaccharide Synthesis	TM0054	Cellulose Binding Protein	3.0
	TM0624	Glucomannan Glycosyltransferase	2.6
	TM0627	Glycosyltransferase	3.4
	TM0628	Glycosyltransferase	1.6
	TM0767	Glucose Glycosyltransferase	9.0
	TM0818	Mannan Glycosyltransferase	2.0
Cyclic di-GMP Regulation	TM1163	Diguanylate Cyclase	1.7
	TM1184	Cyclic di-GMP Phosphodiesterase	-2.6
	TM1788	AdrA Regulator	4.2

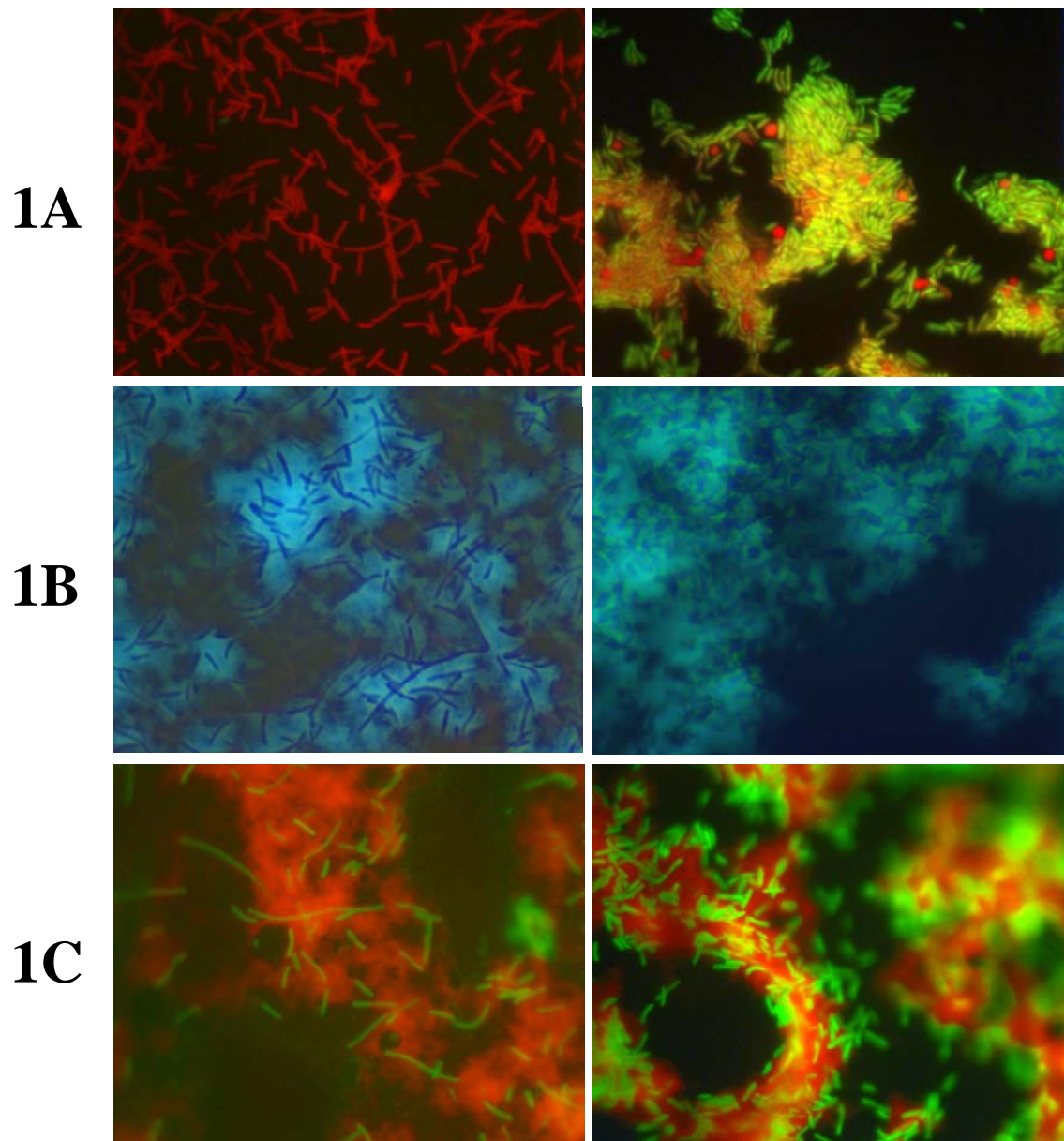


Figure 1. Mono- (*T. maritima*)- (left hand panels) and co-culture (*T. maritima*/*M. jannaschii*) (right hand panels) samples stained with Acridine Orange (1A), Calcofluor (1B), and both dyes (1C). The red staining of the matrix when both acridine orange and calcofluor are present in the stained sample is most likely explained by Fluorescence Resonance Energy Transfer (Dewey and Hammes, 1980); Calcofluor absorbs light in the UV range and emits at a maximum wavelength of 435 nm while Acridine Orange absorbs light in both the UV range but also in the range of 400-500 nm.

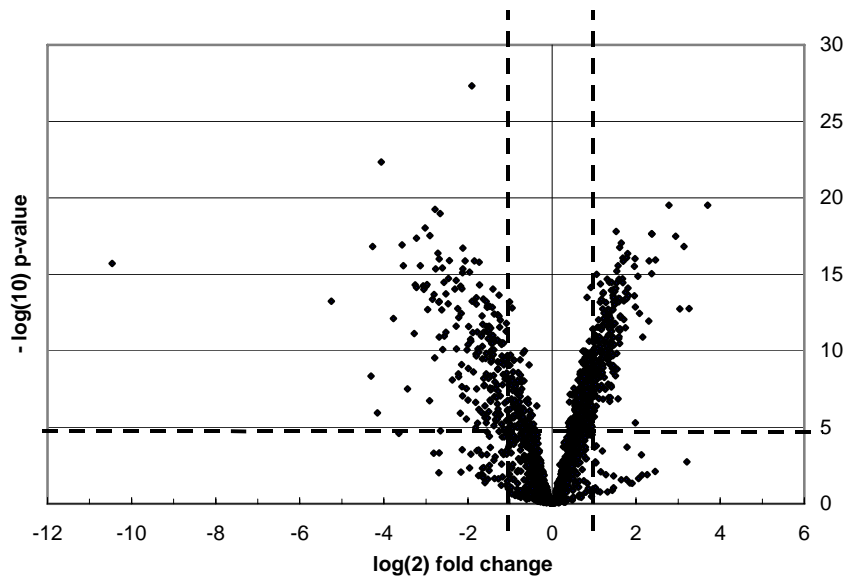
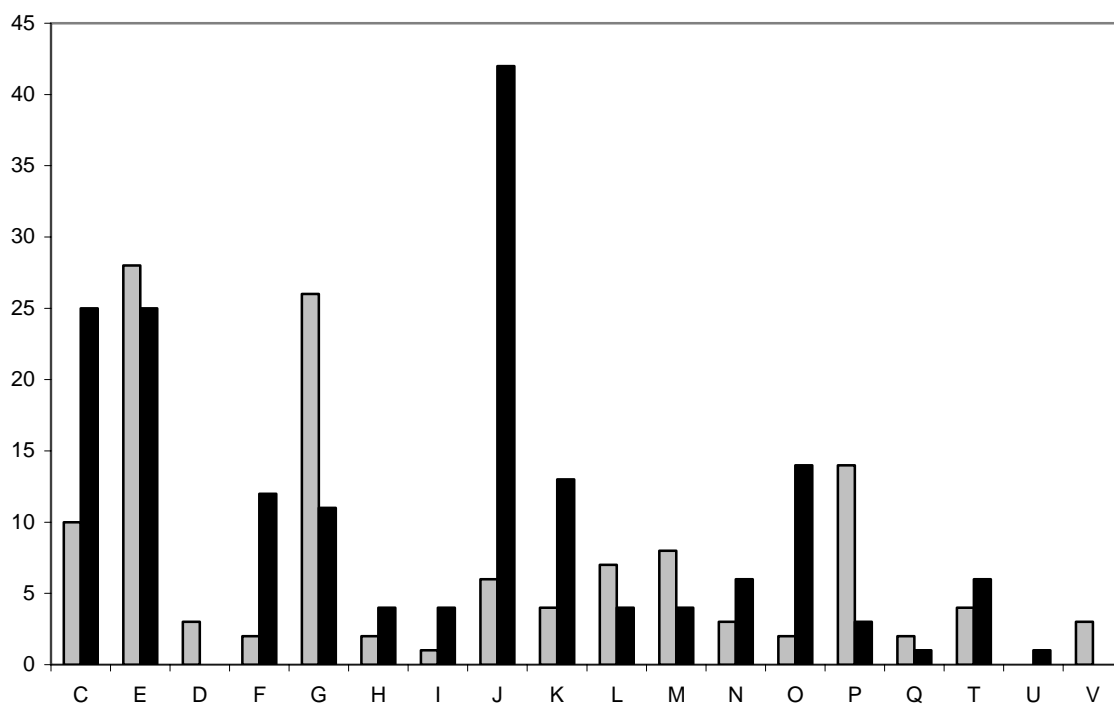


Figure 2A. The log₂ fold change in gene expression between the pure culture and the co-culture. A positive fold change indicates an up-regulation of genes in the co-culture compared to the pure culture. The vertical axis represents the statistical significance of the change in terms of $-\log_{10}$ p-value. The vertical dashed lines represent a 2-fold change. The horizontal dashed lines represent the Bonferroni correction for this experiment.



C	energy production and conversion
E	amino acid transport and metabolism
D	cell division
F	nucleotide transport and metabolism
G	carbohydrate transport and metabolism
H	coenzyme metabolism
I	lipid metabolism
J	translation
K	transcription
L	DNA replication and repair
M	cell envelope biogenesis
N	cell motility and secretion
O	protein repair and chaperones
P	inorganic ion transport and metabolism
Q	secondary metabolites
T	signal transduction
U	protein trafficking and secretion
V	defense mechanisms

Figure 2B. Gene expression changes broken down into functional categories as defined by the COG database. The gray bars represent the number of genes up regulated in the co-culture, while the black bars represent the number of genes down regulated in the co-culture. Not listed are genes unassigned to functional categories, which included 85 genes up-regulated, and 36 genes down-regulated in the co-culture. A 2-fold change cutoff utilized, and the Bonferroni corrected p-value ($\alpha = 0.05$) used to establish statistical significance.

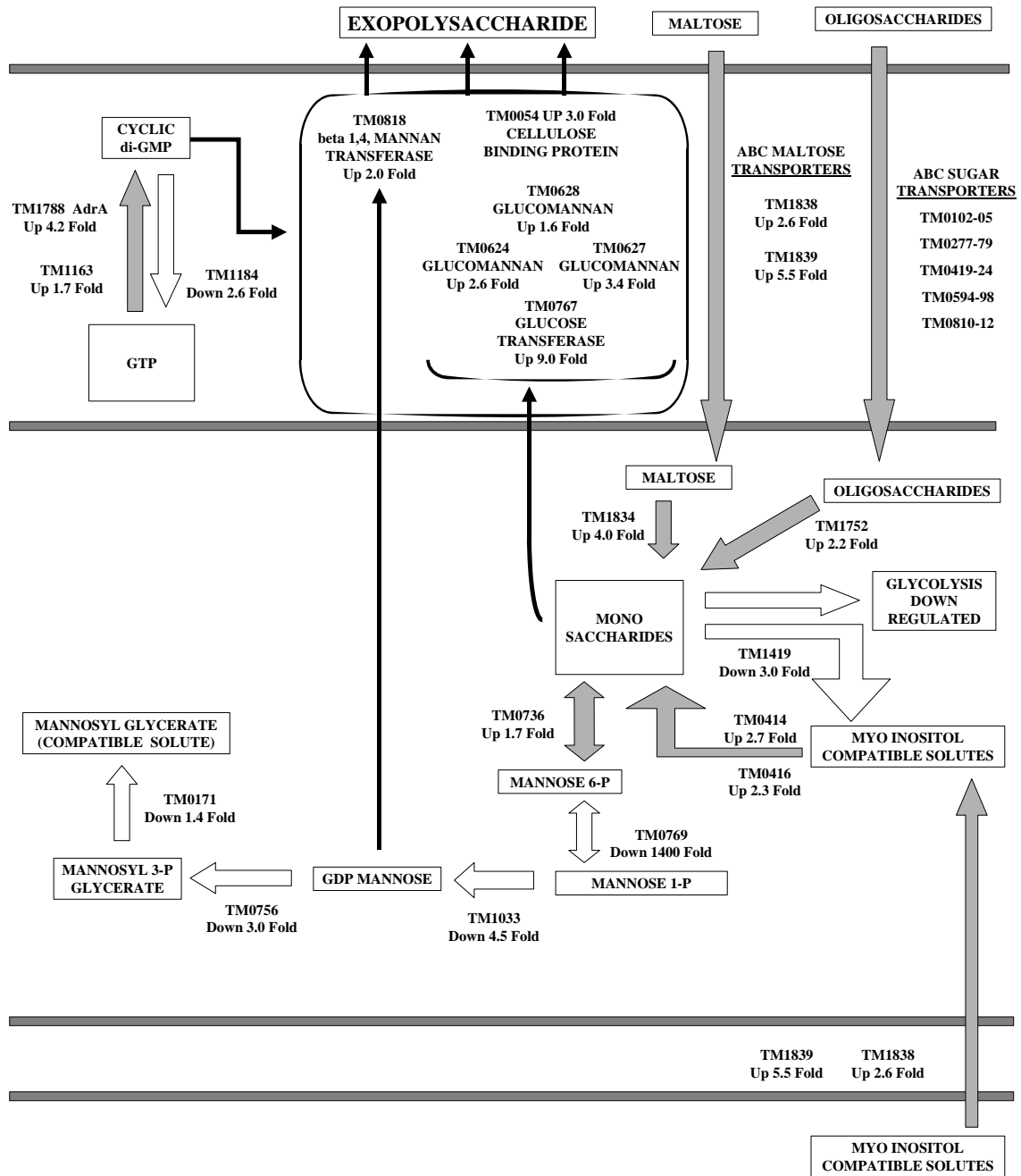


Figure 3. Putative pathway for exopolysaccharide production under high cell density conditions in *T. maritima*. Genes up-regulated under the high cell density co-culture are represented by shaded arrows, while those down-regulated are not shaded. See Table 1 for the list of genes represented.

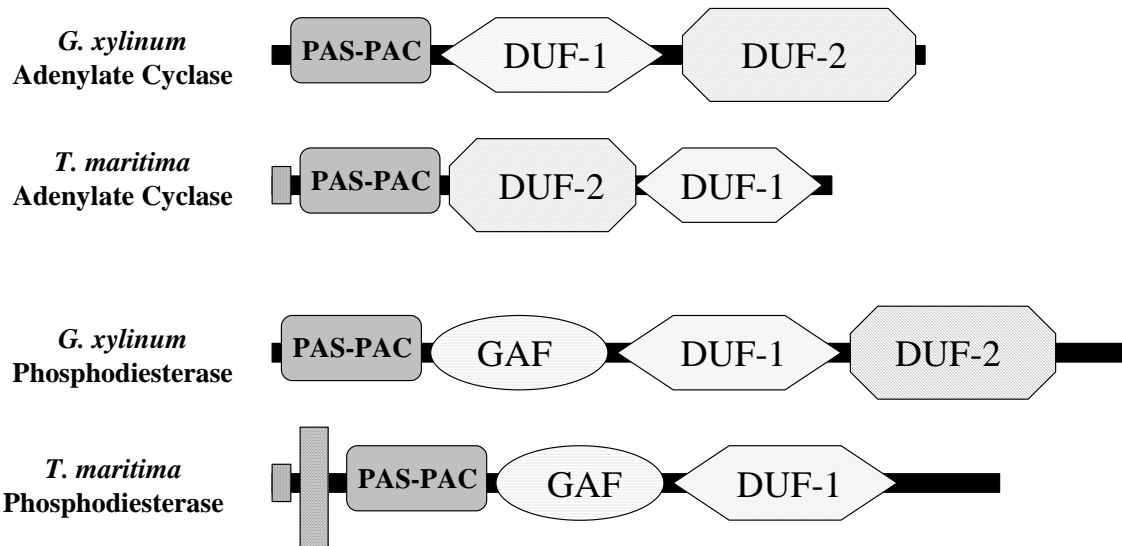


Figure 4. Putative diguanylate cyclase and cyclic di-GMP phosphodiesterase GGDEF domain proteins from *T. maritima*.

Top. The domains of the diguanylate cyclase of *G. xylinum* (O87374) as defined by the SMART database (Letunic *et al.*, 2004) along with the domains of the putative diguanylate cyclase of *T. maritima* (TM1163) as determined by sequence alignment with O87374. The dotted domain signifies a signal peptide sequence.

Bottom. The domains of the cyclic di-GMP phosphodiesterase of *G. xylinum* (O87373) as determined by the SMART database along with the domains of the putative cyclic di-GMP phosphodiesterase of *T. maritima* (TM1184) as determined by sequence alignment with O87373. The dotted domain signifies a signal peptide sequence, while the hashed domain is a predicted trans-membrane region.

5A.

MEAGGFEPSEDGG  PWASPSAARVFALGRDLPRAGCPLPQPS

Predicted Mature Signaling Peptide

5B.

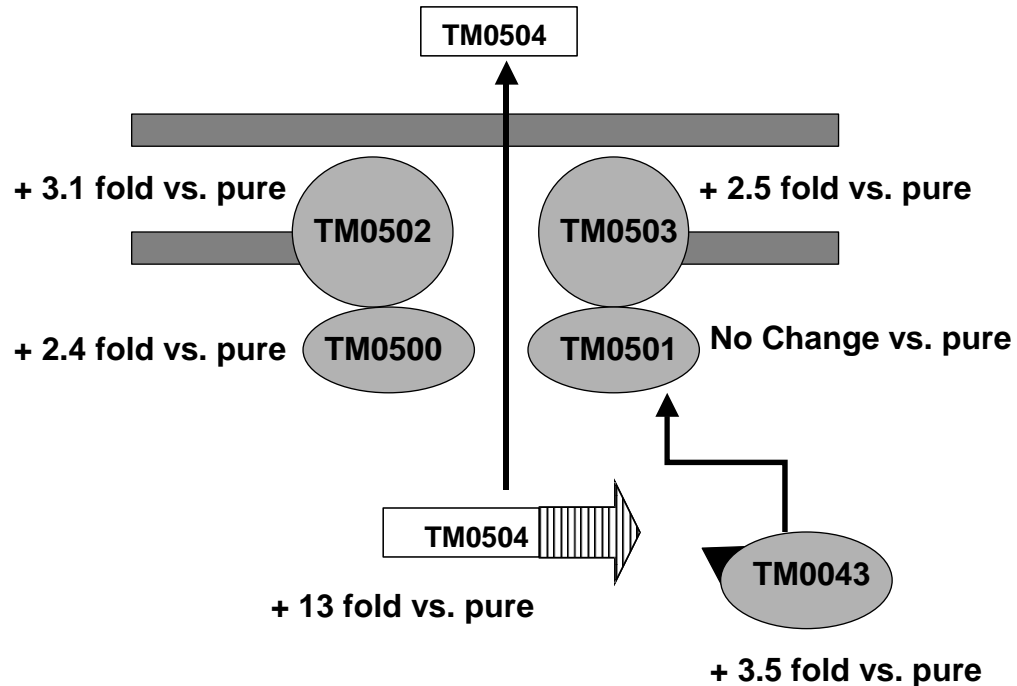


Figure 5. Putative signaling peptide from *T. maritima*.

- A.** Peptide sequence and predicted cleavage site for *T. maritima* protein TM0504. The precursor protein is 43 amino acids long in sequence. Cleavage at the GG residue yields a mature peptide 28 amino acids in length.
- B.** The predicted export pathway for TM0504. Both the ATPase subunits, TM0500 and TM0501, have COG4170 domains identifying them as related to the permease subunits of anti-microbial peptide transporters. In addition, TM0043, an ATPase subunit with a predicted N-terminal double-glycine cleaving domain (COG2274), may be the functional subunit that cleaves the signal precursor.

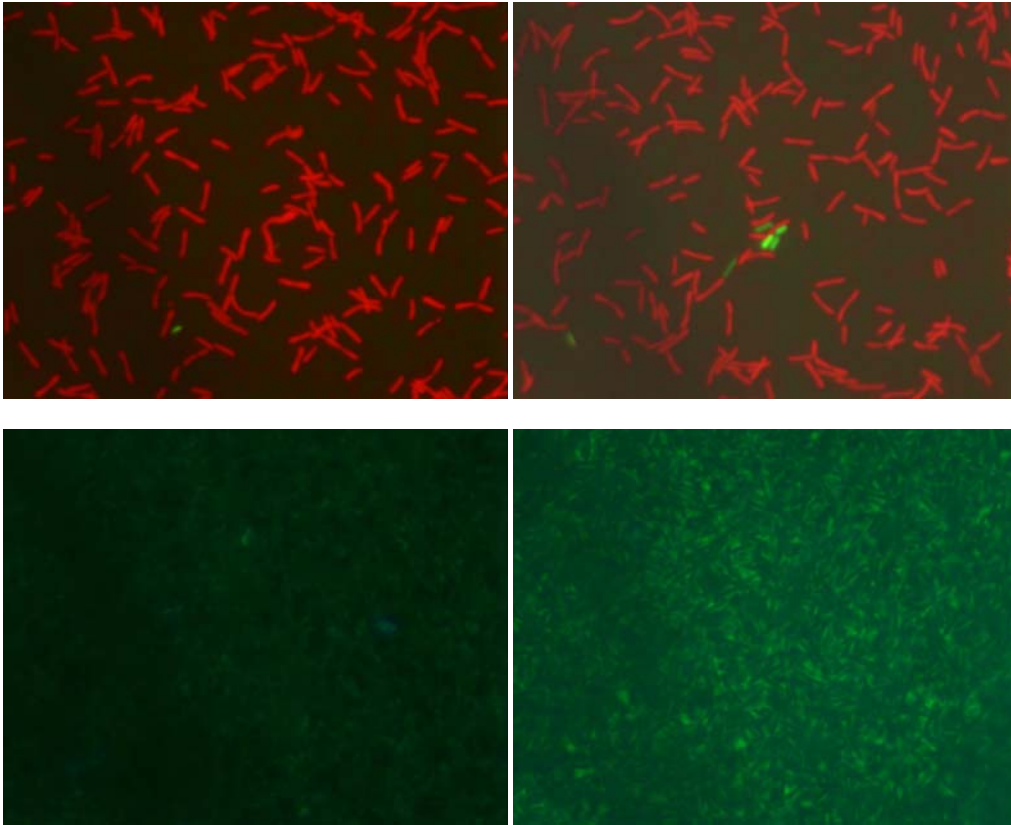


Figure 6. Acridine Orange (top) and Calcofluor (bottom) stained cultures of *T. maritima* 30 minutes after dosing with either buffer (PBS) (left), or synthetic peptide (right). At the time of dosing, both cultures were at a cell density of 5.6×10^7 cells per ml. For Calcofluor staining, 10X the cells were added compared to Acridine Orange staining to enable visualization of EPS at low cell densities. In either staining technique, the same amount of cells was added for both conditions.

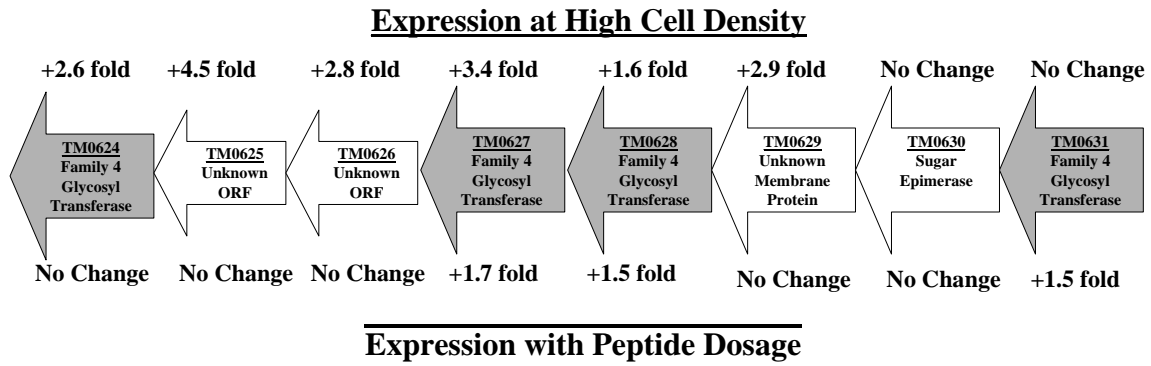


Figure 7. Putative glycosyl transferase operon related to EPS production (TM0624-TM0631). Listed above the ORF's is the fold change in gene expression in the high-cell density co-culture compared to the pure culture. Below the ORFs is the fold change in gene expression of a pure culture of *T. maritima* 30 minutes after adding TM0504 peptide compared to the sample taken before dosing. Note that the pure culture cell density was approximately 1/10 of that found in the co-culture.

**Chapter 4: *Thermotoga maritima* phenotype is impacted by
syntrophic interactions with *Methanococcus jannaschii* in
hyperthermophilic co-culture**

*M.R. Johnson, S.B. Connors, C.I. Montero, K.R. Shockley, and R.M. Kelly**

**Department of Chemical and Biomolecular Engineering
North Carolina State University
Raleigh, NC 27695-7905**

Accepted to: Applied and Environmental Microbiology (October, 2005)

***Address correspondence to:**

Robert M. Kelly

Dept. of Chemical and Biomolecular Engineering
North Carolina State University
Raleigh, NC 27695-7905

Phone: (919) 515-6396

Fax: (919) 515-3465

Email: rmkelly@eos.ncsu.edu

ABSTRACT

Significant growth phase-dependent differences were noted in the transcriptome of the hyperthermophilic bacterium *Thermotoga maritima* when it was co-cultured with the hyperthermophilic archaeon *Methanococcus jannaschii*. For the mid-log to early-stationary phase transition of a *T. maritima* monoculture, 24 genes (1.3% of the genome) were differentially expressed 2-fold or more. In contrast, methanogenic co-culture gave rise to 292 genes differentially expressed in *T. maritima* at this level (15.5% of the genome) for the same growth phase transition. Interspecies H₂ transfer resulted in three- to five-fold higher *T. maritima* cell densities than in the monoculture with concomitant formation of exopolysaccharide (EPS)-based cell aggregates. Differential expression of specific sigma factors and genes related to ppGpp-dependent stringent response suggest involvement in the transition into stationary phase and aggregate formation. Cell aggregation was growth phase-dependent, such that it was most prominent during mid-log phase and decayed as cells entered stationary phase. The reduction in cell aggregation was coincidental with down-regulation of genes encoding EPS-forming glycosyltransferases and up-regulation of genes encoding β -specific glycosyl hydrolases; the latter were presumably involved in hydrolysis of β -linked EPS to release cells from aggregates. Detachment of aggregates may facilitate colonization of new locations in natural environments where *T. maritima* coexists with other organisms. Taken together, these results demonstrate that syntrophic interactions can impact the transcriptome of heterotrophs in methanogenic co-culture, and this factor should be considered in examining the microbial ecology in anaerobic environments.

INTRODUCTION

Despite the fact that microorganisms interact significantly within their ecological niche, this factor is usually not taken into account in the context of microbial physiology. One key limitation in this regard is that methodologies for examining the influence of one microbial species on another are typically based on either identification (e.g., 16S rRNA phylogeny (46)) or enumeration (e.g., FISH (12)). Additional insights into functional outcomes of interspecies interactions are difficult to obtain. Yet such information is needed to relate pure culture cellular physiology to the beneficial and antagonistic elements present in microbial ecosystems.

Syntrophic relationships between microorganisms with complementary growth physiologies are a key part of microbial ecosystems. One such example in certain anaerobic niches is the association between fermentative H₂-producers and methanogenic H₂-consumers, whereby the inhibitory H₂ formed as the by-product of sugar or peptide metabolism serves as an energy source for the generation of methane (26). This syntrophy can be found in niches ranging from the mammalian digestive tract (24) to anaerobic digesters used for domestic waste treatment (12). Molecular hydrogen is also a key chemical species in hydrothermal environments (1), and likely supports this form of syntrophy; indeed, the pairing of hyperthermophilic fermentative anaerobes and methanogens in laboratory co-cultures leads to faster growth rates and higher biomass yields of heterotrophs compared to monocultures (5). Furthermore, growth rates of certain hyperthermophilic methanogens appear to be contingent upon the supply of

available H₂ that can be maximized through close spatial proximity with fermentative anaerobes (26).

The hyperthermophilic bacterium *Thermotoga maritima* grows heterotrophically by fermenting a variety of carbohydrates, producing H₂ as an auto-inhibitory by-product (16). In syntrophic co-culture with a hydrogenotrophic methanogen, such as *Methanococcus jannaschii* (7), this inhibition is relieved and cell population density is enhanced through the interspecies transfer of hydrogen (26). In addition to the utilization of sugars as carbon and energy sources (8, 28), *T. maritima* also has been shown to produce exopolysaccharides (EPS) that serve as the basis for biofilms (35, 36). In fact, when grown to high cell densities through co-culture with the hyperthermophilic methanogen *M. jannaschii*, *T. maritima* produces EPS that leads to formation of stable cellular aggregates, which presumably facilitate interspecies H₂-transfer (26). Cellular aggregation was found to occur initially during mid-log phase in high cell density co-cultures, apparently driven, at least in part, by quorum sensing and cyclic di-GMP regulation (18, 37). Calcofluor staining indicated that in exopolysaccharide was produced in pure cultures but at a level much lower than that of the co-culture, with aggregation noted only in the co-culture (18). Carbohydrate analysis of the aggregates indicated the exopolysaccharide consisted of a polymer of ribose, glucose and mannose, and was likely beta linked due to the positive calcofluor staining (18). Transcriptional profiling of exponential phase *T. maritima* present in cell aggregates indicated an increase in uptake of extracellular sugars when compared to the pure culture at the same stage of growth. However, sugar uptake by *T. maritima* in the exponential phase co-culture was not

coupled to glycolysis and compatible solute formation but rather directed toward the production of EPS (18).

The response of the *T. maritima* transcriptome during the transition into, and existence in, stationary phase in both pure and syntrophic culture has not been examined. In general, the transition from log to stationary phase, and transitions within stationary phase, follow different trajectories for microorganisms that depend on the causative agents that decelerate growth, such as growth substrate limitation (29), accumulation of inhibitory by-products (5), and imposition of certain forms of stress (43). The onset of stationary phase is known to be related to the action of specific regulators, such as sigma factors, that establish stationary phase phenotypes involving changes in morphology, virulence, and survival strategy (29). Indeed, transcriptional analysis of microorganisms driven into stationary phase by nutrient depletion has highlighted the importance of global regulators, such as σ^H , RpoS, and ppGpp, in limiting cellular processes and promoting scavenging and other survival activities (6, 43).

The influence of interspecies interactions is typically not considered when examining growth phase transitions but clearly can have a significant impact on microbial physiology. To examine this issue, a cDNA microarray-based functional genomics approach was used to determine the influence of interspecies H₂ transfer on growth phase-related transcriptional phenotypes of *T. maritima* in co-culture with *M. jannaschii*. It is clear from the results of this study that markedly different physiological and transcriptional states arise from interspecies interactions that are variable both between and within growth phases. While the focus of this work is on hyperthermophilic

microorganisms, the findings point out the importance of ecological relationships in examining microbial physiology in anaerobic environments.

MATERIALS AND METHODS

Growth of microorganisms. *T. maritima* strain MSB8 and *M. jannaschii* strain DSM2661 were grown at 80°C on media (BSMII) containing: 40 g/l sea salts, 5 g/l tryptone, 3 g/l yeast extract, 3 g/l maltose, 3 g/l Piperazine-1,4-bis(2-ethanesulfonic acid) (PIPES), 0.5 mg/l NaSeO₃•5H₂O, 0.5 mg/l NiCl₂•6H₂O, 0.25 g/l NH₄Cl, 10 mg/l Fe(NH₄)₂(SO₄)₂•6H₂O, 1.25 g/l sodium acetate anhydrate, 1 ml/l 1% Resazurin, 10 ml/l Wolfe's trace elements and 10ml/l Wolfe's trace vitamins solution (all Sigma Aldrich, Components of Wolfe's vitamin and mineral solutions can be found in ATCC medium no. 1343). The media was adjusted to pH 7.0, autoclaved for sterility, and stored at 4°C until use. For H₂ inhibition experiments, 400 ml of media was dispensed into a 1-liter glass jar sealed with a rubber septum (Corning, Corning, NY) and heated to 80°C. The media was then sparged through a syringe needle with the appropriate gas (100% N₂ or 80% H₂:20% CO₂) for one minute, and reduced with 4 ml of a 10% sodium sulfide:10% l-cysteine HCl solution (pH 8.0) (Sigma-Aldrich). A 1% inoculum of log phase cells was used. Culture bottles were agitated at 100 rpm in an oil bath at 80°C. To study the effects of hydrogen removal three cases were examined in 400 ml batch culture. The first case was a reference culture grown with an enclosed headspace initially filled with nitrogen. The second case tested the effect of N₂-sparging on *T. maritima* monocultures by having two syringe needles inserted through the bottle septum, the first of which was supplied

with 250 ml per minute of nitrogen and the second was used as a vent. For the co-culture of *T. maritima* growth with *M. jannaschii*, both species were inoculated simultaneously into a bottle with an initial atmosphere 80% H₂:20% CO₂ (2 bar). Duplicate cultures for all conditions were harvested at mid-log phase and pooled with equal amounts of RNA.

For growth phase experiments, *T. maritima* was grown with and without *M. jannaschii* at 80°C in a 16-liter Microgen sterilizable-in-place fermenter (New Brunswick Scientific). Ten liters of non-sterile BSMII media adjusted to pH 7.0 was charged to the fermenter, which was sterilized-in-place by heating to 100°C for 20 minutes. The fermenter was then cooled to 80°C and stirred at 500 RPM with three Rushton style impellers for agitation. Temperature was controlled by utilizing the sterilization mode on the fermenter, which heats with steam through an internal heat exchanger. Once at 80°C, sparging was started using N₂ fed at 0.25 l/min to maintain anaerobic conditions. The media was reduced by the addition of 60 ml of 10% sodium sulfide through a septum, and 200 ml of inoculum was then added via a growth flask fitted with a dip tube. Anaerobic inoculum (200 ml of either *T. maritima* or *T. maritima*/*M. jannaschii* co-culture) was forced into the fermenter via positive pressure with nitrogen gas through an addition port on the fermenter. Sparging was not utilized after inoculation in the co-culture experiment in order to prevent removing hydrogen essential for methanogen growth. Samples from both the pure and co-culture were taken at mid-log, early stationary, and late stationary phases, after completing duplicate trial runs of each growth condition to determine an accurate growth curves.

Fluorescence microscopy. Cells were enumerated by fixing culture samples with glutaraldehyde (Sigma Aldrich, 0.25% final concentration) for 5 min, then staining the cells by adding small aliquots (~10 μ L) to 5 ml of 0.05% acridine orange (Sigma), and filtering the cells onto 0.2 micron polycarbonate filter membranes (Osmonics), with the goal of having 100-300 cells in the field of view. Ten replicate counts were completed using an eyepiece grid (Nikon). Error analysis yielded a 15% error associated with counting 100-300 cells per field of view. To capture images, an epifluorescence microscope (Nikon) with appropriate filter sets (Southern Micro Instruments, Marietta GA) that was fitted with a digital camera (Spot system, Diagnostic Instruments Inc.) was utilized.

Microarray protocols. A *T. maritima* microarray was synthesized from PCR products as discussed previously (8), representing over 99% of the open reading frames in the sequenced genome (28). For each RNA extraction, 400 ml samples were harvested, split into four 100 ml samples, and quickly cooled to 0°C by immersion in ice water. The harvested cells were then immediately centrifuged at 13,000 x g (25 min at 4°C). Supernatant was discarded and the RNA was extracted from cell pellets, from which cDNA was synthesized, labeled through indirect incorporation, and hybridized to the microarray following the methods described previously (38). The experimental designs for the gene expression studies were completed following recommended guidelines (20) by utilizing independent loops for both the hydrogen removal study (3 condition loop) and the comparison of growth phases (6 condition loop). Microarray slides were scanned using the appropriate laser power to balance the cy3 and cy5 signals with a Perkin Elmer

ExpressLite Scanner (Perkin-Elmer). Raw uncorrected quantitation of spots was completed using ScanArray (Perkin-Elmer), and data analysis was completed as discussed previously (8), utilizing a mixed model ANOVA-based analysis to generate both least squared mean expression data, and the Bonferroni-corrected (47) fold-change data. Unless otherwise noted, gene annotation is from the COG database at NCBI (44).

The cross-hybridization of *M. jannaschii* labeled cDNA with the *T. maritima* microarray was expected to be minimal since *M. jannaschii* comprised a small fraction of the co-culture and the genomes for these two organisms show less than 80% identity at the nucleotide level (32, 48). To verify, RNA from *M. jannaschii* was labeled using the protocols explained above and tested for cross hybridization by hybridizing the labeled samples to the *T. maritima* microarray. No cross-hybridization of the *M. jannaschii* RNA was detected on the scanned slides at full laser power.

Independent confirmation with Real-Time PCR. A biological repeat of both the pure and co-culture growth curve experiments were completed, with selected genes analyzed for expression in both replicate experiments. The following genes and primers were utilized: TM0767 (5'-CGCATTGCCACAAGAAAGTA-3', 5'-CCCGTGTTCACATAGGGAAT-3'), TM1451 (5'-AGGCTTGTTGTCAGTATAGCCA-3', 5'-CTACCGCCTTCAGAAGTCCTAT-3'), TM1598 (5'-GATGTCGTTTCAGGATGTGTTTT-3', 5'-GACATTCACGGCTATCCTGTAG-3'), TM1662 (5'-TTGCGTACTCCACTACAGGAAC-3', 5'-ACGATGAGATCGACCCTTTTAT-3'), and TM1834 (5'-AGGAGCAGATTCTGAAATAGGC-3', 5'-GGACGGATTTCTTTGATGAAC-3'). cDNA for each growth condition and replicate was synthesized using superscript III (Invitrogen). Real-time PCR reactions were carried out

with iQ SYBR Green Supermix (Bio-Rad) with 20 μ L reactions containing both primers at a concentration of 250 nM, using the iCycler iQ real-time PCR detection system (Bio-Rad). Template cDNA was added to the test reactions at 2.4 ng per reaction, and a standard curve was completed for each gene represented using cDNA added in 4-fold serial dilutions in the range from 0.15 ng to 38.4 ng of cDNA. The PCR efficiency and cycle thresholds (Ct) were calculated using the iCycler iQ software (Bio-Rad), and the fold-changes were calculated by the method of Pffafli (33). A melt curve analysis was completed and confirmed homogeneous PCR products were generated with no non-specific amplification. Calculated fold-changes from real-time PCR for both biological repeats were in agreement with the microarray results (Table 3).

RESULTS and DISCUSSION

The objective of this study was to examine transcriptional and physiological changes with respect to growth phase and population density in *T. maritima* as a consequence of syntrophic co-culture with *M. jannaschii*. A whole genome cDNA microarray was used to interrogate samples of *T. maritima* obtained at different stages of growth in both pure and co-culture. The fact that no significant cross-hybridization of the *T. maritima* microarray with *M. jannaschii* was noted facilitated the functional genomics approach described here.

Transition from log to stationary phase in *T. maritima* pure and co-culture.

Cell densities (Figure 1B), epifluorescence micrographs (Figure 1A) and volcano plots (Figure 1C) are shown for *T. maritima* pure culture and co-culture with *M. jannaschii* as

a function of growth phase, comparing mid-log phase (ML), early stationary phase (ES) and late stationary phase (LS). While the growth rates of the pure and co-culture was similar (Figure 1B), the corresponding maximum cell densities were appreciably different; the co-culture peaked at more than 10^9 cells/ml compared to $2\text{-}3 \times 10^8$ cells/ml for the monoculture. The lower cell density of the *T. maritima* pure culture relative to the co-culture was apparently more the result of H_2 inhibition than nutrient limitation, and could be the reason for the more abrupt transition to stationary phase in the pure culture. Genes encoding starvation response proteins, such as SurE, an acid phosphatase that acts to scavenge phosphate under conditions of phosphorus limitation (51), and known carbohydrate utilization pathways in *T. maritima* (8) did not respond in the transition from mid-log to early-stationary phase in the pure culture. In addition, regulatory proteins, including sigma factors, were not differentially expressed during this transition. A likely cause for the onset of stationary phase in the pure culture was the build-up of inhibitory H_2 , bottlenecking core metabolic processes in *T. maritima*.

Indeed, differential expression contrasts between a quiescent pure culture, a pure culture sparged with inert gas to remove inhibitory H_2 , and a co-culture with *M. jannaschii* supported this hypothesis. ABC transporters for amino acids, peptides, and sugars were up-regulated in both the sparged and co-culture cases relative to the quiescent culture, suggesting that hydrogen inhibition was alleviated to some extent by H_2 removal (see Supplemental Table S1). In the quiescent culture, compared to the other two cases, up-regulation of core metabolism genes was noted, consistent with reduced metabolic efficiency attributed to H_2 inhibition and a shift to a lower redox state. Furthermore, heterotrophic thermophiles have been observed to form lactate and ethanol

as by-products in the absence of elemental sulfur (45). Ethanol accumulation in *T. maritima* could be responsible for the observed up-regulation of σ^E , known to be responsive to thermal stress in *T. maritima* (34). In *E. coli* mutants resistant to elevated ethanol concentrations, the over-expression of chaperones was found to be necessary for survival (13). Here, chaperones and protein repair-related ORFs were expressed at highest levels in the quiescent pure culture.

Not only was population density a distinguishing factor between pure and co-culture, but the corresponding transcriptomes were substantially different (see Figure 1C). Transcriptional response analysis showed that 24 genes changed 2-fold or more in the pure culture (1.3 % of the *T. maritima* genome) between mid-log and early stationary phase (Table 1). Of note was the down-regulation of molecular chaperones, such as GroES (8-fold) and GroEL (9-fold), presumably a reflection of decreased protein synthesis in stationary phase. In contrast to the pure culture, 292 genes responded 2-fold or more (15.5 % of the *T. maritima* genome) for the same phase transition in the co-culture (see Supplementary Table S2). Cell aggregation was extensive during mid-log phase (when cell densities reached 5×10^8 cells/ml). In mesophilic microorganisms, aggregate formation leading to biofilms can be triggered by stresses, such as starvation (10), or by a cell density-dependent response, such as quorum sensing (11). Indeed, previous work showed that population density-triggered EPS formation occurred in *T. maritima* co-cultures during exponential phase (18). Here, however, aggregation was significantly reduced as the co-culture entered stationary phase and non-existent in late stationary phase (Figure 1B). The reasons for this may be related to observations that some mesophilic bacteria deliberately detach during certain growth phases to escape from

the biofilm matrix (3, 19, 39). The mechanism for detachment is usually enzyme-based, with specific activity towards elements comprising the biofilm (3, 19). Furthermore, microorganisms clustered together stand a greater chance colonizing new environments compared to individual cells; this is especially important in situations where syntrophic relationships exist so that deliberate detachment is advantageous compared to gradual biofilm erosion (39). A similar strategy may have been operational in the *T. maritima* co-culture. While transporters and nutrient-scavenging genes are often more highly expressed in stationary phase due to nutrient limitation (15), this does not appear to be the case in the co-culture. ABC transporters and carbohydrate-active enzymes up-regulated during the stationary phase transition were from a broad distribution of carbohydrate-active enzymes (Table 2). Despite the fact that the growth medium was maltose-based, maltose-directed ABC transporters (TM1836, TM1839) and related glycosidases (TM1835) were down-regulated, while genes encoding enzymes for the degradation of β -glycans (e.g., TM0024, TM0070, TM1231, TM1524, TM1752) were up-regulated during the transition to stationary phase in the co-culture (Table 2). This suggests that the β -linked saccharide components of EPS produced during exponential growth may have been degraded, released, and transported back into the cell to be re-used. It also appears that the onset of stationary phase for *T. maritima* in the co-culture was not driven by nutrient limitation. For example, no differential expression was noted for the gene encoding a stationary phase survival protein SurE (TM1662), and as mentioned above, the maltose-specific transport and degradation genes were down-regulated in the co-culture. In addition, the rich growth medium used here had relatively high carbon and nitrogen content compared to the quantity of biomass produced. Neither cell aggregate

formation nor differential expression of any carbohydrate-active enzymes and transporters was noted in the pure culture during the transition into stationary phase.

Comparisons between phase-dependent phenotypes in pure culture and co-culture. In addition to tracking differential expression for points along the growth curves for the pure and co-cultures, transcriptional contrasts between the pure and co-cultures for the equivalent points on their growth phase trajectories were examined. Thirty-five genes were differentially expressed two-fold or more between ML of the pure culture and ML of the co-culture, including 24 genes up-regulated in the pure culture mostly related to central metabolism and chaperones (see Supplemental Table S3). The 11 genes up-regulated in the co-culture included an α -glucuronidase (41) (TM0434, +2.0-fold in co-culture), an α -glucosidase (4) (TM1834, +4.6-fold in co-culture), and several hypothetical proteins. Forty-four genes were differentially expressed two-fold or more between LS pure culture compared to LS co-culture, mainly central metabolism genes (see Supplemental Table S3). Late stationary phase cells in both the pure and co-culture were comparable in appearance, characterized by a shift in *T. maritima* from the rod-like morphology noted in exponential growth to a coccoid-like morphology in stationary phase with no evidence of dividing cells. To investigate the viability of *T. maritima* and *T. maritima* / *M. jannaschii* co-culture in extended stationary phase, both were inoculated and allowed to grow at 80°C into stationary phase. Samples were drawn from each culture every 12 hours and inoculated as a 1% inoculum into fresh, sterile media. Even after 120 hours at 80°C, both cultures contained viable cells, which grew quickly (lag phase of less than 3 hours) to cell densities characteristic of pure culture and co-cultures.

The most significant differences between the pure and co-culture were associated with ES phase, where 240 genes were differentially expressed 2-fold or more (see Supplemental Table S3). These consisted of 127 genes expressed higher in the pure culture, of which over half were central metabolism-related genes, and 113 genes detected at higher levels in the co-culture. Genes up-regulated in the stationary phase co-culture included a large number of ABC transporter components (30 genes in all), and carbohydrate hydrolases, including an α -glucosidase (TM1834, +3.8 fold), a pectate lyase (TM0433, +3.5 fold), an α -mannosidase (TM1231, +3.0 fold), two alpha-glucuronidases (TM0055, +2.1 fold; TM1068, +2.6), two endoglucanases (TM0305, +2.0 fold; TM1751 +2.1 fold), a laminarinase (TM0024, 2.1 fold), an α -galactosidase (TM0310, +2.1 fold), and an endoxylanase (TM0061, +2.2 fold). The up-regulation of the carbohydrate hydrolases and transporters in the co-culture likely reflects the processing of EPS associated with cell aggregates discussed above.

Differential expression of regulatory proteins. Regulatory mechanisms in *T. maritima* that potentially contribute to the transition between growth phases and aggregation, maturation and detachment of cell aggregates include sigma factors, ppGpp, and cyclic di-GMP. Equally important to note are stationary phase regulatory proteins that apparently do not exist in the *T. maritima* genome, but are present and necessary for survival in model mesophilic microorganisms. Examples of such regulatory proteins not encoded in the *T. maritima* genome include: starvation response regulators FadR (14) and Lrp (52), global regulators UspA (23) and RpoS (21), the programmed cell death system mazEF (2), DNA protection protein Dps (27) and the SOS polymerase system which

facilitates beneficial mutations (49). The role of the few regulatory systems that do exist in *T. maritima* are likely to be particularly important for growth phase transitions and survival. Expression profiles (based on least squares mean, LSM) of four identifiable sigma factors in the *T. maritima* genome (σ^H (TM0534), σ^{28} (TM0902), σ^A (TM1451), and σ^E (TM1598) (28)) were examined (see Figure 2). σ^H responds strongly during stationary phase in *Bacillus subtilis*, controlling the formation of spores and inducing the organism into stationary phase (6). Here, the σ^H homolog (TM0534) was not differentially expressed during or between exponential and stationary phases for either pure or co-culture (Figure 2). Many genes under control of σ^H in *B. subtilis* are involved in adaptation to nutrient deficiency (6). Since *T. maritima* was grown here in a nutrient-rich medium, the fact that σ^H was not differentially expressed is not surprising. In *E. coli*, RpoS (σ^S) is required for stationary phase survival along with a required lipoprotein (NlpD), an L-isoaspartate methyltransferase (Pcm), and a stationary phase survival protein (SurE) (51). An RpoS ortholog has yet to be identified in *T. maritima* and, therefore, a different sigma factor or regulatory protein likely regulates stationary phase physiology. Putative *T. maritima* homologs do exist for NlpD (TM0409) and Pcm (TM0704), and SurE (TM1662) (51). It is interesting to note that all three genes were not differentially expressed in the growth phase contrasts, nor in the sparged culture and co-culture comparisons.

Both σ^A and σ^E were up-regulated during the transition from mid-log to early stationary phase in the co-culture (Figure 2). σ^E in mesophilic bacteria is often involved in cellular stress responses, such as heat shock (50), protein aggregation (50), and

oxidative stress (29). σ^A in mesophiles is known to regulate house-keeping functions and RNA genes transcribed during active growth (6). In previous studies with *T. maritima*, it was noted that σ^A was up-regulated in biofilm cells compared to planktonic cells (35), and under conditions of heat stress (34). In this study, σ^A and σ^E both responded to H₂ inhibition in the quiescent pure culture during exponential growth and were up-regulated compared to conditions of hydrogen removal (σ^A +4.0-fold vs. co-culture, +4.3-fold vs. sparged; σ^E +2.1-fold vs. co-culture, +2.1-fold vs. sparged). Up-regulation of σ^A and σ^E likely reflects a lowered metabolic efficiency and increased levels of stress in H₂-inhibited *T. maritima*, which in the absence of sulfur may generate lactate and ethanol as by-products (45), leading to intracellular protein denaturation.

TM0902, which belongs to the COG1191 group of σ^{28} -related regulators, was down-regulated in both sparged and co-culture, compared to the quiescent culture (-2.5 fold co-culture, -2.4 fold sparged pure culture). Members of this COG have been shown to induce the expression of flagellar proteins in *E. coli* (22). For example, the σ^{28} -related sigma factor identified in the genome of another hyperthermophilic bacterium, *Aquifex aeolicus*, and closely related to TM0902 (31% identity, 60% similarity over 90% of the protein), was shown to restore the motility of an *E. coli* σ^{28} mutant (40). Higher expression of TM0902 in the pure culture perhaps indicates an attempt of *T. maritima* cells to move from stressful conditions. Hydrogen levels have been shown to modulate flagella expression in *M. jannaschii* (25), and it could be hypothesized a similar system may exist in *T. maritima*. Several chemotaxis genes were down-regulated in both the sparged and co-cultures, with a greater number down-regulated in the co-culture (listed

here are fold changes in co-culture and sparged culture, respectively; NC indicates less than 2-fold): TM0429 (-3.1, -2.8), TM0701 (-2.8, NC), TM0702 (-4.5, -2.6), TM0718 (-2.2, NC), TM0904 (NC, -2.0), TM0918 (-2.2, NC), TM1428 (-2.0, NC), and predicted flagellar proteins TM0219 (-3.1, NC) and TM0908 (2.1, NC).

Secondary messengers. Secondary messengers, such as guanosine-3',5'-(bis)pyrophosphate (ppGpp) and cyclic di-GMP, play a role in regulating gene expression in microorganisms by influencing the binding efficiency of sigma factors to RNA polymerase (29-31), and modulating enzyme activity (17), respectively. ppGpp, a hormone-like nucleotide which mediates the preferential binding of sigma factors in response to the nutritional quality of the extracellular environment, is produced by two different classes of enzymes that are utilized to detect amino acid starvation (RelA), and carbon starvation or stress (SpoT) (29). *T. maritima* contains putative homologs to RelA (TM0729) and its accessory gene GppA (TM0195), while a homolog to SpoT has yet to be identified. In *T. maritima*, TM0195 was up-regulated nearly 2-fold during the transition from mid-log to early-stationary phase in the co-culture, while TM0729 was up-regulated during the same transition in both the pure and co-culture (+2.4 fold co-culture, +2.5 fold pure), suggesting an enhanced ability to detect amino acid starvation in both cultures in stationary phase.

Cyclic di-GMP is apparently involved in controlling biofilm formation processes in *T. maritima* (18, 37) as well as in mesophilic bacteria, such as *Acetobacter xylinum* (42). Here, differential expression of cyclic di-GMP-related genes was not observed during the transition to stationary phase in either the pure or co-cultures. However, differential regulation of this system was seen during batch growth comparing the co-

culture to the hydrogen accumulating condition. In particular, a putative cyclic di-GMP cyclase (TM1788) was up-regulated 4.2-fold in the co-culture compared to the quiescent pure culture, while the putative cyclic di-GMP phosphodiesterase (TM1184) was down-regulated 2.6-fold under the same comparison. In the comparison between the sparged and quiescent cultures, TM1184 was down-regulated 3.4-fold. Because GGDEF domain proteins are known to respond to environmental factors for the regulation of cyclic di-GMP (17), it may be that the differential expression of these genes relates to the nutritional quality of the extracellular environment more so than to growth rate or population density.

Summary. In this study, it was shown that, when grown at high cell densities through syntrophic co-culture with *M. jannaschii*, *T. maritima* cycles through aggregate formation, maturation, and detachment likely mediated by the action of carbohydrate active enzymes and transporters. While it is likely the transition to stationary phase in the *T. maritima* co-culture falls under the control of specific sigma factors and ppGpp regulation, the aggregation lifecycle may also be affected by quorum sensing. It has been previously shown the aggregation process appears to be regulated, at least in part, by TM0504, a small peptide that induces the transcription of EPS-forming glycosyltransferases upon its accumulation in the culture supernatant (18). In this study, the expression of this gene changes very little during the transition from mid-log phase to early stationary phase in the co-culture. However, it is already expressed within the top 7 percent of all genes in mid-log phase, suggesting that the maximum dynamic range of this sensing system may have been reached early in co-culture growth.

The importance of interspecies interaction in examining microbial physiology is underlined by the results of this study. *T. maritima* grown in pure batch culture was driven into stationary phase at a relatively low cell density by H₂ inhibition. The cell aggregation cycle and the effects of population density were only seen for *T. maritima* when grown in high-density co-culture with *M. jannaschii*. Overall, this work illustrates the point that ecological interactions are an essential element to be considered in studying microbial physiology, and that functional genomics approaches can be used to complement classical microbiological methods to this purpose.

ACKNOWLEDGMENTS

This work was supported was supported in part through grants from the NASA Exobiology Program, NSF Biotechnology Program and the DOE Energy Biosciences Program.

REFERENCES CITED

1. **Adams, M. W. W.** 1990. The metabolism of hydrogen by extremely thermophilic, sulfur-dependent archaeobacteria. *FEMS Microbiol. Rev.* **75**:219-238.
2. **Aizenman, E., H. Engelberg-Kulka, and G. Glaser.** 1996. An *Escherichia coli* chromosomal "addiction module" regulated by guanosine 3',5'-bispyrophosphate: a model for programmed bacterial cell death. *P. Natl. Acad. Sci. USA* **93**:6059-6063.
3. **Allison, D. G., B. Ruiz, C. SanJose, A. Jaspe, and P. Gilbert.** 1998. Extracellular products as mediators of the formation and detachment of *Pseudomonas fluorescens* biofilms. *FEMS Microbiol. Lett.* **167**:179-184.
4. **Bibel, M., C. Brettl, U. Goslar, G. Kriegshauser, and W. Liebl.** 1998. Isolation and analysis of genes for amylolytic enzymes of the hyperthermophilic bacterium *Thermotoga maritima*. *FEMS Microbiol. Lett.* **158**:9-15.
5. **Bonch-osmolovskaya, E. A., and K. O. Stetter.** 1991. Interspecies hydrogen transfer in cocultures of thermophilic Archaea. *Syst. Appl. Microbiol.* **14**:205-208.
6. **Britton, R., P. Eichenberger, J. Gonzales-Pastor, P. Fawcett, R. Monson, R. Losick, and A. D. Grossman.** 2002. Genome-wide analysis of the stationary phase sigma factor (sigma H) regulon of *Bacillus subtilis*. *J. Bacteriol.* **184**:4881-4890.
7. **Bult, C. J., O. White, G. J. Olsen, L. Zhou, R. D. Fleischmann, G. G. Sutton, J. A. Blake, L. M. FitzGerald, R. A. Clayton, J. D. Gocayne, A. R. Kerlavage, B. A. Dougherty, J. F. Tomb, M. D. Adams, C. I. Reich, R. Overbeek, E. F. Kirkness, K. G. Weinstock, J. M. Merrick, A. Glodek, J. L. Scott, N. S. Geoghagen, and J. C. Venter.** 1996. Complete genome sequence of the methanogenic Archaeon, *Methanococcus jannaschii*. *Science*:1058-1073.
8. **Chhabra, S., K. R. Shockley, S. Conners, K. Scott, R. Wolfinger, and R. Kelly.** 2003. Carbohydrate induced differential gene expression patterns in the hyperthermophilic bacterium *Thermotoga maritima*. *J. Biol. Chem.* **278**:7540-7552.
9. **Conners, S. B., C. I. Montero, D. A. Comfort, K. R. Shockley, M. R. Johnson, S. Chhabra, and R. M. Kelly.** 2004. An expression-driven approach to the prediction of carbohydrate transport and utilization regulons in the hyperthermophilic bacterium *Thermotoga maritima*. **in submission**.
10. **Costerton, J. W.** 1995. Overview of Microbial Biofilms. *J. Ind. Microbiol.* **15**:137-140.
11. **Davies, D. G., M. R. Parsek, J. P. Pearson, B. H. Iglewski, J. W. Costerton, and E. P. Greenberg.** 1998. The involvement of cell-to-cell signals in the development of a bacterial biofilm. *Science* **280**:295-298.
12. **de los Reyes, F. L., D. B. Oerther, M. F. de los Reyes, M. Hernandez, and L. Raskin.** 1998. Characterization of filamentous foaming in activated sludge

- systems using oligonucleotide hybridization probes and antibody probes. *Water Sci. Technol.* **37**:485-493.
13. **Echave, P., M. Esparza-Cerón, E. Cabisco, J. Tamarit, J. Ros, J. Membrillo-Hernández, and E. C. C. Lin.** 2002. DnaK dependence of mutant ethanol oxidoreductases evolved for aerobic function and protective role of the chaperone against protein oxidative damage in *Escherichia coli*. *P. Natl. Acad. Sci. USA* **99**:4626-4631.
 14. **Farewell, A., A. Diez, C. C. Di Russo, and T. Nystrom.** 1996. Role of the *Escherichia coli* FadR regulator in stasis survival and growth phase dependent expression of the *uspA*, *fad*, and *fab* genes. *J. Bacteriol.* **178**:6443-6450.
 15. **Ferenci, T.** 1999. Regulation by nutrient limitation. *Curr. Opin. Microbiol.* **2**:208-213.
 16. **Huber, R., T. A. Langworthy, H. König, M. Thomm, C. R. Woese, U. B. Sleytr, and K. O. Stetter.** 1986. *Thermotoga maritima* sp-nov represents a new genus of unique extremely thermophilic eubacteria growing up to 90 degrees C. *Arch. Microbiol.* **144**:324-333.
 17. **Jenal, U.** 2004. Cyclic di-guanosine-monophosphate comes of age: a novel secondary messenger involved in modulating cell surface structures in bacteria. *Curr. Opin. Microbiol.* **7**:185-191.
 18. **Johnson, M. R., C. I. Montero, S. B. Connors, K. R. Shockley, S. L. Bridger, and R. M. Kelly.** 2004. Population density-dependent regulation of exopolysaccharide formation in the hyperthermophilic bacterium *Thermotoga maritima*. *Mol. Microbiol.* **55**:664-674.
 19. **Kaplan, J. B., C. Raganath, N. Ramasubbu, and D. H. Fine.** 2003. Detachment of *Actinobacillus actinomycetemcomitans* biofilm cells by an endogenous beta-hexosaminidase activity. *J. Bacteriol.* **185**:4693-4698.
 20. **Kerr, M. K., and G. A. Churchill.** 2001. Experimental design for gene expression microarrays. *Biostatistics* **2**:183-201.
 21. **King, T., and T. Ferenci.** 2005. Divergent roles of RpoS in *Escherichia coli* under aerobic and anaerobic conditions. *FEMS Microbiol Lett.* **244**:323-327.
 22. **Kundu, T. K., S. Kusano, and A. Ishihama.** 1997. Promoter selectivity of *Escherichia coli* RNA polymerase sigmaF holoenzyme involved in transcription of flagellar and chemotaxis genes. *J. Bacteriol.* **179**:4264-4269.
 23. **Kvint, K., L. Nachin, A. Diez, and T. Nystrom.** 2003. The bacterial universal stress protein: function and regulation. *Curr. Opin. Microbiol.* **6**:140-145.
 24. **Morvan, B., F. Bonnemoy, G. Fonty, and P. Gouet.** 1996. Quantitative determination of H₂-utilizing acetogenic and sulfate-reducing bacteria and methanogenic archaea from digestive tract of different mammals. *Curr. Microbiol.* **32**:129-133.
 25. **Mukhopadhyay, B., E. F. Johnson, and R. S. Wolfe.** 2000. A novel p(H₂) control on the expression of flagella in the hyperthermophilic strictly hydrogenotrophic methanarchaeon *Methanococcus jannaschii*. *P. Natl. Acad. Sci. USA* **97**:11522-11527.

26. **Muralidharan, V., K. D. Rinker, I. S. Hirsh, E. J. Bouwer, and R. M. Kelly.** 1997. Hydrogen transfer between methanogens and fermentative heterotrophs in hyperthermophilic cocultures. *Biotechnol. Bioeng.* **56**:268-278.
27. **Nair, S., and S. E. Finkel.** 2004. Dps protects cells against multiple stresses during stationary phase. *J Bacteriol.* **186**:4192-4198.
28. **Nelson, K. E., R. A. Clayton, S. R. Gill, M. L. Gwinn, R. J. Dodson, D. H. Haft, E. K. Hickey, L. D. Peterson, W. C. Nelson, K. A. Ketchum, L. McDonald, T. R. Utterback, J. A. Malek, K. D. Linher, M. M. Garrett, A. M. Stewart, M. D. Cotton, M. S. Pratt, C. A. Phillips, D. Richardson, J. Heidelberg, G. G. Sutton, R. D. Fleischmann, J. A. Eisen, O. White, S. L. Salzberg, H. O. Smith, J. C. Venter, and C. M. Fraser.** 1999. Evidence for lateral gene transfer between Archaea and Bacteria from genome sequence of *Thermotoga maritima*. *Nature* **399**:323-329.
29. **Nystrom, T.** 2002. Aging in bacteria. *Curr. Opin. Microbiol.* **5**:596-601.
30. **Nystrom, T.** 2003. Conditional senescence in bacteria: death of the immortals. *Mol. Microbiol.* **48**:17-23.
31. **Nystrom, T.** 2004. Growth versus maintenance: a trade-off dictated by RNA polymerase availability and sigma factor competition? *Mol. Microbiol.* **54**:855-862.
32. **Peterson, J., L. Umayam, T. Dickinson, E. K. Hickey, and O. White.** 2001. The comprehensive microbial resource. *Nucleic Acids Res.* **29**:123-125.
33. **Pfaffl, M. W.** 2001. A new mathematical model for relative quantification in real-time RT-PCR. *Nucleic Acids Res.* **29**:e45.
34. **Pysz, M., D. Ward, K. Shockley, C. Montero, S. Conners, M. Johnson, and R. Kelly.** 2004. Transcriptional analysis of dynamic heat-shock response by the hyperthermophilic bacterium *Thermotoga maritima*. *Extremophiles* **8**:209-217.
35. **Pysz, M. A., S. C. Conners, C. I. Montero, K. R. Shockley, M. R. Johnson, D. E. Ward, and R. M. Kelly.** 2004. Transcriptional analysis of biofilm formation in the anaerobic hyperthermophilic bacterium *Thermotoga maritima*. *Appl. Environ. Microbiol.* **70**:6098-6112.
36. **Rinker, K. D., and R. M. Kelly.** 2000. Effect of carbon and nitrogen sources on growth dynamics and exopolysaccharide production for the hyperthermophilic archaeon *Thermococcus litoralis* and bacterium *Thermotoga maritima*. *Biotechnol. Bioeng.* **69**:537-547.
37. **Ryjenkov, D. A., M. Tarutina, O. V. Moskvina, and M. Gomelsky.** 2005. Cyclic Diguanylate Is a Ubiquitous Signaling Molecule in Bacteria: Insights into Biochemistry of the GGDEF Protein Domain. *J. Bacteriol.* **187**:1792-1798.
38. **Shockley, K. R., D. E. Ward, S. Chhabra, S. Conners, C. Montero, and R. Kelly.** 2003. Heat shock response by the hyperthermophilic archaeon *Pyrococcus furiosus*. *Appl. Environ. Microbiol.* **69**:2365-2371.
39. **Stoodley, P., S. Wilson, L. Hall-Stoodley, J. D. Boyle, H. M. Lappin-Scott, and J. W. Costerton.** 2001. Growth and detachment of cell clusters from mature mixed-species biofilms. *Appl. Environ. Microbiol.* **67**:5608-5613.

40. **Studholme, D. J., and M. Buck.** 2000. The alternative sigma factor 28 of the extreme thermophile *Aquifex aeolicus* restores motility to an *Escherichia coli* fliA mutant. FEMS Microbiol. Lett. **191**:103-107.
41. **Suresh, C., A. A. Rus'd, M. Kitaoka, and K. Hayashi.** 2002. Evidence that the putative alpha-glucosidase of *Thermotoga maritima* MSB8 is a pNP alpha-D-glucuronopyranoside hydrolyzing alpha-glucuronidase. FEBS Lett. **517**:159-162.
42. **Tal, R., H. C. Wong, R. Calhoon, D. Gelfand, A. L. Fear, G. Volman, R. Mayer, P. Ross, D. Amikam, H. Weinhouse, A. Cohen, S. Sapir, P. Ohana, and M. Benziman.** 1998. Three cdg operons control cellular turnover of cyclic di-GMP in *Acetobacter xylinum*: Genetic organization and occurrence of conserved domains in isoenzymes. J. Bacteriol. **180**:4416-4425.
43. **Tani, T. H., A. Khodursky, R. M. Blumenthal, P. O. Brown, and R. G. Matthews.** 2002. Adaptation to famine: A family of stationary-phase genes revealed by microarray analysis. P. Natl. Acad. Sci. USA **99**:13471-13476.
44. **Tatusov, R., D. Natale, I. Garkavtsev, T. Tatusova, U. Shankavaram, B. Rao, B. Kiryutin, M. Galperin, N. Fedorova, and E. Koonin.** 1997. The COG database: new developments in phylogenetic classification of proteins from complete genomes. Nucleic Acids Res. **29**:22-28.
45. **van Niel, E. W., P. A. Claassen, and A. J. M. Stams.** 2003. Substrate and product inhibition of hydrogen production by the extreme thermophile, *Caldicellulosiruptor saccharolyticus*. Biotechnol. Bioeng. **81**:255-262.
46. **Woese, C. R.** 1998. The universal ancestor. P. Natl. Acad. Sci. USA:6854-6859.
47. **Wolfinger, R., G. Gibson, E. Wolfinger, L. Bennet, H. Hamadeh, P. Bushel, C. Afshari, and R. Paules.** 2001. Assessing gene significance from cDNA microarray expression data via mixed models. J. Comp. Biol. **8**:625-637.
48. **Wu, L. Y., D. K. Thompson, G. S. Li, R. A. Hurt, J. M. Tiedje, and J. Z. Zhou.** 2001. Development and evaluation of functional gene arrays for detection of selected genes in the environment. Appl. Environ. Microbiol. **67**:5780-5790.
49. **Yeiser, B., E. D. Pepper, M. F. Goodman, and S. E. Finkel.** 2002. SOS-induced DNA polymerases enhance long-term survival and evolutionary fitness. P. Natl. Acad. Sci. USA **99**:8737-8741.
50. **Yoon, S., M. Han, S. Lee, K. Jeong, and J. Yoo.** 2003. Combined transcriptome and proteome analysis of *Escherichia coli* during high cell density culture. Biotechnol. Bioeng. **81**:753-767.
51. **Zhang, R. G., T. Skarina, J. E. Katz, S. Beasley, A. Khachatryan, S. Vyas, C. H. Arrowsmith, S. Clarke, A. Edwards, A. Joachimiak, and A. Savchenko.** 2001. Structure of *Thermotoga maritima* stationary phase survival protein SurE: A novel acid phosphatase. Structure **9**:1095-1106.
52. **Zinser, E. R., and R. Kolter.** 2000. Prolonged stationary-phase incubation selects for lrp mutations in *Escherichia coli* K-12. J Bacteriol. **182**:4361-4365.

TABLES

Table 1. Differentially expressed genes in <i>T. maritima</i> during the transition from mid-log (ML) to early stationary phase (ES) in pure culture growth. All fold changes are significant based on the Bonferroni correction.		
Gene_ID	Annotation	Fold-change ES-ML
TM_rnpB	RNAse P RNA	3.0
TM0317	Cation transport ATPase	2.2
TM0373	Molecular chaperone	-5.5
TM0374	small heatshock chaperone	-3.4
TM0456	Ribosomal protein L10	-2.0
TM0504	Predicted signaling peptide (15)	2.2
TM0505	Co-chaperonin GroES	-7.9
TM0506	Chaperonin GroEL	-8.8
TM0571	Trypsin-like serine proteases	2.3
TM0729	ppGpp synthetases	2.5
TM0807	Peroxiredoxin	-3.5
TM0849	DnaJ-class molecular chaperone	-2.3
TM1286	Methionine synthase II	-3.1
TM1369	Possible ABC-type transport system	2.5
TM1370	Possible ABC-type transport system	2.5
TM1371	Selenocysteine lyase	2.8
TM1372	NifU homolog (Fe-S clusters)	2.0
TM1375	Spermidine-binding periplasmic protein	2.0
TM1434	conserved hypothetical protein	2.0
TM1435	Predicted CoA-binding protein	2.0
TM1533	Ferredoxin-like protein	2.2
TM1536	Predicted membrane protein	4.0
TM1867	Malate/lactate dehydrogenases	2.2
TM1874	Cold shock proteins	2.4

Table 2. Carbohydrate-active enzymes and ABC transporters in *T. maritima* that were differentially regulated during the transition from mid-log (ML) to early stationary phase (ES) in co-culture with *M. jannaschii*. No statistically significant fold changes were noted for the same transition in the pure culture. Annotations are based from the work of Connors et al. (9), with the exception of TM0624, and TM0627 which are annotated from the COG database (44).

Gene ID	Annotation	Co-culture ES-ML
TM0024	Laminarinase	3.0
TM0030-31	β -glucan ABC transporter subunits	2.1, 3.4
TM0070	Xylanase	2.2
TM0071	Xylan ABC transporter subunit	7.2
TM0114	Putative monosaccharide ABC transporter subunit	2.5
TM0123	Metal ABC transporter subunit	2.4
TM0300-302	Unknown ABC transporter subunits	3.3, 2.1, 2.0
TM0310	Galactosidase	2.2
TM0418	Maltose ABC transporter subunit	2.2
TM0430-432	Putative pectin ABC transporter subunits	3.1, 2.5, 4.4
TM0433	Pectate lyase	2.4
TM0533	Unknown ABC transporter	-2.1
TM0624	F1 Glycosyltransferase	2.4
TM0627	F1 Glycosyltransferase	-2.0
TM0633	Predicted GH73	2.6
TM0752	Glucuronidase	2.3
TM0767	Maltosyltransferase	-3.3
TM0958	Ribose ABC transporter subunit	2.7
TM1064	Rhamnose ABC transporter subunit	2.0
TM1068	Glucuronidase	1.9
TM1199	Lactose ABC transporter subunit	2.0
TM1223	β -glucan ABC transporter subunit	2.3
TM1227	Mannase	1.9
TM1231	Mannosidase	2.9
TM1232-35	Unknown ABC transporter subunits	3.4, 2.1, 2.7, 5.3
TM1524	Endoglucanase	2.1
TM1525	Endoglucanase	1.8
TM1650	Amylase	2.1
TM1746-49	Mannan ABC transporter subunits	2.1, 2.9, 2.4, 2.1
TM1751	Endoglucanase	2.0
TM1752	Endo mannase	2.0
TM1834	Glucosidase	NC
TM1835	Cyclomaltodextrinase	-1.9
TM1836	Maltose ABC transporter subunit	-2.3
TM1839	Maltose ABC transporter subunit	-2.8
TM1840	Amylase	1.9
TM1848	Cellobiose phosphorylase	2.1
TM1851	Mannosidase	3.0
TM1853-55	Putative sugar ABC transporter subunits	2.9, 5.7, 22.6

Table 3. Confirmation of microarray-based transcriptional results with Real-Time PCR complemented with an independent biological repeat. All microarray-deduced fold changes are significant based on the Bonferroni correction. Real-time PCR data analysis was conducted as previously described (33).

Gene ID	Annotation	Biological Repeat 1	Biological Repeat 2	Biological Repeat 1	Biological Repeat 1	Biological Repeat 2	Biological Repeat 1
		Real-Time PCR Co-culture ES-ML	Real-Time PCR Co-culture ES-ML	Array Results Co-culture ES-ML	Real-Time PCR Pure Culture ES-ML	Real-Time PCR Pure Culture ES-ML	Array Results Pure Culture ES-ML
TM0767	maltosyltransferase	-1.8	-2.6	-3.3	-1.1	-1.0	NC
TM1451	RNA polymerase, sigma A subunit	3.3	2.2	2.0	1.6	1.1	NC
TM1598	RNA polymerase, sigma E subunit	6.6	4.0	5.0	1.3	1.8	NC
TM1662	surE stationary phase survival protein	1.0	-1.3	NC	-1.2	1.1	NC
TM1834	alpha-glucosidase	-1.3	-1.9	NC	-1.1	-1.1	NC

Figure 1A.

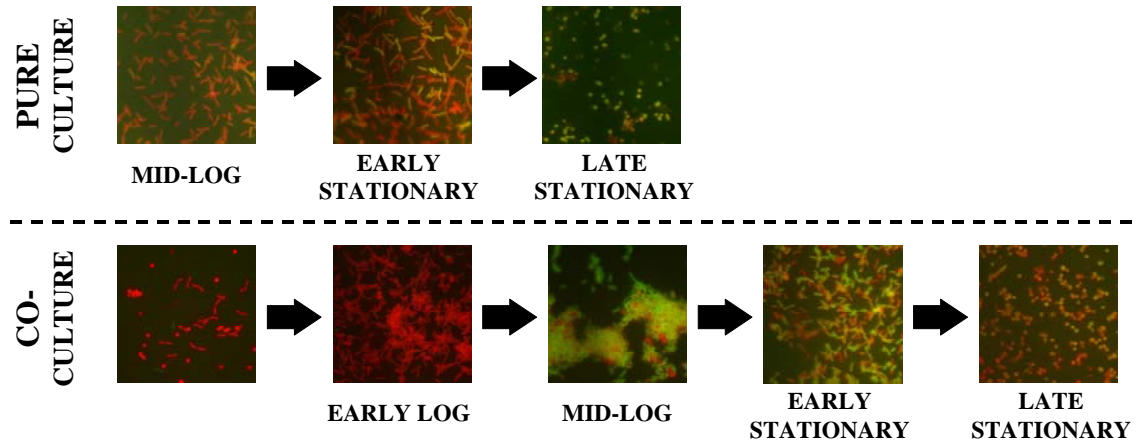


Figure 1B.

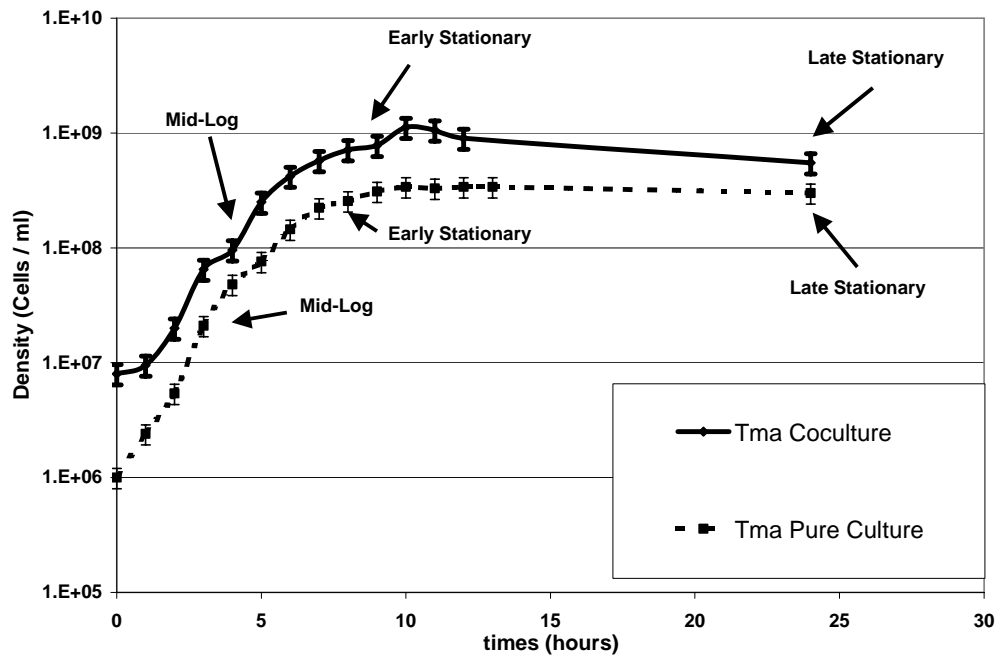


Figure 1C.

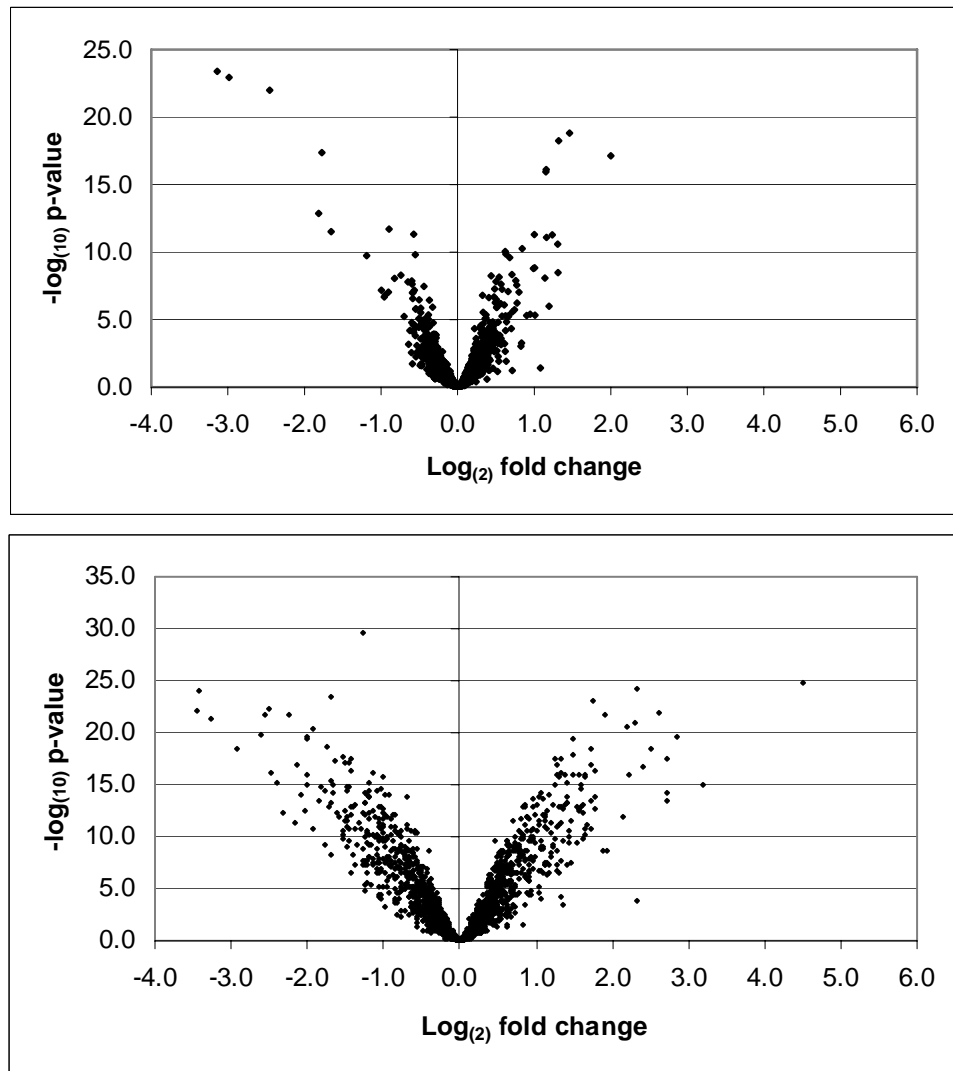


Figure 1. Growth of *T. maritima* in pure culture and in co-culture with *M. jannaschii*.

1A. Epifluorescence micrographs of pure and co-culture corresponding to growth curve are shown from left to right. After inoculation, the pure culture grew without aggregating to a density of above 10^8 cells/ml before entering a prolonged stationary phase during which time *T. maritima* cell morphology changed from rods to cocci. The co-culture began to aggregate once cell densities reached approximately 5×10^8 cells/ml until entering stationary phase ($\sim 10^9$ cells/ml). In stationary phase, cells detached from aggregates and by 24 hours displayed cocci morphology similar to what is seen in the pure culture during late stationary phase.

1B. Growth curves for *T. maritima* grown in pure culture and in co-culture with *M. jannaschii*.

1C. Volcano plots comparing expression profiles of pure (top) *T. maritima* culture and co-culture (bottom) of *T. maritima* with *M. jannaschii* during the transition of growth phases from mid-log to early stationary phase. The x-axis is the log₂ fold change from mid-log to early stationary phase and the y-axis is the $-\log_{10}$ p-value for the calculated fold change.

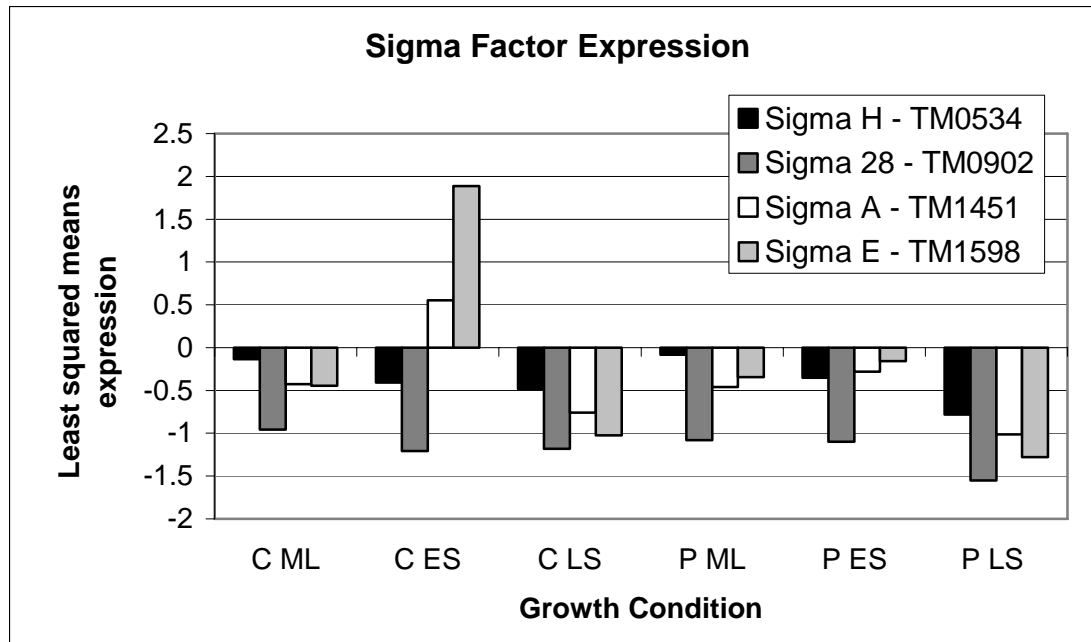


Figure 2. Relative expression as shown by the least squares mean expression of putative sigma factors in *T. maritima* under conditions of hydrogen removal (C, co-culture) compared to that of hydrogen accumulation (P, quiescent pure culture) for mid-log (ML), early stationary (ES), and late stationary (LS) phases transitions.

Table S1. Genes that were significantly differentially expressed in either the sparged pure culture compared to the pure culture, or in the co-culture compared to the pure culture.

gene ID	Fold Change Sparge-Reference	Sparge-ref negative log(10) p-value	Fold Change Coculture-Reference	Co-ref negative log(10) p-value	COG Annotation	TIGR Annotation
TM0002	2.2	10.5	5.2	17.6		hypothetical protein
TM0003	1.3	2.7	2.4	11.8		hypothetical protein
TM0004	4.1	8.1	9.6	12.8		hypothetical protein
TM0015	-3.3	10.6	-6.8	15.3	Pyruvate:ferredoxin oxidoreductase	pyruvate ferredoxin oxidoreductase, gamma
TM0016	-3.7	9.4	-6.4	13.2	Pyruvate:ferredoxin oxidoreductase	pyruvate ferredoxin oxidoreductase, delta
TM0017	-3.1	9.1	-5.8	13.7	Pyruvate:ferredoxin oxidoreductase	pyruvate ferredoxin oxidoreductase, alpha
TM0018	-1.7	8.1	-3.3	15.8	Pyruvate:ferredoxin oxidoreductase	pyruvate ferredoxin oxidoreductase, beta
TM0019	-3.7	9.3	-4.9	11.6	Dehydrogenaseswith different specificities	oxidoreductase, short chain dehydrogenase
TM0020	-2.1	8.3	-1.7	7.0	Integral membrane protein possiblyinvolved	conserved hypothetical protein
TM0027	2.1	7.1	2.7	9.9	ABC-type dipeptide/oligopeptide/nickel transport system,ATPase	oligopeptide ABC transporter, ATP-binding
TM0028	1.9	7.6	2.4	10.8	ABC-type dipeptide/oligopeptide/nickel transport system,ATPase	oligopeptide ABC transporter, ATP-binding
TM0029	2.3	7.2	3.1	10.5	ABC-type dipeptide/oligopeptide/nickel transport systems,permease	oligopeptide ABC transporter, permease
TM0030	2.7	9.0	3.3	11.5	ABC-type dipeptide/oligopeptide/nickel transport systems,permease	oligopeptide ABC transporter, permease
TM0031	2.5	7.5	2.7	8.6	ABC-type dipeptide transport system,periplasmic	oligopeptide ABC transporter, periplasmic
TM0033	2.0	8.6	3.0	13.4	Dipeptidyl aminopeptidases/acylaminoacyl-peptidases	hypothetical protein
TM0034	2.3	11.7	2.3	12.7	Uncharacterized Fe-S center protein	iron-sulfur cluster-binding protein
TM0035	-2.6	16.6	-3.8	27.3		hypothetical protein
TM0036	-2.1	4.7	-2.0	5.0	Predicted nucleotide kinase	conserved hypothetical protein
TM0039	-2.8	10.5	-2.7	11.0	Uncharacterized conserved protein	conserved hypothetical protein
TM0040	-2.6	9.5	-2.0	7.8	Dihydropteroate synthase and relatedenzymes	dihydropteroate synthase
TM0041	-2.5	11.4	-1.4	4.8	7,8-dihydro-6-hydroxymethylpterin-pyrophosphokinase	2-amino-4-hydroxy-6-hydroxymethylidihydrop
TM0043	2.1	8.9	3.5	14.1	ABC-type multidrug transport system,ATPase	ABC transporter, ATP-binding protein
TM0044	6.7	18.2	6.9	19.5		hypothetical protein
TM0047	1.7	6.2	2.1	9.2	Transposase and inactivated derivatives	transposase, putative

Table S1, Continued						
TM0049	2.2	8.1	2.7	11.0	Ferredoxin	iron-sulfur cluster-binding protein
TM0054	1.6	9.0	3.1	16.8		hypothetical protein
TM0056	2.2	7.8	2.3	8.6	ABC-type dipeptide transport system,periplasmic	oligopeptide ABC transporter, periplasmic
TM0059	2.1	5.7	2.8	8.4	ABC-type dipeptide/oligopeptide/nickel transport systems,permease	oligopeptide ABC transporter, permease
TM0063	2.5	7.1	1.4	2.2		hypothetical protein
TM0064	4.3	12.6	2.1	8.2	Glucuronate isomerase	uronate isomerase, putative
TM0067	3.0	4.0	-3.4	5.3	Sugar kinases, ribokinase family	2-keto-3-deoxygluconate kinase
TM0080	2.2	7.8	2.4	9.9	ABC-type Fe ³⁺ -hydroxamate transport system,periplasmic	iron(III) ABC transporter, periplasmic
TM0087	1.9	6.8	2.5	10.1	Predicted dioxygenase	conserved hypothetical protein
TM0088	1.4	3.6	2.0	9.5	Type II secretory pathway,component	comE protein, putative
TM0089	1.9	8.6	2.8	13.5		hypothetical protein
TM0091	1.6	4.0	2.6	9.5		hypothetical protein
TM0092	1.5	6.3	2.8	13.9		hypothetical protein
TM0093	2.3	11.8	3.2	15.9		hypothetical protein
TM0097	1.3	2.3	2.0	8.1	Nicotinic acid mononucleotide adenyltransferase	conserved hypothetical protein
TM0098	1.3	1.4	2.0	6.1	Predicted GTPase	conserved hypothetical protein
TM0101	1.5	4.8	2.1	10.2		hypothetical protein
TM0102	2.1	9.7	2.6	12.6	Uncharacterized ABC-type transport system,periplasmic	basic membrane protein
TM0104	1.5	6.2	2.0	10.9	Uncharacterized ABC-type transport system,permease	sugar ABC transporter, permease protein
TM0105	2.1	7.1	3.0	10.8	Uncharacterized ABC-type transport system,permease	sugar ABC transporter, permease protein
TM0106	2.0	7.3	2.4	10.0	Predicted nuclease (RecB family)	conserved hypothetical protein
TM0112	1.7	4.5	2.3	7.7	Ribose/xylose/arabinose/galactoside ABC-type transporter,permease	sugar ABC transporter, permease protein
TM0121	2.9	8.2	2.1	6.4	Lysine 2,3-aminomutase	conserved hypothetical protein
TM0127	-3.3	4.3	-1.1	0.3	Signal transduction histidine kinase	sensor histidine kinase
TM0135	1.9	7.0	2.3	9.8	Transposase and inactivated derivatives	transposase, putative
TM0136	1.5	3.9	2.0	7.8	Predicted Fe-S-cluster redox enzyme	conserved hypothetical protein
TM0146	-2.1	8.8	-4.4	15.4	ATP-dependent protease Clp, ATPasesubunit	ATP-dependent Clp protease, ATPase
TM0147	-2.8	9.9	-2.9	11.3	Uncharacterized homolog of plantIojap	conserved hypothetical protein
TM0148	-2.8	12.0	-3.3	14.3	Glucosamine 6-phosphate synthetase	glucosamine--fructose-6-phosphate aminotransferase
TM0151	-3.7	11.7	-2.7	10.5	Predicted metal-binding, possibly nucleicacid-binding	conserved hypothetical protein
TM0155	2.3	9.0	1.9	8.3	Prephenate dehydratase	chorismate mutase/prephenate dehydratase
TM0156	2.3	11.5	2.8	14.0	Alkaline phosphatase	alkaline phosphatase
TM0160	1.2	1.8	2.4	9.8	Uncharacterized conserved protein	conserved hypothetical protein

Table S1, Continued						
TM0162	2.5	9.0	3.3	12.0		hypothetical protein
TM0164	1.1	0.6	2.4	10.5	Predicted membrane protein	conserved hypothetical protein
TM0166	1.9	6.7	1.9	7.5	Folylpolyglutamate synthase	folylpolyglutamate synthase/dihydrofolate
TM0173	1.8	6.1	2.1	8.4	Reverse gyrase	reverse gyrase
TM0174	2.1	10.9	1.7	9.3		pyrophosphatase, proton-translocating
TM0179	1.3	2.8	2.3	12.1		hypothetical protein
TM0180	2.1	7.6	1.4	3.7		hypothetical protein
TM0182	1.9	8.2	2.0	10.2	Fe-S oxidoreductase	conserved hypothetical protein
TM0188	1.7	7.8	3.2	14.7	Uncharacterized conserved protein	conserved hypothetical protein
TM0189	1.8	6.4	2.4	10.3	ABC-type Fe ³⁺ -hydroxamate transport system,periplasmic	iron(III) ABC transporter, periplasmic
TM0190	1.9	8.1	2.7	12.7	ABC-type Fe ³⁺ -siderophore transport system,permease	iron(III) ABC transporter, permease prote
TM0191	1.8	9.6	2.6	14.5	ABC-type cobalamin/Fe ³⁺ -siderophores transport systems,ATPase	iron(III) ABC transporter, ATP-binding
TM0192	2.9	12.3	3.9	15.5	Uncharacterized protein conserved inbacteria	spoVS-related protein
TM0193	1.9	8.0	2.2	10.7	ABC-type uncharacterized transport system,permease	conserved hypothetical protein
TM0196	1.1	0.4	2.4	8.3	Uncharacterized conserved protein	conserved hypothetical protein
TM0197	2.5	10.9	2.1	10.6	Predicted ATPase of thePP-loop	conserved hypothetical protein
TM0199	-2.1	7.4	-2.7	10.6	Predicted ATP-dependent serine protease	DNA repair protein
TM0202	1.7	4.6	2.6	9.2	ABC-type nitrate/sulfonate/bicarbonate transporter,periplasmic	hypothetical protein
TM0203	1.7	5.5	2.3	9.5	ABC-type nitrate/sulfonate/bicarbonate transporter,permease	ABC transporter, permease protein, cystTW
TM0208	-5.6	2.9	-17.8	5.9	Pyruvate kinase	pyruvate kinase
TM0209	-2.3	6.7	-4.7	12.2	6-phosphofructokinase	6-phosphofructokinase
TM0212	-1.3	0.9	-2.3	5.2	Glycine cleavage system Hprotein	glycine cleavage system H protein
TM0219	-1.8	6.0	-3.1	11.7	Flagellar biosynthesis/type III secretorypathway	flagellar export/assembly protein
TM0222	1.5	4.4	2.0	9.3	ABC-type cobalt transport system,ATPase	ABC transporter, ATP-binding protein
TM0228	2.6	12.9	3.4	16.1	NADH:ubiquinone oxidoreductase, NADH-binding (51kD)	NADP-reducing hydrogenase, subunit C
TM0231	1.6	6.3	2.2	10.6	UDP-N-acetylmuramate-alanine ligase	UDP-N-acetylmuramate--alanine ligase
TM0233	2.3	9.0	2.8	11.7	Bacterial cell division membraneprotein	cell division protein, rodA/ftsW/spoVE
TM0234	2.6	14.3	3.1	17.0	UDP-N-acetylmuramoylalanine-D-glutamate ligase	UDP-N-acetylmuramoylalanine--D-glutamate
TM0257	-2.0	6.3	-2.3	10.5		
TM0258	-2.5	9.5	-2.1	8.4	Topoisomerase IA	DNA topoisomerase
TM0262	1.7	5.2	2.0	8.0	DNA polymerase sliding clampsubunit	DNA polymerase III, beta subunit
TM0265	-2.0	5.0	-1.5	2.9	Nuclease subunit of theexcinuclease	excinuclease ABC, subunit C
TM0266	2.1	8.1	3.1	12.2	Bacterial nucleoid DNA-binding protein	DNA-binding protein, HU

Table S1, Continued						
TM0267	1.6	4.9	2.0	7.8	Predicted GTPase	thiophene oxidation protein ThdF-related
TM0272	-1.5	6.2	-6.3	19.0	Phosphoenolpyruvate synthase/pyruvate phosphate dikinase	pyruvate, orthophosphate dikinase
TM0273	-2.7	12.6	-4.4	16.7	Fructose/tagatose bisphosphate aldolase	fructose-bisphosphate aldolase
TM0275	-5.3	11.4	-8.0	14.2	Transcriptional regulators	transcriptional regulator, GntR family
TM0277	2.6	10.5	3.3	13.3		
TM0278	2.3	9.5	3.3	13.3	ABC-type sugar transport systems, permease	sugar ABC transporter, permease protein
TM0279	2.7	10.3	3.1	12.3	ABC-type sugar transport system, permease	sugar ABC transporter, permease protein
TM0280	2.5	13.1	3.0	15.6	Uncharacterized protein conserved in bacteria	hypothetical protein
TM0282	1.7	8.3	2.0	11.4	Galactose mutarotase and related enzymes	aldose 1-epimerase
TM0283	2.8	13.2	2.9	14.4	Ribulose-5-phosphate 4-epimerase and related epimerases	sugar isomerase
TM0284	2.1	5.4	1.9	5.1	Sugar (pentulose and hexulose) kinases	sugar kinase, FGGY family
TM0285	1.8	8.7	2.1	11.5	Glycerol dehydrogenase and related enzymes	araM protein, putative
TM0286	2.1	8.8	2.2	10.3	Predicted transcriptional regulators	conserved hypothetical protein
TM0291	1.2	0.7	-2.6	9.7	3-isopropylmalate dehydratase large subunit	3-isopropylmalate dehydratase
TM0293	1.0	0.2	-2.5	10.7	Gamma-glutamyl phosphate reductase	gamma-glutamyl phosphate reductase
TM0295	-2.8	6.8	-2.7	7.5	Transaldolase	transaldolase-related protein
TM0296	2.2	9.4	3.4	13.8	Sugar kinases, ribokinase family	fructokinase
TM0306	2.0	5.1	-2.8	8.4		alpha-L-fucosidase, putative
TM0309	2.5	7.6	1.7	4.6	ABC-type dipeptide transport system, periplasmic	oligopeptide ABC transporter, periplasmic
TM0330	1.7	5.4	2.2	8.6	Predicted metal-dependent hydrolase with the	conserved hypothetical protein
TM0335	1.9	10.6	2.3	13.4	Dihydroorotase and related cyclic amidohydrolases	dihydroorotase
TM0336	2.3	10.0	2.6	12.3	Hydrolases of the alpha/beta superfamily	conserved hypothetical protein
TM0337	2.3	7.2	2.9	9.8	Fe-S oxidoreductase	conserved hypothetical protein
TM0343	2.4	8.8	2.6	10.4	3-deoxy-D-arabino-heptulosonate 7-phosphate (DAHP) synthase	chorismate mutase, putative
TM0345	2.8	11.6	3.0	13.2	5-enolpyruvylshikimate-3-phosphate synthase	3-phosphoshikimate-1-carboxyvinyltransferase
TM0347	2.0	8.0	2.3	10.0	Chorismate synthase	chorismate synthase
TM0348	2.5	13.2	2.2	13.2	Shikimate kinase	shikimate kinase/3-dehydroquinate synthase
TM0352	-3.4	6.0	-1.4	1.6	ABC-type antimicrobial peptide transport system,	ABC transporter, ATP-binding protein
TM0356	2.1	9.6	2.3	11.4	Threonine dehydratase	threonine dehydratase catabolic
TM0358	1.9	9.2	2.2	12.0	Sphingosine kinase and enzymes related	conserved hypothetical protein
TM0362	2.1	7.5	2.0	7.2	Endonuclease IV	deoxyribonuclease IV
TM0363	2.3	10.6	2.2	11.5	Predicted RNA-binding protein homologous to	fibronectin-binding protein, putative
TM0365	1.0	0.0	-2.2	4.9	Aspartyl aminopeptidase	aminopeptidase, putative

Table S1, Continued						
TM0366	1.7	7.2	2.0	10.0	Predicted EndoIII-related endonuclease	endonuclease III
TM0368	2.8	13.6	3.5	16.4	Permeases of the major facilitator	Permeases of the major facilitator superfamily
TM0371	1.1	0.3	3.0	6.9	Arginine repressor	arginine repressor
TM0374	-1.1	0.3	-2.7	9.3	Molecular chaperone (small heatshock	heat shock protein, class I
TM0381	-2.3	7.7	-5.9	14.5	Pyruvate/2-oxoglutarate dehydrogenase complex	dihydrolipoamide dehydrogenase
TM0384	-6.0	7.4	-1.6	1.6		anaerobic ribonucleoside-triphosphate
TM0388	1.5	6.7	2.0	11.4	ABC-type multidrug transport system,permease	ABC-type multidrug transport system, permease
TM0390	3.6	11.3	8.8	16.8		hypothetical protein
TM0391	1.6	6.4	2.8	13.0		hypothetical protein
TM0394	-2.9	4.4	-4.4	7.0	Glutamate synthase domain 3	conserved hypothetical protein
TM0395	-3.0	4.0	-38.0	13.2	Uncharacterized NAD(FAD)-dependent dehydrogenases	NADH oxidase, putative
TM0396	-3.5	8.8	-19.2	16.8	Fe-S-cluster-containing hydrogenase components 2	iron-sulfur cluster-binding protein
TM0397	-1.1	0.2	-3.3	9.9	Glutamate synthase domain 2	glutamate synthase, alpha subunit
TM0399	-1.9	5.5	-2.3	7.8	Response regulators consisting of aCheY-like	response regulator
TM0409	1.7	5.7	2.2	9.5	Membrane proteins related to metalloendopeptidases	conserved hypothetical protein
TM0412	2.7	13.6	3.2	16.1	Threonine dehydrogenase and related Zn-dependent	alcohol dehydrogenase, zinc-containing
TM0413	2.5	12.9	2.9	15.2	Uncharacterized protein, putative amidase	creatinine amidohydrolase, putative
TM0414	2.4	11.8	2.7	13.9	Predicted dehydrogenases and related proteins	dehydrogenase
TM0416	2.0	7.7	2.3	9.9	Sugar phosphate isomerases/epimerases	D-tagatose 3-epimerase-related protein
TM0419	1.8	9.9	2.3	13.8	ABC-type sugar transport systems,permease	sugar ABC transporter, permease protein
TM0420	2.4	11.1	2.8	13.2	ABC-type sugar transport system,permease	sugar ABC transporter, permease protein
TM0423	1.9	4.7	-7.2	13.4	Glycerol dehydrogenase and related enzymes	glycerol dehydrogenase
TM0424	2.0	6.3	2.6	9.6	Predicted permeases	conserved hypothetical protein
TM0429	-2.8	7.6	-3.1	9.5	Methyl-accepting chemotaxis protein	methyl-accepting chemotaxis protein
TM0432	2.6	4.4	-1.2	0.5	ABC-type sugar transport system,periplasmic	sugar ABC transporter, periplasmic
TM0439	-1.3	1.8	-2.2	8.2	Transcriptional regulators	transcriptional regulator, GntR family
TM0440	1.8	4.3	2.3	6.8		hypothetical protein
TM0455	-1.8	4.3	-2.1	6.1	Ribosomal protein L1	ribosomal protein L1
TM0456	2.4	6.7	4.9	12.0	Ribosomal protein L10	ribosomal protein L10
TM0457	3.5	7.8	8.2	12.7	Ribosomal protein L7/L12	ribosomal protein L7/L12
TM0459	-2.7	7.9	-2.5	7.8	DNA-directed RNA polymerase, beta'subunit/160	DNA-directed RNA polymerase, beta' subunit
TM0465	-2.9	4.8	-3.5	6.6		hypothetical protein
TM0466	-3.2	8.7	-7.9	14.3	Uncharacterized conserved protein	conserved hypothetical protein

Table S1, Continued						
TM0467	-3.8	8.6	-3.1	8.2	Serine phosphatase RsbU, regulator of	regulatory protein, putative
TM0472	-1.9	8.7	-2.1	11.3	Predicted glutamine amidotransferase involved in	amidotransferase, putative
TM0474	1.8	5.3	2.0	7.0	Nicotinic acid phosphoribosyltransferase	conserved hypothetical protein
TM0475	1.6	4.2	2.0	7.3	Amidases related to nicotinamidase	pyrazinamidase/nicotinamidase-related protein
TM0480	-2.0	8.2	-1.6	6.1	Excinuclease ATPase subunit	excinuclease ABC, subunit A
TM0481	2.0	8.9	2.0	9.7	Uncharacterized conserved protein	conserved hypothetical protein
TM0482	2.2	8.9	1.9	8.6	Activator of 2-hydroxyglutaryl-CoA dehydratase (HSP70-class)	(R)-2-hydroxyglutaryl-CoA dehydratase
TM0484	2.4	11.0	1.7	7.5	ABC-type nitrate/sulfonate/bicarbonate transporter, periplasmic	pyrimidine precursor biosynthesis enzyme
TM0485	2.4	12.1	2.4	13.2	ABC-type nitrate/sulfonate/bicarbonate transport system, permease	ABC transporter, permease protein, cysteine
TM0488	1.9	8.3	1.5	6.0	Methylase of polypeptide chain release	hemK protein
TM0494	1.8	7.9	2.0	9.7	Predicted transcriptional regulator containing the	conserved hypothetical protein
TM0499	2.2	8.7	2.5	11.1		hypothetical protein
TM0500	1.9	7.7	2.4	10.6	ABC-type dipeptide/oligopeptide/nickel transport system, ATPase	oligopeptide ABC transporter, ATP-binding
TM0502	2.9	10.0	3.1	11.3	ABC-type dipeptide/oligopeptide/nickel transport system, permease	oligopeptide ABC transporter, permease
TM0503	2.0	11.6	2.5	14.7	ABC-type dipeptide/oligopeptide/nickel transport system, permease	oligopeptide ABC transporter, permease
TM0504	3.2	11.9	13.0	19.5		hypothetical protein
TM0505	3.7	9.9	-1.7	4.6	Co-chaperonin GroES (HSP10)	groES protein
TM0506	3.9	9.6	-3.5	9.8	Chaperonin GroEL (HSP60 family)	groEL protein
TM0510	-1.8	8.3	-3.6	15.9	Mn-dependent transcriptional regulator	iron-dependent transcriptional repressor,
TM0511	-1.5	1.8	-2.0	4.2	Uracil-DNA glycosylase	conserved hypothetical protein
TM0514	2.1	4.5	1.5	2.6	Prolyl-tRNA synthetase	prolyl-tRNA synthetase
TM0515	2.4	15.1	2.9	17.8	Predicted Fe-S oxidoreductase	conserved hypothetical protein
TM0516	1.3	1.3	2.5	7.8		clostripain-related protein
TM0519	2.2	7.5	1.9	7.1	GAF domain-containing protein	conserved hypothetical protein
TM0522	-1.3	3.1	-2.3	10.5	ATP-dependent protease HslVU (ClpYQ), ATPase	heat shock protein HslU
TM0525	2.0	7.3	2.3	9.4	tRNA delta(2)-isopentenylpyrophosphate transferase	tRNA delta-2-isopentenylpyrophosphate transferase
TM0528	1.8	6.0	2.1	8.6	Methionyl-tRNA formyltransferase	methionyl-tRNA formyltransferase
TM0533	1.6	3.7	2.7	9.0	ABC-type dipeptide/oligopeptide/nickel transporter, permease	oligopeptide ABC transporter, permease protein
TM0535	1.4	2.1	2.7	7.7		hypothetical protein
TM0537	2.6	12.0	2.7	13.6		hypothetical protein

Table S1, Continued						
TM0542	2.0	6.9	1.9	7.1	Malic enzyme	malate oxidoreductase
TM0545	-1.5	3.2	-2.7	9.9	Homoserine kinase	homoserine kinase, putative
TM0546	-1.3	0.9	-2.5	5.9	Threonine synthase	threonine synthase
TM0547	-1.9	8.4	-2.6	12.4	Homoserine dehydrogenase	aspartokinase II
TM0548	-1.4	2.1	-2.0	5.6	Thiamine pyrophosphate-requiring enzymes	acetolactate synthase, large subunit
TM0549	-2.5	7.0	-11.6	15.6	Acetolactate synthase, small (regulatory) subunit	acetolactate synthase, small subunit
TM0550	-1.2	1.0	-2.7	9.4	Ketol-acid reductoisomerase	ketol-acid reductoisomerase
TM0552	-1.4	1.2	-2.4	4.7	Isopropylmalate/homocitrate/citramalate synthases	2-isopropylmalate synthase, putative
TM0553	-1.4	1.6	-2.4	6.2	Isopropylmalate/homocitrate/citramalate synthases	2-isopropylmalate synthase
TM0554	-1.5	2.2	-2.6	7.0	3-isopropylmalate dehydratase large subunit	3-isopropylmalate dehydratase
TM0558	2.1	5.2	-1.2	1.2	Carbamoylphosphate synthase small subunit	carbamoyl-phosphate synthetase
TM0560	-1.1	0.9	2.6	12.1	Protein distantly related to bacterial	conserved hypothetical protein
TM0572	1.8	6.4	2.0	8.3	Predicted pyridoxal phosphate-dependent enzyme apparently	lipopolysaccharide biosynthesis protein,
TM0576	-2.2	10.8	-1.3	4.9	DNA polymerase III, alpha subunit	DNA polymerase III, alpha subunit
TM0578	2.2	11.6	2.7	14.5	Pyrroline-5-carboxylate reductase	pyrroline-5-carboxylate reductase
TM0590	1.9	6.0	3.0	10.9	Cell division protein FtsI/penicillin-binding protein	penicillin-binding protein 2
TM0591	2.4	10.3	1.7	7.5	ABC-type polar amino acid transport	amino acid ABC transporter, ATP-binding
TM0592	2.7	9.7	2.2	8.7	ABC-type amino acid transport system,	amino acid ABC transporter, permease
TM0593	8.7	18.8	2.2	10.9	ABC-type amino acid transport/signal transduction	amino acid ABC transporter
TM0594	2.8	11.8	2.7	12.7	Permeases	conserved hypothetical protein
TM0595	5.7	16.7	3.2	14.5	ABC-type sugar transport system, periplasmic	sugar ABC transporter, periplasmic
TM0596	2.4	9.8	2.6	11.4	ABC-type sugar transport systems, permease	sugar ABC transporter, permease protein
TM0597	1.9	6.5	2.7	10.5		hypothetical protein
TM0598	2.3	8.6	2.7	10.2	ABC-type sugar transport system, permease	sugar ABC transporter, permease protein
TM0599	2.3	9.2	1.9	8.4		hypothetical protein
TM0600	1.8	7.9	2.0	9.3	Uncharacterized FAD-dependent dehydrogenases	conserved hypothetical protein
TM0606	-1.4	3.0	2.1	8.5		hypothetical protein
TM0607	1.0	0.0	2.3	9.1	Zn-dependent hydrolases, including glyoxylases	hypothetical protein
TM0616	3.1	7.6	1.9	5.1	Predicted ATPase (AAA+ superfamily)	conserved hypothetical protein
TM0624	-1.1	0.9	2.6	10.2	Glycosyltransferase	N-acetylglucosaminyl-phosphatidylinositol
TM0625	1.9	4.6	4.5	10.9		hypothetical protein
TM0626	1.8	5.5	2.8	10.4	Uncharacterized proteins of the AP	hypothetical protein
TM0629	1.6	3.1	2.9	8.8		hypothetical protein
TM0656	-2.3	4.3	-1.7	2.8	Predicted transcriptional regulators	conserved hypothetical protein

Table S1, Continued						
TM0665	2.6	7.8	1.2	1.2	Cysteine synthase	cysteine synthase
TM0666	2.5	4.8	1.2	0.6	Serine acetyltransferase	serine acetyltransferase
TM0669	2.1	5.7	1.9	5.6		hypothetical protein
TM0686	-1.1	0.5	-2.7	9.6	DNA polymerase III, gamma/tausubunits	DNA polymerase III, gamma and tau subunit
TM0687	-2.4	3.9	-13.7	12.1	Uncharacterized protein conserved inbacteria	conserved hypothetical protein
TM0688	-1.1	0.6	-5.0	14.0	Glyceraldehyde-3-phosphate dehydrogenase	glyceraldehyde-3-phosphate dehydrogenase
TM0689	-1.7	3.5	-7.0	13.7	3-phosphoglycerate kinase	phosphoglycerate kinase/triose-phosphate
TM0690	-4.3	9.1	-7.8	12.7	Uncharacterized conserved protein	conserved hypothetical protein
TM0691	-3.2	10.6	-5.5	14.7	SAM-dependent methyltransferases	conserved hypothetical protein
TM0692	-2.8	6.2	-2.4	5.8	Phosphopantetheinyl transferase (holo-ACP synthase)	holo-(acyl carrier protein) synthase
TM0693	-8.2	12.7	-9.6	14.3		hypothetical protein
TM0694	-4.9	11.2	-8.4	14.2	FKBP-type peptidyl-prolyl cis-trans isomerase	trigger factor, putative
TM0695	-2.1	9.8	-2.5	12.4	Protease subunit of ATP-dependentClp	ATP-dependent Clp protease, proteolytic
TM0701	-1.8	6.1	-2.8	11.1	Chemotaxis signal transduction protein	purine-binding chemotaxis protein
TM0702	-2.6	8.1	-4.5	12.4	Chemotaxis protein histidine kinaseand	chemotaxis sensor histidine kinase CheA
TM0705	1.9	7.0	2.0	8.0	ABC-type antimicrobial peptide transportsystem,	ABC transporter, ATP-binding protein
TM0707	1.9	6.9	2.1	9.1	Predicted S-adenosylmethionine-dependent methyltransferase	glucose-inhibited division protein B
TM0714	-2.5	9.8	-3.5	13.5		hypothetical protein
TM0717	-6.7	13.6	-11.8	16.9	Biotin carboxyl carrier protein	propionyl-CoA carboxylase, gamma subunit
TM0718	-1.9	5.8	-2.2	8.4	Chemotaxis signal transduction protein	purine-binding chemotaxis protein
TM0720	-1.9	5.9	-2.4	9.3	Glycine/serine hydroxymethyltransferase	serine hydroxymethyltransferase
TM0721	-2.8	10.2	-4.5	14.2	Uracil phosphoribosyltransferase	uracil phosphoribosyltransferase
TM0728	2.6	10.3	3.5	13.6	Permeases of the drug/metabolitetransporter	conserved hypothetical protein
TM0729	2.2	8.2	3.9	13.6	Guanosine polyphosphate pyrophosphohydrolases/synthetases	(p)ppGpp synthetase
TM0747	-1.2	1.6	-2.0	9.7	Periplasmic protease	carboxyl-terminal protease
TM0753	-2.0	5.4	-3.0	9.5	Methylase involved in ubiquinone/menaquinonebiosynthesis	ubiquinone/menaquinone biosynthesis methylase
TM0755	-1.3	1.9	-3.0	9.8	Uncharacterized flavoproteins	conserved hypothetical protein
TM0756	-2.7	4.5	-3.0	5.6	FOG: TPR repeat	galactosyltransferase-related protein
TM0762	-2.1	7.6	-1.3	2.9	Ribosomal protein S2	ribosomal protein S2
TM0765	1.7	6.4	2.2	9.9	ABC-type multidrug transport system,ATPase	ABC transporter, ATP-binding protein
TM0769	-1.9	1.3	-1414.4	15.7	Phosphomannomutase	phosphomannomutase
TM0770	-2.0	10.6	-2.4	13.6	Fe-S oxidoreductase	conserved hypothetical protein

TM0772	-2.0	5.3	-1.8	5.0	Uncharacterized homolog of PSP1	conserved hypothetical protein
TM0780	2.2	9.8	1.7	7.4	Peroxiredoxin	bacterioferritin comigratory protein, ahp
TM0786	-1.3	2.0	-2.3	9.7	Uncharacterized conserved protein	hypothetical protein
TM0802	1.9	8.7	2.0	10.1	3-oxoacyl-(acyl-carrier-protein) synthase	3-oxoacyl-(acyl carrier protein) synthase
TM0803	-1.8	10.8	-2.0	13.2	CTP synthase (UTP-ammonia lyase)	CTP synthetase
TM0804	-1.7	6.9	-2.4	11.5	Histidinol phosphatase and related hydrolases	conserved hypothetical protein
TM0805	-2.7	9.4	-2.6	10.1	UDP-N-acetylmuramyl pentapeptide phosphotransferase	lipophilic protein, putative
TM0806	1.6	5.0	2.0	8.2		hypothetical protein
TM0807	1.5	5.5	2.3	11.6	Peroxiredoxin	alkyl hydroperoxide reductase, putative
TM0810	1.9	6.7	2.1	8.9	ABC-type sugar transport system, periplasmic	sugar ABC transporter, periplasmic
TM0811	2.6	10.2	2.8	11.8	ABC-type sugar transport systems, permease	sugar ABC transporter, permease protein
TM0812	2.1	4.7	2.6	6.9	ABC-type sugar transport system, permease	sugar ABC transporter, permease protein,
TM0815	2.0	9.6	3.9	16.0	Na ⁺ -driven multidrug efflux pump	conserved hypothetical protein
TM0817	2.0	13.3	2.1	15.0	Predicted exporters of the RND	hypothetical protein
TM0818	1.1	0.5	2.0	5.7	Teichoic acid biosynthesis proteins	lipopolysaccharide biosynthesis protein,
TM0823	1.2	0.7	-2.8	6.0	Transcriptional regulator	transcriptional regulator, TetR family
TM0835	1.6	2.6	2.6	7.0	Actin-like ATPase involved in cell	cell division protein FtsA, putative
TM0842	-2.0	6.4	-2.7	10.0	FOG: CheY-like receiver	response regulator
TM0849	5.8	13.8	1.1	0.4	DnaJ-class molecular chaperone with C-terminal	dnaJ protein
TM0852	2.4	10.6	2.6	12.0	Putative translation factor (SUA5)	conserved hypothetical protein
TM0866	-1.9	5.4	-3.7	11.2	Membrane protease subunits, stomatin/prohibitin homologs	conserved hypothetical protein
TM0870	-1.2	1.3	2.0	9.1	Cell division protein FtsI/penicillin-binding protein	penicillin-binding protein 2
TM0872	-2.2	6.9	-1.7	5.3	Predicted S-adenosylmethionine-dependent methyltransferase	conserved hypothetical protein
TM0874	-3.2	13.0	-2.7	12.8	Inactive homolog of metal-dependent proteases,	conserved hypothetical protein
TM0877	-1.5	2.6	-2.9	8.2	Enolase	enolase
TM0882	2.3	9.8	1.4	4.8	O-acetylhomoserine sulfhydrylase	O-acetylhomoserine sulfhydrylase
TM0896	-2.1	7.7	-3.2	12.3	Galactose-1-phosphate uridylyltransferase	galactose-1-phosphate uridylyltransferase
TM0902	-2.4	4.5	-2.5	5.5	DNA-directed RNA polymerase specialized	RNA polymerase sigma-28 factor, putative
TM0904	-2.0	7.9	-1.6	6.1	Chemotaxis protein CheC, inhibitor of	chemotaxis protein CheC
TM0908	1.5	5.4	2.1	10.7	Flagellar biosynthesis pathway, component FlhA	flagellar biosynthesis protein FlhA
TM0918	-1.5	4.1	-2.2	9.1	Methyl-accepting chemotaxis protein	methyl-accepting chemotaxis protein
TM0922	1.3	3.1	2.0	9.0	Uncharacterized conserved protein	conserved hypothetical protein
TM0923	1.8	8.1	2.0	10.6		hypothetical protein
TM0924	1.6	4.0	2.0	7.1	Uncharacterized Fe-S protein PflX, homolog	conserved hypothetical protein

Table S1, Continued						
TM0927	2.7	9.5	3.1	11.4	Ferredoxin	ferredoxin
TM0932	1.4	3.7	2.0	8.5	Predicted endonuclease distantly related to	conserved hypothetical protein
TM0935	2.0	6.2	2.7	8.9	FOG: CBS domain	conserved hypothetical protein
TM0943	-1.4	2.5	-3.2	11.0	Glutamine synthetase	glutamine synthetase
TM0949	-2.2	5.1	-1.1	0.3	Transcriptional regulators	transcriptional regulator, LacI family
TM0953	2.1	9.3	2.5	11.9		
TM0955	2.0	6.9	2.5	9.5	Ribose/xylose/arabinose/galactoside ABC-type transporter, permease	ribose ABC transporter, permease protein
TM0956	2.1	7.2	2.3	8.9	ABC-type sugar transport system, ATPase	ribose ABC transporter, ATP-binding protein
TM0960	1.9	8.4	2.1	10.6	Sugar kinases, ribokinase family	ribokinase
TM0962	2.0	9.3	2.5	12.7	Beta-propeller domains of methanol dehydrogenase	conserved hypothetical protein
TM0964	2.3	11.5	1.8	9.9	Uncharacterized conserved protein	conserved hypothetical protein
TM0968	1.4	1.7	2.7	7.6	Acetyltransferases, including N-acetylases of ribosomal	conserved hypothetical protein
TM0978	2.2	10.0	2.3	11.6	Predicted redox protein, regulator of	conserved hypothetical protein
TM0979	2.0	5.4	-1.3	1.9	Uncharacterized conserved protein involved in	conserved hypothetical protein
TM0980	2.1	2.3	-3.5	5.0	Uncharacterized protein involved in the	Uncharacterized protein involved in the oxidation
TM0982	2.8	8.3	-1.0	0.2	Predicted transporter component	conserved hypothetical protein
TM0983	2.2	8.2	-1.3	3.2	Predicted redox protein, regulator of	conserved hypothetical protein
TM0985	2.2	7.7	1.7	5.6		hypothetical protein
TM0986	1.6	4.5	2.2	8.3	Uncharacterized protein conserved in bacteria	conserved hypothetical protein
TM0989	2.8	13.3	1.4	5.5		conserved hypothetical protein
TM1000	2.1	7.5	2.7	10.9	Uncharacterized conserved protein related to	conserved hypothetical protein
TM1001	2.4	10.4	3.0	13.4	Predicted nucleotidyltransferases	conserved hypothetical protein
TM1007	1.9	6.9	2.2	9.5		
TM1011	2.3	9.6	2.6	11.9	Predicted ATPase (AAA+ superfamily)	conserved hypothetical protein
TM1027	2.9	14.5	2.3	13.7		hypothetical protein
TM1032	1.7	5.3	2.2	9.3	Permeases of the major facilitator	permease, putative
TM1033	-2.5	2.8	-4.5	5.9	Mannose-1-phosphate guanylyltransferase	mannose-1-phosphate guanylyltransferase
TM1054	-1.6	5.4	-2.1	9.7	ABC-type (unclassified) transport system, ATPase	ABC transporter, ATP-binding protein
TM1056	1.9	8.6	2.6	12.4	Uncharacterized protein involved in tolerance	periplasmic divalent cation tolerance protein
TM1057	1.8	7.5	2.6	11.9	Kef-type K ⁺ transport systems, predicted	potassium channel, putative
TM1059	5.9	17.1	5.2	17.6	Uncharacterized protein conserved in bacteria	spoVS-related protein
TM1060	1.7	6.6	2.0	9.8	Permeases of the major facilitator	conserved hypothetical protein

Table S1, Continued						
TM1063	1.9	6.5	2.2	8.7	ABC-type dipeptide/oligopeptide/nickel transport system,ATPase	oligopeptide ABC transporter, ATP-binding
TM1066	1.8	7.4	2.0	9.3	ABC-type dipeptide/oligopeptide/nickel transport systems,permease	oligopeptide ABC transporter, permease
TM1067	2.1	7.8	2.2	9.2	ABC-type dipeptide transport system,periplasmic	oligopeptide ABC transporter, periplasmic
TM1082	-1.8	7.2	-2.9	12.8	SOS-response transcriptional repressors	lexA repressor
TM1083	-1.4	1.0	-3.0	6.4	Uncharacterized conserved protein	conserved hypothetical protein
TM1088	1.7	6.5	2.1	10.0		
TM1101	1.9	8.3	2.0	9.4	Predicted phosphoesterase	conserved hypothetical protein
TM1103	1.8	6.1	2.0	8.2	Histone acetyltransferase	conserved hypothetical protein
TM1104	2.6	12.2	3.0	14.7	Multisubunit Na ⁺ /H ⁺ antiporter, MnhCsubunit	conserved hypothetical protein
TM1105	2.5	9.0	3.0	11.4	Formate hydrogenlyase subunit 3/MultisubunitNa ⁺ /H ⁺	NADH dehydrogenase, putative
TM1106	1.8	6.3	2.0	8.5		hypothetical protein
TM1112	2.4	8.8	-1.0	0.2	Predicted enzyme of thecupin	hypothetical protein
TM1115	1.7	10.3	2.2	14.4		hypothetical protein
TM1116	1.8	8.4	2.1	10.9		hypothetical protein
TM1117	1.7	8.0	2.1	11.0	Type II secretory pathway,component	general secretion pathway protein D
TM1118	1.9	6.8	2.4	9.7		hypothetical protein
TM1122	1.8	4.4	2.0	6.0	ABC-type sugar transport system,permease	glycerol-3-phosphate ABC transporter, permease
TM1136	1.8	6.1	2.1	8.6	Branched-chain amino acid ABC-typertransport	branched chain amino acid ABC transporter
TM1137	1.9	9.1	2.4	12.5	Branched-chain amino acid ABC-typertransport	branched chain amino acid ABC transporter
TM1150	2.2	7.6	1.4	3.6	ABC-type dipeptide transport system,periplasmic	oligopeptide ABC transporter, periplasmic
TM1151	2.2	6.3	1.5	3.7	ABC-type dipeptide/oligopeptide/nickel transport system,ATPase	oligopeptide ABC transporter, ATP-binding
TM1152	1.9	5.4	1.4	2.9	ABC-type dipeptide/oligopeptide/nickel transport system,ATPase	oligopeptide ABC transporter, ATP-binding
TM1153	2.5	8.1	2.7	9.7	ABC-type dipeptide/oligopeptide/nickel transport systems,permease	oligopeptide ABC transporter, permease
TM1155	-1.3	0.7	-2.3	4.4	Glucose-6-phosphate 1-dehydrogenase	glucose-6-phosphate 1-dehydrogenase
TM1158	2.0	7.1	2.7	10.6	GMP synthase - Glutamineamidotransferase	conserved hypothetical protein
TM1159	1.7	5.6	2.0	8.1		hypothetical protein
TM1165	-2.1	6.3	-1.6	4.7	Pyruvate:ferredoxin oxidoreductase	2-oxoacid ferredoxin oxidoreductase, beta
TM1167	-1.1	0.6	3.4	13.4		hypothetical protein
TM1169	1.9	7.8	1.9	8.6	Dehydrogenaseswith different specificities	3-oxoacyl-(acyl carrier protein) reductase

Table S1, Continued						
TM1170	2.5	9.7	2.8	11.8	HD-GYP domain	ABC transporter, periplasmic
TM1184	-3.4	8.9	-2.6	7.6	FOG: GGDEF domain	pleD-related protein
TM1191	1.9	9.0	2.0	11.0	Galactose-1-phosphate uridylyltransferase	galactose-1-phosphate uridylyltransferase
TM1204	1.6	3.3	2.2	6.9	Maltose-binding periplasmic proteins/domains	maltose ABC transporter, periplasmic malt
TM1224	-2.1	4.3	-2.8	6.7	Transcriptional regulator/sugar kinase	transcriptional regulator, XylR-related
TM1226	-1.2	0.5	-2.5	5.4	ABC-type dipeptide transport system,periplasmic	oligopeptide ABC transporter, periplasmic
TM1232	1.5	3.7	2.0	7.7		sugar ABC transporter, ATP-binding protein
TM1240	-2.3	8.9	-1.5	5.1	Predicted GTPase, probable translation factor	conserved hypothetical protein
TM1241	-5.5	4.0	-2.1	1.5		hypothetical protein
TM1243	-1.1	0.3	-4.4	15.1	Phosphoribosylaminoimidazolesuccinocarboxamide (SAICAR)	phosphoribosylaminoimidazole-succinocarboxamide
TM1244	-1.7	1.9	-3.1	5.8	Phosphoribosylformylglycinamide (FGAM) synthase	conserved hypothetical protein
TM1245	-2.0	0.8	-12.5	4.6	Phosphoribosylformylglycinamide (FGAM) synthase	phosphoribosylformylglycinamide synthase
TM1246	1.1	0.3	-2.0	6.2	Phosphoribosylformylglycinamide (FGAM) synthase	phosphoribosylformylglycinamide synthase
TM1249	-1.2	0.9	-2.1	5.4	AICAR transformylase/IMP cyclohydrolase PurH	phosphoribosylaminoimidazolecarboxamide
TM1250	-1.3	2.1	-2.0	6.9	Phosphoribosylamine-glycine ligase	phosphoribosylamine--glycine ligase
TM1263	1.7	5.0	2.0	7.2	ABC-type phosphate transport system,permease	phosphate ABC transporter, permease protein
TM1265	-1.1	0.5	2.4	7.5	Predicted ATPase (AAA+ superfamily)	conserved hypothetical protein
TM1266	1.1	0.7	2.0	8.6		hypothetical protein
TM1271	2.3	5.2	2.6	6.7	Type II secretory pathway,pseudopilin	type IV pilin-related protein
TM1273	1.0	0.1	-2.7	7.5	Asp-tRNAAsn/Glu-tRNAGln amidotransferase B subunit	glutamyl tRNA-Gln amidotransferase
TM1276	2.3	9.5	2.6	11.6		sugar ABC transporter, ATP-binding protein
TM1286	-1.7	4.2	-2.3	7.0	Methionine synthase II (cobalamin-independent)	5-methyltetrahydropteroyltriglutamate
TM1287	-2.3	8.5	-1.5	4.9	Mannose-6-phosphate isomerase	conserved hypothetical protein
TM1288	-2.9	10.0	-2.4	9.2	Fe-S oxidoreductases	conserved hypothetical protein
TM1289	-2.0	6.9	-2.2	8.4	Ferredoxin	ferredoxin
TM1290	-1.9	4.9	-2.1	6.1	Uncharacterized conserved protein	conserved hypothetical protein
TM1291	-5.2	12.2	-4.0	11.6	MinD superfamily P-loop ATPasecontaining	iron-sulfur cluster-binding protein
TM1297	2.3	11.2	2.9	14.1	Predicted oxidoreductases	oxidoreductase, putative
TM1322	1.8	8.3	2.5	12.2		conserved hypothetical protein

Table S1, Continued						
TM1323	2.3	10.7	2.7	13.4		hypothetical protein
TM1340	2.0	6.6	2.6	9.6	Ferredoxin subunits of nitrite reductase	oxidase-related protein
TM1343	1.5	3.1	2.2	7.5		
TM1346	-3.1	7.6	-4.1	10.1	Predicted Zn-dependent peptidases	processing protease, putative
TM1352	2.5	9.7	1.9	8.1	Predicted metal-dependent phosphoesterases (PHPfamily)	hypothetical protein
TM1360	-2.9	4.7	-6.9	9.5	FOG: CheY-like receiver	response regulator
TM1363	-2.9	11.2	-5.4	15.9	Protein chain release factorA	peptide chain release factor RF-1
TM1381	-1.9	3.9	-3.1	7.7		hypothetical protein
TM1382	-2.2	7.0	-2.4	8.8		conserved hypothetical protein
TM1389	3.0	9.9	3.9	12.9	SAM-dependent methyltransferases	ubiquinone/menaquinone biosynthesis
TM1391	-1.9	6.6	-2.1	8.5	ATPases with chaperone activity,ATP-binding	ATP-dependent Clp protease, ATPase subunit
TM1400	1.1	1.5	-16.7	22.3	Serine-pyruvate aminotransferase	aspartate aminotransferase, putative
TM1401	1.1	0.7	-7.5	17.5	Phosphoglycerate dehydrogenase and related dehydrogenases	D-3-phosphoglycerate dehydrogenase
TM1413	1.4	4.9	2.0	9.5		hypothetical protein
TM1414	-2.5	9.6	-1.9	8.0	Beta-fructosidases (levanase/invertase)	beta-fructosidase
TM1416	-1.5	4.2	-2.9	11.6	ABC-type transport system involvedin	conserved hypothetical protein
TM1417	-1.2	0.6	-2.1	4.6	ABC-type transport system involvedin	ABC transporter, ATP-binding protein
TM1418	2.0	7.9	1.2	1.5		
TM1419	-1.8	3.9	-3.0	8.5	Myo-inositol-1-phosphate synthase	myo-inositol-1-phosphate synthase-related
TM1420	-1.3	1.4	-9.4	14.1	NADH:ubiquinone oxidoreductase 24 kDsubunit	hypothetical protein
TM1421	-1.8	2.5	-3.2	6.0	Ferredoxin	hydrogenase, putative
TM1422	-2.0	3.9	-5.9	11.0	Predicted Fe-S protein	rnfB-related protein
TM1423	-1.3	1.3	-2.8	6.8		hypothetical protein
TM1424	2.7	2.0	-19.8	8.3	NADH:ubiquinone oxidoreductase 24 kDsubunit	Fe-hydrogenase, subunit gamma
TM1425	-1.5	1.8	-6.4	10.9	Ferredoxin	Fe-hydrogenase, subunit beta
TM1426	-2.3	7.1	-8.8	15.6	NADH dehydrogenase/NADH:ubiquinone oxidoreductase	Fe-hydrogenase, subunit alpha
TM1427	-2.0	4.9	-8.3	14.0	AT-rich DNA-binding protein	conserved hypothetical protein
TM1428	-1.9	4.5	-2.0	5.6	Methyl-accepting chemotaxis protein	methyl-accepting chemotaxis protein
TM1432	-3.3	7.2	-1.9	4.6	Predicted dehydrogenase	conserved hypothetical protein
TM1434	-3.5	7.2	-4.0	8.9		hypothetical protein
TM1440	-2.2	7.0	-2.4	8.8	Translation initiation factor 2Bsubunit,	translation initiation factor, eIF-2B alp
TM1442	-3.0	9.2	-3.4	11.2	Anti-anti-sigma regulatory factor	anti-sigma factor antagonist, putative
TM1443	-2.4	6.8	-3.4	10.1	Cytidylate kinase	cytidylate kinase

Table S1, Continued						
TM1444	-2.0	7.7	-1.8	7.7	Penicillin tolerance protein	lytB protein
TM1445	-2.7	8.4	-3.2	10.3		
TM1451	-4.3	10.0	-4.0	10.4	DNA-directed RNA polymerase, sigma subunit	RNA polymerase sigma-A factor
TM1453	-2.0	4.4	-2.5	6.5	Ribosomal protein S9	ribosomal protein S9
TM1454	-2.4	6.9	-3.8	10.8	Ribosomal protein L13	ribosomal protein L13
TM1469	-1.7	2.3	-2.2	4.4	Transcriptional regulator/sugar kinase	glucokinase
TM1470	-2.1	7.9	-1.4	4.3	Transcription termination factor	transcription termination factor Rho
TM1471	-2.9	6.6	-3.0	7.8	Ribosomal protein L17	ribosomal protein L17
TM1472	-2.7	11.5	-3.9	15.2	DNA-directed RNA polymerase, alphasubunit/40	DNA-directed RNA polymerase, alpha subunit
TM1473	-4.1	7.3	-6.1	10.1	Ribosomal protein S4 and related	ribosomal protein S4
TM1474	-4.2	8.8	-4.8	10.1	Ribosomal protein S11	ribosomal protein S11
TM1475	-3.1	3.7	-4.1	5.5	Ribosomal protein S13	ribosomal protein S13
TM1477	-2.5	9.7	-2.8	11.5		
TM1478	-3.8	12.3	-3.7	13.2	Methionine aminopeptidase	methionine aminopeptidase
TM1479	-4.2	11.1	-4.7	12.8	Adenylate kinase and related kinases	adenylate kinase
TM1483	-3.0	4.7	-3.0	5.3	Ribosomal protein S5	ribosomal protein S5
TM1484	-2.2	4.9	-2.4	5.9	Ribosomal protein L18	ribosomal protein L18
TM1485	-6.2	11.6	-6.2	12.7	Ribosomal protein L6P/L9E	ribosomal protein L6
TM1486	-3.4	5.8	-3.3	6.2	Ribosomal protein S8	ribosomal protein S8
TM1487	-1.9	7.2	-2.2	9.4	Ribosomal protein S14	ribosomal protein S14
TM1488	-5.2	7.9	-4.6	8.3	Ribosomal protein L5	ribosomal protein L5
TM1489	-3.1	4.4	-2.9	4.7	Ribosomal protein L24	ribosomal protein L24
TM1490	-2.1	8.4	-2.0	9.1	Ribosomal protein L14	ribosomal protein L14
TM1491	-4.2	6.9	-4.1	7.5	Ribosomal protein S17	ribosomal protein S17
TM1492	-5.4	11.3	-6.5	13.2	Ribosomal protein L29	ribosomal protein L29
TM1493	-5.3	14.2	-6.6	16.4	Ribosomal protein L16/L10E	ribosomal protein L16
TM1494	-8.9	16.1	-9.3	17.4	Ribosomal protein S3	ribosomal protein S3
TM1495	-5.1	8.7	-4.5	9.1	Ribosomal protein L22	ribosomal protein L22
TM1496	-12.8	7.1	-10.8	7.5	Ribosomal protein S19	ribosomal protein S19
TM1497	-3.8	8.8	-2.5	7.0	Ribosomal protein L2	ribosomal protein L2
TM1498	-6.4	14.8	-6.4	16.0	Ribosomal protein L23	ribosomal protein L23
TM1500	-5.2	8.0	-4.7	8.5	Ribosomal protein L3	ribosomal protein L3
TM1501	-5.4	12.0	-5.5	13.1	Ribosomal protein S10	ribosomal protein S10
TM1502	-6.1	17.6	-6.9	19.3	GTPases - translation elongation factors	translation elongation factor Tu

Table S1, Continued						
TM1503	-2.5	5.3	-2.0	4.7	Translation elongation factors (GTPases)	translation elongation factor G
TM1504	-3.5	7.6	-3.7	8.6	Ribosomal protein S7	ribosomal protein S7
TM1505	-2.1	7.4	-1.5	4.2	Ribosomal protein S12	ribosomal protein S12
TM1509	-2.2	7.8	-6.1	15.4	Predicted metal-dependent hydrolase	conserved hypothetical protein
TM1510	-1.9	2.6	-2.9	5.6		hypothetical protein
TM1515	-2.1	5.1	-1.2	0.9	Fe ²⁺ /Zn ²⁺ uptake regulation proteins	ferric uptake regulation protein
TM1519	-1.5	3.0	-2.6	8.4	Tetrahydrodipicolinate N-succinyltransferase	2,3,4,5-tetrahydropyridine-2-carboxylate
TM1520	-1.4	3.0	-2.0	8.1	Dihydrodipicolinate reductase	dihydrodipicolinate reductase
TM1522	-1.3	1.4	-2.0	5.2	Diaminopimelate epimerase	diaminopimelate epimerase
TM1533	-1.5	3.5	-2.7	10.5	Ferredoxin-like protein	ferredoxin
TM1546	2.2	9.3	2.1	9.9	Single-stranded DNA-specific exonuclease	single stranded DNA-specific exonuclease,
TM1566	-2.0	5.0	-2.2	6.6	Ribosomal protein S16	ribosomal protein S16
TM1568	-2.0	3.7	-1.9	4.1	RimM protein, required for 16S	16S rRNA processing protein, putative
TM1569	-4.9	7.2	-4.4	7.7	tRNA-(guanine-N1)-methyltransferase	tRNA guanine-N1 methyltransferase
TM1570	-3.1	12.5	-3.0	13.2		conserved hypothetical protein
TM1571	-2.3	4.4	-2.5	5.5	Ribosomal protein L19	ribosomal protein L19
TM1578	-2.3	9.6	-2.2	10.5	Preprotein translocase subunit SecA	preprotein translocase SecA subunit
TM1590	-2.8	9.6	-3.1	11.2	Translation initiation factor 3(IF-3)	translation initiation factor IF-3
TM1591	-2.4	6.4	-3.8	10.6	Ribosomal protein L35	ribosomal protein L35
TM1598	-2.1	7.3	-2.1	8.2	DNA-directed RNA polymerase specializedsigma	RNA polymerase sigma-E factor
TM1602	-3.4	7.4	-2.0	4.5	Predicted small molecule bindingprotein	transcriptional regulator, biotin repress
TM1605	-3.3	12.7	-2.9	13.0	Translation elongation factor Ts	translation elongation factor Ts
TM1607	-2.8	10.6	-2.8	11.6	Ribosome-associated protein Y (PSrp-1)	conserved hypothetical protein
TM1608	-4.3	12.8	-4.4	14.1	Uncharacterized protein conserved inbacteria	conserved hypothetical protein
TM1609	-1.8	6.7	-2.5	10.7	FOF1-type ATP synthase, epsilon subunit	ATP synthase F1, subunit epsilon
TM1610	-1.6	7.0	-2.7	14.0	FOF1-type ATP synthase, betasubunit	ATP synthase F1, subunit beta
TM1611	-4.2	6.7	-9.7	11.1	FOF1-type ATP synthase, gammasubunit	ATP synthase F1, subunit gamma
TM1612	-1.8	7.4	-2.8	12.9	FOF1-type ATP synthase, alphasubunit	ATP synthase F1, subunit alpha
TM1613	-3.0	11.5	-8.1	18.0	FOF1-type ATP synthase, deltasubunit	ATP synthase F1, subunit delta
TM1615	-1.3	1.6	-2.1	6.7	FOF1-type ATP synthase, subunitc/Archaeal/vacuolar-type	ATP synthase F0, subunit c
TM1624	-3.2	5.4	-2.0	3.3	Beta-galactosidase/beta-glucuronidase	beta-mannosidase, putative
TM1626	-2.5	6.9	-2.6	8.0	Peptidyl-tRNA hydrolase	peptidyl-tRNA hydrolase
TM1627	-3.1	10.8	-4.9	14.6	Ribosomal protein L25 (generalstress	general stress protein Ctc
TM1628	-2.1	9.6	-4.2	15.9	Phosphoribosylpyrophosphate synthetase	phosphoribosyl pyrophosphate synthetase

TM1629	-1.7	7.7	-2.4	12.3	N-acetylglucosamine-1-phosphate uridyltransferase	UDP-N-acetylglucosamine pyrophosphorylase
TM1633	-3.6	2.6	-6.3	4.8	ATP-dependent Lon protease, bacterialtype	ATP-dependent protease LA
TM1634	2.1	7.8	1.8	6.8		hypothetical protein
TM1641	1.4	3.4	2.7	11.3	Dihydrofolate reductase	dihydrofolate reductase
TM1657	-2.2	9.6	-2.0	9.7	Ribosomal protein S20	ribosomal protein S20
TM1658	-2.2	11.4	-2.1	11.8	S-adenosylmethionine synthetase	S-adenosylmethionine synthetase
TM1670	1.9	6.4	2.0	8.0		hypothetical protein
TM1675	1.9	8.4	2.0	10.1	Predicted membrane protein	conserved hypothetical protein
TM1681	-1.9	6.7	-1.4	3.4		hypothetical protein
TM1683	-7.2	16.6	-1.7	7.3	Cold shock proteins	cold shock protein
TM1698	1.5	3.9	2.0	8.6	Aspartate/tyrosine/aromatic aminotransferase	aspartate aminotransferase
TM1704	-7.2	5.8	-7.5	6.7	Parvulin-like peptidyl-prolyl isomerase	hypothetical protein
TM1706	-3.3	4.8	-2.8	4.4	Transcription elongation factor	transcription elongation factor, greA/gre
TM1707	-2.9	7.2	-2.8	7.6	Predicted transcriptional regulator	conserved hypothetical protein
TM1723	1.2	1.6	2.0	9.3	Imidazolonepropionase and related amidohydrolases	conserved hypothetical protein
TM1729	2.4	9.2	1.6	5.5		outer membrane protein
TM1734	-1.4	0.9	-4.0	6.8	Phosphate uptake regulator	phosphate transport system regulator PhoU
TM1752	-1.3	3.3	2.2	10.6	Endoglucanase	endoglucanase
TM1754	1.3	1.9	2.7	9.1	Butyrate kinase	butyrate kinase, putative
TM1763	-2.0	4.8	-1.9	5.0	Translation elongation factor P(EF-P)/translation	translation elongation factor P
TM1764	-1.9	3.5	-2.4	6.0	Uncharacterized protein conserved inbacteria	conserved hypothetical protein
TM1765	-2.1	7.8	-3.5	13.1	Transcription termination factor	N utilization substance protein B
TM1776	-2.1	2.9	-5.2	8.1	Fe ²⁺ /Zn ²⁺ uptake regulation proteins	ferric uptake regulation protein
TM1780	-1.2	1.7	-3.1	13.4	Argininosuccinate synthase	argininosuccinate synthase
TM1781	-1.3	3.2	-2.3	10.4		
TM1784	1.0	0.1	-2.8	11.4	Acetylglutamate kinase	acetylglutamate kinase
TM1788	1.4	2.5	4.2	12.5	FOG: GGDEF domain	conserved hypothetical protein, GGDEF
TM1799	2.0	6.4	1.0	0.0	Predicted helicases	conserved hypothetical protein
TM1800	1.9	7.4	1.5	5.4	Uncharacterized protein predicted tobe	hypothetical protein
TM1802	2.1	4.7	1.2	0.6		hypothetical protein
TM1809	-1.4	1.9	-3.5	9.7	Uncharacterized protein predicted tobe	conserved hypothetical protein
TM1810	-1.2	1.4	-2.9	10.8	Uncharacterized protein predicted tobe	hypothetical protein
TM1820	-1.8	2.3	-2.6	5.1	GMP synthase - Glutamineamidotransferase	GMP synthase

Table S1, Continued						
TM1830	1.8	5.8	2.5	9.6	FOG: GGDEF domain	conserved hypothetical protein
TM1832	2.1	6.2	1.8	5.3	Transposase and inactivated derivatives	transposase
TM1833	2.2	9.1	4.1	14.9		methyl-accepting chemotaxis-related
TM1834	1.1	0.1	4.0	5.3	Alpha-galactosidases/6-phospho-beta-glucosidases	alpha-glucosidase
TM1838	1.8	7.0	2.6	11.6		hypothetical protein
TM1839	2.8	10.6	5.5	15.9	Maltose-binding periplasmic proteins/domains	maltose ABC transporter, periplasmic
TM1841	1.4	4.3	2.4	11.8		hypothetical protein
TM1845	-3.5	7.9	-1.3	1.4	Type II secretory pathway,pullulanase	pullulanase
TM1847	1.6	4.2	2.0	7.6	Transcriptional regulator/sugar kinase	ROK family protein
TM1849	1.2	1.6	-2.4	12.0		hypothetical protein
TM1850	-1.3	1.3	-5.8	11.2		hypothetical protein
TM1851	-3.1	8.2	-2.4	7.4	Alpha-mannosidase	alpha-mannosidase, putative
TM1858	-3.1	6.6	-3.5	7.5	Uncharacterized protein conserved inbacteria	recX protein, putative
TM1868	1.9	7.7	2.6	11.7	ABC-type cobalt transport system,permease	conserved hypothetical protein

Table S2. Genes in *T. maritima* /*M. jannaschii* co-culture that were differentially regulated during mid-log (ML) to early stationary phase (ES) in co-culture transition. Annotations are from the COG database (44) with the exception of those marked with a (*), which are based on Connors et al. (9).

gene_id	BLAST / COG_function	Fold Change	gene_id	BLAST / COG_function	Fold Change
TM0012	NADH:ubiquinone oxidoreductase	2.2	TM0300	ABC-type dipeptide transport system,periplasmic	3.3
TM0015	Pyruvate:ferredoxin oxidoreductase	-2.0	TM0301	ABC-type dipeptide transport systems,permease	2.1
TM0016	Pyruvate:ferredoxin oxidoreductase	-3.2	TM0302	ABC-type dipeptide transport systems,permease	2.0
TM0017	Pyruvate:ferredoxin oxidoreductase	-2.3	TM0309	ABC-type dipeptide transport system,periplasmic	2.8
TM0024	Beta-glucanase/Beta-glucan synthetase*	3.0	TM0310	Beta-galactosidase	2.2
TM0030	ABC-type dipeptide transport systems,permease*	2.2	TM0319	hypothetical protein	2.2
TM0031	ABC-type dipeptide transport system,periplasmic*	3.4	TM0369	Predicted transcriptional regulators	2.4
TM0032	Transcriptional regulator/sugar kinase	3.7	TM0373	Molecular chaperone	4.6
TM0035	hypothetical protein	-2.4	TM0374	small heatshock chaperone	6.2
TM0053	esterase, putative	2.6	TM0375	hypothetical protein	3.0
TM0062	hypothetical protein	2.0	TM0379	Uncharacterized NAD-dependent dehydrogenases	-2.9
TM0065	Transcriptional regulator	2.8	TM0380	frame shift containing	-2.7
TM0067	Sugar kinases, ribokinase family	2.0	TM0381	Pyruvate/2-oxoglutarate dehydrogenase	-2.8
TM0068	Mannitol-1-phosphate/altronate dehydrogenases	2.6	TM0384	anaerobic ribonucleoside-triphosphate reductase	-6.1
TM0070	endo-1,4-beta-xylanase B	2.2	TM0385	ribonucleoside-triphosphate reductase	-4.5
TM0071	ABC-type dipeptide transport system,periplasmic*	7.2	TM0392	Glycosyltransferase	-7.5
TM0110	Transcriptional regulator/sugar kinase	2.3	TM0393	Transcriptional regulator/sugar kinase	-5.7
TM0114	ABC-type sugar transport system,periplasmic*	2.5	TM0403	Nitrogen regulatory protein PII	2.0
TM0122	Fe2+/Zn2+ uptake regulation proteins	3.3	TM0418	Maltose-binding periplasmic proteins/domains	2.2
TM0123	ABC-type metal ion transport system	2.4	TM0423	Glycerol dehydrogenase and related enzymes	-3.2
TM0131	frame shift containing	3.3	TM0426	Predicted dehydrogenases and related proteins	3.8
TM0132	Flagellin and related hook-associated	2.5	TM0430	ABC-type sugar transport system,permease	3.1
TM0137	Tryptophan synthase alpha chain	-3.3	TM0431	ABC-type sugar transport systems,permease	2.5
TM0139	Phosphoribosylanthranilate isomerase	-2.0	TM0432	ABC-type sugar transport system,periplasmic	4.4
TM0140	Indole-3-glycerol phosphate synthase	-2.2	TM0433	pectate lyase	2.4
TM0153	hypothetical protein	-2.2	TM0436	Threonine dehydrogenase	2.3
TM0206	Hypoxanthine-guanine phosphoribosyltransferase	-2.0	TM0454	Ribosomal protein L11	-2.9
TM0207	Predicted Zn-dependent hydrolases	-2.1	TM0455	Ribosomal protein L1	-4.3
TM0208	Pyruvate kinase	-2.0	TM0456	Ribosomal protein L10	-5.6
TM0211	Glycine cleavage system T protein	3.1	TM0457	Ribosomal protein L7/L12	-4.1
TM0212	Glycine cleavage system H protein	-2.0	TM0463	Lipoprotein signal peptidase	-3.1
TM0215	Putative translation initiation inhibitor, yjgF	-2.0	TM0464	Methylase chemotaxis proteins	-2.3
TM0236	UDP-N-acetylmuramyl pentapeptide synthase	3.7	TM0465	hypothetical protein	-2.8
TM0269	hypothetical protein	2.5	TM0471	FOG: GGDEF domain	-2.0
TM0277	frame shift containing	2.4	TM0472	Predicted glutamine amidotransferase	-2.0

Table S2, Continued

gene id	BLAST / COG_function	Fold Change
TM0490	NAD-dependent protein deacetylases	-2.3
TM0497	Uncharacterized membrane protein	2.0
TM0505	Co-chaperonin GroES (HSP10)	3.1
TM0506	Chaperonin GroEL (HSP60 family)	3.1
TM0533	ABC-type dipeptide systems,permease	-2.1
TM0545	Homoserine kinase	-2.0
TM0549	Acetolactate synthase	-3.6
TM0550	Ketol-acid reductoisomerase	-2.1
TM0551	Dihydroxyaciddehydratase dehydratase	-2.6
TM0552	Isopropylmalate synthases	-2.0
TM0553	Isopropylmalate synthases	-2.4
TM0554	3-isopropylmalate dehydratase	-2.2
TM0555	3-isopropylmalate dehydratase	-2.0
TM0557	Carbamoylphosphate synthase	-2.1
TM0558	Carbamoylphosphate synthase	-2.7
TM0560	hypothetical protein	-9.6
TM0565	DNA-binding protein	2.7
TM0571	Trypsin-like serine proteases	6.6
TM0575	Holliday junction resolvosome	2.4
TM0603	Ribosomal protein S6	-2.6
TM0604	Single-stranded DNA-binding protein	-2.8
TM0606	hypothetical protein	-10.9
TM0614	Predicted nucleotidyltransferases	3.1
TM0624	Glycosyltransferase	2.4
TM0627	Glycosyltransferase	-2.0
TM0629	hypothetical protein	-2.3
TM0630	Nucleoside-diphosphate-sugar epimerases	-3.5
TM0632	Sugar transferases	2.1
TM0633	Muramidase (flagellum-specific)*	2.6
TM0654	Spermidine synthase	-2.3
TM0656	Predicted transcriptional regulators	-2.1
TM0657	Rubryerthrin	-3.4
TM0658	Desulfoferrodoxin	-4.0
TM0659	Rubredoxin	-3.0
TM0665	Cysteine synthase	-2.6

gene_id	BLAST / COG_function	Fold Change
TM0666	Serine acetyltransferase	-2.7
TM0668	Predicted pyridoxal phosphate-dependent enzyme	2.6
TM0669	hypothetical protein	-2.1
TM0688	Glyceraldehyde-3-phosphate dehydrogenase	-4.1
TM0689	3-phosphoglycerate kinase	-5.0
TM0691	SAM-dependent methyltransferases	-2.4
TM0695	ATP-dependent Protease subunit	-3.2
TM0720	Glycine/serine hydroxymethyltransferase	-2.0
TM0723	Uncharacterized conserved protein	-2.0
TM0724	Ca2+/Na+ antiporter	-2.1
TM0729	ppGpp synthetases	2.4
TM0752	Alpha-galactosidases*	2.3
TM0757	Glycosyltransferases	2.7
TM0762	Ribosomal protein S2	-2.9
TM0767	Maltosyltransferase *	-3.3
TM0784	hypothetical protein	3.3
TM0785	Uncharacterized protein, linocin/CFP29 homolog	-2.3
TM0786	Uncharacterized conserved protein	-2.1
TM0798	(acyl-carrier-protein) S-malonyltransferase	-3.8
TM0799	Uncharacterized conserved protein	-2.8
TM0800	Dioxygenase	-2.1
TM0801	3-hydroxymyristoyl dehydratases	-2.9
TM0802	3-oxoacyl-(acyl-carrier-protein) synthase	-2.8
TM0808	Transcriptional regulator/sugar kinase	2.1
TM0816	Transcriptional regulators	2.3
TM0823	Transcriptional regulator	6.6
TM0824	Predicted Fe-S oxidoreductases	6.6
TM0826	hypothetical protein	2.6
TM0840	hypothetical protein	2.2
TM0850	Molecular chaperone GrpE	2.7
TM0851	Transcriptional regulator of heatshock	2.7
TM0860	Preprotein translocase subunit SecD	-2.1
TM0881	Homoserine trans-succinylase	-2.0
TM0894	Zn-dependent hydrolases	-2.0
TM0895	Glycogen synthase	-2.2

Table S2, Continued

gene_id	BLAST / COG_function	Fold Change
TM0896	Galactose-1-phosphate uridylyltransferase	-2.8
TM0898	hypothetical protein	-2.3
TM0899	hypothetical protein	-2.2
TM0943	Glutamine synthetase	-2.1
TM0958	ABC-type sugar transport system,periplasmic	2.7
TM0963	Oligoendopeptidase F	3.3
TM0972	FOG: GGDEF domain	2.2
TM0991	Uncharacterized conserved protein	-2.3
TM1005	AraC-type DNA-binding domain	3.0
TM1015	Glutamate dehydrogenase	5.0
TM1016	hypothetical protein	2.4
TM1039	Imidazoleglycerol-phosphate dehydratase	-2.1
TM1042	ATP phosphoribosyltransferase	-2.2
TM1059	Uncharacterized protein conserved in bacteria	2.3
TM1064	ABC-type dipeptide transport system,ATPase*	2.0
TM1069	Transcriptional regulators of sugar metabolism	2.2
TM1097	Ornithine carbamoyltransferase	-2.3
TM1098	Predicted metal-dependent membrane protease	-2.3
TM1112	hypothetical protein	2.8
TM1145	HD-GYP domain	2.1
TM1148	Isocitrate dehydrogenases	-2.7
TM1164	Pyruvate:ferredoxin oxidoreductase	-2.2
TM1168	frame shift containing	-4.0
TM1172	6Fe-6S prismatic cluster-containing protein	-2.1
TM1190	Galactokinase	2.4
TM1199	ABC-type dipeptide transport system,periplasmic*	2.0
TM1223	ABC-type dipeptide transport system,periplasmic*	2.3
TM1231	Alpha-mannosidase	2.9
TM1232	sugar ABC transporter, ATP-binding	3.4
TM1233	ABC-type sugar transport system,permease	2.1
TM1234	ABC-type sugar transport systems,permease	2.7
TM1235	conserved hypothetical protein	5.3
TM1239	Uncharacterized protein conserved in bacteria	-2.3
TM1245	Phosphoribosylformylglycinamide synthase	-2.1
TM1266	hypothetical protein	-2.8

gene_id	BLAST / COG_function	Fold Change
TM1267	Thiamine biosynthesis enzyme ThiH	-5.9
TM1269	Biotin synthase and related enzymes	-2.9
TM1270	Cystathionine beta-lyases	-2.0
TM1273	Asp-tRNAAsn/Glu-tRNA ^{Gln} amidotransferase	-2.1
TM1274	hypothetical protein	-2.3
TM1275	hypothetical protein	2.5
TM1276	sugar ABC transporter, ATP-binding	2.0
TM1286	Methionine synthase II (cobalamin-independent)	-2.2
TM1307	hypothetical protein	2.3
TM1330	Predicted transcriptional regulators	2.2
TM1345	Polyribonucleotide nucleotidyltransferase	-2.3
TM1347	IMP dehydrogenase/GMP reductase	-2.1
TM1359	Signal transduction histidine kinase	2.7
TM1364	Flagellar basal body protein	3.2
TM1365	Flagellar basal body rod protein	2.8
TM1366	Flagellar hook-basal body protein	2.1
TM1384	Adenine/guanine phosphoribosyltransferases	-2.4
TM1400	Serine-pyruvate aminotransferase	-10.8
TM1405	Glycosyltransferase	2.9
TM1421	Ferredoxin	-2.3
TM1423	hypothetical protein	-2.1
TM1425	Ferredoxin	-3.3
TM1426	NADH dehydrogenase	-4.7
TM1427	AT-rich DNA-binding protein	-3.1
TM1428	Methyl-accepting chemotaxis protein	-2.4
TM1429	Glycerol uptake facilitator	2.5
TM1431	Glycerol-3-phosphate responsive antiterminator	2.6
TM1432	Predicted dehydrogenase	2.0
TM1438	point mutation containing	-2.1
TM1439	Uncharacterized protein conserved in bacteria	-2.5
TM1451	DNA-directed RNA polymerase, sigma A	2.0
TM1461	Preprotein translocase subunit YidC	-2.4
TM1469	Transcriptional regulator/sugar kinase	-2.0
TM1470	Transcription termination factor	-2.3
TM1471	Ribosomal protein L17	-2.4

Table S2, Continued

gene_id	BLAST / COG_function	Fold Change
TM1472	DNA-directed RNA polymerase	-2.5
TM1473	Ribosomal protein S4 and related	-2.4
TM1479	Adenylate kinase	-2.7
TM1480	Preprotein translocase subunit SecY	-2.0
TM1481	Ribosomal protein L15	-2.1
TM1483	Ribosomal protein S5	-2.1
TM1485	Ribosomal protein L6P/L9E	-2.8
TM1486	Ribosomal protein S8	-2.0
TM1488	Ribosomal protein L5	-2.4
TM1494	Ribosomal protein S3	-2.0
TM1495	Ribosomal protein L22	-2.0
TM1497	Ribosomal protein L2	-2.7
TM1498	Ribosomal protein L23	-4.0
TM1499	Ribosomal protein L4	-3.3
TM1500	Ribosomal protein L3	-2.7
TM1501	Ribosomal protein S10	-2.4
TM1502	GTPases - translation elongation factors	-4.4
TM1503	Translation elongation factors (GTPases)	-2.3
TM1504	Ribosomal protein S7	-2.0
TM1524	endoglucanase	2.1
TM1541	Flagellar basal body P-ring biosynthesis	2.0
TM1576	Predicted rRNA methylase	2.1
TM1598	DNA-directed RNA polymerase, sigma E	5.0
TM1599	hypothetical protein	3.0
TM1600	hypothetical protein	2.6
TM1602	Predicted small molecule binding protein	3.1
TM1607	Ribosome-associated protein Y (PSrp-1)	-2.1
TM1609	F ₀ F ₁ -type ATP synthase, epsilon subunit	-2.1
TM1610	F ₀ F ₁ -type ATP synthase, beta subunit	-2.4
TM1611	F ₀ F ₁ -type ATP synthase, gamma subunit	-2.6
TM1612	F ₀ F ₁ -type ATP synthase, alpha subunit	-2.1
TM1628	Phosphoribosylpyrophosphate synthetase	-2.7
TM1629	N-acetylglucosamine-1-phosphoryltransferase	-2.0
TM1643	Predicted dinucleotide-utilizing enzyme	2.2
TM1650	Glycosidases*	2.1

gene_id	BLAST / COG_function	Fold Change
TM1658	S-adenosylmethionine synthetase	-2.7
TM1683	Cold shock proteins	-5.3
TM1684	Ribosomal protein L31	-2.2
TM1685	Predicted RNA binding protein	-3.2
TM1704	Parvulin-like peptidyl-prolyl isomerase	-2.3
TM1746	ABC-type dipeptide transport system, periplasmic*	2.1
TM1747	ABC-type dipeptide transport systems, permease*	2.9
TM1748	ABC-type dipeptide transport systems, permease*	2.4
TM1749	ABC-type dipeptide transport system, ATPase*	2.1
TM1751	Endoglucanase	2.0
TM1752	Endoglucanase	2.0
TM1756	Butyrate kinase	2.0
TM1768	Exonuclease VII, large subunit	-2.1
TM1774	Predicted phosphoglycerate mutase	-2.3
TM1776	Fe ²⁺ /Zn ²⁺ uptake regulation proteins	2.1
TM1807	Uncharacterized protein	-2.7
TM1808	Uncharacterized protein	-3.8
TM1809	Uncharacterized protein	-3.4
TM1810	hypothetical protein	-2.0
TM1811	Predicted hydrolase of the HD family	-2.3
TM1812	hypothetical protein	-2.4
TM1836	ABC-type sugar transport system, permease	-2.3
TM1837	maltose transport system permease protein	-2.0
TM1839	Maltose-binding periplasmic proteins/domains	-2.8
TM1848	Cellobiose phosphorylase	2.1
TM1849	hypothetical protein	4.9
TM1850	hypothetical protein	3.1
TM1851	Alpha-mannosidase	3.0
TM1852	Predicted glycosylase	2.2
TM1853	ABC-type sugar transport system, permease	2.9
TM1854	ABC-type sugar transport systems, permease	5.7
TM1855	ABC-type sugar transport system, periplasmic	22.6
TM1856	Transcriptional regulators	9.2
TM1866	Transcriptional regulator	2.3
TM1878	5'-nucleotidase/2',3'-cyclic phosphodiesterase	4.7

Table S3. Differential gene expression in *T. maritima* between similar growth phases in pure culture and co-culture with *M. jannaschii*

Table S3A. Genes that were differentially expressed in the comparison of the co-culture in mid-log phase, to the pure culture at mid-log phase.

gene ID	Fold Change CML-PML	negative log(10) p-value	COG Annotation	TIGR Annotation
TM0004	2.1	11.4		hypothetical protein
TM0051	-2.3	8.8	Fe2+ transport system proteinB	iron(II) transport protein B
TM0053	-2.2	8.3		esterase, putative
TM0373	-6.1	22.7	Molecular chaperone	dnaK protein
TM0374	-3.6	17.9	Molecular chaperone (small heatshock)	heat shock protein, class I
TM0379	3.2	13.8	Uncharacterized NAD(FAD)-dependent dehydrogenases	NADH oxidase
TM0380	2.6	8.0		
TM0381	2.4	13.1	Pyruvate/2-oxoglutarate dehydrogenase complex	dihydrolipoamide dehydrogenase
TM0390	2.0	8.9		hypothetical protein
TM0395	-3.3	10.8	Uncharacterized NAD(FAD)-dependent dehydrogenases	NADH oxidase, putative
TM0396	-3.4	19.9	Fe-S-cluster-containing hydrogenase components	iron-sulfur cluster-binding protein
TM0397	-3.2	10.9	Glutamate synthase domain 2	glutamate synthase, alpha subunit
TM0398	-2.1	6.2	Glutamate synthase domain 1	conserved hypothetical protein
TM0434	2.0	15.2	Alpha-galactosidases/6-phospho-beta-glucosidases	alpha-glucosidase, putative
TM0505	-14.5	26.0	Co-chaperonin GroES (HSP10)	groES protein
TM0506	-16.4	26.3	Chaperonin GroEL (HSP60 family)	groEL protein
TM0547	-2.1	14.0	Homoserine dehydrogenase	aspartokinase II
TM0549	-2.0	7.3	Acetolactate synthase, small (regulatory)subunit	acetolactate synthase, small subunit
TM0606	2.0	8.8		hypothetical protein
TM0654	2.1	9.4	Spermidine synthase	spermidine synthase
TM0755	-2.1	8.8	Uncharacterized flavoproteins	conserved hypothetical protein
TM0807	-4.0	14.0	Peroxiredoxin	alkyl hydroperoxide reductase, putative
TM0849	-3.0	12.5	DnaJ-class molecular chaperone	dnaJ protein
TM0965	-2.1	15.4	NCAIR mutase (PurE)-related proteins	phosphoribosylaminoimidazole carboxylase

Table S3A, Continued

TM0979	-2.6	15.2	Uncharacterized conserved protein	conserved hypothetical protein
TM0980	-3.4	8.5	Uncharacterized protein	Uncharacterized protein involved oxidation
TM0981	-2.4	7.6	Uncharacterized conserved protein	Uncharacterized ACR protein
TM0982	-2.3	4.7	Predicted transporter component	conserved hypothetical protein
TM0983	-2.0	11.1	Predicted redox protein	conserved hypothetical protein
TM1155	-2.4	8.6	Glucose-6-phosphate 1-dehydrogenase	glucose-6-phosphate 1-dehydrogenase
TM1245	-2.4	15.0	Phosphoribosylformylglycinamide (FGAM) synthase	phosphoribosylformylglycinamide synthase
TM1286	-2.7	10.1	Methionine synthase II (cobalamin-independent)	5-methyltetrahydropteroyltriglutamate
TM1799	2.0	11.3	Predicted helicases	conserved hypothetical protein
TM1834	4.6	17.1	Alpha-galactosidases/6-phospho-beta-glucosidases	alpha-glucosidase
TM1874	2.9	13.4	Cold shock proteins	cold shock protein

Table S3B. Genes that were differentially expressed in the comparison between the co-culture in early stationary phase and the pure culture at early stationary phase.

gene ID	Fold Change CES-PES	negative log(10) p-value	COG Annotation	TIGR Annotation
TM0004	2.0	8.7		hypothetical protein
TM0010	-2.2	5.3	Ferredoxin	NADP-reducing hydrogenase, subunit C
TM0015	-2.6	12.6	Pyruvate:ferredoxin oxidoreductase	pyruvate ferredoxin oxidoreductase, gamma
TM0016	-4.0	13.5	Pyruvate:ferredoxin oxidoreductase	pyruvate ferredoxin oxidoreductase, delta
TM0017	-2.5	12.3	Pyruvate:ferredoxin oxidoreductase	pyruvate ferredoxin oxidoreductase, alpha
TM0024	2.1	7.7	Beta-glucanase/Beta-glucan synthetase	laminarinase
TM0027	2.1	7.1	ABC-type dipeptide/oligopeptide/nickel transport system,ATPase	oligopeptide ABC transporter, ATP-binding
TM0029	2.1	11.3	ABC-type dipeptide/oligopeptide/nickel transporter,permease	oligopeptide ABC transporter, permease
TM0030	3.2	8.9	ABC-type dipeptide/oligopeptide/nickel transporter,permease	oligopeptide ABC transporter, permease
TM0031	5.3	14.1	ABC-type dipeptide transport system,periplasmic	oligopeptide ABC transporter, periplasmic
TM0032	4.3	19.3	Transcriptional regulator/sugar kinase	transcriptional regulator, XylR-related
TM0035	-2.1	17.2		hypothetical protein
TM0055	2.1	6.8		alpha-glucuronidase

Table S3B, Continued				
TM0056	2.3	9.8	ABC-type dipeptide transport system,periplasmic	oligopeptide ABC transporter, periplasmic
TM0061	2.2	5.6		endo-1,4-beta-xylanase A
TM0062	2.4	8.0		hypothetical protein
TM0065	3.2	10.0	Transcriptional regulator	transcriptional regulator, IclR family
TM0067	2.2	10.3	Sugar kinases, ribokinase family	2-keto-3-deoxygluconate kinase
TM0068	2.5	9.7	Mannitol-1-phosphate/altronate dehydrogenases	D-mannonate oxidoreductase, putative
TM0070	2.7	11.7		endo-1,4-beta-xylanase B
TM0071	8.1	17.4	ABC-type dipeptide transport system,periplasmic	oligopeptide ABC transporter, periplasmic
TM0110	2.2	9.5	Transcriptional regulator/sugar kinase	transcriptional regulator, XylR-related
TM0111	2.1	9.3	Alcohol dehydrogenase, class IV	alcohol dehydrogenase, iron-containing
TM0112	2.1	5.9	Ribose/xylose/arabinose/galactoside ABC-type transporter,permease	sugar ABC transporter, permease protein
TM0114	3.2	7.1	ABC-type sugar transport system,periplasmic	sugar ABC transporter, periplasmic
TM0122	4.2	12.7	Fe2+/Zn2+ uptake regulation proteins	ferric uptake regulation protein
TM0123	2.7	11.3	ABC-type metal ion transportsystem,	zinc ABC transporter, periplasmic zinc-binding
TM0131	2.1	4.7		
TM0132	3.1	10.7	Flagellin and related hook-associatedproteins	flagellin, putative
TM0137	-2.4	9.1	Tryptophan synthase alpha chain	tryptophan synthase, alpha subunit
TM0139	-2.1	11.5	Phosphoribosylanthranilate isomerase	phosphoribosylanthranilate isomerase
TM0153	-2.8	5.3		hypothetical protein
TM0208	-2.1	5.5	Pyruvate kinase	pyruvate kinase
TM0211	2.1	4.5	Glycine cleavage system Tprotein	aminomethyltransferase
TM0215	-2.4	11.5	Putative translation initiation inhibitor,yjgF	protein synthesis inhibitor, putative
TM0236	2.5	4.4	UDP-N-acetylmuramyl pentapeptide synthase	UDP-related synthase
TM0277	2.2	4.6		
TM0291	-2.5	14.1	3-isopropylmalate dehydratase large subunit	3-isopropylmalate dehydratase
TM0293	-2.0	8.6	Gamma-glutamyl phosphate reductase	gamma-glutamyl phosphate reductase
TM0300	2.9	12.3	ABC-type dipeptide transport system,periplasmic	oligopeptide ABC transporter, periplasmic
TM0301	2.2	5.4	ABC-type dipeptide/oligopeptide/nickel transport systems,permease	oligopeptide ABC transporter, permease
TM0302	2.2	4.3	ABC-type dipeptide/oligopeptide/nickel transport systems,permease	oligopeptide ABC transporter, permease
TM0305	2.0	5.1		endoglucanase, putative
TM0309	3.6	15.2	ABC-type dipeptide transport system,periplasmic	oligopeptide ABC transporter, periplasmic
TM0310	2.1	10.1	Beta-galactosidase	beta-D-galactosidase
TM0311	2.8	10.4		hypothetical protein
TM0317	-2.3	13.2	Cation transport ATPase	cation-transporting ATPase, P-type
TM0369	3.3	15.9	Predicted transcriptional regulators	Predicted transcriptional regulators

TM0370	2.4	11.2	RecA-superfamily ATPases implicated insignal	Rad55/RecA (clusters with archaeal proteins)
TM0373	4.1	16.4	Molecular chaperone	dnaK protein
TM0374	5.8	17.9	Molecular chaperone (small heatshock	heat shock protein, class I
TM0384	-2.9	12.1		anaerobic ribonucleoside-triphosphate red
TM0385	-2.3	4.3	Oxygen-sensitive ribonucleoside-triphosphate reductase	conserved hypothetical protein
TM0390	2.0	5.9		hypothetical protein
TM0392	-5.5	14.6	Glycosyltransferase	conserved hypothetical protein
TM0393	-5.3	19.0	Transcriptional regulator/sugar kinase	transcriptional regulator, XylR-related
TM0395	-4.8	10.8	Uncharacterized NAD(FAD)-dependent dehydrogenases	NADH oxidase, putative
TM0396	-3.9	17.4	Fe-S-cluster-containing hydrogenase components 2	iron-sulfur cluster-binding protein
TM0397	-2.4	7.1	Glutamate synthase domain 2	glutamate synthase, alpha subunit
TM0418	3.0	12.3	Maltose-binding periplasmic proteins/domains	sugar ABC transporter, periplasmic
TM0423	-3.3	6.1	Glycerol dehydrogenase and relatedenzymes	glycerol dehydrogenase
TM0426	2.6	4.2	Predicted dehydrogenases and relatedproteins	PHT4-related protein
TM0430	2.2	5.2	ABC-type sugar transport system,permease	sugar ABC transporter, permease protein
TM0431	3.1	12.2	ABC-type sugar transport systems,permease	sugar ABC transporter, permease protein
TM0432	5.6	11.8	ABC-type sugar transport system,periplasmic	sugar ABC transporter, periplasmic
TM0433	3.5	17.4		pectate lyase
TM0434	2.2	13.0	Alpha-galactosidases/6-phospho-beta-glucosidases	alpha-glucosidase, putative
TM0435	2.3	9.2	Acetyl esterase (deacetylase)	acetyl xylan esterase-related protein
TM0436	3.0	11.1	Threonine dehydrogenase and relatedZn-dependent	alcohol dehydrogenase, zinc-containing
TM0437	2.6	8.1		exo-poly-alpha-D-galacturonosidase
TM0438	2.5	7.2	6-phosphogluconate dehydrogenase	6-phosphogluconate dehydrogenase
TM0455	-2.5	6.6	Ribosomal protein L1	ribosomal protein L1
TM0463	-2.1	6.4	Lipoprotein signal peptidase	lipoprotein signal peptidase
TM0465	-2.1	5.7		hypothetical protein
TM0471	-2.1	8.3	FOG: GGDEF domain	hypothetical protein-GGDEF domain
TM0472	-2.3	9.2	Predicted glutamine amidotransferase involvedin	amidotransferase, putative
TM0490	-2.2	8.8	NAD-dependent protein deacetylases, SIR2family	regulatory protein, SIR2 family
TM0533	-2.2	7.7	ABC-type dipeptide/oligopeptide/nickel transport systems,permease	oligopeptide ABC transporter, permease
TM0543	-2.0	8.3	ABC-type Na+ efflux pump,permease	conserved hypothetical protein
TM0545	-2.9	9.7	Homoserine kinase	homoserine kinase, putative
TM0547	-2.2	11.4	Homoserine dehydrogenase	aspartokinase II
TM0548	-2.5	7.3	Thiamine pyrophosphate-requiring enzymes	acetolactate synthase, large subunit
TM0549	-5.4	13.2	Acetolactate synthase, small (regulatory)subunit	acetolactate synthase, small subunit

TM0550	-2.5	4.9	Ketol-acid reductoisomerase	ketol-acid reductoisomerase
TM0551	-2.6	5.6	Dihydroxyaciddehydratase/phosphogluconate dehydratase	dihydroxy-acid dehydratase
TM0553	-2.1	4.7	Isopropylmalate/homocitrate/citramalate synthases	2-isopropylmalate synthase
TM0554	-2.1	6.1	3-isopropylmalate dehydratase large subunit	3-isopropylmalate dehydratase
TM0558	-2.3	4.0	Carbamoylphosphate synthase small subunit	carbamoyl-phosphate synthetase
TM0560	-4.5	13.7	Protein distantly related to bacterial	conserved hypothetical protein
TM0571	3.5	7.0	Trypsin-like serine proteases, typically periplasmic,	heat shock serine protease, periplasmic
TM0575	2.1	11.1	Holliday junction resolvase, endonuclease subunit	crossover junction endodeoxyribonuclease
TM0580	-3.3	14.3	ATP-dependent Zn proteases	cell division protein FtsH
TM0606	-5.4	14.9		hypothetical protein
TM0614	2.2	4.9	Predicted nucleotidyltransferases	conserved hypothetical protein
TM0624	2.3	6.4	Glycosyltransferase	N-acetylglucosaminyl-phosphatidylinositol
TM0630	-3.2	12.2	Nucleoside-diphosphate-sugar epimerases	nucleotide sugar epimerase, putative
TM0632	2.6	4.1	Sugar transferases involved in lipopolysaccharide	extracellular polysaccharide biosynthesis
TM0657	-2.7	5.1	Rubryerythrin	rubryerythrin
TM0658	-3.9	15.9	Desulfoferrodoxin	neelaredoxin
TM0659	-2.8	8.5	Rubredoxin	rubredoxin
TM0665	-4.4	14.6	Cysteine synthase	cysteine synthase
TM0666	-5.2	14.9	Serine acetyltransferase	serine acetyltransferase
TM0688	-4.7	11.6	Glyceraldehyde-3-phosphate dehydrogenase	glyceraldehyde-3-phosphate dehydrogenase
TM0689	-5.8	10.6	3-phosphoglycerate kinase	phosphoglycerate kinase/triose-phosphate
TM0691	-2.7	5.0	SAM-dependent methyltransferases	conserved hypothetical protein
TM0693	-2.4	11.3		hypothetical protein
TM0694	-2.0	5.3	FKBP-type peptidyl-prolyl cis-trans isomerase	trigger factor, putative
TM0695	-4.4	13.9	Protease subunit of ATP-dependent Clp	ATP-dependent Clp protease, proteolytic
TM0696	-2.0	7.2	Uncharacterized conserved protein	ray-related protein
TM0698	-2.2	6.4	Flagellar biosynthesis pathway, component FlIP	flagellar biosynthesis protein FlIP
TM0714	-2.0	10.2		hypothetical protein
TM0753	-2.0	9.5	Methylase involved in ubiquinone/menaquinone biosynthesis	ubiquinone/menaquinone biosynthesis
TM0755	-3.5	11.1	Uncharacterized flavoproteins	conserved hypothetical protein
TM0757	2.6	8.2	Glycosyltransferases involved in cell wall	hypothetical protein
TM0758	3.0	15.1	Flagellin and related hook-associated proteins	flagellin
TM0780	-2.0	8.4	Peroxioredoxin	bacterioferritin comigratory protein, ahp
TM0784	2.2	14.7		hypothetical protein
TM0798	-2.5	5.3	(acyl-carrier-protein) S-malonyltransferase	malonyl CoA-acyl carrier protein transacy

Table S3B, Continued				
TM0799	-2.0	4.4	Uncharacterized conserved protein	bioY protein
TM0800	-2.4	6.7	Dioxygenases related to 2-nitropropanedioxygenase	conserved hypothetical protein
TM0801	-2.3	11.5	3-hydroxymyristoyl/3-hydroxydecanoyl dehydratases	(3R)-hydroxymyristoyl-(acyl carrier protein
TM0804	-2.4	9.0	Histidinol phosphatase and related hydrolases	conserved hypothetical protein
TM0805	-2.3	9.4	UDP-N-acetylmuramyl pentapeptide phosphotransferase	lipophilic protein, putative
TM0808	2.0	4.6	Transcriptional regulator/sugar kinase	transcriptional regulator, XylR-related
TM0823	4.5	12.1	Transcriptional regulator	transcriptional regulator, TetR family
TM0824	4.9	9.8	Predicted Fe-S oxidoreductases	astB/chuR-related protein
TM0840	2.5	11.0		hypothetical protein
TM0842	2.6	4.7	FOG: CheY-like receiver	response regulator
TM0847	-2.3	12.6	GTPase	conserved hypothetical protein
TM0850	2.3	10.6	Molecular chaperone GrpE (heatshock	grpE protein, putative
TM0851	2.7	6.7	Transcriptional regulator of heatshock	heat shock operon repressor HrcA
TM0881	-3.8	13.9	Homoserine trans-succinylase	homoserine O-succinyltransferase
TM0882	-2.9	12.2	O-acetylhomoserine sulfhydrylase	O-acetylhomoserine sulfhydrylase
TM0886	-2.0	11.1	Membrane carboxypeptidase (penicillin-binding protein)	penicillin-binding protein, class 1A
TM0893	-2.1	12.0	Uncharacterized bacitracin resistance protein	bacitracin resistance protein
TM0896	-2.7	10.8	Galactose-1-phosphate uridylyltransferase	galactose-1-phosphate uridylyltransferase
TM0943	-2.4	7.3	Glutamine synthetase	glutamine synthetase
TM0958	3.0	6.5	ABC-type sugar transport system, periplasmic	ribose ABC transporter, periplasmic ribose
TM0963	2.0	9.4	Oligoendopeptidase F	oligoendopeptidase, putative
TM0965	-2.4	14.3	NCAIR mutase (PurE)-related proteins	phosphoribosylaminoimidazole carboxylase
TM0972	2.2	4.5	FOG: GGDEF domain	conserved hypothetical protein, GGDEF dom
TM0975	2.1	8.4		hypothetical protein
TM0980	-2.6	4.6	Uncharacterized protein involved in the	Uncharacterized protein involved in oxidation
TM0981	-2.0	4.2	Uncharacterized conserved protein involved in	Uncharacterized ACR
TM1005	2.0	6.3	AraC-type DNA-binding domain-containing proteins	transcriptional regulator, putative
TM1016	2.3	10.9		hypothetical protein
TM1017	2.3	9.3	Permeases of the drug/metabolite transporter	conserved hypothetical protein
TM1037	-2.0	9.3	Phosphoribosylformimino-5-aminoimidazole carboxamide ribonucleotide	phosphoribosylformimino-5-aminoimidazole
TM1039	-2.1	11.6	Imidazoleglycerol-phosphate dehydratase	imidazoleglycerol-phosphate dehydratase
TM1043	-2.0	9.2	Histidyl-tRNA synthetase	histidyl-tRNA synthetase-related protein
TM1059	2.1	4.8	Uncharacterized protein conserved in bacteria	spoVS-related protein
TM1068	2.6	7.8	Alpha-galactosidases/6-phospho-beta-glucosidases	alpha-glucosidase, putative
TM1120	2.5	11.8	ABC-type sugar transport system, periplasmic	glycerol-3-phosphate ABC transporter, permease

Table S3B, Continued				
TM1135	-2.3	11.6	ABC-type branched-chain amino acid transport	branched chain amino acid ABC transporter
TM1145	2.0	9.6	HD-GYP domain	conserved hypothetical protein
TM1148	-2.1	9.4	Isocitrate dehydrogenases	isocitrate dehydrogenase
TM1155	-2.6	7.8	Glucose-6-phosphate 1-dehydrogenase	glucose-6-phosphate 1-dehydrogenase
TM1164	-2.1	4.6	Pyruvate:ferredoxin oxidoreductase and related 2-oxoacid:ferredoxin	2-oxoacid ferredoxin oxidoreductase, alpha
TM1168	-2.3	8.5		
TM1176	2.2	4.3	Predicted transcriptional regulators	transcriptional regulator, metal-sensing
TM1199	2.1	8.9	ABC-type dipeptide transport system, periplasmic	oligopeptide ABC transporter, periplasmic
TM1200	2.0	6.4	Transcriptional regulators	transcriptional regulator, LacI family
TM1223	3.1	9.1	ABC-type dipeptide transport system, periplasmic	oligopeptide ABC transporter, periplasmic
TM1227	2.0	6.0		endo-1,4-beta-mannosidase
TM1231	3.0	8.4	Alpha-mannosidase	alpha-mannosidase-related protein
TM1232	2.2	9.4		sugar ABC transporter, ATP-binding protein
TM1233	2.0	6.1	ABC-type sugar transport system, permease	sugar ABC transporter, permease protein,
TM1234	2.9	12.8	ABC-type sugar transport systems, permease	sugar ABC transporter, permease protein
TM1235	4.6	13.4		conserved hypothetical protein
TM1238	-2.1	8.3	Superfamily I DNA and RNA	ATP-dependent DNA helicase
TM1239	-2.6	9.8	Uncharacterized protein conserved in bacteria	conserved hypothetical protein
TM1240	-2.3	13.1	Predicted GTPase, probable translation factor	conserved hypothetical protein
TM1245	-5.3	18.8	Phosphoribosylformylglycinamide (FGAM) synthase	phosphoribosylformylglycinamide synthase
TM1246	-2.6	9.1	Phosphoribosylformylglycinamide (FGAM) synthase, synthetase domain	phosphoribosylformylglycinamide synthase
TM1248	-2.9	10.8	Folate-dependent phosphoribosylglycinamide formyltransferase PurN	phosphoribosylglycinamide formyltransferase
TM1249	-2.4	7.6	AICAR transformylase/IMP cyclohydrolase PurH	phosphoribosylaminoimidazolecarboxamide
TM1250	-2.3	10.8	Phosphoribosylamine-glycine ligase	phosphoribosylamine--glycine ligase
TM1252	-2.1	7.4		hypothetical protein
TM1267	-3.0	13.1	Thiamine biosynthesis enzyme ThiH	thiH protein, putative
TM1271	2.0	4.6	Type II secretory pathway, pseudopilin	type IV pilin-related protein
TM1274	-2.6	12.3		hypothetical protein
TM1275	2.2	8.3		hypothetical protein
TM1276	3.0	14.6		sugar ABC transporter, ATP-binding protein
TM1307	2.3	7.1		hypothetical protein
TM1326	-2.0	5.2	ABC-type multidrug transport system, permease	conserved hypothetical protein
TM1345	-2.0	10.3	Polyribonucleotide nucleotidyltransferase (polynucleotide phosphorylase)	polynucleotide phosphorylase
TM1364	2.8	7.3	Flagellar basal body protein	flagellar basal-body rod protein FlgB
TM1365	2.2	13.0	Flagellar basal body rod protein	flagellar basal-body rod protein FlgC

TM1369	-2.9	8.3	ABC-type transport system involvedin	conserved hypothetical protein
TM1370	-3.3	11.0	ABC-type transport system involvedin	hypothetical protein
TM1371	-2.9	15.9	Selenocysteine lyase	aminotransferase, class V
TM1375	-2.7	11.9	Spermidine/putrescine-binding periplasmic protein	spermidine/putrescine ABC transporter
TM1400	-22.5	23.9	Serine-pyruvate aminotransferase/archaeal aspartate aminotransferase	aspartate aminotransferase, putative
TM1423	-2.3	8.0		hypothetical protein
TM1425	-3.6	11.4	Ferredoxin	Fe-hydrogenase, subunit beta
TM1426	-5.4	20.0	NADH dehydrogenase/NADH:ubiquinone oxidoreductase 75kD	Fe-hydrogenase, subunit alpha
TM1427	-2.8	12.8	AT-rich DNA-binding protein	conserved hypothetical protein
TM1429	2.9	5.6	Glycerol uptake facilitator andrelated	glycerol uptake facilitator protein
TM1479	-2.3	12.2	Adenylate kinase and relatedkinases	adenylate kinase
TM1498	-2.0	5.7	Ribosomal protein L23	ribosomal protein L23
TM1499	-2.1	14.2	Ribosomal protein L4	ribosomal protein L4
TM1502	-2.8	9.9	GTPases - translation elongationfactors	translation elongation factor Tu
TM1533	-2.1	8.2	Ferredoxin-like protein	ferredoxin
TM1536	-4.4	14.7	Predicted membrane protein	conserved hypothetical protein
TM1562	-2.1	15.0		hypothetical protein
TM1598	4.1	19.0	DNA-directed RNA polymerase specializedsigma	RNA polymerase sigma-E factor
TM1599	3.0	10.8		hypothetical protein
TM1600	2.0	9.4		hypothetical protein
TM1608	-2.8	16.0	Uncharacterized protein conserved in bacteria	conserved hypothetical protein
TM1609	-2.2	9.0	F0F1-type ATP synthase, epsilon subunit	ATP synthase F1, subunit epsilon
TM1610	-3.5	13.8	F0F1-type ATP synthase, beta subunit	ATP synthase F1, subunit beta
TM1611	-4.4	12.0	F0F1-type ATP synthase, gamma subunit	ATP synthase F1, subunit gamma
TM1612	-2.9	14.6	F0F1-type ATP synthase, alpha subunit	ATP synthase F1, subunit alpha
TM1613	-2.7	12.5	F0F1-type ATP synthase, delta subunit	ATP synthase F1, subunit delta
TM1616	-2.1	4.9	F0F1-type ATP synthase, subunit a	ATP synthase F0, subunit a
TM1631	-2.0	10.5	Uncharacterized conserved protein	conserved hypothetical protein
TM1683	-3.7	9.7	Cold shock proteins	cold shock protein
TM1685	-2.1	5.9	Predicted RNA binding protein(contains	conserved hypothetical protein
TM1746	2.7	11.9	ABC-type dipeptide transport system,periplasmic	oligopeptide ABC transporter, periplasmic
TM1747	2.4	8.0	ABC-type dipeptide/oligopeptide/nickel transport systems,permease	oligopeptide ABC transporter, permease
TM1748	2.8	10.4	ABC-type dipeptide/oligopeptide/nickel transport systems,permease	oligopeptide ABC transporter, permease
TM1749	2.7	9.3	ABC-type dipeptide/oligopeptide/nickel transport system,ATPase	oligopeptide ABC transporter, ATP-binding
TM1750	2.1	4.9	ABC-type dipeptide/oligopeptide/nickel transport system,ATPase	oligopeptide ABC transporter, ATP-binding

Gene ID	Fold Change	negative log(10) p-value	COG Annotation	TIGR Annotation
TM1751	2.1	6.6	Endoglucanase	endoglucanase
TM1754	2.2	10.3	Butyrate kinase	butyrate kinase, putative
TM1767	-2.0	9.9	5,10-methylene-tetrahydrofolate dehydrogenase	methylenetetrahydrofolate dehydrogenase
TM1808	-2.6	13.1	Uncharacterized protein predicted to be	conserved hypothetical protein
TM1822	-2.1	7.5	Membrane protease subunits, stomatin/prohibitin homologs	ftsH protease activity modulator HflK
TM1834	3.8	13.2	Alpha-galactosidases/6-phospho-beta-glucosidases	alpha-glucosidase
TM1836	-2.1	4.7	ABC-type sugar transport system, permease	maltose ABC transporter, permease protein
TM1839	-2.3	6.7	Maltose-binding periplasmic proteins/domains	maltose ABC transporter, periplasmic malt
TM1848	2.5	9.8	Cellobiose phosphorylase	cellobiose-phosphorylase
TM1849	6.2	18.9		hypothetical protein
TM1850	2.0	6.1		hypothetical protein
TM1852	2.2	5.5	Predicted glycosylase	conserved hypothetical protein
TM1853	3.1	11.3	ABC-type sugar transport system, permease	sugar ABC transporter, permease protein
TM1854	5.1	15.6	ABC-type sugar transport systems, permease	sugar ABC transporter, permease protein
TM1855	19.8	21.9	ABC-type sugar transport system, periplasmic	sugar ABC transporter, periplasmic
TM1856	8.2	12.7	Transcriptional regulators	transcriptional regulator, LacI family
TM1878	4.3	12.8	5'-nucleotidase/2',3'-cyclic phosphodiesterase and related esterases	UDP-sugar hydrolase

Table S3C. Genes that were differentially expressed in the comparison between the co-culture in late stationary phase and the pure culture at late stationary phase.

gene ID	Fold Change CLS-PLS	negative log(10) p-value	COG Annotation	TIGR Annotation
TM0047	-2.0	10.6	Transposase and inactivated derivatives	transposase, putative
TM0089	-2.2	12.9		hypothetical protein
TM0092	-2.0	10.8		hypothetical protein
TM0093	-2.0	7.6		hypothetical protein
TM0126	2.0	5.9	Response regulators	response regulator
TM0139	2.0	14.7	Phosphoribosylanthranilate isomerase	phosphoribosylanthranilate isomerase
TM0153	-2.0	4.5		hypothetical protein
TM0166	-2.1	8.5	Folypolyglutamate synthase	folypolyglutamate synthase

TM0173	-2.0	7.1	Reverse gyrase	reverse gyrase
TM0217	-2.2	7.0	Glycyl-tRNA synthetase, beta subunit	glycyl-tRNA synthetase, beta subunit
TM0228	-2.0	7.3	NADH:ubiquinone oxidoreductase, NADH-binding (51kD)	NADP-reducing hydrogenase, subunit C
TM0233	-2.1	9.0	Bacterial cell division membraneprotein	cell division protein, rodA/ftsW/spoVE fa
TM0234	-2.4	7.0	UDP-N-acetylmuramoylalanine-D-glutamate ligase	UDP-N-acetylmuramoylalanine--D-glutamate
TM0297	2.0	14.3	Dehydrogenaseswith different specificities	oxidoreductase, short chain dehydrogenase
TM0330	-2.0	8.9	Predicted metal-dependent hydrolase	conserved hypothetical protein
TM0336	-2.0	7.1	Hydrolases of the alpha/beta superfamily	conserved hypothetical protein
TM0396	2.2	14.5	Fe-S-cluster-containing hydrogenase components	iron-sulfur cluster-binding protein
TM0400	2.1	6.9	Signal transduction histidine kinase	sensor histidine kinase
TM0425	-2.0	8.4	Predicted dehydrogenases and related proteins	oxidoreductase, putative
TM0461	-2.0	8.2	DNA polymerase III, alphasubunit	DNA polymerase III, alpha subunit
TM0474	-2.0	8.2	Nicotinic acid phosphoribosyltransferase	conserved hypothetical protein
TM0477	-2.0	4.4		outer membrane protein alpha
TM0520	-2.1	9.9	Predicted tRNA(5-methylaminomethyl-2-thiouridylate) methyltransferase	tRNA methyltransferase
TM0528	-2.0	11.4	Methionyl-tRNA formyltransferase	methionyl-tRNA formyltransferase
TM0537	-2.0	7.9		hypothetical protein
TM0626	-2.0	6.5	Uncharacterized proteins of theAP	hypothetical protein
TM0690	2.4	12.0	Uncharacterized conserved protein	conserved hypothetical protein
TM0729	-2.0	15.0	Guanosine polyphosphate pyrophosphohydrolases	(p)ppGpp synthetase
TM0785	2.1	9.4	Uncharacterized protein, linocin/CFP29 homolog	bacteriocin
TM0818	2.2	8.4	Teichoic acid biosynthesis proteins	lipopolysaccharide biosynthesis protein,
TM0832	-2.0	6.3		hypothetical protein
TM0835	-2.0	6.7	Actin-like ATPase involved incell	cell division protein FtsA, putative
TM0935	-2.0	10.8	FOG: CBS domain	conserved hypothetical protein
TM0953	-2.1	11.8		
TM0956	-2.2	11.6	ABC-type sugar transport system,ATPase	ribose ABC transporter, ATP-binding protein
TM1027	2.0	11.4		hypothetical protein
TM1163	-2.0	13.4	FOG: GGDEF domain	conserved hypothetical protein, GGDEF domain
TM1193	2.2	9.0	Beta-galactosidase/beta-glucuronidase	beta-galactosidase
TM1201	2.2	14.0		arabinogalactan endo-1,4-beta-galactosidase
TM1389	-2.2	10.7	SAM-dependent methyltransferases	ubiquinone biosynthesis methyltransferase
TM1416	2.0	7.3	ABC-type transport system	conserved hypothetical protein
TM1723	2.2	15.9	Imidazolonepropionase and related amidohydrolases	conserved hypothetical protein
TM1755	2.5	13.5	Phosphotransacetylase	phosphate butyryltransferase

**Chapter 5: Evidence for AI-2 based cell-to-cell signaling in
hyperthermophilic archaea and bacteria: Proposed pathway for AI-2
biosynthesis in *Pyrococcus furiosus***

M.R. Johnson¹, J.D. Nichols¹, S.B. Connors¹, E. Pfeiler², C.J. Chou¹, S. Tachdjian¹, D.A. Comfort¹, J.K. Michel¹, C.I. Montero¹, B. Pridgen¹, K.R. Shockley³, and R.M. Kelly^{1}*

¹Department of Chemical and Biomolecular Engineering

²Department of Food Science
North Carolina State University
Raleigh, NC 27695-7905

³The Jackson Laboratory
Bar Harbor, ME 04609

Accepted to: *Applied and Environmental Microbiology* (October, 2005)

***Address correspondence to:**

Robert M. Kelly

Dept. of Chemical and Biomolecular Engineering
North Carolina State University
911 Partners Way, EB-1
Box 7905
Raleigh, NC 27695-7905

Phone: (919) 515-6396

Fax: (919) 515-3465

Email: rmkelly@eos.ncsu.edu

ABSTRACT

Intercellular communication, often referred to as quorum sensing, is widespread among the mesophilic bacteria but not yet found in other prokaryotes. Cell-free extracts from *Pyrococcus furiosus* and *Thermotoga maritima*, a hyperthermophilic archaeon growing optimally near 100°C, were found to trigger bioluminescence in *Vibrio harveyi* reporter strains. This indicated that the production of a recognizable form of AI-2, a furanosyl borate diester and known universal autoinducer of quorum sensing in mesophilic bacteria. Because these hyperthermophiles lack a key enzyme (LuxS) involved in AI-2 biosynthesis found in mesophilic bacteria, an alternative pathway must be involved. This issue was pursued through the purification of AI-2 biosynthetic enzymes from *P. furiosus* crude cell extracts using the *V. harveyi* reporter strain bioassay to follow quorum sensing activity. Indeed, it was shown that fractionated cell-free extracts could convert adenosine to a species that triggered quorum sensing in *V. harveyi*. Based on genome sequence information, an alternative pathway for AI-2 biosynthesis in *P. furiosus* could be proposed. This pathway involves the conversion of adenosine to adenine and ribose-1'-phosphate by a eukaryotic-like MTA-phosphorylase (PF0016) encoded in the *P. furiosus* genome. In fact, the recombinantly produced MTA phosphorylase could complement fractionated *P. furiosus* biomass to produce enhanced levels of AI-2 activity from adenosine at 90°C. Other enzymatic components of the pathway are under investigation but likely include a ribose phosphoisomerase (PF1258) to produce ribulose-1'-phosphate. A potentially unique contribution of thermal energy in the conversion of ribulose-1'-phosphate to (4S)-4,5-

dihydroxy-2,3-pentanedione (DPD), precursor to AI-2, is proposed such that this step is significantly accelerated over rates observed at mesophilic temperatures. These results suggest AI-2 should be considered as phenomena that can occur in organisms that lack LuxS, and that temperature may play an important role in the execution of cell-to-cell signaling in hyperthermophiles.

INTRODUCTION

It is becoming clear that microbial behaviors are coordinated through the production and detection of extracellular signaling molecules that accrue in proportion to population density within the microenvironment, which in turn regulate gene expression (28). Such signaling allows for a direct regulatory link between population density and phenotypes, and has been implicated in controlling biofilm formation, competence, virulence, and growth rate (25).

Interspecies communication in the Bacterial domain has been found to occur through the production and detection of a signal molecule known as AI-2, which is a furanosyl borate diester (8) produced from the metabolic byproducts of the activated methyl cycle through the actions of two highly conserved proteins LuxS and Pfs (20). To date, 239 microbial genomes have been fully sequenced, with ten per cent of those being members of the Archaea (<http://www.ncbi.nlm.nih.gov/Genomes>). Of those, nearly forty per cent contain a predicted LuxS protein, while LuxS is found in none of the Archaeal genomes (16). Processes controlled by AI-2 include many of the defining features of microbial pathogens: motility, toxin production, luminescence, and biofilm formation. This has made the AI-2 signaling system an important target for the study of anti-microbial treatments (24). In addition, the involvement of AI-2 as part of the detoxification pathway for the activated methyl cycle is an intriguing from an evolutionary perspective due to the fact this is a pathway found in almost all living organisms, utilizing highly conserved enzymes (20). In the activated methyl cycle, S-adenosyl homocysteine (SAH) is produced as a byproduct of DNA and protein methylation. As SAH is a potent inhibitor of methyltransferases, organisms have either a

SAH hydrolase or a Pfs nucleosidase, which can cleave SAH to either adenosine and homocysteine in the case of the SAH hydrolase, or S-ribosyl homocysteine (SRH) and adenine if Pfs is utilized (20). The further processing of SRH to AI-2 involves the LuxS enzyme, which is able to cleave the homocysteine from SRH and open the ribose moiety in a process that yields (4S)-4,5-dihydroxy-2,3-pentanedione (DPD), a compound that can spontaneously convert to AI-2 in the presence of boron (8, 18).

Evidence does exist that intra-species quorum sensing occurs in the hyperthermophilic bacteria (11), and preliminary studies have shown that a member of the halophilic archaea may produce a compound similar to the homoserine lactone signal molecules used for intra-species signaling in gram-negative bacteria (15). However, no evidence exists to date to suggest that members of the Archaea nor any other thermophile or hyperthermophile produce or detect inter-species signaling molecules akin to AI-2. All archaeal and thermophilic bacterial genomes that have been sequenced to indicate a putative SAH hydrolase and lack a putative LuxS in their genomes, such that they have not been examined for the production of the AI-2 signal molecule. However, this issue should be investigated if only for the reason that processing pathways for the degradation products of SAH hydrolase have not been identified.

Determining if interspecies communication occurs in the Archaea is key for the understanding of ecology in a broad spectrum of environments ranging from the oceans where archaea are estimated to constitute over one-fourth of the prokaryote biomass, to the GI tract flora of higher Eukaryotes, where archaea are major contributors to the digestive process (7). Evolutionarily, archaea share characteristics of both bacteria and eukaryotes (12). While the latter two domains have well-characterized systems for interspecies

communication, genomic homogeneity-based analysis of archaea has yet to identify any putative extracellular communication systems. If interspecies communication does occur in the archaea, it would provide insight into the evolution of cell-to-cell signaling, and the development of multi-cellularity.

MATERIALS AND METHODS

Growth of microorganisms. *P. furiosus* (DSM strain 3638) was grown at 90°C in BSMII media, while *T. maritima* strain MSB8 and *M. jannaschii* strain DSM2661 were grown at 80°C in BSMII media all without shaking. BSMII media contained the following (11): 40 g/l sea salts, 5 g/l tryptone, 3 g/l yeast extract, 3 g/l maltose, 3 g/l Piperazine-1,4-bis(2-ethanesulfonic acid) (PIPES), 0.5 mg/l NaSeO₃•5H₂O, 0.5 mg/l NiCl₂•6H₂O, 0.25 g/l NH₄Cl, 10 mg/l Fe(NH₄)₂(SO₄)₂•6H₂O, 1.25 g/l sodium acetate anhydrate, 1 ml/l 1% resazurin, 10 ml/l Wolfe's trace elements and 10ml/l Wolfe's trace vitamins solution (all Sigma Aldrich, Components of Wolfe's vitamin and mineral solutions can be found in ATCC medium no. 1343). The media was adjusted to pH 7.0, autoclaved for sterility, and stored at 4°C until use. For growth 50 mL of media was dispensed into 100 mL serum bottles, which were then capped, heated to the relevant growth temperature, sparged with nitrogen, and reduced with 0.5 mL of 10% L-cysteine / 10% sodium sulfide. Once reduced the cultures were inoculated with a 1% inoculum.

For autoinducer assays, *V. harveyi* strains were provided through the generosity of Dr. Bonnie Bassler, Department of Molecular Biology, Princeton University, Princeton, NJ. Strain BB152 (luxM::tn5Kan) (1) was used as a positive control for AI-2 production, while

strain MM32 (luxN::Cm, luxS::Tn5Kan) (14) was utilized in the *V. harveyi* bioassay (1). All were grown in AB media (1), with the respective antibiotic (chloramphenicol 30 ug/ml, kanamycin 50 ug/ml) added when necessary.

Screening of model hyperthermophiles for autoinducer production. Bioassays for autoinducers were developed following the methods of Bassler et al. (1). Luminescence was detected with a microplate reader (Perkin Elmer, HTS 7000 Plus), in dark-walled 96 well plates (Corning, 3603), with 200 μ L of culture added per well. The luminescence reading in relative light units (RLU) was read with an integration time of 150 ms, and a gain of 150. Cultures of the MM32 sensor strain were used for screening for the presence of AI-2, as MM32 is able to respond to AI-2 through the induction of luminescence, but cannot produce AI-2 or sense the species-specific quorum-sensing molecule AI-1. MM32 was grown overnight at 30°C in AB media with antibiotic and diluted 1/500 f with fresh AB media (with antibiotic).

For detection of autoinducers in culture supernatants, *P. furiosus*, *T. maritima*, and *M. jannaschii* cultures were harvested in late log phase through centrifugation, and the supernatant was filtered through a sterile 0.2 μ m filter (Millipore). For the bioassay, *V. harveyi* cultures were grown in capped 14 mL tubes (Bectin Dickinson) with shaking to minimize the inhibition of *V. harveyi* growth due to reducing agents present in some of the hyperthermophilic supernatants. Samples were drawn every 2 hours from the culture tubes, and read for luminescence with the maximum luminescence used for the purpose of analysis. Each culture tube contained 0.5 mL of the filtered supernatant, 4.5 mL of diluted *V. harveyi*

in AB media with appropriate antibiotics, and the cultures were grown in triplicate at 30°C with shaking at 225 RPM.

For detection of autoinducer synthesis activity in protein samples, reactions were carried out in sealed 96-well PCR plates (USA Scientific). Reaction mixtures included 15 µL 0.1X Phosphate Buffered Saline (Gibco), 5 µL of substrate, and 5 µL of protein sample. The reaction mixture was mixed and sealed, incubated at 90°C for one hour, cooled to room temperature and assayed for the presence of autoinducer by adding 20 µL of the reaction products to 180 µL of diluted *V. harveyi*. The mixture was loaded into dark-walled 96 well plates (Corning, 3603), and incubated 15 hrs in a microplate reader (Perkin Elmer, HTS 7000 Plus) at 30°C, with luminescence read every 3 hrs using the parameters listed above. Maximum luminescence was often detected at 9 hours. All assays were replicated at least three times.

Fractionation of native *P. furiosus* cell-free extract. *P. furiosus* was grown at 90°C in a 16-liter Microgen sterilizable-in-place fermenter (New Brunswick Scientific). Twelve liters of BSMII media adjusted to pH 7.0 was charged to the fermenter, which was heated to 90°C and stirred at 500 RPM with a single three-blade marine impellor for agitation. Temperature was controlled by utilizing the sterilization mode on the fermenter, which heats with steam through an internal heat exchanger. Once at 90°C, sparging was started using N₂ fed at 0.5 l/min to maintain anaerobic conditions. The media was reduced by the addition of 30 ml of 10% sodium sulfide / 10% L-cysteine through a septum, and 200 ml of inoculum was then added via a growth flask fitted with a dip tube. Anaerobic inoculum was forced into the fermenter via positive pressure with nitrogen gas through an addition port on the

fermenter. Cells were harvested in log phase (3×10^8 cells/mL) through centrifugation and were washed in 40 g/L sea salts (Sigma), and centrifuged again. The cell pellet was resuspended in 1X phosphate buffered saline (Gibco), and sonicated to lyse the cells. Cell debris was removed through centrifugation, and the cell-free extract was filtered through a 0.2 μ m filter (Millipore). The extract was dialyzed four times against 10 mM Tris (pH 7.0) using a 10 kDa Amicon stirred cell (Millipore). The resulting sample contained 15 g of crude protein as determined by the Bio-Rad protein assay (Bio-Rad).

The resulting sample was further purified using a DEAE Fast-Flow column (GE Healthcare, 100 mL column volume) eluted over a linear gradient from 0-2M NaCl (50 mM Tris, pH 7.0) with a flow rate of 3 mL/min. The resulting fractions were tested for activity using the microplate *V. harveyi* assay listed above with 50 mM adenosine as the substrate, and the fractions yielding greater than 5000 RLU in activity were pooled and resulted in 1.2 g of protein. The active pool was re-dialyzed against 10 mM Tris (pH 7.0), and purified again with the DEAE Fast-Flow column with elution occurring over a linear gradient from 200mM to 1M NaCl (50 mM Tris, pH 7.0) at a flow rate of 3 mL/min. The fractions were again tested using the *V. harveyi* assay, and active fractions were pooled, and dialyzed against water three times.

Large-scale *in-vitro* production of AI-2. The proposed autoinducer was synthesized for transcriptional studies in 100 mL sealed serum bottles containing 5 mL of *P. furiosus* crude extract (obtained from 2.5 L of *P. furiosus* culture), and 45 mL of 0.1X phosphate buffered saline (Gibco), with the reaction mixture heated with agitation for 1 hour at 90°C. A control was made utilizing the same procedure except 5 mL of 0.1X PBS was substituted in

place of the crude extract. Both samples were filtered after the heat incubation through a 10 kDa filter to remove proteins, and heated for 20 min at 90°C, sparged with nitrogen for 1 min, and reduced with 0.5 mL of 10% sodium sulfide, 10% L-cysteine. *V. harveyi* bioassays confirmed the production of over 20,000 RLU of luminescence in the autoinducer sample, with less than 10 RLU of activity in the control. It should be noted adenosine was not added to the synthesis reaction as it was found to greatly inhibit the ability to extract RNA in gene expression experiments. Activity was not dependant upon the addition of adenosine most likely due to the well-characterized ability of several *P. furiosus* proteins (e.g. PFsahH and PFMTAP) to bind adenosine in their active site (3, 17).

For small molecule mass spectra analysis, the same procedure as above was followed for synthesizing a control sample without crude extract and a sample reacted with crude extract with the exception that adenosine was added to both reactions at a final concentration of 1 mM to enhance the presence of the reaction substrates and products over the mass spectra background. Confirmation of activity was completed with the MM32 bioassay, and mass spectra analysis of the reaction products were completed by the Analytical Instrument Group (Raleigh, NC). The instrument utilized was a modified Varian MAT 212 double focusing reverse Nier/Johnson (magnet/electric field) high-resolution mass spectrometer. Molecular weight analysis of reaction products was completed using Fast Atom Bombardment (FAB) analysis with glycerol or mNBA (nitro-benzyl-alcohol) as a matrix. Electron Impact (EI) ionization was utilized for quantitative analysis at 70eV using a direct inlet system heated from 20°C - 380°C.

Microarray protocols. To examine the effects of AI-2 on *P. furiosus* gene expression, transcriptional studies were completed examining the effect of AI-2 addition to an actively growing culture. Two identical 400 mL cultures of *P. furiosus* were grown in 1 L bottles with septums (Corning), with one of the cultures dosed with 20 mL of synthesized autoinducer and the other culture dosed with the control. Both cultures were dosed at a cell density of 5×10^7 cells/mL, and the cultures were harvested and RNA was extracted 60 min after dosing.

A *P. furiosus* microarray was synthesized from PCR products as discussed previously (19), representing over 99% of the open reading frames in the sequenced genome. For each RNA extraction, 400 ml cultures were harvested, and quickly cooled to 0°C by immersion in ice water. The harvested cells were then immediately centrifuged at 13,000 x g (25 min at 4°C). Supernatant was discarded and the RNA was extracted from cell pellets, from which cDNA was synthesized, labeled through indirect incorporation, and hybridized to the microarray following the methods as described previously (11). Microarray slides were scanned using the appropriate laser power to balance the cy3 and cy5 signals with an ExpressLite Scanner (Perkin-Elmer). Raw uncorrected quantitation of spots was completed using ScanArray (Perkin-Elmer), and data analysis was completed as discussed previously (9), utilizing a mixed model ANOVA-based analysis to generate both least squared mean expression data, and the Bonferroni-corrected (27) fold-change data. Unless otherwise noted, gene annotation is from the COG database at NCBI (23).

Recombinant production of *P. furiosus* methylthioladenosine phosphorylase (PF0016). Primers utilized to amplify PF0016 were 5'-

ATATCATATGCCGAAGATAGGGATAATCG-3' and 5'-ATATGGATCCTCACACAAACATCGTCTT-3', which introduced a NdeI and BamHI sites respectively. The PCR products were purified and digested using NdeI and BamHI, and ligated into a similarly digested pET11A (Novagen). Sequence analysis of the insert confirmed no internal mutations existed. The resulting insert was transformed into BL21 Codon Plus (Stratagene), and 1-L of culture was grown under induction with 1 mM IPTG for 12 hours in LB media with 50 mg/L carbenicillin. The resulting culture was centrifuged at 7700 RPM for 20 minutes, with the cell pellet washed twice with fresh LB and re-centrifuged, and the resulting cell pellet was re-suspended in water and disrupted through sonication. Cell debris was removed by centrifugation, and the resulting crude extract was dialyzed twice against 10 mM Tris, pH 8.0, to remove AI-2 in the BL21 extract, and incubated at 80°C for 1 hour to denature the mesophilic BL21 proteins. The heat-treated extract was centrifuged at 15,000 RPM for 20 minutes, and filtered through a 0.2 µm filter (Millipore). The resulting extract was dialyzed two times against 0.1X PBS buffer, heated again to 80°C for 30 minutes to process substrate bound in the active site, and dialyzed two more times against 0.1X PBS. The presence of the recombinant enzyme was confirmed through the use of SDS-PAGE.

RESULTS

Autoinducer AI-2 activity in hyperthermophile supernatants. AI-2 activity was noted in the mid-log phase supernatants of the hyperthermophilic organisms *P. furiosus*, *Thermotoga maritima*, and *Methanococcus jannaschii*. The level of AI-2 activity in *P. furiosus* and *T. maritima* was about half of that found in BB152, which is expected due to the much lower maximum cell density of the hyperthermophilic cultures (mid 10⁸ cells / mL)

than BB152. *M. jannaschii*, which was grown to a maximum cell density one order of magnitude less than the other hyperthermophiles, displayed AI-2 activity that was about 12 per cent of that found in BB152, but was four times higher than that found in the BSMII media.

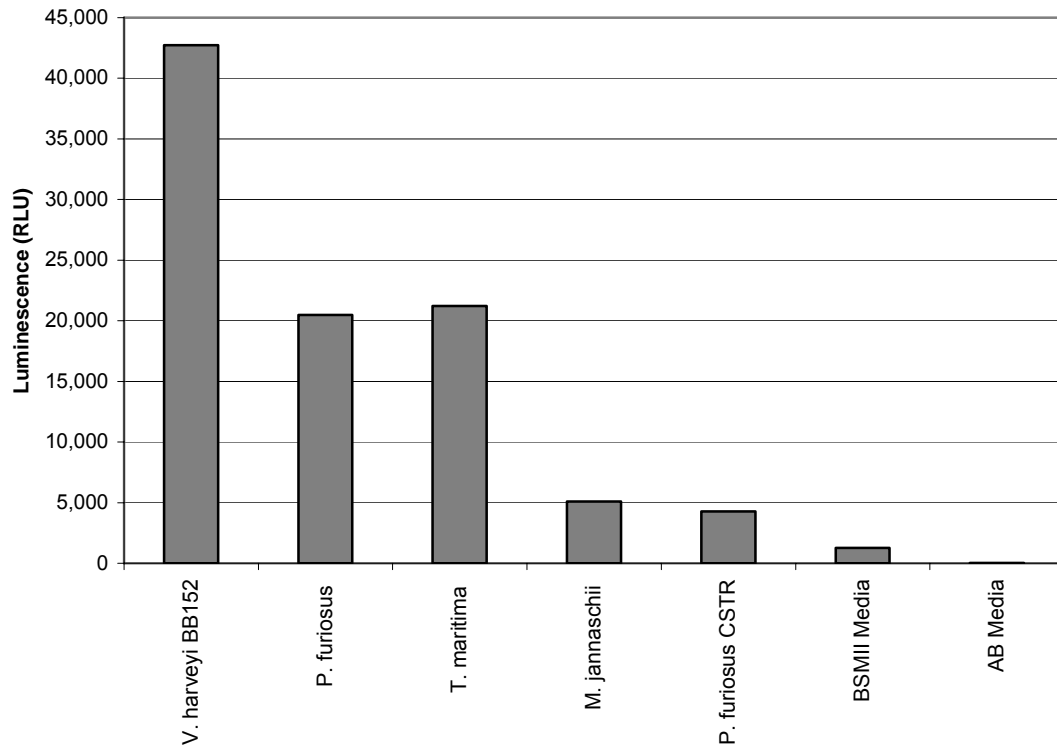


Figure 1. The induction of luminescence in *V. harveyi* strain MM32 by hyperthermophilic supernatants. Cultures of *P. furiosus*, *T. maritima*, and *M. jannaschii* were grown in BSMII media and tested with the *V. harveyi* bioassay. In addition a supernatant sample from continuous-culture grown *P. furiosus* ($D = 0.45$) was tested for supernatant activity. For a positive control, *V. harveyi* strain BB152 supernatant was tested.

P. furiosus grown in a continuous culture at a constant cell density of 2×10^8 cells per mL had AI-2 activity in its supernatant comparable to *M. jannaschii*, which is expected as autoinducers will not accumulate in the continuous culture environment.

Crude extract autoinducer synthesis activity in *P. furiosus*. As AI-2 is produced in mesophilic organisms from S-adenosyl homocysteine (SAH), a byproduct of the activated methyl cycle, it was hypothesized that AI-2 may be produced from SAH in *P. furiosus* as well. Crude *P. furiosus* protein extracts displayed autoinducer synthesis activity in the MM32 bioassay that was increased substantially in the presence of SAH (Table 1). To test the inactivation of the synthesis activity, the sample was both autoclaved and treated with EDTA. For EDTA treatment, an equal volume of 500 mM EDTA (Sigma-Aldrich) was added to a sample of crude extract protein, and the sample was incubated at room temperature for 1 hour. The sample was then dialyzed into pure water and concentrated to the original volume using a Centricon 10 kDa concentrator (Millipore). The activity was clearly disrupted by either autoclaving the crude extract for 20 minutes at 121°C, or also by treating the crude extract with EDTA.

Table 1. The induction of luminescence in *V. harveyi* strain MM32 by crude extracts of *P. furiosus*. Samples were prepared and heated at 90°C for 20 and 60 minutes, and then tested for autoinducer activity with the *V. harveyi* MM32 bioassay. Units are relative light units (RLU) measured as explained in the methods section.

Sample	20 min	60 min
30°C + no substrate	6	6
90°C + no substrate	2,666	15,354
30°C + SAH	7	7
90°C + SAH	10,660	25,353
Autoclaved 90°C + SAH	7	12
EDTA Treated 90°C + SAH	6	7

The production of AI-2 is an enzymatic reaction with adenosine as the proposed substrate. Following initial screening of the *P. furiosus* supernatants, an attempt was made

to purify the native enzymes responsible for AI-2 synthesis activity as LuxS, the synthesis enzyme in mesophilic AI-2 producing bacteria, is not apparently present in *P. furiosus* based from genomic analysis. Initial screening of crude extracts fractionated with a DEAE ion exchange resin indicated a substantial loss of activity with SAH as the substrate for AI-2 synthesis. As the *P. furiosus* genome encodes a SAH hydrolase that has been confirmed to have the ability to cleave SAH to adenosine and homocysteine (17), we hypothesize that the ribose moiety of adenosine could be the substrate utilized to produce AI-2. Upon the utilization of adenosine as the substrate, AI-2 synthesis activity was recovered in the fractionated proteins. AI-2 activity was not detected with ribose as the reaction substrate, nor was any substrate including adenosine activity in the enzymatic reaction without the addition of heat. In addition, adenosine heated in the presence of protein controls (bovine serum albumin) was not active. Active fractions were pooled and fractionated again utilizing the DEAE ion exchange resin with a reduced ion gradient. Active fractions were collected, and separated utilizing a Superdex 75 gel filtration column. The resulting active fractions were analyzed via peptide mapping to identify the genes encoding the proteins present in the partially purified protein.

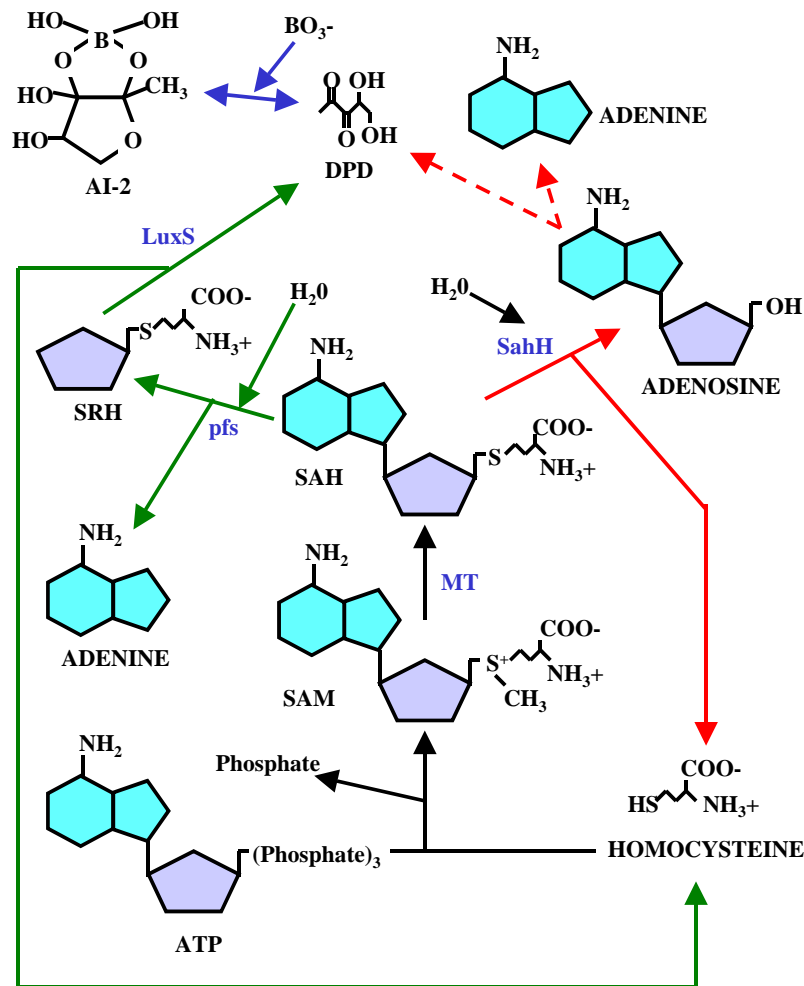


Figure 2. The production pathway for AI-2 in mesophilic organisms (green) and the proposed pathway in *P. furiosus* (red). The steps labeled in black are conserved in nearly all living organisms (20).

Proposed pathway for AI-2 production in *P. furiosus*. Adenosine has been shown as the substrate for the production of AI-2 from partially purified intracellular proteins from *P. furiosus*. The conversion of adenosine to DPD, the precursor to AI-2, would theoretically involve the cleaving of the ribose moiety from adenosine followed by the opening of the ribose ring followed by tautomerization. One enzyme that has been well characterized in *P. furiosus* that has been shown to cleave ribose from adenosine yielding phosphorylated ribose is Methylthioadenosine phosphorylase (PfMTAP, PF0016) (3, 5).

To examine if AI-2 synthesis activity with PF0016 in the presence of adenosine, PF0016 was produced recombinantly in *E. coli* and partially purified through a heat treatment, taking advantage of the proteins inherent thermal stability. AI-2 activity assays demonstrated PF0016 did not have the ability to form AI-2 from adenosine, but the activity of the purified native protein was complemented by PF0016 (Figure 3).

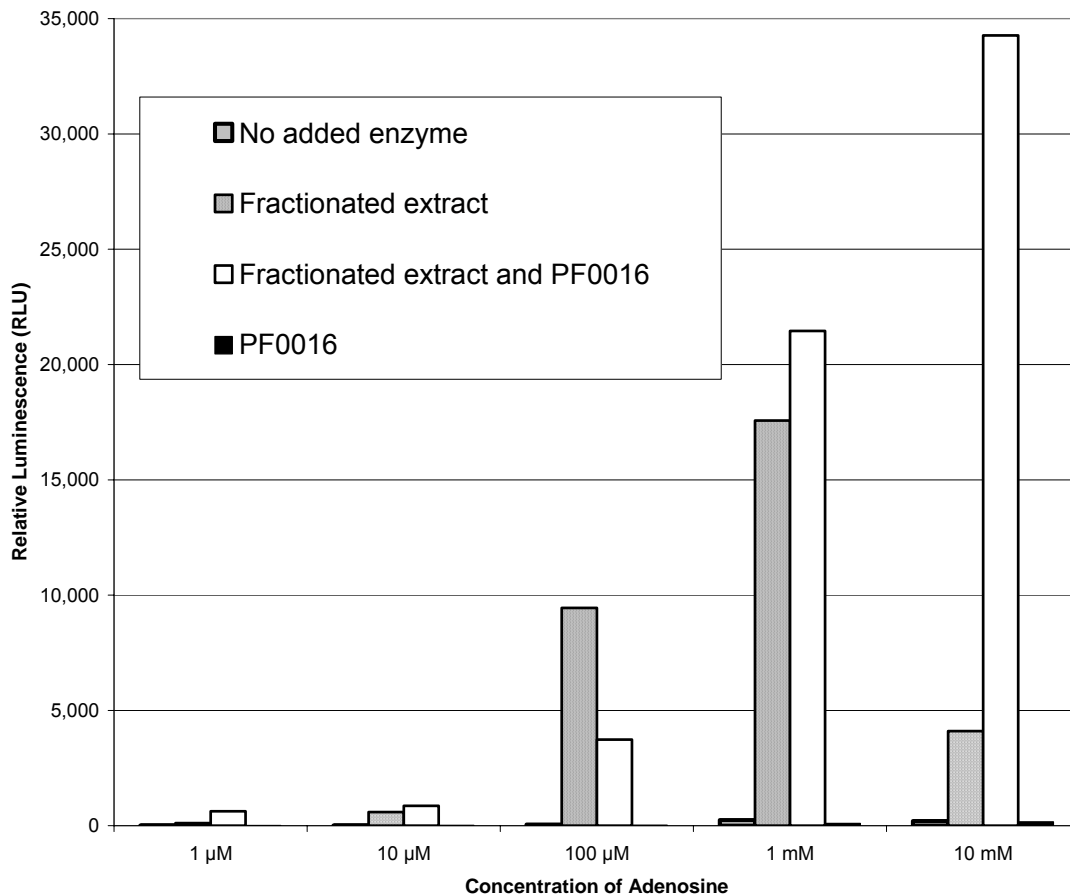


Figure 3. The effect of adenosine concentration on activity of purified *P. furiosus* crude extract. No activity was detected with heated and unheated adenosine without the presence of the purified crude extract. Purified extract without substrate both heated and unheated resulted in no detectable activity. In addition, no activity was detected with the MTA phosphorylase with adenosine.

Recently it has been shown that ribulose 5-phosphate can be converted to DPD, the precursor to AI-2, through a non-enzymatic spontaneous reaction (10). We hypothesize therefore that

the activity of PF0016 can be complemented with a ribose phosphoisomerase to yield ribulose 5-phosphate, which could spontaneously convert to DPD, which in the presence of abundant marine boron yields AI-2.

To examine the native enzyme reaction in more detail mass spectra analysis was completed on *in-vitro* produced AI-2 and control synthesis reaction products (Figure 4). Analysis of the 0.1X PBS buffer utilized for both reactions indicated peaks at m/z 114.9, 207.1 and 281.0 were resultant of the 0.1X PBS buffer, while background peaks at 120.9, 163.1, 205.1, 297.1 m/z occurred in all samples.

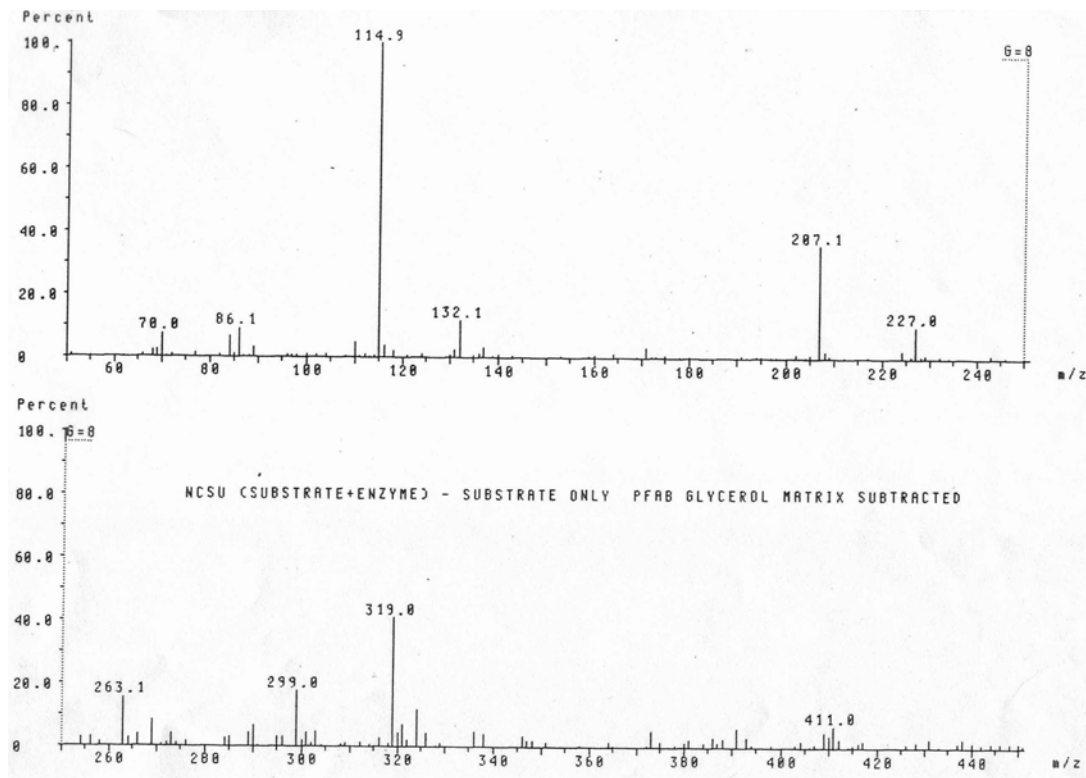


Figure 4. Background subtracted mass spectra analysis of *in-vitro* produced AI-2. Mass peaks at 132.1 and 227.0 are predicted to correspond to DPD and phosphorylated ribose, respectively.

Of significance was the presence of mass peaks at 132.1 and 227.0, which are in good agreement with that of DPD and phosphorylated ribose/ribulose, respectively. These findings support the hypothesis that a ribose moiety is cleaved from adenosine and phosphorylated and isomerized, after which it proceeds to DPD and AI-2.

Additional quantitative mass spectra analysis of the reaction products suggests that approximately 20% of the adenosine was converted in the reaction mixture (data not shown), which is not surprising given the reversible nature of the enzymatic conversion of adenosine by MTA phosphorylase. Given these results, 1-10% of the ribose moiety available in adenosine is converted to AI-2, which would place the half activation range of the *in-vitro* produced AI-2 somewhere in the micro-molar range, consistent measurements previously obtained for AI-2 induction in *V. harveyi* (18, 26). 4-hydroxy-5-methyl-3(2H) furanone (MHF), a commonly produced metabolic byproduct similar to AI-2 has been found to induce light production as well in *V. harveyi*, but with a half-induction point of around 1 mM (18); this level that has been confirmed in our laboratory (data not shown), and which is a much greater concentration than the products of our AI-2 *in-vitro* reaction. This suggests the products of the *P. furiosus in-vitro* reaction are of a similar activity level to that of *V. harveyi* produced AI-2.

Transcriptional response to *in-vitro* produced AI-2. In order to understand what, if any, biological response occurs in *P. furiosus* to the presence of AI-2 a transcriptional study was completed comparing a culture dosed with synthesized AI-2 to one dosed with a control reaction without enzyme. Fifteen genes were differentially expressed 1.7-fold or more using the Bonferroni correction (27) for statistical significance (Table 2). A low level

of induction was expected as the AI-2 autoinducer is being added to the culture in addition to AI-2 that is already present in the culture (Figure 1). Four genes were expressed at higher levels in the AI-2 dosed culture compared to the control, including putative ribose ABC transporter subunits which were each expressed higher in the AI-2 dosed culture.

Table 2. Differential gene expression in between an AI-2 and control dosed culture of *P. furiosus*.

	Fold Change AI2 - Control	neglog10 P-value	Predicted COG Function function
PF1676	1.8	4.3	Biotin-(acetyl-CoA carboxylase) ligase
PF1689	1.7	8.7	Transketolase, C-terminal subunit
PF1696	1.8	4.2	ABC-type uncharacterized transport systems, ATPase subunit
PF1697	2.3	11.3	Uncharacterized ABC-type transport system, permease subunit
PF0202	-1.7	5.5	Isocitrate dehydrogenases
PF0722	-2.7	13.2	Peroxiredoxin
PF0829	-1.6	4.8	hypothetical protein
PF1003	-1.7	6.9	ABC-type phosphate transport system,periplasmic
PF1020	-1.7	4.9	Phosphate/sulphate permeases
PF1264	-1.8	6.3	Translation elongation factor P(EF-P)/translation
PF1335	-1.7	7.5	Hydroxyethylthiazole kinase, sugar kinasefamily
PF1338	-2.1	11.4	Putative transcription activator
PF1530	-1.8	11.0	Flavoprotein involved in thiazolebiosynthesis
PF1751	-2.3	7.8	ABC-type thiamine transport system,periplasmic
PF1881	-2.3	9.6	Archaeal DNA-binding protein

The higher expression of the putative ribose transporters is of interest, as they do not seem to be sugar responsive when *P. furiosus* is grown on a wide variety of sugars (unpublished data). In *Escherichia coli* and *Salmonella typhimurium*, it has been found that the Lsr ABC transporter, which is highly similar to ribose ABC transporters, actively transports AI-2 inside of the cells, where it is phosphorylated and regulates gene expression (21, 22, 29). Whether these transporters function to transport AI-2 in *P. furiosus* is yet to be confirmed, but evidence does exist that the dosing of AI-2 into an actively growing *P. furiosus* culture actually leads to the reduction of AI-2 in the culture supernatants.

Supernatants saved from the dosed culture samples used for transcriptional analysis were screened for the presence of AI-2 activity using the MM32 bioassay, and it was found that substantially less AI-2 activity was noted in the AI-2 dosed culture (13,551 RLU) compared to the control (32,605 RLU). This result suggests the expressed transporters may be induced by the increased concentration of AI-2 in the AI-2 dosed culture, in turn triggering the uptake of AI-2 from the extracellular environment. In a follow up experiment, supernatant samples of *P. furiosus* were collected at different phases of growth and it was found autoinducer activity was phase dependant, with AI-2 activity decreasing sharply in stationary phase (Table 3).

Table 3. The induction of luminescence in MM32 by the supernatants of *P. furiosus* at different growth phases.

	Cell density (cells/mL)	Luminescence (RLU)
<i>P. furiosus</i> Early Log	4.2E+06	844
<i>P. furiosus</i> Late Log	1.0E+08	20,468
<i>P. furiosus</i> Stationary	3.0E+08	217

A notable gene expressed at reduced levels in the AI-2 dosed culture compared to the control was the putative transcription factor (PF1338). While a function for this activator is unknown, it is likely that a transcription regulator will be differentially expressed in response to AI-2 concentrations as a means to link population density to a expression response.

DISCUSSION

In this study we demonstrate AI-2 activity is present in the culture supernatants of several hyperthermophilic microorganisms, all of which based on the available genomic information lack the luxS and pfs enzymes required for AI-2 production in mesophilic organisms. In *P. furiosus*, the AI-2 activity is produced utilizing adenosine as the ribose moiety donor, through a process that likely occurs via the phosphorylation and isomerization of the ribose moiety, followed by the spontaneous conversion to DPD, and then AI-2, in the presence of boron.

One enzyme that seems to play a complimentary role in this pathway is MTA phosphorylase (PF0016), which has the unique feature of having exceptional activity against adenosine. While it is not uncommon that MTA phosphorylases (MTAP) have activity against adenosine, it is often at greatly reduced levels compared to their primary substrate (2). The *P. furiosus* genome contains two putative MTAPs based on sequence homology, including the above-mentioned PF0016 which has been characterized (5), and PF0853 which is a hypothetical MTAP. MTAPs are classified under the purine nucleotide phosphorylase (PNP) family based upon sequence homology and are grouped into two classes, low molecular weight and high molecular weight PNPs (2). High molecular weight PNPs form homohexameric complexes and are classified with having broad substrate utilization including MTA, adenosine, guanosine, and inosine. Low molecular weight PNPs form homotrimeric complexes, and are classified as having activity inosine and guanosine, but not adenosine. Based on sequence analysis, PF0853 belongs to the class II high molecular weight PNPs, while PF0016 is a class I low molecular weight PNPs, with an extremely high sequence identity (52%) to the characterized human trimeric class I PNP, while having

extremely high activity against adenosine (3). The key to the high activity against adenosine lies in a key amino acid substitution in PF0016 that allows it to recognize bind adenosine. It has been found that in the mouse class I PNP, which is nearly identical to the human class I PNP, substituting Asn-243 with Asp allows the binding of the C6-amino group found of adenosine (13). Alignment of the mouse PNP with PF0016 uncovered that the same exact substitution occurs in PF0016, with the Asn aligned with the mouse Asn-243 replaced with Asp (Figure 5).

```

CLUSTAL FORMAT for T-COFFEE Version_1.41, CPU=0.49 sec, SCORE=95, Nseq=2, Len=299

Mus_musculus_PNP  MENEFTYEDYETTAKWLLQHTEYRPOQVAVICGSLGGLTAHLKEAQIFDYNEIPNFPQST
PF0016             -----MPKIGIIGGSGVYGIFEPKETVKVHTPYGRFSAPVEI
                   *:::* ***: *:   : ...   * . * .

Mus_musculus_PNP  VQGHAGRLVFGLLNGRCCVMMQGRFHMHEGYSLSKVTFPVRVVFHLLGVETLVVINAAGGL
PF0016             GEIEGVEVAF-----IPRHGKYHEFPPEV-PYRANIWALHELGVVERVIAVNAVGS
                   : .. ...*           : *::* : ::   : :* **** :...*.**

Mus_musculus_PNP  NPNFEVGDIMLIRDHINLPGFCGQNPLRGPNDERFGVRFPFAMSDAYDRDMRQKAFTAWKQ
PF0016             KEEYKPGDIVIIDQFIDFTKKREYTFYNGPR-----VAHISMADPFCELRRIETAKE
                   : :: *::**:* :.*:::   . **   * . :*:*: :*: : : *

Mus_musculus_PNP  MGEQRKLQEGTYVMLAGPNFETVAESRLKMLGADAVGMSTVPEVIVARHCGLRVFGFSL
PF0016             LNLVPVH-EKGTIYICIEGPRFSTRAESRMFRQF-ADVIGMTLVPEVNLARELGMCYVNIST
                   :.   : :***: : **.*.* ****::: : *::***: **** :**.* : : : *

Mus_musculus_PNP  ITNKVVMVDYENLEKANHMEVLDAGKAAAQTLERFVSILMESIPLPDRGS-----
PF0016             VTD---YDVWAEKPVDAQEVLRVMKENEKVKLLKRAIPKIPERKCGCADVLKTMFV
                   :*:   *   : .:  *** . *   :.:.:.: : .**   : .

```

Figure 5. Alignment of the mouse class I PNP with PF0016. A key substitution to aspartic acid at the highlighted mouse residue 243 (asparagine) occurs in PF0016. The same substitution in the mouse PNP has been shown to enable activity against adenosine (13).

Temperature may play a role in use of adenosine as a substrate for AI-2 production, as the key amino acid substitution occurring in PF0016 is also seen in the class I MTAPs from *S. solfataricus* (SSO2706), which is active against adenosine (6), and in the hypothetical class I MTAP in *T. maritima* (TM1737). PNPs in mesophilic

organisms that are active against adenosine do not share a high degree of homology with the Eukaryotic PNPs, and utilize a different conserved motif for the active site that binds adenosine (2). In addition, the mesophilic PNPs active against adenosine have broad activities against a wide variety of purines, with their primary activity against inosine and guanosine (2), while the hyperthermophilic MTAP from *P. furiosus* and *S. solfataricus* have a much higher preference for binding adenosine over guanosine or inosine (3, 4). As the reaction from phosphorylated ribose to DPD proceeds very slow at mesophilic temperatures (10), but could be quite rapid at hyperthermophilic temperatures, it may be the primary pathway proposed for AI-2 production in *P. furiosus* is only feasible at elevated temperatures. Such a phenomena would be intriguing as the enzyme classes proposed to be utilized in *P. furiosus* exist in nearly all living organisms. Future work in reproducing the proposed pathway recombinantly in *P. furiosus* and other hyperthermophilic organisms could help resolve the effect of temperature on the evolution of signaling systems.

ACKNOWLEDGEMENTS

This work was supported was supported in part through grants from the NASA Exobiology Program, NSF Biotechnology Program and the DOE Energy Biosciences Program.

REFERENCES CITED

1. **Bassler, B. L., E. P. Greenberg, and A. M. Stevens.** 1997. Cross-species induction of luminescence in the quorum-sensing bacterium *Vibrio harveyi*. *J. Bacteriol.* **179**:4043-4045.
2. **Bzowska, A., E. Kulikowska, and D. Shugar.** 2000. Purine nucleotide phosphorylases: properties, functions, and clinical aspects. *Pharmacol. Ther.* **88**:349-425.
3. **Cacciapuoti, G., C. Bertoldo, A. Brio, V. Zappia, and M. Porcelli.** 2003. Purification and characterization of 5'-methylthioadenosine phosphorylase from the hyperthermophilic archaeon *Pyrococcus furiosus*: substrate specificity and primary structure analysis. *Extremophiles* **7**:159-168.
4. **Cacciapuoti, G., S. Forte, M. A. Moretti, A. Brio, V. Zappia, and M. Porcelli.** 2005. A novel hyperthermostable 5'-deoxy-5'-methylthioadenosine phosphorylase from the archaeon *Sulfolobus solfataricus*. *FEBS J.* **272**:1886-1899.
5. **Cacciapuoti, G., M. A. Moretti, S. Forte, A. Brio, L. Camardella, V. Zappia, and M. Porcelli.** 2004. Methylthioadenosine phosphorylase from the archaeon *Pyrococcus furiosus*. Mechanism of the reaction and assignment of disulfide bonds. *Eur. J. Biochem.* **271**.
6. **Cacciapuoti, G., M. Porcelli, C. Bertoldo, S. Fusco, M. De Rosa, and V. Zappia.** 1996. Extremely thermophilic and thermostable 5'-methylthioadenosine phosphorylase from the archaeon *Sulfolobus solfataricus*. Gene cloning and amino acid sequence determination. *Eur. J. Biochem.* **239**:632-637.
7. **Cavicchioli, R., P. M. G. Curmi, N. Saunders, and T. Thomas.** 2003. Pathogenic archaea: do they exist? *Bioessays* **25**:1119-1128.
8. **Chen, X., S. Schauder, N. Potier, A. Van Dorsselaer, I. Pelczer, B. L. Bassler, and F. M. Hughson.** 2002. Structural identification of a bacterial quorum-sensing signal containing boron. *Nature* **415**:545-549.
9. **Chhabra, S., K. R. Shockley, S. Conners, K. Scott, R. Wolfinger, and R. Kelly.** 2003. Carbohydrate induced differential gene expression patterns in the hyperthermophilic bacterium *Thermotoga maritima*. *J. Biol. Chem.* **278**:7540-7552.
10. **Hauck, T., Y. Hubner, F. Bruhlmann, and W. Schwab.** 2003. Alternative pathway for the formation of 4,5-dihydroxy-2,3-pentanedione, the proposed precursor of 4-hydroxy-5-methyl-3(2H)-furanone as well as autoinducer-2, and its detection as natural constituent of tomato fruit. *Biochim. Biophys. Acta.* **1623**:109-119.
11. **Johnson, M. R., C. I. Montero, S. B. Conners, K. R. Shockley, S. L. Bridger, and R. M. Kelly.** 2004. Population density-dependent regulation of exopolysaccharide formation in the hyperthermophilic bacterium *Thermotoga maritima*. *Mol. Microbiol.* **55**:664-674.
12. **Lopez-Garcia, P., and D. Moreira.** 1999. Metabolic symbiosis at the origin of eukaryotes. *Trends Biochem. Sci.* **24**:88-93.
13. **Maynes, J. T., W. Yam, J. P. Jenuth, R. Gang Yuan, S. A. Litster, B. M. Phipps, and F. F. Snyder.** 1999. Design of an adenosine phosphorylase by active-site modification of murine purine nucleoside phosphorylase. *Enzyme kinetics and*

- molecular dynamics simulation of Asn-243 and Lys-244 substitutions of purine nucleoside phosphorylase. *Biochem. J.* **344**:585-592.
14. **Miller, S. T., K. B. Xavier, S. R. Campagna, M. E. Taga, M. F. Semmelhack, B. L. Bassler, and F. M. Hughson.** 2004. *Salmonella typhimurium* recognizes a chemically distinct form of the bacterial quorum-sensing signal AI-2. *Mol. Cell* **15**:677-687.
 15. **Paggi, R. A., C. B. Martone, C. Fuqua, and R. E. De Castro.** 2003. Detection of quorum sensing signals in the haloalkaliphilic archaeon *Natronococcus occultus*. *FEMS Microbiol. Lett.* **221**:49-52.
 16. **Peterson, J., L. Umayam, T. Dickinson, E. K. Hickey, and O. White.** 2001. The comprehensive microbial resource. *Nucleic Acids Res.* **29**:123-125.
 17. **Porcelli, M., M. A. Moretti, L. Concilio, S. Forte, A. Merlino, G. Graziano, and G. Cacciapuoti.** 2005. S-adenosylhomocysteine hydrolase from the archaeon *Pyrococcus furiosus*: biochemical characterization and analysis of protein structure by comparative molecular modeling. *Proteins* **58**:815-825.
 18. **Schauder, S., K. Shokat, M. G. Surette, and B. L. Bassler.** 2001. The LuxS family of bacterial autoinducers: biosynthesis of a novel quorum-sensing signal molecule. *Mol. Microbiol.* **41**:463-476.
 19. **Shockley, K. R., D. E. Ward, S. Chhabra, S. Conners, C. Montero, and R. Kelly.** 2003. Heat shock response by the hyperthermophilic archaeon *Pyrococcus furiosus*. *Appl. Environ. Microbiol.* **69**:2365-2371.
 20. **Sun, J., R. Daniel, I. Wagner-Dobler, and A. P. Zeng.** 2004. Is autoinducer-2 a universal signal for interspecies communication: a comparative genomic and phylogenetic analysis of the synthesis and signal transduction pathways. *BMC Evol. Biol.* **4**:36.
 21. **Taga, M., S. T. Miller, and B. L. Bassler.** 2003. Lsr-mediated transport and processing of AI-2 in *Salmonella typhimurium*. *Mol. Microbiol.* **50**:1411-1427.
 22. **Taga, M., J. Semmelhack, and B. Bassler.** 2001. The LuxS dependant autoinducer AI-2 controls the expression of an ABC transporter that functions in AI-2 uptake in *Salmonella typhimurium*. *Mol. Microbiol.* **42**:777-793.
 23. **Tatusov, R., D. Natale, I. Garkavtsev, T. Tatusova, U. Shankavaram, B. Rao, B. Kiryutin, M. Galperin, N. Fedorova, and E. Koonin.** 1997. The COG database: new developments in phylogenetic classification of proteins from complete genomes. *Nucleic Acids Res.* **29**:22-28.
 24. **Vendeville, A., K. Winzer, K. Heurlier, C. M. Tang, and K. R. Hardie.** 2005. Making 'sense' of metabolism: autoinducer-2, LuxS and pathogenic bacteria. *Nat. Rev. Microbiol.* **3**:383-396.
 25. **Waters, C. M., and B. L. Bassler.** 2005. Quorum sensing: cell-to-cell communication in Bacteria. *Annu. Rev. Cell Dev. Biol.* **21**:319-346.
 26. **Winzer, K., K. R. Hardie, N. Burgess, N. Doherty, D. Kirke, M. Holden, R. Linfoth, K. Cornell, A. Taylor, P. Hill, and P. Williams.** 2002. LuxS: its role in central metabolism and the *in-vitro* synthesis of 4-hydroxy-5-methyl-3(2H)-furanone. *Microbiol.* **148**:909-922.

27. **Wolfinger, R., G. Gibson, E. Wolfinger, L. Bennet, H. Hamadeh, P. Bushel, C. Afshari, and R. Paules.** 2001. Assessing gene significance from cDNA microarray expression data via mixed models. *J. Comp. Biol.* **8**:625-637.
28. **Xavier, K. B., and B. L. Bassler.** 2003. LuxS quorum sensing: more than just a numbers game. *Curr. Opin. Microbiol.* **6**:191-197.
29. **Xavier, K. B., and B. L. Bassler.** 2005. Regulation of uptake and processing of the quorum-sensing autoinducer AI-2 in *Escherichia coli*. *J. Bacteriol.* **187**:238-248.

**Appendix One: Microarray and Real-Time PCR protocols and manual
Revision 1.4 (04-01-2005)**

Matthew R. Johnson, Clemente I. Montero, C.J. Chou and Keith R. Shockley

**Department of Chemical and Biomolecular Engineering
North Carolina State University
Raleigh, NC 27695-7905**

Date(s) Completed _____

Experiment _____

Researcher _____

RNA Sample Info

RNA Tube	Condition	RNA Conc.	Dye to be Labeled	Date Grown	Media Used	Growth Container	Gel Run on RNA

Slides Info

Slide Barcode	Which Tube for Cy3	Which Tube for Cy5

Key References:

[1]Hasseman, J. (2001). TIGR protocols

[2]Schut et al., 2001 "DNA microarray analysis of the hyperthermophilic archaeon *Pyrococcus furiosus*: evidence for a new type of sulfur-reducing enzyme complex. J. Bact.

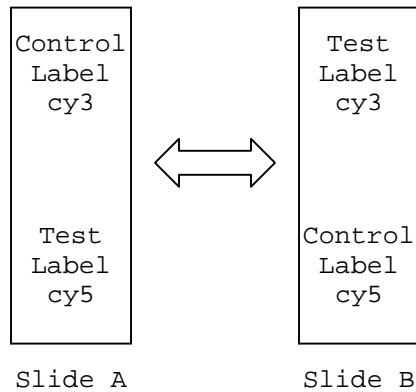
[3]Hegde, et al., 2000. A concise guide to cDNA microarray analysis. Biotechniques.

29:548-562.

Experimental Design:

The key to a proper experiment and good quality results is sitting down and thinking about what questions you want to answer, and how do are you going to answer them with the microarray. Not how can I run some microarrays, and get some questions to answer!!!!

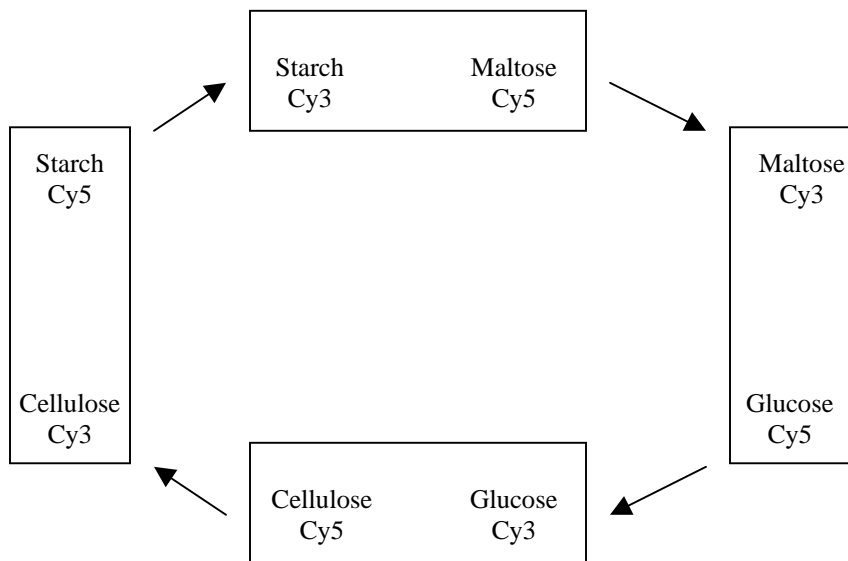
Dye Flips – Good for comparing two samples, i.e. a control (C) and a test (T). Below is shown how to run this experiment with two slides.



Time Course / Multiple Conditions – Read Gary Churchill’s Papers, there is no better source for good information on this.

Kerr and Churchill(2001), [Experimental design for gene expression microarrays](#), Biostatistics, 2:183-201.
Churchill GA. 2002. Fundamentals of experimental design for cDNA microarrays. Nat Gen Supp 32: 490-496.

The example loop below is for an experiment with four different conditions. i.e. four different sugars.



CULTIVATION

MAKING GLUTERALDEHYDE TUBES (for cell preservation)

1. Obtain Gluteraldehyde from freezer and place in the hood to thaw. Check concentration on the bottle.
2. Make 2.5% solution: add 0.9 mL of 50% glut. Solution & 17.1 mL of water. (PREPARE IN HOOD).
3. Use pipettor to aliquot 100 uL into 2 ml tubes. Store in freezer when finished.

GROWING BATCH CULTURES IN STOCK BOTTLES

4. Measure out autoclaved media into each culture bottle required (usually 50 ml).
5. Add additional nutrients (sugar etc.) if needed to bottle. Label aluminum top with date, species, media, and your initials and seal shut.
6. Heat media in shaking incubator set to proper temperature for growth (80C TMA, MJA, SSO / 90C PFU). Heat for about 15 minutes.
7. Insert 2 needles into the top of the bottle, hook up the nitrogen, and lightly sparge for 30 seconds. Add 0.4 ml of reducing agent (10% sodium sulfide, or 10% NaS, 10% cysteine) The media will turn color from a pink to a clear/yellow after a few minutes. Let sit in bath until color change appears.
8. Inoculate using a 1% inoculum from a previously grown culture and return to the bath. Note that MJA is light sensitive and should be covered.
9. Record time of inoculation and monitor growth every hour for a growth curve. TMA and PFU will be to stationary phase within 12 hours, MJA takes about 24 hours, and SSO takes 1-2 days.
10. Grow at least 400 ml in a 1 liter bottle for use for RNA extractions. Make sure to pass the cells at least 3 times before attempted the 400 ml scale.

PROCEDURE FOR COUNTING CELLS WITH THE MICROSCOPE

1. Turn on the microscope to let it warm up.
2. Put on gloves for protection from acridine orange.

3. Replace distilled water in petri dish, glass bottle, and plastic bottle everyday to ensure that the water is sterile. Rinse flask apparatus first with ethanol and then with sterile water.
4. Get materials: 2.5% glutaraldehyde (ga) tubes to preserve cells, test tubes (one for each sample). Soak enough filters (one for each sample) in the petri dish of water.
5. Use a 1 mL syringe; check to make sure the tip is on tight. Withdraw 1 mL of cells from each bottle for sampling, putting the cells in the ga tubes and vortexing.
6. Add 4.7 mL of sterile water to each test tube with 200 uL of acridine orange. Dispose waste properly in labelled containers.
7. Add cells to the test tubes: 80 ul max, but judge by the turbidity of the culture and the time allowed for growth. For good growth, you would expect to count about 30 to 40 cells in a grid for a 5 uL sample of cells.
8. Put a wet filter on the flask top piece and place it on top of a glass prefilter, being careful not to move it once touching (the filter will wrinkle). Clamp the two pieces together and pour a sample into the top piece. Turn of the vacuum pump.
9. Once the sample has completely gone through the filter (i.e. no liquid remains in the top piece), remove the clasp and lift the filter from the flask. Place on a microscope slide with a drop of microscope oil. Put a cover slip on top and press down firmly with top of tweezers. Put another drop of oil on top of the cover slip. A slide can hold up to three filter samples; be sure to label to avoid confusion.
10. Focusing with the microscope: With the lamp warmed, open the gates to let the light reach the slide area. Insert a slide and lower the piece with the coarse adjustment until it just touches the oil on top of the slide. Continue lowering with the coarse adjustment, observing a bright background turning darker through the eyepiece. The orange-stained cells will appear as it begins to turn blacker, and then focus them with the fine adjustment.
11. Count the cells in the grid. Move around the slide to collect 10 total counts of one sample. This can be done while keeping the microscope in focus. Notice if cells are clumped together in regions and scarce in others to correctly represent the cell numbers. Average the 10 counts, and calculate the cell density.

Cell Density (cells per ml) = average *21,000,000 / ul of cells added

RNA Extraction:

- 1) Grow cultures until early/mid log phase or to desired point (0.5-1.0 % inoculum). You need at least 400 ml of culture per sample if harvesting at 10^7 cells per ml or higher.
- 2) If grown on sulfur, filter the culture through a coffee filter (use funnel)
- 3) Spin the cells at 7500 rpm for 22 min, discard the supernatant.
- 4) Resuspend cells in 2.8 mL ice-cold SSM per centrifuge bottle.
- 5) Aliquot into 2.0 ml eppendorf tubes and spin at 13,000 rpm for 30 sec, discard supernatant.
- 6) Resuspend the resulting pellet in 85 ul of ice-cold TE buffer
- 7) Add 625 ul of RNA Lysis buffer (recipe below) to each tube immediately after resuspension in TE
 - cells should lyse almost immediately
 - pass the lysate through a 20 gauge needle to shear the genomic DNA
 - YOU CAN STOP HERE BY PLACING IN -80°C FREEZER UP TO 2 WEEKS
- 8) Add 62.5 ul of 2 M NaAcetate (pH= 4.5) to thawed lysate
- 9) Add an equal volume (approx. 750 ul) of Phenol/Chloroform 5:1 (pH= 4.5, from Ambion) in the fume hood
- 10) Vortex briefly, allow to sit on ice for 5 min then spin 20 min at 13,000 rpm at 4°C
- 11) Pipette off the top layer into a new tube, do not disturb or collect the protein layer floating in the middle of the tube.
- 12) Ethanol Precipitate the RNA (KEEP ICE COLD) by adding 1/10 vol 3 M NaAcetate (pH= 5.5) and 2.5 vol. EtOH to the sample just collected.
- 13) Keep at -20°C overnight or -80°C for 2 hours. Best to do the -20 option if time allows.
- 14) Centrifuge at 13,000 rpm for 30 min, and pour off the supernatant.
- 15) Resuspend each pellet in 500 ul 70% ethanol and spin for 15 min.
- 16) Pour off the supernatant and resuspend pellet in 90 ul of 10 mM Tris (pH 8.5).
- 17) Proceed to Ambion RNA Aqueous Extraction.

Extraction buffer for above steps:

250 g Guanadine thiocynate (6.2 M final)

17.6 ml 0.75 M NaCitrate (pH 7.0)

26.4 ml 10% Sarcosyl

293 ml MilliQ

Note- add 75 ul B-mercaptoethanol/ 10 ml extraction buffer- usually store in 50 ml aliquots

Ambion RNA Purification (2nd Step):

- 1) Add 600 ul of Ambion extraction buffer _____ (Check when completed)
to each tube of RNA
- 2) Add 600 ul of 64% ethanol to each tube of RNA _____ (Check when completed)
- 3) Mix well and apply 600 ul at a time to the Ambion _____ (Check when completed)
Column and centrifuge. Repeat until all is applied.
Empty collection tube after each spin for this step and
All washes listed below.
- 4) Add 700 ul of Ambion wash #1 to column and centrifuge _____ (Check when
completed)
- 5) Add 700 ul of Ambion wash #2/3 to column and centrifuge _____ (Check when
completed)
- 6) Repeat previous step _____ (Check when completed)
- 7) Empty collection tube and centrifuge again 1 minute _____ (Check when completed)
- 8) Place new collection tube on column _____ (Check when completed)
- 9) Elute by adding 60 ul of elution solution **heated to 80 C** _____ (Check when
completed)
- 10) Centrifuge 1 min to collect elution and _____ (Check when completed)
repeat elution into a new collection tube.

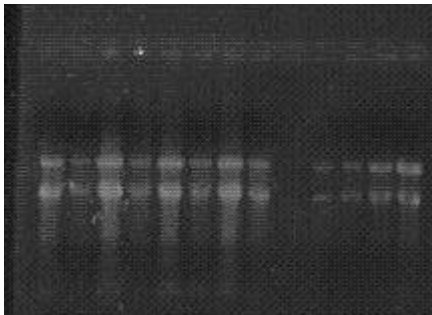
Quality Control: Make a 1/100 dilution (100 ul for each) of each RNA sample and check the absorbance in the GRL. You want a OD₂₆₀ above 1.0, and OD₂₆₀/OD₂₈₀ > 2.0 . A low ratio may mean you extracted protein with RNA.

Quantify: $\text{ug/ul of RNA} = \text{OD}_{260} * 40 * 100 \text{ (the dilution)} / 1000$

GRL SPEC: Click nucleic acids. Click the UV symbol on the bottom of the screen to turn on the UV lamp. Add 100 ul of blank solution (TE) to the small DNA cuvette. Insert into spec and click on blank. Once blanked, remove blank and clean cuvette, add sample and click on read sample. Repeat cleaning and spec additional samples. **Make sure to turn off UV when done !!!!!**

Running the RNA Gel:

- 1) Clean the RNA gel box and combs with RNaseZAP (Ambion)
- 2) Prepare 30 ml of 1% agarose (RNase free) with Sterile 1X TBE.
- 3) Heat the agarose and pour, using the smallest comb for making wells.
- 4) Make dilutions of your RNA so that in a 2-4 ul sample there is 1 ug of RNA (we want to load 1 ug per well).
- 5) Add equal volume Ambion 2X loading buffer and heat at 65 C for 15 minutes.
- 6) Load samples in wells, and run gelbox at 65V.
- 7) Once the gel front has crossed the midpoint in the gel, remove the gel and stain in 1X TBE with 10 mg/ml EtBr. Take a picture with the transilluminator. (CAUTION: EtBr CAN CAUSE CANCER, WEAR GLOVES ALWAYS).
- 8) A gel should look as the one below, with two ribosomal bands and no genomic band. A heavily smeared gel signifies heavily degraded RNA, and the sample should not be used.



No Genomic Present

Ribosomal Bands

Reverse Transcriptase Reaction Option A - Stratagene Protocol:

You need five tubes per slide, per sample. So for a two-condition experiment, with each condition labeled with Cy3 and Cy5, using two slides, you will run ten tubes per sample for a total of twenty tubes. The tubes used are domed PCR tubes for use in the thermocycler

1) Add the following, making the total for all the tubes in each condition in one tube and then dispensing it into individual labeled tubes :

Multiply each sample times 1.10 (extra to make sure to have enough)

Y = ul needed to yield 5 ug

Q = number of RT tubes for that sample (usually = 5)

	Per Tube	Name:	Name:	Name:	Name:	Quantity Needed
Total RNA	Y					Y x 1.1 x Q
Random Primers (3ug/ul)	2 ul					2ul x 1.1 x Q
Water	13-Y					(13-Y) x 1.1 x Q
Total	15 ul					15 x 1.1 x Q

2) Mix Well and Dispense 15 ul into each tube _____ (Check when completed)

3) Incubate at 70°C for 10 min. _____ (Check when completed)

******* Start making dNTP mix and RT master mix *******

4) Place in a dry ice/EtOH bath for 30 sec. _____ (Check when completed)

5) microfuge briefly at 13,000 rpm _____ (Check when completed)

6) Add 5 ul of RT Mix to each tube _____ (Check when completed) and mix well

7) Incubate at 42°C for 2-16 hours _____ (Check when completed)

8) To hydrolyze RNA add 10ul 1N NaOH to each tube _____ (Check when completed)

- 9) To stop reaction add 10ul 0.5M EDTA to each tube _____ (Check when completed)
- 10) Mix and incubate at 65°C for 15 min. _____ (Check when completed)
- 11) Add 10ul 1 N HCl to each _____ (Check when completed)
tube to neutralize reaction mix

RT Master Mix

Add the following:

	<u>Per Tube</u>	<u>Final Conc.</u>	<u>Total Needed</u>
10X Strand Buffer	2ul	1x	_____ 2ul x N x 1.1
*dNTP mix	1ul	1x	_____ 1ul x N x 1.1
StrataScript	2ul	100U	_____ 2ul x N x 1.1

Total	5ul		_____ 5ul x N x 1.1

N = total number of tubes for all samples

*20x dNTP mix	<u>Conc. In 20x Mix</u>	<u>ul per tube</u>	<u>Total Needed</u>
dATP (100 mM Stock)	10mM	0.1	_____ 0.1 x N x 1.1
dGTP (100mM Stock)	10mM	0.1	_____ 0.1 x N x 1.1
dCTP (100mM Stock)	10mM	0.1	_____ 0.1 x N x 1.1
dTTP (100mM Stock)	6mM	0.06	_____ 0.06 x N x 1.1
aa-dUTP (ambion 50mM)	4mM	0.08	_____ 0.08 x N x 1.1
Water (ricco ultrapure)		0.56	_____ 0.56 x N x 1.1

Reverse Transcriptase Reaction Option B - Invitrogen Protocol:

You need one tube per slide, per sample. So for a two-condition experiment, with each condition labeled with Cy3 and Cy5, using two slides, you will run 2 tubes per sample for a total of 4 tubes. The tubes used are domed PCR tubes for use in the thermocycler

1) Add the following, making the total for all the tubes in each condition in one tube and then dispensing it into individual labeled tubes :

Multiply each sample times 1.10 (extra to make sure to have enough)

Y = ul needed to yield 20 ug

Q = number of RT tubes for that sample (usually = 2 since one per slide)

	Per Tube	Name:	Name:	Name:	Name:	Quantity Needed
Total RNA	Y					$Y \times 1.1 \times Q$
Random Primers (3ug/ul)	2 ul					$2ul \times 1.1 \times Q$
Water	10-Y					$(10-Y) \times 1.1 \times Q$
Total	12 ul					$12 \times 1.1 \times Q$

2) Mix Well and Dispense 12 ul into each tube _____ (Check when completed)

3) Incubate at 70°C for 10 min. _____ (Check when completed)

******* Start making dNTP mix and RT master mix *******

4) Place on ice for one minute. _____ (Check when completed)

5) Add 8 ul of RT Mix to each tube _____ (Check when completed)
and mix well

6) Incubate at 42°C for at least 3 hours _____ (Check when completed)

7) To hydrolyze RNA add 10ul 1N NaOH to each tube _____ (Check when completed)

8) To stop reaction add 10ul 0.5M EDTA to each tube _____ (Check when completed)

9) Mix and incubate at 65°C for 15 min. _____ (Check when completed)

10) Add 10ul 1 N HCl to each _____ (Check when completed)
tube to neutralize reaction mix

RT Master Mix

Add the following:

	<u>Per Tube</u>	<u>Final Conc.</u>	<u>Total Needed</u>
5X Strand Buffer	4ul	1x	_____ 4ul x N x 1.1
0.1M DTT	1ul	1x	_____ 1ul x N x 1.1
*dNTP mix	1ul	1x	_____ 1ul x N x 1.1
Superscript III	2ul	400U	_____ 2ul x N x 1.1

Total	8ul		_____ 8ul x N x 1.1

Important Note: Superscript comes in different concentrations. Make sure to add 400U in each reaction. If using higher concentration superscript, add less and replace lost volume with water.

N = total number of tubes for all samples

*20x dNTP mix	<u>Conc. In 20x Mix</u>	<u>ul per tube</u>	<u>Total Needed</u>
dATP (100 mM Stock)	10mM	0.15	_____ 0.15 x N x 1.1
dGTP (100mM Stock)	10mM	0.15	_____ 0.15 x N x 1.1
dCTP (100mM Stock)	10mM	0.15	_____ 0.15 x N x 1.1
dTTP (100mM Stock)	6mM	0.09	_____ 0.09 x N x 1.1
aa-dUTP (ambion 50mM)	4mM	0.12	_____ 0.12 x N x 1.1
Water (ricco ultrapure)		0.34	_____ 0.34 x N x 1.1

NOTE: SINCE IT IS VERY HARD TO MEASURE SMALL AMOUNTS, MAKE A STOCK SOLUTION OF THIS dNTP MIX

RT cDNA Cleanup – Used for either RT option listed above

- 1) Combine all tubes **for each sample** / Dye _____ (Check when completed)
into a labeled tube of appropriate size
- 2) Add five volumes PB Buffer (Qiagen) _____ (Check when completed)
to each tube and mix well
- 3) Add mix 700ul at a time to a labeled Qiagen PCR cleanup column (one for each
sample). Spin at 13,000 rpm for 15 sec., empty collection tube, and repeat until all of the
solution has passed through the column
_____ (Check when completed)
- 4) Complete wash One, add 750 ul of phosphate _____ (Check when completed)
wash buffer to column and spin at 13,000 rpm
for 1 min., empty tube

Phosphate wash buffer (100mL) [5mM KPO₄, pH 8.0, 80% EtOH]
1M KPO₄, pH 8.5 0.5 mL
MSDW 15.25 mL
95% EtOH 84.25 mL

- 5) Complete wash Two, add 750 ul of phosphate _____ (Check when completed)
wash buffer to column and spin at 13,000 rpm
for 1 min., empty tube
- 6) Spin an additional 1 min. with a new collection _____ (Check when completed)
tube and discard the flow through
- 7) Transfer to new 1.5 mL tube, add 30uL phosphate elution buffer
to the membrane and incubate a room temp. for 1 min.
Spin at 13,000 rpm. _____ (Check when completed)

Phosphate elution buffer - dilute 1M KPO₄, pH 8.5 to 4mM with MSDW

- 8) Repeat phosphate elution into _____ (Check when completed)
same tube again using 30ul.

QC of Reaction

Blank GRL spec with 60 ul _____ (Check when completed)
phosphate elution buffer

Check for cDNA by putting entire reaction _____ (Check when completed)
into a 100uL cuvette and reading A₂₆₀ and A₂₈₀
(You need an OD₂₆₀ of at least 1.0 to proceed)

Labeling Reaction

1) Dry all RT samples completely in speed vac _____ (Check when completed)
(about 90 min. total, on low heat check every 20 min.)

2) Make new 1.0 M Sodium Carbonate Buffer _____ (Check when completed)

Buffer Recipe (**must be made fresh every time**) – Add 80 ml ultra pure water to small autoclaved glass bottle along with a clean stir bar (measure water using a sterile 50 ml pipette). Add 10.8 g Sodium Carbonate and allow it to dissolve. Adjust pH to 9.0 using 12 N HCl using a 10ml pipette and a bulb to keep track of amount added (should be about 9 ml). Add water to bring total volume to 100 ml.

3) Make 10 ml of 0.1 M Sodium Carbonate Buffer _____ (Check when completed)

Recipe – Add 9 ml of ultra pure water to a sterile 15 ml screw cap tube and add 1 ml of the fresh 1.0 M buffer made in the previous step.

4) Resuspend each dried sample cDNA in 4.5 uL _____ (Check when completed)
of 0.1M sodium carbonate buffer, pH 9.0

****** Move to a Darkened Area the dyes are VERY light sensitive ******

Get aliquots of dyes for each tube, and make sure to label the tubes for which dye will be added to them. Only get the dyes and thaw them from the – 70C when ready since they degrade quickly once thawed. Aliquots are made by adding 73 ul of DMSO to a tube of amersham cy dye.

5) Add 4.5 uL NHS-ester Cye dye _____ (Check when completed)
(aliquots prepared in DMSO)

6) Incubate for 2 hour at room temperature _____ (Check when completed)
In absolute Darkness

7) Add 35uL of 100mM NaOAc pH 5.2 _____ (Check when completed)
To each tube and mix

8) Add 250ul Buffer PB to each tube and mix _____ (Check when completed)

9) Add each mix to a labeled Qiagen DNA _____ (Check when completed)
Column and spin at 13,000 rpm, empty tube.

10) Wash each column with 750 uL Buffer PE _____ (Check when completed)
(Qiagen) and empty tube

- 11) Spin an additional 1 minute at 13,000 rpm _____ (Check when completed)
And throw away collection tube
- 12) Elute into a new labeled 1.5 ml tube by adding _____ (Check when completed)
30 ul Buffer EB (Qiagen), letting stand 1 min.
at room temp., and then spinning at 13,000 RPM
- 13) Repeat elution into same tube _____ (Check when completed)

Optional: Check cDNA and incorporation **in the darkest setting possible:**

Measure OD at 260, 550, 650.

cDNA => 1 OD = 37 ng/uL; nucleotide pmols =

$[\text{OD}_{260} * \text{vol. (uL)} * 37 \text{ ng/uL} * 1000 \text{ pg/ng}] / (324.5 \text{ pg/pmol})$; pmol Cy3 =

$[\text{OD}_{550} * \text{vol. (uL)}] / 0.15$; pmol Cy5 = $[\text{OD}_{650} * \text{vol. (uL)}] / 0.25$

nucleotides/dye ratio = pmol cDNA/pmol Cy dye

ratio is best with >200 pmol dye incorporated per sample and a ratio less than 50

- 14) Combine different labeled probes as specified in _____ (Check when completed)
The experimental design and dry in a speed vac
On low heat (about 70-80 min.) **Start preheating
prehyb and hyb buffers now**
- 15) Resuspend combined tubes in 20 uL MSDW _____ (Check when completed)

Prehybridization (Start when dyes are nearly dry in SpeedVac)

- 1) Prepare Prehyb buffer fresh _____ (Check when completed)
(225 ml water, 75 ml 20xSSC,
0.3g SDS, 3.0g BSA). Preheat 45 min
at 42C. **Turn 95C heat block on.**
- 2) Place slides in Coplin jar, _____ (Check when completed)
prehybridize at 42°C for 45 min.
Handle slides only by barcode
Put thawed COT1 DNA on ice
- 3) Wash slides by dipping _____ (Check when completed)
5 times in water at room temp.
- 4) Dip twice in isopropanol at room temp, _____ (Check when completed)
dry slides in centrifuge or with nitrogen
and use within 1 hour.

Hybridization:

******* Everything is completed in the Dark *******

- 1) Add 1uL of COT1-DNA (20ug/uL) to _____ (Check when completed)
Each tube that will be hybridized to a slide
- 2) Heat probe mixture to 95°C for 2 min., _____ (Check when completed)
and do a quick spin
- 3) Add 21 ul of 2x hyb. buffer (50% formamide, _____ (Check when completed)
10X SSC, 0.2% SDS) that has been preheated to
42°C to each tube.
- 4) Apply 40ul hyb. mix to slide and cover with a _____ (Check when completed)
20x60 mm polyethylene hydrophobic
coverslip (PGC scientific) avoiding bubbles
- 5) Add 10ul of water to both ends _____ (Check when completed)
of chamber (corning) in wells,
and seal the chamber
- 6) Place in 42°C bath for 16-20 hours _____ (Check when completed)
Cover Very Well with Foil

Slide Wash and Scan

******* Must be completed in the Dark *******

- 1) Preheat wash buffer (1x SSC and 0.2% SDS at 42°C) _____ (Check when completed)
at 42C. Warm up Scanner Lasers for 15 min
- 2) Place slides in dish containing low-stringency _____ (Check when completed)
wash buffer (1x SSC and 0.2% SDS at 42°C)
Agitate for 4 min.
- 3) Wash slides at high stringency wash buffer _____ (Check when completed)
(0.1x SSC and 0.2% SDS) at room temp. for 4 min.
- 4) Wash slides in 0.1x SSC for 4 min. _____ (Check when completed)
- 5) One at a time remove slides from the third wash buffer _____ (Check when completed)
This is important to leave the other slides submerged as
They will photo bleach if removed for greater than 10 minutes
- 6) Dry Slides in the Dark with either the centrifuge _____ (Check when completed)
or with nitrogen gas.

Scanning w/ Perkin Elmer ExpressLite

- 1) Turn on computer and scanner
- 2) Open ScanArray software (allow 10 sec for software to detect scanner)
- 3) Click on laser tabs on right to turn them on, allow 15 minutes for warming.
- 4) Insert slide into scanner on top of metal lip. Do not force the slide, or press down on it. You should feel it stop when it is fully seated. A fully seated slide's barcode will remain visible.
- 5) Go to configure, scan protocol, and either select an existing protocol or ADD a protocol.
- 6) Make sure the scan is set to 10 micron and full speed.
- 7) Select tools
- 8) Select quick scan, select cy3 as the dye to use, and start the scan.
- 9) Stop the scan after scanning about 20 rows.
- 10) At the tools menu select line scan.
- 11) Click show zoom window and draw a line through 30 spots in a row with a mix of intensities. Click OK.
- 12) Click on dye and select cy3. Start the scan, and as soon as the intensities show up on the chart click stop. Add or subtract power until the highest peaks are at about 80%.
- 13) Change dye to cy5 and repeat above step.
- 14) Click accept changes, click finish, click close.
- 15) Now click scan, run scan protocol, select the scan protocol you created.
- 16) Use autosave NCSU, this will save both a tiff image and bitmap of each scan completed, in the order scanned. So for a single slide four files will be present, two for cy3, and two for cy5.
- 17) Click OK to begin scan.
- 18) Record file names below and burn to a CD immediately.

Slide number	Cy3 laser power	Cy5 laser power	File names	CD number

Quantitating the Slides Using ScanArray:

- 1) Open picture file from previous scan.
- 2) Click on configure, click on quantification protocols.
- 3) Select a current protocol or create a new protocol by clicking on ADD.
- 4) Name the protocol if new
- 5) Click on the template tab, and add a gal file from the printer output
(IT IS EXTREMELY IMPORTANT TO USE THE GAL FILE FROM THE PRINTER OUTPUT FOR THE RUN THAT PRINTED THE SLIDE BEING QUANTITATED. MANY HOURS HAVE BEEN WASTED BEING CARELESS ABOUT THIS !!!!)
- 6) A template will appear overlaying your spots. You must now zoom way in and move the template to where your spots are. The best way is to start with moving all subarrays and aligning them with the top left block of spots. Then make sure the angle is right and correct if necessary. Finally, move the subarrays one at a time to make sure all spots are aligned with the templates.
- 7) Click the quantitation and normalization tab and click on histogram and total. Click finish and close.
- 8) Quantitate the slide being displayed by clicking on quantitate, run a protocol, and the protocol you designed. Check spot alignment and click start. Note: this will take a while. The computer is not locked up, it just takes 5+ minutes to quantitate a slide.
- 9) Repeat for the next dye / slide. Save each quantitation as a .csv file.

Optional: If concerned about how the software will quantitate, the software offers an option to see how the spots will be found. Click on the third tab of the quantitation protocol and use the check spot finding option.

RT-PCR For Quality Control:

PRIMER DESIGN

1. OBTAIN GENE SEQUENCE

Example - TM1788

```
GTGAAAGTTTCCGGGGGGGAAGTTTCTCCCTTTTTCAAGGAGGGGTTTTTCTTTACTTCAGAGGAACTGACTCA
TCTTATCAATGTATGTAGTAGCACATCTGCAATTATCTCAGTATTGAAAGACAGTAAGTATAGAAGGTCTTTGG
TCTTATATCTAAAAAGGCCTTTGAGCAAAGATGCTCTTCTTTTGATTGAGACTCTGCTAACTACCCTTGAAAGG
GAAGATCTTTTCGTTTGGTGTAAAAGAACTGGAATACATGGCCTATCACGATCCACTGACAGGGCTTCCAAACAG
GCGTTATTTCTTTGAACTGGGAAACAGATATCTGGACTTAGCAAAGCGCGAGGGAAAAAAGGTATTTCGTTCTTT
TCGTAGATCTTGCTGGGTTTAAGGCGATAAATGACACATACGGCCATCTGTCAGGTGATGAGGTATTGAAGACA
GTTTCAAAAAGGATTCTGGACAGGGTTAGAAGAAGCGATGTGGTGGCTCGATACGGCGGTGATGAGTTTACCAT
TCTCCTCTACGATATGAAAGAAGAGTATCTGAAATCCCTCCTGGAAAGGATTCTTTCCACCTTCAGAGAACCCG
TCAGAGTGGAAAATAAACACTTATCTGTCACACCGAACATAGGAGTTGCCAGATTCCCTGAAGATGGGGAAAAT
CTTGAAGAACTTCTGAAAGTAGCGGATATGAGGATGTACAAAGCAAAGGAAATGAAAGTGCCTTATTTTCAGTCT
CTCATAA
```

2. DEFINE A 300 bp TARGET AREA

If possible, define 600bp sequence (300bp target area + 150 bp upstream +150 bp downstream) input to mfold:

Mfold can be found at:

<http://www.bioinfo.rpi.edu/applications/mfold/old/dna/form1.cgi>

600bp Target area in this example is:

```
TAGTAGCACATCTGCAATTATCTCAGTATTGAAAGACAGTAAGTATAGAAGGTCTTTGGTCTTATATCTAAAAA
GGCCTTTGAGCAAAGATGCTCTTCTTTTGATTGAGACTCTGCTAACTACCCTTGAAAGGGAAGATCTTTTCGTTT
GGTGTAAAAGAACTGGAATACATGGCCTATCACGATCCACTGACAGGGCTTCCAAACAGGCGTTATTTCTTTGA
ACTGGGAAACAGATATCTGGACTTAGCAAAGCGCGAGGGAAAAAAGGTATTTCGTTCTTTTCGTAGATCTTGCTG
GGTTTAAGGCGATAAATGACACATACGGCCATCTGTCAGGTGATGAGGTATTGAAGACAGTTTCAAAAAGGATT
CTGGACAGGGTTAGAAGAAGCGATGTGGTGGCTCGATACGGCGGTGATGAGTTTACCATTCTCCTCTACGATAT
GAAAGAAGAGTATCTGAAATCCCTCCTGGAAAGGATTCTTTCCACCTTCAGAGAACCCGTCAGAGTGGAAAATA
AACACTTATCTGTCACACCGAACATAGGAGTTGCCAGATTCCCTGAAGATGGGGAAAATCTTGAAGAACTTCTG
AAAGTAGC
```

3. INPUT TARGET AREA INTO MFOLD (michael zucker's DNA folding algorithm)

set folding temperature = 55°C (for first iteration)

set 50 mM NaCl

set 3 mM Mg

*Click "Structure Viewing Options"

*View structure

*If structure contains hairpins, increase the temperature parameter and

refold.

*Design primers in regions that lack hairpins.

4. DESIGN PRIMERS WITH GENOMAX (MUST HAVE AN ACCOUNT)

- I. Choose ORFs for real-time analysis
- II. Create a new file in Notepad
 - a. type locus name in upper, left side of document
 - b. press return, add another locus
 - c. continue until all desired ORFs are added to Notepad document
- III. Extract Sequence for selected ORFs
 - a. Go to *Pyrococcus furiosus*, etc. page on TIGR
example: http://www.tigr.org/tigr-scripts/CMR2/gene_table.spl?db=ntpf01
 - b. Go to CMR Batch Download (click “Search”)
 - c. Fill out CMR Batch Download information
 - i. type of sequence = nucleotide
 - ii. Retrieve all sequences from a file of accessions
 - iii. Click “Browse” next to “Retrieve all sequences from a file of accessions”
 - iv. Find the Notepad file
 - v. Submit request (returns a .dbi file with sequences)
- IV. Import Sequence into **Genomax** (or Vector NTI)
 - a. Load Genomax
<http://uncgene.unc.edu/genomax3/cgi-bin/UNCCH/genomax.cgi>
 - b. Click “Local Data Upload”
 - c. Fill in user login (RNA/DNA should be selected)
 - d. On Genomax molecule submission form
 - i. DNA/RNA format = Genomax
 - ii. Add to an existing subset or create new one, depending on objective
 - iii. Click on “Browse” on “Or send data from file” at the bottom and choose appropriate .dbi file.
 - iv. Click on “Submit Molecule to Genomax”
- V. Run Genomax
 - a. Click “Start Genomax Java Client [current version]”
 - b. Type login information
 - c. Click “Sequence Analysis” at top right corner to begin program
 - d. Find appropriate subset under “+DNA/RNA” and double click
- VI. Design Primers
 - a. Select ORFs in subset that you need primers for
 - i. <Shift> and <Ctrl> keys allow multiple selections to be made
 - ii. **Set length of amplicon to be from 75-150 bp long**
 - b. Click on “Primer3” in far right side of toolbar
 - c. Set parameters appropriately and click “ok”
 - i. Primer Size (variable)

- ii. Primer Size (first try) = Min 20, Opt 22, Max 25
 - iii. Primer T_m (first try) = Min 58.0, Opt 59.0, Max 61.0
 - iv. Primer GC% (always) = Min 40, Opt 50, Max 60
 - v. Max T_m Difference (always) = 0.5 (may raise to 1.0 as a last resort)
 - vi. “Advanced Parameters” Try to keep these at 50mM salt conc., 50nM oligo annealing Conc., Max N’s accepted = 0 (may raise to 2 or 3 as a last resort), Max compl. = 8.0 (only change as a last resort), Max 3’ compl. = 3.0 (only change as a last resort)
- d. After all primers have been designed (wait for program to finish running), highlight the relevant ORFs and (copy and paste) into an Excel file for final processing.
 - e. If nothing shows up for a gene, Genomax could not design a primer using the specifications requested. Broaden the criteria used and repeat the design.

5. OPTIONAL: TEST FOR PRIMER DIMERS

free tool available at Qiagen (formerly www.operon.com)

<http://oligos.qiagen.com/oligos/toolkit.php>

*NOTES:

Primer design for QPCR can be a relatively quick or very long and laborious, depending on how much you want to optimize your primers. Keep in mind that the process is experimental (trial and error); do not spend too much time designing primers because even a perfectly designed primer may not work, and sometimes poorly designed primers work well. For a small number of sequences (less than 10), I recommend following steps 1-4 above rather thoroughly, and put much less weight on steps 5-6. Primer dimmers and BLAST search checks may immediately reveal a very obvious flaw in a design, but optimizing 5-6 may take more time than it is worth.

Also, do not run the QPCR rxns more than 2-3 times before ordering new problems. It is recommended to run the rxns twice: if the result will not work, then realize that it will probably take considerably more effort (and \$\$) to optimize the QPCR reactions than to order new primers. Compared to the QPCR, cost of primers is small.

QPCR REACTIONS

Biorad protocols for SYBR GREEN (200 times more fluorescence than background [EtBr is 25x]) recommend performing 50ul reactions for every QPCR reaction. However, I have found that 20ul reactions usually work.

BASICS: For every gene being analyzed with RT-PCR, a standard curve and 3 replicates of each condition must be run. The quantitation requires a complete standard curve, and the replicates of each condition allow for a standard error to be calculated. An example of what a plate would look like for two genes (genes A and B), under a control condition (before heat shock) and one test condition (i.e. after heat shock) are listed below. The standard curve covers the following concentrations of template, 0.15, 0.60, 2.4, 9.6, and 38.4 ng of template cDNA in the 20 ul reaction. Note: template cDNA is from the control condition.

Gene A 0.15 ng	Gene A 0.6 ng	Gene A 2.4 ng	Gene A 9.6 ng	Gene A 38.4 ng			Gene B 0.15 ng	Gene B 0.6 ng	Gene B 2.4 ng	Gene B 9.6 ng	Gene B 38.4 ng
Gene A 2.4ng Control	Gene A 2.4ng Control	Gene A 2.4ng Control					Gene B 2.4ng Control	Gene B 2.4ng Control	Gene B 2.4ng Control		
Gene A 2.4ng Test	Gene A 2.4ng Test	Gene A 2.4ng Test					Gene B 2.4ng Test	Gene B 2.4ng Test	Gene B 2.4ng Test		

Reference:

<u>For 20ul reactions/well</u>	<u>Final Concentration</u>	
iQ SYBR Green Supermix	10 ul	1X
Primer 1	1 ul	250nM
Primer 2	1 ul	250nM
Sterile water	8-x ul	
DNA template	x ul	see below
 Total	 20 ul	

Making dilutions of primers – The freeze dried primers from IDT DNA will have a nMols marking on them, i.e. 25 nMol. We first want to make a 15,000 nM solution. Multiply the nMol on the tube by 1000, then divide this number by 15,000 to get the ml of water to add to the freeze dried primers to make a 15,000 nM solution. Then make add 500 ul of this to

1000 ul of water in a new tube to yield a 5000 nM working stock. Adding 1 ul of this working stock to a 20 ul reaction will yield 250 nM, the desired final concentration.

I. RT-Reaction

The first step is to run a RT reaction as explained above to yield template for running real-time PCR. Run as you would for a microarray except do not use amino allyl in the dNTP mix. Substitute in dTTP in for the amino allyl removed. Once you have the template from the RT reaction, check the OD₂₆₀ and quantitate the cDNA using the formula

$$\text{ng/ul cDNA} = 37 \text{ ng/ul} * \text{OD}_{260}$$

II. Using the Bio-Rad RT-PCR Machine

The manual does an excellent job of covering the use of the software but here are the basics. The first thing is to turn of the machine and the lamp and log in to the thermocycler. Next, start the software and create a new protocol by clicking on the library tab and then create a new protocol. Give the protocol a name and then click on edit the protocol and it will carry over to the workshop tab. Add the following setup.

Cycle	Repeat	Step	Dwell	Setpoint
1	1	1	8:00	95
2	50	1	0:15	95
		2	0:30	calculate
		3	0:30	72
3	1	1	1:00	95

Next, click on Melt Curve under the show options section and 80 repeats of a 0.5 C increase will be added to measure the melting point of any PCR products that will be made.

Next, under the data collection steps section, click on the square next to step 3 in cycle 2 until the camera and Real-Time appear next to the box. This will both have the camera detect the presence of fluorescing double stranded amplified DNA during the extension step, and allow for you to see the data during the run. This is helpful to note if the reactions are working without waiting 3 hours. Save the protocol.

Next, add the plate setup by going to the library tab, view plate setup. Add the standards and samples in a similar method to how they are shown in the example plate layout above. Add the quantities for the standards in terms of ng of cDNA added to the well.

III. Run Gradient

First, you must run a gradient for each ORF in order to experimentally determine the optimal annealing temperature. Fortunately, the iQ machine allows 8 different PCR reactions with 8 different temperatures to be run at the same time, with a different temperature in each row of the machine.

- (A) Make a 20 ul reaction up for each gene, for each row of the thermocycler using 2.4 ng of control as template. Make a new plate template to reflect how you have loaded the wells and save it. Click on the gradient box on the show options section of the workshop protocol, modify the gradient as desired going from -10 the melting temp, to the melting temp itself, and save this as a separate protocol. **Make sure to always centrifuge your 96 well plates or tubes before running the RT-PCR and always use bio-rad optical film to seal the top of the plates.**
- (B) Click on run with this protocol, you will be taken to the run-time central tab. Click on collect well factors from experimental plate, and set well volume to 20 ul. Click begin run. Once run is complete (3 hours), go to the data analysis tab and select a row at a time to view on the graph using the select wells button. You want to find the temperature with the best amplification, and with a single peak on the melting curve (melt curve tab) to use as a melting temp for the actual real-time run. Multiple peaks means non-specific amplification is occurring.

III. QPCR reactions

Run QPCR as you have laid out on your template previously, using the temperature optimum found by running the gradient. Make certain all samples are run with the same amount of cDNA template. It is best to run only a gene or two at a time since the costs of errors are high. Do not run a gradient during the run as all standards and samples must be run at the same temperature. If during the run you would like to add more cycles (i.e. the amplification starts late, on the run-time central tab you have this option to add 10 repeats at a time.

CALCULATIONS

Good reference: <http://www.med.sc.edu:85/pcr/realtime-home.htm>

First, make sure all of the standards and samples both had good amplification (above 750 units of fluorescence), and had no multiple melt curve peaks. Do not use data that doesn't meet this criteria. Next, select PCR base line subtracted on the PCR quant tab of the Data Analysis section, and select user defined for the threshold position. Move the threshold bar to a level at the beginning of the linear amplification section, well above any background.

Next, one set at a time, select the wells that contained the standards, and then click on the PCR standard curve tab. Note down the efficiency for each set of standards (one per gene).

Next, select the sample wells and note down the cycle threshold.

The fold change from one gene to another can be calculated by taking the average of the Ct for the replicates for each condition, and comparing it to the control using the following formula

$$\text{Fold Change} = [(100 + \underline{\% \text{ efficiency}}) / 100] ^ { (Ct_{\text{control}} - Ct_{\text{test}})}$$

Reference in manuscripts - ([M.W. Pfaffl](#)) A new mathematical model for relative quantification in real-time RT-PCR. Nucleic Acids Res. 2001, 29(9):e45).

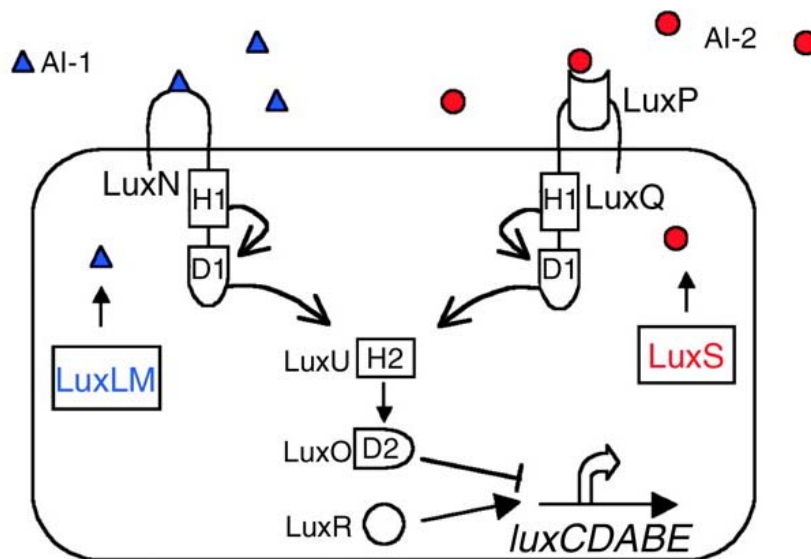
Note: a lower Ct means MORE template was present for that gene, i.e. more mRNA was expressed for that gene.

**Appendix Two: Growth of *Vibrio harveyi* for the detection of
homoserine lactones and the autoinducer AI-2**

Matthew R. Johnson

**Department of Chemical and Biomolecular Engineering
North Carolina State University
Raleigh, NC 27695-7905**

V. harveyi QS systems (J. Clin. Invest. 112:1291-1299 (2003).)



Reporter Strains of *V. harveyi* developed by the Bassler Group at Princeton

<i>V. harveyi</i> Strain	Phenotype	Mutation / antibiotic	Use
BB120	Wild-type	None	Control
BB152	Cannot produce AI-1	-luxM, kanamycin 50 ug/ml final in culture	Over production of AI-2
BB170	Cannot detect AI-1	-luxN, kanamycin 50 ug/ml final in culture	Detection of AI-2
BB886	Cannot detect AI-2	-luxPQ, kanamycin 50 ug/ml final in culture	Detection of AI-1
MM30	Cannot produce AI-2	-luxS, kanamycin 50 ug/ml final in culture	Detection of AI-1
MM32	Cannot produce AI-2, Cannot detect AI-1	-luxN, chloramphenicol (dissolve in ETOH) and 30 ug/ml final in culture -luxS, kanamycin 50 ug/ml final in culture	Improved detection of AI-2 due to the inability to have background luminescence

Cultivation of *V. harveyi*

AB Media –

970 ml water

17.5 g NaCl

12.3 g MgSO₄

2 g Casamino acids (acid hydrolyzed)

pH to 7.5 and autoclave

after cool add sterile...

- 10 ml of 1M Potassium phosphate pH = 7.0
- 10 ml of 0.1M L-arginine
- 10 ml of Glycerol (100%)
- any antibiotics required for the strains utilized

Grow at 30C with shaking w/ slightly slower growth than *E. coli* (doubling time ~1 hr)

If you want to make plates add agar and streak out from a liquid culture

The plate will grow in 1-2 days into a lawn of colonies, which will be good in the cold room for 2 weeks. After which growth is unreliable.

To make glycerol stocks spin down a liquid culture, remove supernatant, and resuspend in fresh media w/ 20% glycerol, and freeze at –80C.

Bioassays

Bioassays are run in clear 96 well plates with black well walls (to prevent luminescence bleed over between wells). They can be used to test supernatants of cultures, or to test activity of enzymes in producing autoinducers.

A typical bioassay is

180 ul of AB media with antibiotic
20 ul of a test sample
5* ul of a freshly grown liquid culture for inoculum

*for bioassays with BB170, BB886, MM30 add cells to a final 1/5000 dilution as background is very high.

Grow overnight with the plate reader reading every 1-4 hours. (30C temp, 150 milliseconds read, 150 gain, no shaking).

All samples are run in duplicate and with controls. Background will increase over time with all strains except MM32.

Supernatant test samples:

Spin down culture of choice
Filter supernatant with a 0.2 micron filter
Use in bioassay (note, reducing agents will hamper aerobic bioassay)

Testing enzyme activity:

To test for the presence of autoinducer synthesis activity with the bioassay:

Using PCR tubes or plates add:

- 5 ul of substrate (around 5 mM is a good place to start)
- 5 ul of enzyme sample
- 20 ul of buffer in 100-200 mM salt range

- seal with PCR caps (not film, will leak)

- heat at growth temperature of organism for 1 hr (longer is not better)

- use 20 ul for bioassay as explained for supernatants

All assays should be done in triplicate.